INVESTIGATION OF THE MULTI-SCALE VARIABILITY OF BEACH PROFILES

by

YING LI

A thesis submitted to the University of Plymouth

in partial fulfilment for the degree of

DOCTOR OF PHILOSOPHY

School of Engineering

Faculty of Technology

November 2005

Investigation of multi-scale variability of beach profiles by Ying Li

Abstract

This work focuses on the multi-scale variability of beach profiles. This includes the spatial variability over a range of scales of surveyed beach profiles and the complex temporal variability of beach elevation at given positions along the profile. The aims of this work are to characterize the variability of beach profiles in both time and space, to identify the predominant spatial and temporal patterns of beach profile changes, to identify the extreme profile changes due to infrequent storms/storm groups, to understand the nature of beach profile change in depth, to quantify the non-stationarity of beach profile and to provide insight into the prediction of beach profiles.

This thesis includes a critical literature review of the existing profile models, such as numerical and data-driven models, to predict beach profiles. Particular focus is on the data-driven models since they characterize the beach in a site-dependent manner. The main weakness of the existing data-driven approaches is that many of the techniques assume stationarity and yet the processes in question are non-stationary, which necessitates more advanced techniques for investigating the variability of beach profiles. Hence in this thesis the wavelet technique is introduced, which is a relatively new technique. It is also shown how the use of a wavelet basis for decomposing the profile signals spatially allows a more satisfactory value for the depth of closure associated with a data set to be defined.

Particular interests are in the beach profile data from the Field Research Facility (FRF) at Duck, North Carolina, USA. The field data and previous works by other researchers are introduced and preliminary studies are conducted including the interpolation of data and the empirical orthogonal function (EOF) analysis. A connection is established between EOF and wavelet analysis. In addition to the identification of basic patterns of beach profile changes, emphasis is given to the non-stationary investigation of beach profile changes in both time and space locally. In this way, the infrequent events are identified at different temporal scales. The responses of beach profile changes to different wave/storm conditions are discussed. The intermittent character of beach profile change is displayed in both time and space, providing much insight to the argument by Southgate and Möller (2000). Also, the depth of closure is presented by analysing the local components of wavelet variance in space, which is scale-dependent. The results agree with Larson and Kraus (1994).

The wavelet analysis is validated on the beach profile data at the Coastal Research Station (CRS), Lubiatowo, Poland. Focus is on the spatial variability across the beach profile. Due to the multi-bar system, the spatial scale contents of beach profile changes at Lubiatowo are more complicated than Duck. The predominant spatial scales indicate that wave breaking may be the major factor of bar formation at this site. This is consistent with Pruszak *et al.* (1997).

LISTS OF CONTENTS

LIST OF NOTATIONS

a	distance parameter
$a_{i,j}$	elements in matrix $\mathbf{A}^{EOF}$
A	dimensional shape parameter dependent only on the sediment size
$\mathbf{A}^{EOF}$	a symmetric correlation matrix
c	variance coefficient
c_k	the k^{th} variance component
c_0	nugget variance
$\mathbf{C}$	covariance matrix
$\tilde{C}_{u,v,m}$	wavelet covariance of variable u and v at scale parameter 2^m
$\tilde{d}_{j,k}$	wavelet coefficient of the AMODWT
$\mathbf{D}$	matrix of wavelet function coefficients
$D_{j,k}$	wavelet coefficient of the DWT
$E(\cdot)$	an additive cost functional
$f(t)$	beach profile elevation in time series
$f(x)$	beach profile elevation in space series
g	acceleration of gravity
$\{g_l\}$	high-pass filter
h	water depth
$h_{i,j}^R$	wavelet filter coefficient of the right side
$h_{i,j}^L$	wavelet filter coefficient of the left side
$h_{x,t}$	the collection of beach profile measurements
H	wavelet filter coefficient

H_{m0} wave height

$\{h_l\}$ lower pass filter

$I_{j,n}$ frequency interval in the nth wavelet packet at exponential scale j

j exponential scale

J_0 Bessel function

k translator in wavelet transforms

l lag in distance or time

$L^2(\Re)$ vector space

m_0 any exponential scale

M number of moment of wavelets

n number of points on variogram

N number of input data

$N(l)$ number of pairs with separate distance/time l

p a positive integer

p_n number of parameter in combined variogram

p_w a threshold in entropy

P_m approximation represent at scale parameter 2^m for a signal

Q mean of the residuals between experimental and simulated model variogram

Q_m detail component at scale parameter 2^m for a signal

$S_{j,k}$ normal cumulated sum of squares at scale parameter 2^m

T_p wave period

$\mathbf{T}_x$ the lagged covariance matrix

$V_{2^{m_0}}$ vector subspace of $L^2(\Re)$

$W_{0,0}$ input data $f(t)$

$W_{j,n}$ the n^{th} wavelet packet at exponential scale j

$W_{j,n,i}$ the discrete wavelet coefficient in the location i of the n^{th} packet at exponential scale j

x_s cross-shore distance from shoreline

x_0 basic sampling of data

$z(x)$ function of a random variable

α exponential parameter in variogram

λ scale parameter in wavelet transforms

λ_0 a fixed dilation step greater than 1

τ threshold of slop cutting off

$\widetilde{\rho}_m$ wavelet correlation between u and v at scale parameter 2^m

γ_k the k^{th} basic variogram

$\gamma(l)$ variogram function

$\hat{\gamma}(l)$ experimental variogram

$\widetilde{\sigma}_j^2$ wavelet variance of the AMODWT at exponential scale j

$\sigma_{j,n}^2$ the n^{th} wavelet variance at exponential scale j

$\delta_{m,n}$ the Kronecker delta function

$\Re$ a set of real numbers

$\varphi(x)$ scaling function

$\psi(x)$ wavelet function

LIST OF TABLES

LIST OF FIGURES

ACKNOWLEDGEMENTS

I would like to express my gratitude to many for their support, which has been very important to fulfil this work. My first great thanks are to the main directors, Professor Dominic Reeve and Dr. Murray Lark who have been the source of strength throughout this work. It is them who initiated this work. I appreciate their commitment and interest in this thesis, the constant patience and guidance during this work. I also owe a debt of gratitude to another director, Dr. Dave Simmonds for the inspiration on the interpretation of the results in this thesis. Thanks are also to director Dr. Qingping Zou for her concern when I was preparing for the viva.

I am grateful to Dr. Grzegorz Różyński from Institute of Hydroengineering of the Polish Academy of Science for the discussion on the work. Also, I express my thanks to many researchers who showed their interest and discussed the work when I was doing a presentation on it.

Grateful thanks are due to many friends for their direct and indirect contribution to this work. I would like to express my gratitude to my parents and my brother and sister for their love and support. Especially I owe many thanks to Zhenghua Zhang for his understanding and caring support. Without all of your support, this work would be harder to finish.

Finally, I offer my gratitude to the Engineering and Physical Sciences Research Council (EPSRC) and Biotechnology and Biological Sciences Research Council (BBSRC) in UK for the financial support throughout my work.

AUTHOR'S DECLARATION

For the degree of Doctor of Philosophy the author has been registered for the University of Nottingham for the first two years and the University of Plymouth for the third year.

This study was funded with the aid of a studentship from the Engineering and Physical Sciences Research Council and Biotechnology and Biological Sciences Research Council and carried out in collaboration with Silsoe Research Institute and Rothamsted Research.

Relevant scientific seminars and conferences were regularly attended at which work was presented. The author presented one internal seminar at University of Nottingham, one internal seminar in Silsoe Research Institute and two internal seminars at University of Plymouth. The author attended the 1st Young Coastal Scientists' and Engineers' Conference (YCSEC), held in Nottingham, UK.

Publications: **Multi-scale variability of beach profiles at Duck: a wavelet analysis,** Coastal Engineering, in press.

Investigation of beach profile variability at different scales using a wavelet technique, presented at Coastal Dynamics'05, Barcelona, April 4-8.

Courses attended: Mathematical methods for coastal engineering, University of Plymouth, 21st June to 30th June 2005

Word count for main body of thesis: 43742

Signed .....

Date Nov. 25. 2005

Chapter 1. INTRODUCTION

1.1 Motivation for This Work

Coastal areas and their resources are critically important to the development and future of coastal communities and nations. Almost half the world's population lives in coastal areas and depends directly on coastal resources for both agriculture and fisheries. People also depend indirectly on the benefits provided by coastal ecosystems, such as protection against sea level rise induced by climate change and storm damage. Sound management of coastal systems is therefore vital for the enhancement of the livelihoods of coastal people. Beaches are a particularly important element of coastal areas that protect economic investments in coastal areas, encouraging a positive contribution to local livelihood development while minimising adverse environmental impacts. In the UK, all of the local maritime councils, the Environment Agency and Defra have responsibilities for developing policy on coastal management.

Traditionally, there are many measures for protecting the shoreline. They mainly include beach nourishment, groynes, detached breakwaters and seawalls as suggested by Krystian (1990). Beaches often form a vital part of the defences, but by default rather than by specific design. Considering the role of beaches in protecting the coast, the recreational opportunities, and the need for environmental conservation, engineers are turning to 'soft' defence options, such as beach nourishment (Brampton, 1992). Therefore, in addition to being fundamental to understanding the morphodynamics of beaches, the spatial and temporal behaviour of beach profiles have a direct application in coastal engineering projects involving beach nourishment and in the siting of coastal structures.

Beach variability can be a major source of uncertainty in shoreline management, therefore clearly understanding the variability of beach profiles is of significance. Since forcing conditions come from several factors including astronomical tides, 'surge' due to atmospheric pressure variations and surface wave activity as well as human intervention, the variability of beach profiles is complex in both space and time. For instance, the ripples evolve at nearly the same time as the orbit motions of water particles as wave passing, as argued by Traykovski *et al.* (1999) whereas

Coco *et al.* (2000) suggested that beach cusps evolve over periods of minutes to hours. Winant *et al.* (1975) suggested that sandbars might respond significantly to seasonal wave conditions so that they have an approximate seasonal cycle, and might evolve over decades (Birkemeier, 1985; Lippmann *et al.* 1993). Failure to understand the changes might result in the shoreline management strategies or sea defence systems being out of balance with the coastal environment.

1.2 Features of Beach Profiles

1.2.1 Profile configurations

There are many ways of categorising beach profiles. According to the bar system, beach profiles can be divided initially into two categories: barred and non-barred. Sediment transport is an important process for the formation of bars. The mechanism of sediment transport consists of waves stirring up the sediment and currents transporting the sediment. Offshore bars can reduce wave energy entering the surf zone by breaking the higher energy incident waves. In this way, offshore bars play a role in protecting the beach. Since the importance of these ubiquitous topographical features has been acknowledged, a number of authors (e. g., Sallenger *et al.*, 1985; Larson and Kraus, 1992; Lippmann *et al.*, 1993; Moor *et al.*, 2003) have studied bar systems.

A few typical profile configurations are shown in Figure 1.1 with the mean water level. The bar and trough labelled on the plot are defined relatively to the mean. For convenience, the cross-shore profile is divided into four zones: dune zone, inner bar zone (surf zone), outer bar zone and upper shoreface as indicated in Figure 1.1. The offshore distance is relative to the baseline where the surveys of the profiles begin.

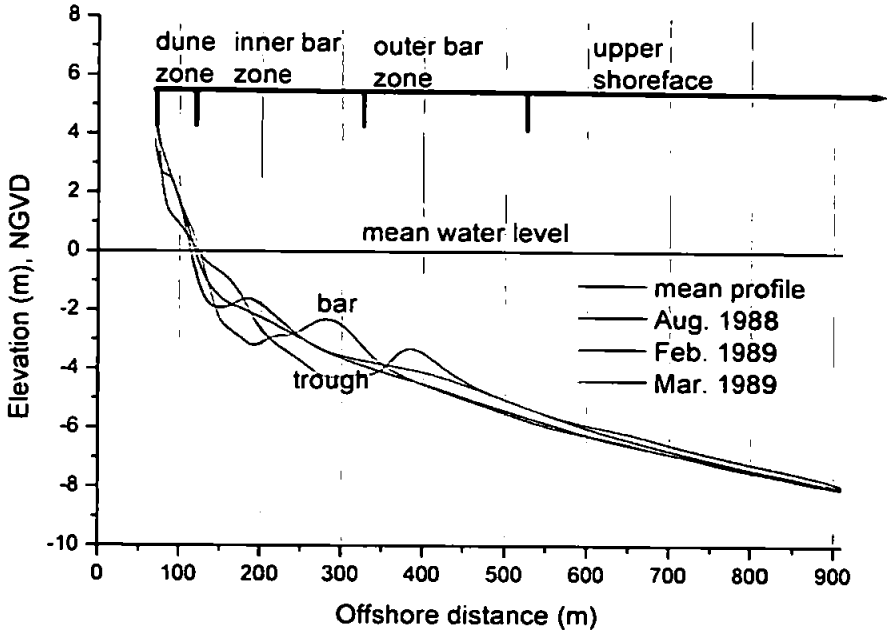

Figure 1.1 Cross-shore profile zone and bar sequence on profile line 62 at Duck, North Carolina USA (the zones are divided according to Lee *at al.*1995).

1.2.2 Depth of closure

An important concept in coastal engineering is the "depth of closure (DoC)". From a practical point of view, it is denoted as the water depth beyond which the beach elevation changes are negligible. Thus the profile is divided into two areas: a nearshore zone which is considered to be morphologically active and an offshore zone where morphological activity is much less and considered insignificant. The DoC has attracted increasing attention due to a number of coastal engineering concerns such as beach-fill design, planning of beach profile surveys, siting of structures. However, it should be acknowledged that DoC is a relative rather than an absolute concept and depends on different definitions. For instance, the time interval and the critical value of the 'negligible' beach elevation changes to identify the DoC often vary in different definitions.

The previous studies are based on the mathematical formulae of Hallermeier (1978, 1981), who related DoC to the properties of incident waves, in the absence of beach profile measurements or physiographic indicators. In Hallermeier's formulae the DoC is a fixed depth based on extreme wave heights with an adjustment for wave steepness. Moreover, the parameters in the mathematical formulas are based on a range of sediment sizes. However, the sediment transport is due to a

number of factors and their interaction, such as waves, currents, water level, which suggests that the DoC should be not be decided only by wave parameters. It is essential to examine the DoC by considering all these factors together. Further, the temporal and spatial scale and site dependency should also be considered since the scales will affect the results of the DoC at a particular field site.

1.3 Previous Study of Beach Profiles and Current Problems

The investigation of beach profile changes is hampered by a lack of data and by the prohibitive computational complexity of applying deterministic dynamic equations for fluid flow and sediment transport over even the relatively short periods of a single storm. Therefore, much effort has been focused on simplified models. Roelvink and Broker (1993) classified the different modelling techniques into four categories: descriptive models; empirical models; equilibrium models and process-based models. Progress in this area of investigation has changed from simple phenomenological description to sophisticated numerical models. Most present models are either equilibrium or process-based.

1.3.1 Equilibrium of beach profiles

The principle behind the equilibrium beach description is that a beach responds to the environmental conditions (waves and water levels) imposed upon it and if such environmental conditions are constant the beach shape should remain relatively constant. The resulting profile is defined as the equilibrium profile. Although equilibrium of beach profiles might never be achieved in nature, the topic has been investigated extensively because of the practical significance in coastal engineering. The conditions for equilibrium on beaches and associated slopes and profile shapes have been a topic of research since the 1950s. The investigation of the equilibrium of beach profiles by previous researchers generally concentrated on justification of an exponential relationship, which was proposed by Bruun (1954) based on field data from the Danish West coast and from California. The empirical correlations from Brunn (1954) and Dean (1977) between a scale parameter and the sediment size were proposed as:

$$h = Ax_s^{2/3}, \tag{1.1}$$

in which h is the water depth at a distance x_s from the shoreline and A is a dimensional shape parameter that depends only on the sediment size.

Vellinga (1983) investigated dune zone erosion using a wave tank test and developed the erosion profile that included the effect of significant wave height in deep water and sediment fall velocity. Dean (1991) modified the equilibrium beach profiles to quantify the shoreline response due to the elevated water levels and wave heights on natural and seawalled shorelines. By modifying the classical concave equilibrium profile (Bruun, 1954; Dean, 1977), a few more realistic descriptions of the equilibrium beach profile were proposed by Larson. (1991, 1996) and by Larson *et al.* (1999a).

Further work has been carried out to develop the theory of an equilibrium profile. More parameters were included in the exponential beach profile shape function by Bodge (1992) and Komar and McDougal (1994). They considered the local incident wave and bottom sediment characteristics and provided greater flexibility to the dimensional shape parameter allowing for the indeterminate nature of the water line. González *et al.* (1999) presented a beach profile equilibrium model for perched beaches with the assumption that wave reflection is the most important process to modify Dean's equilibrium model. With the recognition of the difficulty of parameter selection, Romaniczyk *et al.* (2005) studied the shape function of equilibrium beach profiles in conjunction with a Taylor expansion for the nearshore and above water portion of profiles.

The equilibrium of profiles was presented to quantify the shoreline response due to elevated water levels and wave heights on natural and sea wall shorelines. However a number of simplifications were made by in order to obtain simple analytical expressions. First, it was assumed the rate of cross-shore wave energy dissipation was constant in a given water depth. Second, the waves were described as linear shallow water waves and the wave heights in the surf zone were taken to be proportional to the water depth. These simplifications in equilibrium-based models are inappropriate because variations of morphology about mean states are mainly the result of internal dynamics between the morphology and the external forcing such as waves, currents and tides, and not simply a linear response to the forcing.

1.3.2 Process-based models of beach profile changes

The traditional approach to studying beach profile changes relies on the cause-effect chain of energy transfer. The waves and currents induce sediment transport, which usually changes the beach morphology. On this basis of the laws of conservation of mass, momentum and energy plus sediment transport formulae, various process-based models can be built up. The process-based models have a common structure, consisting of submodels, representing: (1) the hydrodynamics such as wave propagation, tide-, wind- and wave-driven currents, (2) the associated sediment transport patterns and (3) bed level changes, implemented in a loop system to ensure feedback and dynamic interaction of the elements of the morphodynamic system.

There are many examples of predictive process-based models of beach profiles, such as HR Wallingford COSMOS (Southgate and Nairn, 1993; Nairn and Southgate, 1993), UNIBEST-TC of Delft Hydraulics (Reniers *et al.*, 1995; Bosboom *et al.*, 1997), CROSMOR2000 of University of Utrech (Van Rijn and Wijnberg, 1994, 1996; Van Rijn, 1997, 1998, 2000), BEACH1/3D of University of Liverpool (O'Connor *et al.*, 1998; O'Connor and Nicholson, 1999) and CIIRC of University of Catalunya (Rivero and Sánchez-Arcilla, 1994; Sierra and Sánchez-Arcilla, 1999).

Those process-based models generally operate on short-term scales that describe periods of up to a week or so, corresponding to the effect of storm events. Even in the short-term the quality and application of process-based models is limited by a few shortcomings such as the uncertainty and the calibration of parameters. However, predictions of beach profile changes are required over large periods of time into the future to design beaches and sea defences (typically 50 years). The process-based models are not sufficient to model the beach profile behaviour accurately and do not provide reliable and robust predictions over the time scales of 50 years, indicating that the process-based models might not be the best choice in this case.

1.3.3 Statistical methods

Basic statistics can be very useful for analysing beach profile changes for deriving simple empirical relationship to be used for predictive purpose (Larson *et al.*, 2003). Basic statistical measures such as the mean, standard deviation, range and correlation, have been employed to

characterize beach profile changes traditionally. A growing body of observations, suitable for analysing the long-term behaviour of beaches, is now becoming available. In parallel with this, new statistical techniques for identifying trends, quasi-periodic behaviour and other measures of predictability continue to be developed. For instance, one of these methods, the empirical orthogonal function (EOF) was first applied by Winant *et al.* (1975), and is now an established statistical method for analysing coastal morphology.

The non-stationarity of beach profile changes has been acknowledged recently. Lippmann *et al.* (1993) suggested that the bar system at Duck, North Carolina, USA shows non-stationary behaviour. However in many statistical methods, such as EOF, stationarity is assumed. Stationarity means that the moments of a distribution of random variables are the same everywhere. If all the moments are constant, then we have full stationarity; if only the first and second moments, i. e. the mean, variance and covariance function, are, then we have second-order or weak stationarity; if only the spatial differences are stationary, then we call the process intrinsic (Webster, 2000). What we talk about often in coastal engineering is second-order stationarity, which will be simply referred to as stationarity for convenience in this thesis.

Fourier theory assumes that a signal is stationary and periodic in nature. The EOF method assumes a certain separability of the spatial and temporal variation such that the spatial observations provide replicate information at any time and vice versa. This is a serious assumption that we wish to avoid. The complex variability of beach profiles in space and time means that Fourier-type and EOF analyses are not always the most appropriate. Therefore, more advanced statistical techniques are needed.

The recently developed wavelet transform might be appropriate since it has been formulated to deal with data that show various kinds of non-stationarity. Wavelet transforms have been used widely in disciplines where there is a need to examine the non-stationarity processes with long data series or data compression, such as in signal analysis (Mallat, 1989), in geophysics (Kumar and Foufoula-Georgiou, 1994), in earthquake analysis (Iyama and Kuwamura, 1999), in the study of sea ice properties (Lindsay *et al.*, 1996) and in vibration analysis (Smallwood, 1999). Hence wavelet techniques are expected to provide new insight into the variability of beach profiles.

1.4 Objectives and Organization of This Work

1.4.1 Scope of this thesis

The identification of the patterns of beach profile changes at different spatial and temporal scales is of significance. Therefore, the aim of this work is to investigate the long-term beach statistics at two sites using wavelet techniques for analysing the spatial and temporal variability of beach profiles. The main objectives of this thesis are as follows:

- Review existing methods that are based on field data sets in respect of the intended use of the results.
- Introduce wavelet techniques and methods to measure changes in the variability of beach profiles.
- Gather together data sets of long-term field beach profile surveys.
- Analyse the long-term data sets at Duck, North Carolina USA using wavelet techniques to investigate both time and space statistics and examine the non-stationarity.
- Validate the techniques on another field data set.
- Investigate the DoC based on wavelet techniques.

The techniques are expected to be computationally efficient so that useful input for design and coastal management can be provided. The methods introduced in this thesis are applied to the specific problems of describing the variability of beach profiles. However, the techniques have some general relevance to the measurement and statistical understanding of complex processes, and it is anticipated that the methods might be used for problems in related fields important for the successful management of the environment.

1.4.2 Structures of this thesis

The organisation of this thesis is as follows. The existing statistical methods that are based on field data are reviewed in the **Chapter 2**. The wavelet transforms and techniques to identify changes in wavelet variance are presented in **Chapter 3**. The prime data set at Duck is described in **Chapter 4**, together with the methods used for interpolation. Also, in this chapter the earlier work

of other researchers is reviewed. Subsequently, EOF analysis is performed for the sake of later comparison with the wavelet analysis. This is the core work, which will be presented in **Chapter 5** and **Chapter 6**. Scale-dependent analyses are performed to determine characteristic temporal and spatial scales of beach profile changes as well as the local variability in time and space. In addition, an effort is made to relate the changes in wavelet variance to the most active zone and the DoC of beach profiles. In **Chapter 7**, the techniques in **Chapter 3** are used to investigate the spatial variability of the beach profiles at Lubiatowo, Poland so that the wavelet techniques are validated against different data sets. In **Chapter 8**, the key conclusions from the above studies are given and discussed. Finally, possible future work based on this thesis is proposed.

Chapter 2. DATA-DRIVEN MODELS

2.1 Comparison between Data-driven and Process-based Models

It has been acknowledged that coastal morphology is a non-linear dissipative system maintained away from equilibrium, which responds to the complicated interactions, feedbacks and couplings in the nearshore zone (De Vriend, 1991; Larson and Kraus, 1995). This non-linear dissipative system can alternate between periodic and chaotic behaviour. The chaotic behaviour means that a deterministic non-linear dynamic system can produce random looking results. A chaotic system must have a fractal dimension, and exhibit sensitive dependence on initial conditions. The term 'fractal' refers to self-similar geometric objects or time series, which means their statistical properties are related to the time scale used for observation. These properties suggest that it will be difficult to predict the coastal morphology using the process-based models.

Generally, the prior assumptions on coefficients of process-based models that are often nested can generate bias. The beach (foreshore) and dune zones are dominated by the tide and storm surge levels, low-frequency and wave run-up phenomena and 3D morphology. These factors make the choice of parameters in the process-based models more difficult.

With the recent growth of available beach profile data from novel measurement technologies such as remote sensing (e.g. satellite imageries, aerial photos and surf zone video monitoring), the variability of beach profiles can be investigated with greater confidence. By analysing the data and establishing generic system properties, the variability of beach profiles on yearly and decadal timescales can be understood, modelled and predicted. This new kind of study is known as the data-driven model (statistical method). In data-driven models the dominant features that result from the interactions of couplings of different forcing conditions can be studied. The strength of this approach has been addressed by Różyński (2003b), Larson *et al.* (2003) and Southgate *et al.* (2003).

Data-driven modelling is more objective than process-based models considering the coastal morphology and forcing conditions at different field sites. This is especially important in comparative studies of different sites, as the patterns that characterize the data sets under study

provide unbiased clues on key phenomena at each site. For instance, although seasonal variation is a general characteristic of nearshore morphological behaviour, the degree of seasonality varies widely at different field sites (Van Rijn *et al.*, 2003).

However, data-driven models also have problems. Similarly to the interpretation of the process-based models, data-driven models also need a critical examination. Therefore, the aim of this chapter is to review the existing data-driven models so that both their advantages and disadvantages can be recognized.

2.2 Statistical Methods for Studying Beach Profile Changes

2.2.1 Introduction

The aim of this section is to critically review the statistical methods that are currently employed to study the variability of beach profiles. Basic statistical measures such as the mean, standard deviation, range and correlation, have been employed to characterize beach profile change traditionally. The standard deviation is a basic statistic that describes how tightly all the observations are clustered around the mean in a set of data. Lippmann *et al.* (1993) computed the monthly averaged standard deviation time series to study the bar variability at Duck, N. C. To quantify the variability in elevation along the profile, the standard deviations over time of cross-shore profiles were computed at fixed locations by several authors, including Kraus and Harikai (1983), Birkemeier (1985), and Howd and Birkemeier (1987).

Different kinds of Fourier transforms have also been used to study the variability of coastal morphology so that the cyclic behaviour can be characterized using sinusoidal functions. One such study was the application of Random Sine Function (RSF) by Pruszak and Różyński (1998). They argued that RSF is especially useful for describing the local geometrical properties of bar movement.

Różyński (2003b), Larson *et al.* (2003) and Southgate *et al.* (2003) reviewed the recent work on the statistical methods used for characterizing coastal morphology. Beach profile changes were previously studied using statistical methods such as empirical orthogonal functions (EOF), principal oscillation patterns (POP), singular spectrum analysis (SSA) and canonical correlation

analysis (CCA). All these methods are connected with the EOF method somewhat, therefore it is necessary to have a close look at the EOF method.

2.2.2 Empirical Orthogonal Function (EOF)

EOF analysis is also known as principal component analysis (PCA), which is a method that has been extensively used to identify spatial patterns in coastal morphology data. It was first proposed by Winant *et al.* (1975) for analysing the variability of beach profiles.

Beach profile data were used to generate sets of empirical eigenvectors. In order to generate empirical eigenvector a symmetric correlation matrix $\mathbf{A}^{\mathbf{EOF}}$ is formed with elements

$$a_{i,j} = \frac{1}{n_x n_t} \sum_{t=1}^{n_t} h_{i,t} h_{j,t} . \tag{2.1}$$

in which $h_{x,t}$ are the collection of beach profile measurements. The subscript x is an index ranging between 1 and n_x, the total number of points along the profile, and the subscript t refers to the time index at which varies between 1 and n_t, the total number of times at which profiles were recorded.

The diagonal elements of this matrix are

$$a_{x,x} = \frac{1}{n_x n_t} \sum_{t} h_{x,t}^2 . \tag{2.2}$$

and represent the mean square value of the date in time divided by n_x. The sum of the diagonal elements defined as the trace of $\mathbf{A}^{\mathbf{EOF}}$ is

$$TrA = \sum_{x=1}^{n_x} a_{x,x} = \frac{1}{n_x n_t} \sum_{x=1}^{n_x} \sum_{t=1}^{n_t} h_{x,t}^2 . \tag{2.3}$$

Thus TrA is equal to the mean square value of all the data. The square matrix $\mathbf{A}^{\mathbf{EOF}}$ possesses a set of eigenvalues λ_n and a set of corresponding eigenvectors $e_{n,x}$, which are defined by the matrix equation

$$A^{EOF} e_n = \lambda_n e_n . \tag{2.4}$$

A direct result of this definition is that the sum of all the eigenvalues is equal to the mean square value of all the data. Consequently, each eigenvalue represents a portion of that mean square value.

$$h_{x,t} = \sum_n c_{n,t} e_{n,x} . \tag{2.5}$$

If we require that:

$$\sum_n e_{n,x} e_{m,x} = \delta_{m,n} . \tag{2.6}$$

where $\delta_{m,n}$ is the Kronecker delta function, a set of eigenvectors normalized to unity is formed, and $e_{n,x}$ are orthonormal. The power of EOF lies in the fact that the choice of the eigenvector guarantees they best fit the data in the least squares sense.

Resulting from the orthonormal property, the coefficients $c_{n,t}$ are obtained from:

$$c_{n,t} = \sum_{x=1}^{n_t} h_{x,t} e_{n,x} . \tag{2.7}$$

It can be shown that:

$$c_{n,t} = \sum c_{n,t} c_{m,t} = \delta_{n,m} \lambda_n n_n . \tag{2.8}$$

so if we define $c^*_{n,t} = c_{n,t} / (\lambda_n n_x n_t)^{1/2}$, the function $c^*_{n,t}$ form another orthonormal set:

$$\sum_{t=1}^{n_t} c^*_{n,t} c^*_{m,t} = \delta_{n,m} . \tag{2.9}$$

Equation (2.9) consists of eigenvectors of the other symmetric correlation matrix $\mathbf{B}^{EOF}$ with elements

$$b_{i,j} = \frac{1}{n_x n_t} \sum_{x=1}^{n_x} h_{x,i} h_{x,j} . \tag{2.10}$$

Although the sizes of both matrices differ in general, they have the same non-zero eigenvalues.

Winant *et al.* (1975) came to a few significant conclusions from studying Torrey Pines Beach using the method described above. The eigenvector with the largest value is the mean beach function. They concluded from the North Range that the first largest eigenvector apart from the mean accounted for 39.4% of the all variance that was referred as the bar-berm function. And the second largest eigenvector apart from the mean accounted for 46.7% of the all variance that was referred as terrace function. They gave the similar analysis to the South Range and Indian Canyon Range.

Another earlier employment of EOF in coastal engineering is by Aubery (1979) who related the mean profile shape, bar and berm features, and the low-tide terrace to the first, second and third EOF eigenvector, respectively. After these pioneering works, EOF method has become a fairly common method to investigate beach profile changes in time.

EOF was performed by Hashimoto and Uda (1982) to study the response of beach profiles to incident waves. The analysis was based on data at Ajigaura Beach and concluded that the second eigenvector was associated with the beach changes due to onshore-offshore sand transport caused by changes of wave heights.

Later on, Birkemeier (1985) examined the time scales of nearshore profile changes at Duck with EOF using over three years of surveys. It was found that the first two eigenvectors, which accounted for 64.8% of the variance because of two different double bar configurations, resulted from storm sequences.

A Dutch data set, which included large-scale morphological changes, was investigated by Wijnberg and Terwindt (1995) using EOF. It was impossible to schematise the various bar systems with one common set of morphological empirical eigenvector. This implied that in EOF analysis simultaneously taking into account the alongshore and temporal variation in the whole profile would fail to schematise the various bar systems (Ostrowski *et al*, 1991). Therefore, a moving window approach was employed by the authors to quantify particular large-scale morphological features.

Larson *et al.* (1999b) analysed the topographic data from three different beach nourishment projects using EOF to determine the response of the fills at different temporal and spatial scales at three fields. Most recently, EOF was used by Różyński (2003b) to investigate the long-term bathymetric surveys at a coastal segment of the southern Baltic coast to determine the characteristic evolution patterns of multiple longshore bars. The author employed EOF to give grounds for the application of canonical correlation analysis that will be introduced in the next section. Medina *et al.* (1991) separated the temporal and spatial variability of the onshore and offshore sediment transport through laboratory and field data of beach profile changes according to the main components of EOF.

A particular employment of EOF by Reeve *et al.* (2001) was to investigate the 2-D behaviour of beaches by treating the 2-D data set as 1-D array. By this study, the long-term morphological behaviour at Great Yarmouth, UK was successfully investigated.

On the basis of the model proposed by Winant *et al.* (1975), Hsu *et al.* (1994) developed a 2-D EOF model. They used beach profile data that were measured every two months along six segmented detached breakwaters to generate spatial and temporal orthogonal eigenvectors. The spatial and temporal eigenvectors were examined from data sets in different time intervals by Hsu *et al.* who concluded that the 2-D EOF provides a better prediction of the global changes near coastal structures than the 1-D EOF.

There are some other examples of the application of the 2-D-EOF. The multi-scale shore variability at Lubiatowo and Cecina Mare Beach was studied by Aminti *et al.* (1995) employing EOF. They argued that for both sites better description of shore profiles was ensured by the 1-D EOF while the 2-D EOF could be recommended for studies aimed at the investigation of general trends of shore variability.

EOF has some very strong advantages. First of all, spatial structure of the analysed system can be separated. Each eigenvector can be examined separately and an attempt can be made to assign to it a physical process that it should account for. Secondly, EOF permits identification of the dominant patterns of beach profile changes. Most variability is usually contained in a few modes only while the remaining ones represent either insignificant phenomena or noise. The larger eigenvalues explain the majority of the variability.

EOF does have serious limitations. One problem of EOF is essentially an attempt to handle the non-stationarity of beach profile changes with the assumption of stationarity. The assumption that the temporal series gives effectively replication of spatial series is the most serious problem of EOF.

2.2.3 Canonical Correlation Analysis (CCA)

Canonical correlation analysis was developed by Hotelling (1936) for application in the social sciences. It was Glahn (1968) who initialized the application of this technique to geophysical data. CCA was used to study if there are any patterns occurring simultaneously in two different data sets

and the correlation between the two different patterns. This method is not suitable for the work in this thesis; therefore the CCA is given a quite short description for the background of the current data-driven models.

The main idea of CCA is to form a new set of variables from the original two data sets so that the new variables are linear combinations of the old ones and maximally correlated. Usually, EOF proceeds CCA to reduce the noise in the data. With the pioneering work by Barnett and Preisendorfer (1987), CCA began to be used widely in geophysics, especially in meteorology and oceanography. Sometimes singular value decomposition (SVD) was used as an alternative to CCA.

There are two investigations that apply CCA in studying coastal morphology. An 11-year long measurement time series of waves and profiles from Duck, North Carolina, was analysed by Larson *et al.* (2000) using CCA. Based on the correlation between the dominant patterns in the wave heights and profile changes established through CCA, a regression matrix was derived that related the profile response to wave heights. They suggested that linear statistical analysis based on data processing, such as CCA, are useful for analysing profile response to waves.

Różyński (2003a) evaluated the importance of interactions among multiple longshore bars at a segment of the southern Baltic coast employing CCA. By maximizing the correlation among the bars, the author predict the inner bar behaviour with the outer bar. The most important conclusion of the study is that outer bars control the long-term variability of the inner bar by more than 60%, suggesting the significant interaction between the outer and inner bars at that site.

Though the above investigation initiated application of the CCA in coastal morphodynamics, the critical examination of the stationarity and the transferability of the regression matrix are needed to forecast profile evolution using CCA.

2.2.4 Principal Oscillation Patterns (POP)

POP is a linearized form of the more general Principal Interaction Patterns (PIP) that was developed by Hasselmann (1988). Storch *et al.* (1988) presented a successful application of POP method in meteorology and concluded that POP can identify "coherent, migrating, standing or otherwise changing patterns of the system without prior knowledge of the system dynamics". In POP analysis the patterns are derived based on approximate forms of certain dynamic equations.

The POPs are defined as the normal modes of linear dynamical representation of the data in terms of first-order autoregressive vector process with residual noise.

So far, there are two applications of this method in coastal morphology. The shoreline evolution in the vicinity of Vliehors was analysed by Jansen (1997) using POP. Subsequently, this method was employed by Różyński and Jansen (2002) to investigate the multi-bar system at Lubiatowo.

The POP patterns should account for more signal variance than the EOF patterns, because they include lag-1 covariance. However, it is usually accompanied by EOF analysis because of difficulties in the interpretation of POP patterns. POP postulates the system's (linear) dynamics in advance through the POP system matrix. This assumption does not make POP patterns reflect actual developments in coastal morphodynamics. Another drawback is that the POP patterns are not orthogonal. Considering the drawbacks of POP, it is not employed in this thesis.

2.2.5 Singular Spectrum Analysis (SSA)

SSA was developed, described and tested upon artificially generated time series by Vautard *et al.* (1992). SSA can be seen as a particular application of the EOF analysis, where the column vectors of the data matrix contains the time series delayed in time up to the maximum shift, known as the embedding. The selecting of the embedding dimension d is crucial in the analysis. Vaultard *et al.* (1992) argued that in practice d should not exceed $N/3$, where N is the number of values recorded in time.

SSA is useful for noise-reduction, de-trending, and identification of oscillatory components and deterministic chaos. Compared with the traditional EOF analysis, SSA provides information on the dynamics of the underlying system. The method is based on the Karhunen-Loéve expansion that requires stationarity of the analyzed time series. In the expansion the covariance matrix ($\mathbf{T}_\tau$) of the analysed time series with lags of $N/3$ is utilized. SSA allows for detailed decomposition of the original time series. First, it is possible to separate the 'true' signal from noise by extracting reconstructed components (RC-s) associated with the largest eigenvalues of the matrix $\mathbf{T}_\tau$. Second, a pair of almost equal eigenvalues associated with two significant RC-s reflects an oscillation present in signals, which will not be discussed in this thesis.

The use of this method in coastal morphology is a very recent thing. Różyński *et al.* (2001) use the SSA method to analyse the temporal and spatial variation in shoreline position at Lubiatowo. Also, Southgate *et al.* (2003) used SSA to extract long-term trends from measurements of the variation at several beaches around the world in order to detect oscillatory behaviour in the filtered signals. Stive *et al.* (2002) investigated the causes and factors for the variability and the resulting possible evolutions of wave-dominated shores and shorelines, in which SSA was employed to extract the long-term trends.

As mentioned above, SSA is a particular application of EOF, therefore the stationary assumption still holds. It is determined that SSA is still not the appropriate choice for the non-stationary process. Another disadvantage is the selecting of the embedding dimension that might bring bias to the SSA analysis.

2.3 Discussion

Existing statistical methods for investigating the variability of beach profile have been reviewed in the above sections. Among these methods, EOF was the earliest to be used in coastal morphology, and allows the dominant modes of variability of beaches to be selected. Moreover, it should be noted that all of the POP, CCA and SSA are based on or related to EOF, but CCA, POP and SSA are not as well widely used as EOF. Therefore these methods will need further calibration on more data sets.

Although these statistical methods discussed in this chapter are useful in specific aspects for understanding and predicting the variability of beach profiles, they are essentially an attempt to handle non-stationarity by assuming that multiple observations at time locations give independent information on the spatial variation. This is actually an important motivation on the later wavelet analysis, since wavelet analysis is well suited for investigating non-stationary process.

A natural step prior to data-driven model development is analysis of the data to establish basic properties and degree of association between these properties (Larson *et al.*, 2003). Considering the complexity of beach profile changes in both space and time over a range of scales, it is obvious that the existing data-driven models have not given a comprehensive understanding of the properties of

data. From this point of view, wavelet analysis is highly appropriate because it allows a multiresolution analysis by dividing the variation into a range of scales.

Another common application related to the variability of beach elevation is to determine the DoC (Hallermeier, 1981). It is apparent that the existing statistical methods have not dealt with this aspect. Hence, an introduction is given for wavelet analysis and a related method to identify the DoC is also presented in next chapter. It is expected that wavelet analysis will provide an in-depth understanding of the variability of beach profiles.

Chapter 3. METHODOLOGY DEVELOPMENT

3.1 Wavelet Technique

3.1.1 Wavelet

In Fourier analysis, which breaks down a signal into constituent sinusoids of different frequencies, the signal is transformed using sine functions. For many signals, Fourier analysis is extremely useful because the frequency content of the signal is of great importance. Fourier analysis has a serious drawback. In transforming to the frequency domain, time/space information is lost. When looking at a Fourier transform of a signal, it is impossible to tell when a particular event takes place, since a particular Fourier coefficient describes the amplitude and phase of a sinusoid exponent of the signal that is assumed to be constant everywhere. Hence the Fourier transform is not enough to study non-stationary signals.

Wavelet technique that is suitable for analysing the non-stationary process was developed in the 1980s by Morlet, Grossmann, Meyer, Mallet, and others. It was the work of Daubechies (1988) that caught the attention of the wider applied mathematics communities in signal processing, statistics, and numerical analysis. The most attractive property of wavelet analysis is time (or space)–scale localization so that the signal variance at a particular scale is related to a particular time (location). Another important property is that wavelets enable a multiresolution analysis to be performed, which partitions the variance of a signal according to a range of scales. Unlike Fourier analysis, which uses harmonic sine and cosine functions, in wavelet analysis the basis is an analysing kernel called a mother wavelet, which is localised in time or space.

Wavelet analysis represents a windowing technique with variable-sized regions. Figure 3.1 shows how the wavelet transform partitions a time (space) frequency plane so that high frequency components are analysed in a short window, and low frequency components in a large window. A wavelet represents variation over some interval of temporal (spatial) frequency defined by its gain function.

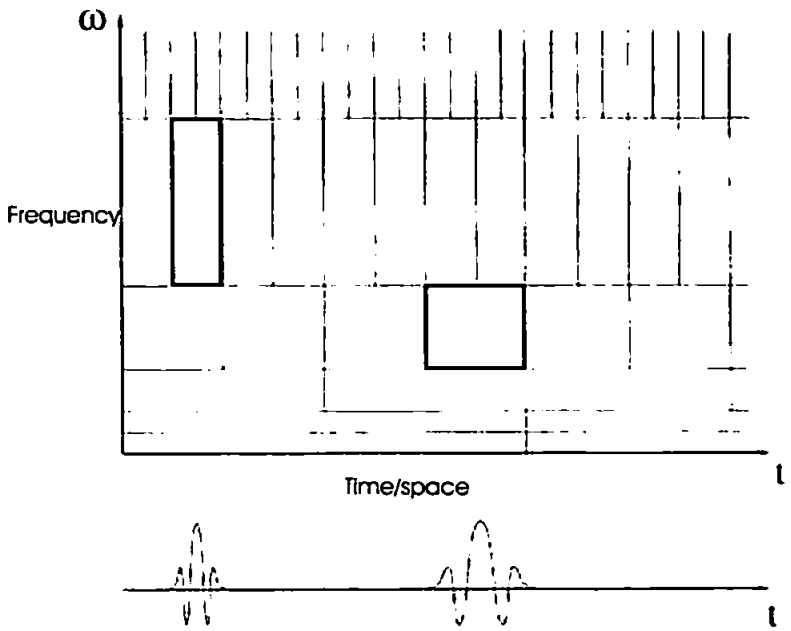

Figure 3.1 Wavelet basis.

3.1.2 Applications of wavelet transforms

Though wavelet transforms have not been employed to investigate variability of beach profiles, the wavelet transform has been used widely in disciplines where there is a need to examine intermittent or variable phenomena in long data series. Some limited applications can be found in relevant areas where the data set is large. For one thing, wavelet transforms have been used in oceanography to study wave and turbulence characteristics. Liu (1994) initialized the employment of the wavelet spectrum to study ocean wind waves, followed by Massel (2001) and Panizzo *et al.* (2002). The application of wavelet transforms on turbulence data can be found from the work by Everson and Sirovich (1989), Meneveau (1991), Farge (1992a, 1992b) and Hudgrins (1992). Subtidal coastal sea level fluctuations were studied by Percival and Mofjeld (1997) using the maximal overlap discrete wavelet transform. Różyński and Reeve (2005) characterized the time series of water surface elevation and current collected at Lubiatowo using wavelet transforms. The only work on studying beaches was by Short and Trembanis (2004) who used the continuous wavelet transform to investigate the patterns of beach width (longshore variability).

Wavelet transforms have not been previously applied to the analysis of beach profiles, perhaps because the data sets are quite small. Therefore, in what follows the wavelet transforms are

introduced and methods for identifying changes in variance are developed. This is necessary considering the highly non-linear dynamic system of coastal morphology. Another aim of the introduction is to pave the way for other potential uses of the wavelet technique in coastal engineering.

3.2 The Wavelet Transforms

3.2.1 General properties of wavelet transforms

The mother wavelet, denoted by $\psi(x)$, belongs to families of wavelets. There are several families of wavelets. The most common of these include the Haar, Morlet, Mexican hat and Daubechies wavelet families. They have some basic properties in common. The differences depend to some extent on the phenomena they are intended to describe although the subject is complicated by the variety of conventions and notation.

The key properties of a wavelet are that:

1. Its mean is zero

$$\int_{-\infty}^{\infty} \psi(x)\,dx = 0. \tag{3.1}$$

2. Its squared norm is 1

$$\int |\psi(x)|^2 dx = 1. \tag{3.2}$$

3. It has compact support, by which is meant that a wavelet damps rapidly to zero and so operates very locally.

The wavelet is an analysing kernel that oscillates locally like a wave and damps rapidly to zero on either side of its centre. Because of the compact support the coefficient describes the local variation at some scale. Wavelet analysis uses a collection of analysing kernels all derived from the mother wavelet. They are denoted by $\psi_{\lambda,k}(x)$. Each kernel is determined by two parameters λ and k, the scale and location parameter respectively. The general formula is:

$$\psi_{\lambda,k}(x) = \frac{1}{\sqrt{\lambda}}\psi\left(\frac{x-k}{\lambda}\right), \quad \lambda > 0, \quad k \in \Re, \tag{3.3}$$

where $\Re$ is the set of real numbers that defines the set of local kernels. Changing λ dilates or contracts the wavelet and changing k translates it. To divide the time series into contributions from different frequency bands, we need to perform filtering at several different scales. If we increase λ, then the interval over which the wavelet takes non-zero values is expanded so that the low frequency components of a signal over a wider time (space) interval can be investigated. Conventionally k, representing a translation, is centred at $k = 0$ for the mother wavelet $\psi(x)$ so that the local variation of a signal can be investigated in different portions by increasing k.

3.2.2 The discrete wavelet transform

Broadly speaking, there are two main wavelet transforms. One is known as the continuous wavelet transform (CWT), which is designed to work with time series defined over the entire real axis. Another is discrete wavelet transform (DWT), which deals with series defined essentially over a range of integers. The beach profile data are finite and discrete and exact reconstructions are required, therefore the DWT is introduced and employed in this thesis.

The discrete equivalent of Equation (3.3) is given by

$$\psi_{j,k}(x) = \frac{\psi}{\sqrt{\lambda_0^j}}\left(\frac{x - kx_0\lambda_0^j}{\lambda_0^j}\right) = \lambda_0^{-j/2}\psi\left(\lambda_0^{-j}x - kx_0\right) \tag{3.4}$$

where j is the exponential scale and λ_0 is a fixed dilation step greater than 1 and x_0 is the sampling interval in time or space. Therefore the translation can be discretized in steps $x = kx_0\lambda_0^j$. Following the common convention of $\lambda_0 = 2$ and $x_0 = 1$, the Equation (3.4) becomes

$$\psi_{j,k}(x) = 2^{-j/2}\psi(2^{-j}x - k). \tag{3.5}$$

A set of wavelets that provides a complete orthonormal basis for all functions $f(x)$ of finite variance can be constructed. That is, every wavelet is orthogonal to its dilation and translations. Thus the discrete wavelet transform is:

$$D_{j,k} = \left\langle f, \psi_{j,k} \right\rangle. \tag{3.6}$$

The inner products, $D_{j,k}$ in Equation (3.6) are the wavelet coefficients.

Thus, any data with finite variance can be approximated as precisely as we can by the sum of the products of the wavelet coefficients and the wavelets as:

$$f(x) = \sum_{j=-\infty}^{\infty} \sum_{k=-\infty}^{\infty} \langle f, \psi_{j,k} \rangle \psi_{j,k}. \tag{3.7}$$

3.2.3 Multiresolution analysis

We need to deal with the infinite summations of Equation (3.7) to make a discrete transform of data at discrete points. This is the reason that we introduce multiresolution analysis. A multiresolution analysis is to write f as a limit of successive approximations, each of which is a smoothed version of f, with more and more concentrated smoothing functions (Daubechies, 1988). In practice, Equation (3.7) is approximated to include scale components larger than any arbitrary exponential scale m_0 as

$$P_{m_0} f(x) = \sum_{j=m_0+1}^{\infty} \sum_{k=-\infty}^{\infty} \langle f, \psi_{j,k} \rangle \psi_{j,k}. \tag{3.8}$$

This is a smooth approximation to the data, since all components corresponding to this scale or finer have been discarded. The discarded component, $Q_{m_0} f(x)$ for scale parameter 2^{m_0} is called the detail. Thus,

$$Q_{m_0} f(x) = \sum_{k=-\infty}^{\infty} \langle f, \psi_{m_0,k} \rangle \psi_{m_0,k}. \tag{3.9}$$

Therefore, Equation (3.7) can be expressed by Equation (3.8) and (3.9) as

$$f(x) = P_{m_0} f(x) + \sum_{j=-\infty}^{m_0} Q_j f(x). \tag{3.10}$$

Since the scale m_0 is selected arbitrarily, Equation (3.10) can also be written as

$$P_{m_0-1} f(x) + \sum_{j=-\infty}^{m_0-1} Q_j f(x) = P_{m_0} f(x) + \sum_{j=-\infty}^{m_0} Q_j f(x). \tag{3.11}$$

and so

$$P_{m_0-1} f(x) = P_{m_0} f(x) + Q_{m_0} f(x). \tag{3.12}$$

That is, the smooth representation at some scale is equal to the smooth representation at the next coarsest scale plus the corresponding detail component.

Considering the increasingly smooth representations $P_{m_0} f(x)$, $P_{m_0+1} f(x)$, $P_{m_0+2} f(x)$,... Mallat (1989) expressed each of these as a vector belonging to the vector space $L^2(\Re)$ of one-dimensional functions of x with finite variance. The function $f(x)$ also belongs to this vector space. The vector space comprising the representations for scale parameters 2^{m_0} of all vectors in $L^2(\Re)$ is defined as $V_{2^{m_0}}$. Since any element of $V_{2^{m_0}}$ is also an element of $L^2(\Re)$, $V_{2^{m_0}}$ is a subspace of $L^2(\Re)$. In Equation (3.12), all the information in the smooth representations for scale parameters $P_{m_0} f(x)$ is contained in the representation $P_{m_0-1} f(x)$ for all m_0. This indicates that the vector subspaces corresponding to these representations are nested. Each subspace contains all those space corresponding to smoother representations, thus

$$V_{2^{m_0+2}} \subset V_{2^{m_0+1}} \subset V_{2^{m_0}} \subset V_{2^{m_0-1}} \subset \cdots \subset L^2(\Re).$$

The important consequence here is that the scaling functions provide an orthonormal basis for the nested subspaces. The existence of a scaling function φ was shown by Mallat (1989). The scaling function is the 'conjugate mirror' that corresponds to the wavelet function. That is, once we choose the wavelet function, the scaling function is determined. It is analogous to the wavelet function, in that scaling functions are generated from the basic scaling function by scaling and translation as expressed in Equation (3.13)

$$\varphi_{j,k}(x) = 2^{-j/2} \varphi(2^{-j} x - k). \tag{3.13}$$

The scaling functions and the corresponding wavelet functions together generate a multiresolution analysis as:

$$P_j f(x) = \sum_{k=-\infty}^{\infty} \langle f, \varphi_{j+1,k} \rangle \varphi_{j+1,k} + \sum_{k=-\infty}^{\infty} \langle f, \psi_{j+1,k} \rangle \psi_{j+1,k}. \tag{3.14}$$

Therefore Equation (3.10) can be written as:

$$f(x) = \sum_{k=-\infty}^{\infty} \langle f, \varphi_{m_0,k} \rangle \varphi_{m_0,k} + \sum_{j=-\infty}^{m_0} \sum_{k=-\infty}^{\infty} \langle f, \psi_{j,k} \rangle \psi_{j,k}. \tag{3.15}$$

This is multiresolution analysis. Using this equation, the beach profile elevations $f(x)$ can be expressed as the smooth representation at the scale parameter 2^{m_0} together with the detail components identified by the wavelet functions with scale parameters 2^{m_0}, 2^{m_0-1}, ...and 2.

The multiresolution analysis is carried out using the pyramid algorithm, as described by Press *et al.* (1992). In this algorithm, input data must consist of $N = 2^p$ equally spaced observations, where p is a positive integer. It can be regarded the input as a discrete representation of the underlying $f(x)$ where $m = 0$. Filtering the data separately with wavelet filters and scaling filters, we keep the wavelet coefficients and filter the smooth representation. The process is repeated until two detail coefficients and two mother function coefficients remain. The final output of the algorithm consists of 2^p values, the two mother function coefficients and $2^p - 2$ wavelet coefficients for scale 2^1 to 2^{p-1}. The algorithm can be inverted to give an exact reconstruction of the original data from all 2^p coefficients. Alternatively, if all the coefficients are set to zero before inversion, save for all the wavelet coefficients corresponding to scale 2^{m_0}, then the output is simply the detail components, and the inversion corresponds to Equation (3.9).

3.2.4 Wavelet choice

The number of vanishing moments of a wavelet function, M, is a critical parameter of a wavelet. As M increases the wavelets become smoother but also less localized. If a wavelet has M vanishing moments then

$$\int x^c \psi(x)\,\mathrm{d}x = 0,\ c = 0, 1, 2, \ldots M-1. \tag{3.15}$$

The choice of wavelet and its moments was discussed by Kumar (1997). We wish to use an orthogonal wavelet basis with as compact a support as possible and an adaptation to the finite interval. For this reason the Daubechies' (1988, 1992) wavelet family with M =2 is chosen to study the local features of beach profile changes in this thesis. There are four filter coefficients for the Daubechies' wavelet with two vanishing moments. This wavelet has orthogonal property and a compact support. This is preferred as our interest is in analysing the variance of profile in time and

space. If we were mainly concerned to compress or de-noise the data we would choose a wavelet with more vanishing moments for its greater smoothness.

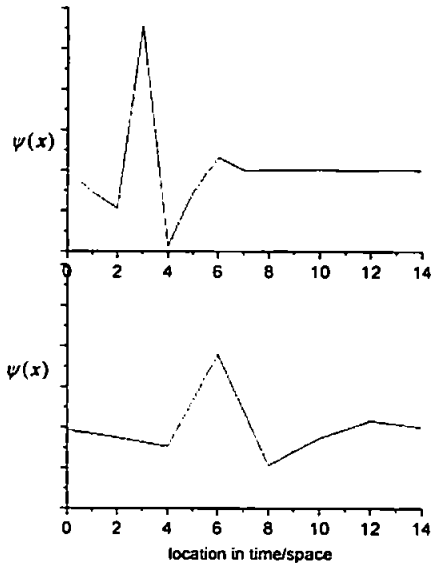

Figure 3.2 Translation and scaling of a Daubechies wavelet with two vanishing moments.

The Daubechies wavelet with two vanishing moments, abbreviated as the db2 wavelet, is illustrated in Figure 3.2, where the wavelet in the lower graph illustrates a dilation and translation of the wavelet in the upper graph. Thus the latter would yield an analysis of details in the time series at a coarser scale and at a different location within the data series.

3.3 The Adapted Maximal Overlap Discrete Wavelet Transform (AMODWT)

3.3.1 The MODWT

Daubechies (1992) argued that the DWT partitions the variance of a signal over all scales if the mother wavelet satisfies certain additional conditions. Therefore, if the sum of squared differences from the mean of a sequence of N data $u = f(x)$ is denoted $SS_0 f(x)$, and the equivalent sum of squares for the smooth representation of the data at scale parameter 2^m is $SS_j f(x)$, then

$$SS_0 f(x) = SS_j f(x) + \sum_{j=1}^{m} \sum_{k=1}^{k_j} D_{j,k}^2 . \tag{3.16}$$

The contribution to the variance of u for scale parameter 2^m is known as the sample wavelet variance (Percival, 1995).

$$\hat{\sigma}_{u,m}^2 = \frac{1}{2^m k_j} \sum_{j=1}^{k_j} D_{m,j}^2 . \tag{3.17}$$

The translation step in the DWT is equivalent to subsampling the output of a convolution of data with a wavelet filter. This, among other conditions, ensures orthogonality of the wavelet basis. By not subsampling the convolution of the wavelet with the data as in the DWT analysis, but rather by retaining all the values, the wavelet variances can be estimated more efficiently (Percival and Guttorp, 1994). This is called the maximal overlap discrete wavelet transform (MODWT). However, because the MODWT coefficients are obtained without the subsampling steps, the new coefficients at any scale are no longer orthogonal to each other so it is possible to generate correlated wavelet coefficients within and between different scales. A major advantage of the MODWT is that it can be readily applied to data where N is not an integer power of 2 in number, which is a very important consideration for our relatively small set of beach profile data.

The variance of the MODWT is defined as:

$$\tilde{\sigma}_m^2 = \frac{1}{2^m \tilde{n}_m} \sum_{k=1}^{\tilde{n}_m} \tilde{d}_{m,k}^2 . \tag{3.18}$$

This is a measure of the variance associated with dilation 2^m of one wavelet, where the tildes over symbols denote that the coefficients comprise the maximal overlap set and not the subsampled set used in the ordinary DWT. Since near the beginning and the end of the data sequence the wavelet filters overlap the ends. Percival and Guttorp (1994) discarded those locations simply so that $\tilde{n}_m < N$ coefficients are generated. Since the MODWT coefficients are not orthogonal, the MO wavelet variance is estimated with an effective number of degrees of freedom that is somewhat less than $\tilde{n}_m$. It can be referred to Percival (1995) for more details. Similarly the contribution to the covariance can be estimated from the MODWT as:

$$\tilde{C}_{u,v,m} = \frac{1}{2^m \tilde{n}_j} \sum_{n=1}^{\tilde{n}_j} \tilde{d}_{m,n}^u \tilde{d}_{m,n}^v , \tag{3.19}$$

where $\widetilde{d}^{u}_{m,n}$ and $\widetilde{d}^{v}_{m,n}$ are the MODWT coefficients for scale 2^m and location n for variable u and v, respectively.

Whitcher *et al.* (2000b) developed the wavelet correlation from the MODWT wavelet variances and covariance. The wavelet correlation between u and v at scale 2^m is estimated by

$$\widetilde{\rho}_m = \frac{\widetilde{C}_{u,v,m}}{\widetilde{\sigma}_{u,m}\widetilde{\sigma}_{v,m}}. \tag{3.20}$$

3.3.2 The AMODWT

Any wavelet filter will overlap the ends of a sequence of data so that the conventional filter cannot be used to generate wavelet coefficients. In signal processing there are many more data than the features of interest, so generally the data are just discarded where this occurs (e.g. Percival, 1995). However the beach profile data are not long enough to allow data at the end to be discarded. Few wavelet coefficients might remain if we just follow Percival (1995). Therefore the adapted wavelet filters of Cohen *et al.* (1993) were used in this thesis to generate adapted maximal overlap discrete wavelet transform (AMODWT) coefficients. The filters are denoted as a set of coefficients $H = \{h_{i,j}\}, i = 1,2,\cdots,2^j + 2(2^j - 1)$. There will be N coefficients for each scale parameter with N input data by:

$$\begin{aligned}
\widetilde{d}_{j,k} &= \sum_{i=1}^{2^{j+1}-1} h^L_{i,j} f(k+i-1), k = 1,2,...,2^j - 1 \\
&= \sum_{i=1}^{2^j+2(2^j-1)} h_{i,j} f(k-2^j+i), k = 2^j, 2^j+1, ...N - 2(2^j-1) \\
&= \sum_{i=1}^{2^{j+1}-1} h^R_{i,j} f(k-2^{j+1}+i+1), \quad k = N-2^{j+1}+3, N-2^{j+1}+4, ..., N.
\end{aligned} \tag{3.21}$$

where $h^R_{i,j}$ and $h^L_{i,j}$ are the filter coefficients of the right and left side respectively. The adaptation will introduce bias, which will not be discussed here in detail. The bias is especially obvious at the first two finer scales, so the first two and the first four coefficients from the adapted wavelet coefficients are discarded. Further details may be found in Lark and Webster (2001).

Though these scale-specific statistics are useful, they lose the local information that wavelet coefficients contain because they are summed over all locations. Therefore, the local contributions

to the wavelet variances are also discussed. The local wavelet variance components and standard deviation at different scales are defined as

$$\tilde{d}_{j,k}^2 / 2^j \ , \tag{3.22}$$

and

$$\sqrt{\tilde{d}_{j,k}^2 / 2^j} \ , \tag{3.23}$$

separately in this thesis.

3.4 Procedures of Identifying Changes in Wavelet Variances

3.4.1 General

It has been generally acknowledged that the variability of beach profiles in both space and time is non-stationary. Therefore wavelet variances are also expected to vary with offshore distance in space or in time series. Identifying the locations of discontinuous changes in spatial and temporal wavelet variances will provide much insight into the variability of beach profiles. For these purposes a method is needed to detect changes in wavelet variances. A suitable method using the MODWT was proposed by Whitcher *et al.* (2000a) who applied to the data on measurements of the water level of the Nile River. Lark and Webster (2001) used the method to detect changes in variance of soil properties on a linear transect. Here the method is introduced briefly based on the AMODWT coefficients.

First of all, the wavelet coefficients of beach profiles were computed using the AMODWT. The normalized cumulative sum of squares of the AMODWT coefficients at scale 2^j is defined as:

$$S_{j,k} = \frac{\sum_{i=1}^{k} \tilde{d}_{j,k}^2}{\sum_{i=1}^{N} \tilde{d}_{j,k}^2}, \qquad k = 1,2,\ldots, N-1. \tag{3.24}$$

Under the null hypothesis, which assumes that beach profiles have uniform wavelet variances, $S_{j,k}$ is expected to increase linearly over $k = 1,2,\ldots, N-1$. If there is a single change in variance at some point in the sequence say $k=k^{'}$, then the graph of $S_{j,k}$ against k is expected to approximate a

bilinear piecewise function with the break point at k^*. Any individual realization of a random process of uniform variance will show some breaks of slope in the $S_{j,k}$ plot. Therefore, the strength of evidence against the null hypothesis can be measured using the B-statistic with

$$B = \max(B^+, B^-), \tag{3.25}$$

where

$$B^+ \equiv \max_{1 \le k \le N-1} \left(\frac{k}{N-1} - S_{j,k} \right), \tag{3.26}$$

and

$$B^- \equiv \max_{1 \le k \le N-1} \left(S_{j,k} - \frac{k-1}{N-1} \right). \tag{3.27}$$

For a given sequence the value of B arises from the largest change in slope of $S_{j,k}$ at some k. The size of B is a measure of the magnitude of the change in variance. Finding the value of k that gives rise to large values of B identifies candidate a change point at which the variance change is significant.

As mentioned above, the variation of beach profiles is not constant along the profile, so the purpose is to test and reject the null hypothesis of uniform variances, and further to identify the positions of changes in wavelet variances using Equations (3.25)-(3.27). To test the null hypothesis, a diagnostic distribution of B under the null hypothesis of uniform variances is needed; however there is no tractable form for the sample distribution of B for the MODWT. Therefore, in this thesis the critical values of B for the null hypothesis of uniform variances are estimated by Monte Carlo methods. In the following the method of obtaining the diagnostic statistic distribution B is introduced. In brief, they are:

1. The experimental variogram of beach profiles was computed and modelled. The experimental variogram and some variogram functions are introduced below. The experimental variogram of beach profiles was computed and modelled using some combinations of variogram functions.

2. A covariance matrix C is generated by employing the coefficients of variogram functions modelled in the above procedure of beach profile data.

3. A series of realizations with uniform variance of a random process was computed using the Cholesky factorization of the covariance matrix (Goovaerts, 1997). The random process is the elevation at given locations of beach profiles in time series or elevation distribution in space series in given surveyed beach profiles.

4. The wavelet coefficients of the series of realizations generated in the above procedure were computed using the AMODWT.

5. The B statistic was computed at each scale. Subsequently the 95th percentile of the modelled scales of B are set as critical values to check the candidate change in wavelet variances of beach profile data at each scale.

3.4.2 Variogram

With reference to the above section, in the development of B statistics the variogram was used. It is seldom used in coastal engineering; hence the aim of this section is to introduce the concept. Variogram is a measure of the variance between data as a function of distance. It is used in the geostatistic methods, widely applied in mining, petroleum, meteorology, geology, soil science and ecology. The variogram function for a random variable $f(x)$ is defined as:

$$\gamma(l) = \frac{1}{2} Var\{f(x+l) - f(x)\}, \tag{3.28}$$

where $f(x)$ is a random function of the location, x, and l is a lag. In this thesis, the lag may correspond to a spatial distance along the profile or an interval of time.

The variogram was computed from experimental data following the estimator of Matheron (1962):

$$\hat{\gamma}(l) = \frac{1}{2 \cdot N(l)} \sum_{k=1}^{N(l)} \{f(x_k + l) - f(x_k)\}^2, \tag{3.29}$$

where $N(l)$ is the number of data pairs of values in which the separation distance is equal to l.

The experimental variogram can be modelled by appropriate continuous functions. All standard variogram functions will define a positive definite covariance structure. They include the linear model, circular model (in 1 or 2-D), spherical model, exponential model, Wackernagel function, Bessel function, sine function and others. In addition, the nugget variance can be used to quantify

the positive intercept of semivariance at $|l|=0$, which represents the random variation that is entirely uncorrelated in space. In following, the variogram models used in this thesis are introduced.

The spherical function is one of the most frequently used models in geostatistics, in one, two and three dimensions. It is defined as

$$\gamma(l)=\begin{cases} c\left\{\dfrac{3l}{2a}-\dfrac{1}{2}\left(\dfrac{l}{a}\right)^3\right\} & for\ l\le a \\ c & for\ l>a \end{cases}, \tag{3.30}$$

where c is the variance and a is a distance parameter, the range of the variogram.

If the variogram is concave upward at short lags, indicating locally smooth variation, then the Wackernagel model is preferred:

$$\gamma(l)=c\left\{1-\exp\left(-\frac{l^{\alpha}}{a^{\alpha}}\right)\right\}, \tag{3.31}$$

where α is an exponential parameter less than 2. In some instances the variogram decreases from its maximum to a local minimum and then increases again. This is called the *hole effect*, which might indicate periodic variation. When the hole effect is present, a sine function should be considered. A damped version of the sine function might also be used:

$$\gamma(l)=(c_1\cos\theta+c_2\sin\theta)/\theta\,. \tag{3.32}$$

Another model that can be satisfactorily used to describe less pronounced hole effect incorporates the Bessel function J_0 as follows:

$$\gamma(l)=c\left\{1-\exp(-l/r)J_0\left(\frac{2\pi l}{\omega_J}\right)\right\}. \tag{3.33}$$

Each of these functions describes simple components of variances. Usually the additive combination of a few models is necessary to model the variogram of real data. In order to match the fluctuations in the experimental variogram of beach profiles closely, several combinations of these models are compared to find the ideal modelling functions for every series of beach profile data. The combinations of these models used in this thesis are from nugget, Wackernagel, and sine function (WS); nugget, Wackernagel and Bessel function (WB); nugget, spherical and Bessel function (SB); and nugget, spherical and sine function (SS).

The combined models of variogram are assembled in nested form as:

$$\gamma(l) = c_0 + c_1\gamma_1(l) + c_2\gamma_2(l) + \cdots + c_n\gamma_n(l), \tag{3.34}$$

where c_0 is the nugget variance and each c_k is a component of the model with a basic variogram function γ_k, such as the spherical, sine, Wackernagel and Bessel function.

Akaike's (1973) information criterion (AIC) is adopted to identify the best models appropriate for the variogram so that a balance is achieved between the number of nested parameters and the closeness of fit. A small value of AIC signifies a more efficient fit between the modelled and experimental variogram. The AIC is defined as:

AIC =-2 ln (maximized likelihood) + 2(number of parameters)

It can be estimated by

$$AIC = \left\{ n_l \ln\left(\frac{2\pi}{n_l}\right) + n_l + 2 \right\} + n_l \ln Q + 2p_n, \tag{3.35}$$

where n_l is the number of points on the variogram, and p_n is the number of parameters in the model. According to Equation (3.34), the parameter number is $n+1$ if each variogram has one parameter. Q is the mean of the squared residuals between the experimental values and the modelled values (Webster and Oliver, 2001).

3.4.3 *B* statistic development and identifying changes in variances

The overall variance of the random function modelled from Equation (3.34) is thus

$$\sigma^2 = \sum_{k=0}^{n} c_k \,. \tag{3.36}$$

The data have a covariance matrix **C**, in which $\mathbf{C}(i, j)$ is the covariance of the i^{th} and j^{th} datum. **C** is the matrix that was used for simulation. The covariance of datum i with datum j depends only on $l_{i,j}$ under the null hypothesis of second-order stationarity. It is given by

$$C(i,j) = \begin{cases} \sigma^2 & if\ i = j \\ \sigma^2 - \gamma(l_{i,j}) & otherwise \end{cases}. \tag{3.37}$$

A FORTRAN program that used both CHFAC and RNMVN subroutines in IMSL (1994) was written to get a series of data with uniform variance based on the covariance in Equation (3.37).

The Cholesky factorization of the covariance matrix of a set of modelled data, which is then assumed to be a realization of the random process with the specified variogram of beach profile data, was computed using the routine CHFAC. Subsequently, the realization of 5000 random sequences with uniform variances was computed using the IMSL routine RNMVN with the Cholesky factorization.

The 5000 sequences of data with uniform variances were decomposed into a range of scales using the AMODWT. Another FORTRAN program was written to compute the B statistics with different length of wavelet coefficients from the AMODWT at each scale. The different lengths were set in increments of 25 units to the full length. The 25 unites was randomly chosen considering the full length as well as the identifying the changes efficiently. Finally, the 95th percentile of the B statistics at each scale from the 5000 sequences was defined as the critical values for rejecting the null hypothesis corresponding to the different length of data.

With the critical value of the B statistics, the candidate changes in spatial wavelet variance for each surveyed beach profile can be identified. First, B for the sequence of wavelet coefficients are computed at a particular scale. Second, B are tested against the critical values for a particular scale at full length of data. If B is larger than the critical value, the location k is considered as a significant change in wavelet variances. Third, the checking procedure is repeated for segments 1 to $k-1$ and k to N until data are divided into segments of uniform variance.

3.4.4 Specification of the procedure using beach profile data

Before giving a detailed introduction of the data used in this thesis, we jump first to the results of variogram and B statistic based on the Duck data. The purpose of this is to make the work easy to follow. Another consideration is that these results will not meddle in the core problems addressed in this thesis. The experimental variograms of all the 267 surveys of beach elevation along the profile line 62 at Duck were computed and modelled. The envelope of experimental variograms of the 267 surveys along the profile is shown in Figure 3.3 against the lags in space of 2m, 4m ... 420m. The corresponding modelled variogram is also depicted in Figure 3.3.

Similarly, the experimental variogram of all the 421 cross-shore profile points of beach elevation in the time series are also computed and modelled. The envelope of the variogram is shown in Figure 3.4 against the lags in time of 1 month, 2 months ...133 months. The corresponding modelled variograms of these are displayed in Figure 3.4 as well. The parameters of the modelled variograms of combined functions in Figures 3.3 and 3.4 are listed in Table 3.1.

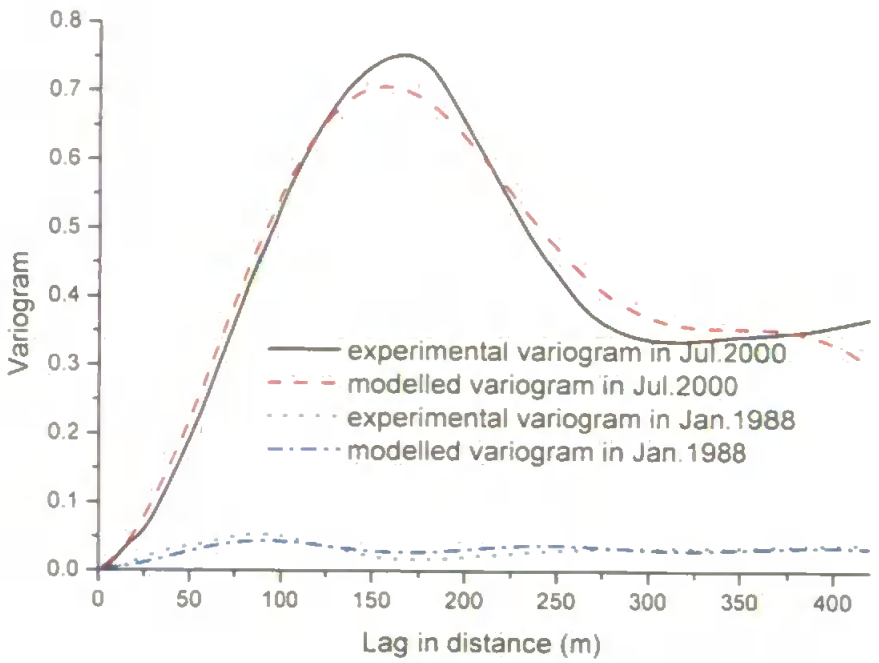

Figure 3.3 Range of variogram in space for profile line 62.

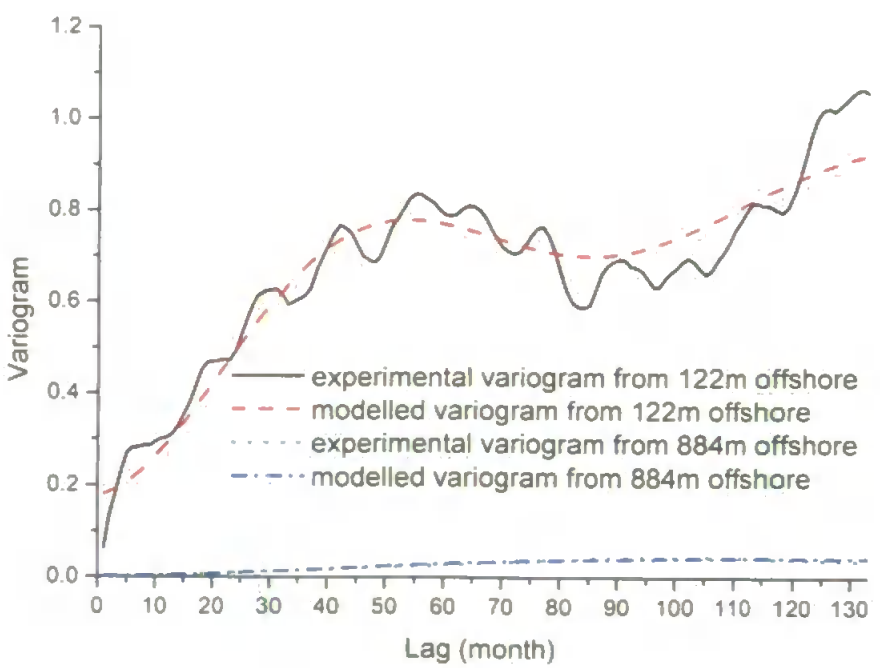

Figure 3.4 Range of variogram in time for profile line 62.

Table 3.1 Modelled variograms of combined functions.

	Simulation variogram functions	*errors*
Jul.2000 (S+B)	$r(l) = 0.018 + 0.00015 \times (1.5 \times \frac{l}{25.9752}) - 0.5 \times (\frac{l}{25.9752})^3 + 0.5654 \times (1 - \exp(-\frac{l}{419.9968}) + J_0(\frac{2\pi l}{269.1920})$	0.000852
Jan.1988 (S+B)	$r(l) = 0.0028 + 0.000003 \times (1.5 \times \frac{l}{264.4533}) - 0.5 \times (\frac{l}{264.4533})^3 + 0.0307 \times (1 - \exp(-\frac{l}{420.0000}) + J_0(\frac{2\pi l}{152.1382})$	0.000026
122m (W+B)	$r(l) = 0.17666 + 0.4544 \times (1.0 - \exp(-\frac{l}{132.9986})^{2.0}) + 0.4228 \times (1 - \exp(-\frac{l}{132.9981}) \times J_0(\frac{2\pi l}{84.2346})$	0.003778
884m (W+B)	$r(l) = 0.0017 + 0.0381 \times (1.0 - \exp(-\frac{l}{62.2445})^{1.9988}) + 0.0041 \times (1 - \exp(-\frac{l}{123.3646}) \times J_0(\frac{2\pi l}{132.6501})$	0.000006

Using the Monte Carlo method described in Section 3.4.3, a series of critical values for each survey can be obtained despite the difference between the variograms in Figure 3.3 and Figure 3.4. Due to the high correlation among the surveys, the critical values from them are quite similar; therefore the average 95% percentile of B statistic from all of the surveys was used to identify candidate points exhibiting significant changes in spatial variances for all the surveys. Table 3.2 lists the average spatial critical values for segments of different lengths under dilations corresponding to $j = 1,2,\cdots,6$ of the Daubechies's wavelet with two vanishing moments. In Table 3.2, S_j denotes the spatial scale. For $j = 1$, the spatial scale is $2^1 \times 2$ m=4m, and so on. It can be seen that generally the critical values decrease with the increasing of the length of segment. Moreover, the critical values increase when the scale parameters increase.

Table 3.2 The 95th percentile of the spatial B statistics scale by scale

Length of segments	S_1	S_2	S_3	S_4	S_5	S_6
25	0.397	0.4725	0.5225	0.5815	0.562	0.507
50	0.291	0.353	0.421	0.5065	0.5365	0.507
75	0.24	0.341	0.3665	0.459	0.5015	0.507
100	0.2095	0.257	0.3305	0.419	0.483	0.5045
125	0.1855	0.2325	0.2975	0.392	0.466	0.4795
150	0.1705	0.2135	0.283	0.375	0.4545	0.4615
175	0.1575	0.197	0.2625	0.3535	0.4415	0.4574
200	0.1495	0.1875	0.254	0.341	0.4415	0.455
225	0.141	0.178	0.2365	0.332	0.4315	0.448
250	0.135	0.1685	0.227	0.3215	0.4275	0.448
275	0.1275	0.159	0.2175	0.30820	0.419	0.4455
300	0.123	0.156	0.2125	0.3025	0.4165	0.4455
325	0.117	0.1485	0.2025	0.298	0.4105	0.4415
350	0.114	0.1445	0.1965	0.2895	0.409	0.4385
375	0.11	0.139	0.191	0.2885	0.409	0.436
400	0.1065	0.1375	0.1950	0.2885	0.409	0.433
421	0.1065	0.1375	0.1950	0.2885	0.4090	0.433

Note: The full length segment is 421 since profile data from 70m to 910m are interpolated in 2m interval.

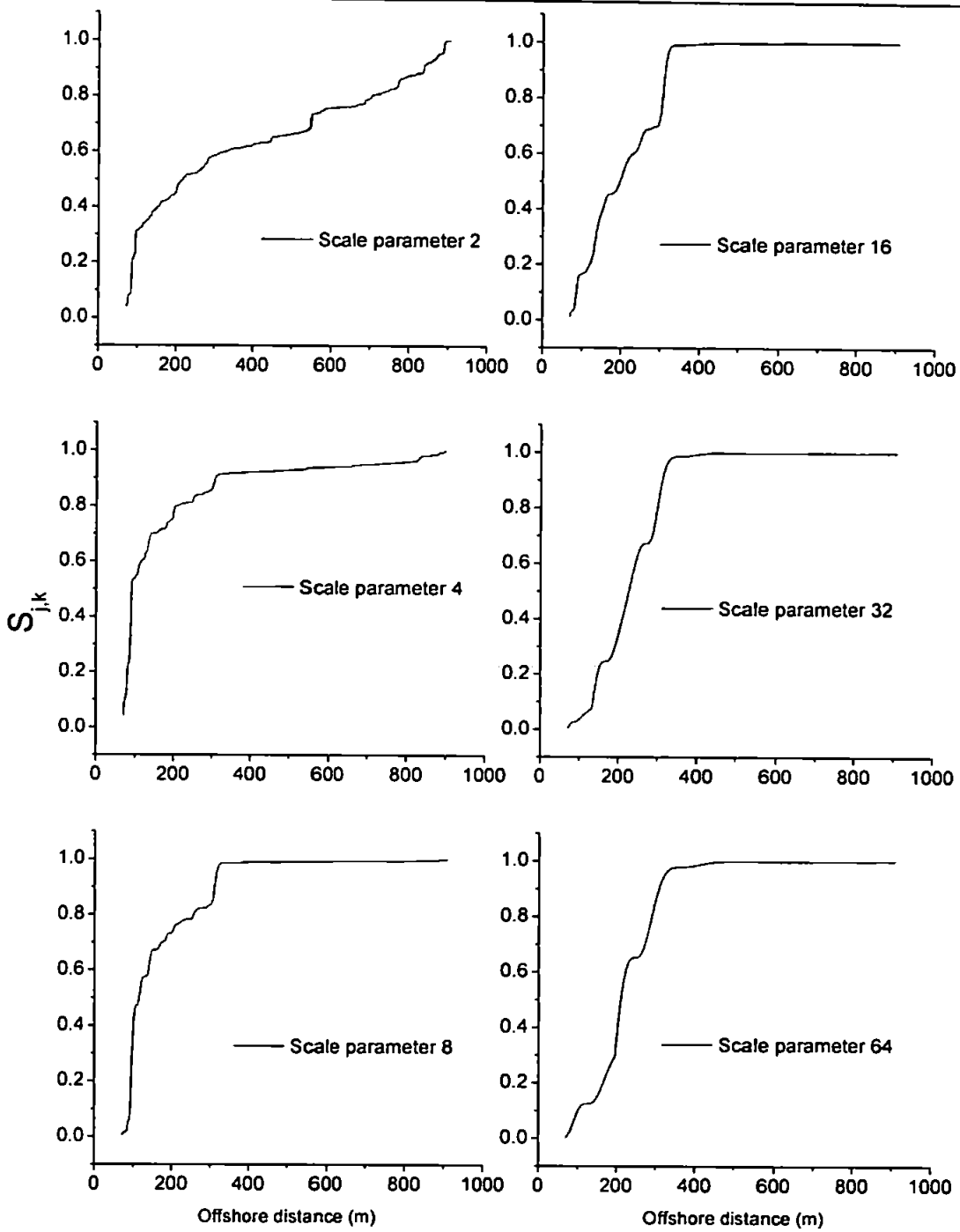

Figure 3.5 Plots of $S_{j,k}$ against cross-shore positions at different values of the scale parameter.

Table 3.3 The 95th percentile of the temporal B statistics scale by scale

Length of segments	S_1	S_2	S_3	S_4	S_5	S_6
25	0.3960	0.4670	0.5330	0.5665	0.5505	0.5355
50	0.2860	0.3465	0.4327	0.5052	0.5247	0.5355
75	0.2390	0.2925	0.3770	0.4715	0.4930	0.5355
100	0.2045	0.2530	0.3410	0.4490	0.4805	0.5030
125	0.1860	0.2295	0.3160	0.4310	0.4705	0.4375
150	0.1710	0.2135	0.2950	0.4210	0.4685	0.3895
175	0.1580	0.1995	0.2820	0.4092	0.4620	0.3540
200	0.1480	0.1860	0.2695	0.4000	0.4555	0.3540
225	0.1400	0.1790	0.2630	0.3975	0.4511	0.3540
250	0.1330	0.1790	0.2630	0.3975	0.4460	0.3540
267	0.1300	0.1790	0.2630	0.3975	0.4435	0.3540

The survey at Duck in March 1996 was used to specify this procedure in a particular case. The AMODWT coefficients in the spatial series of profile data for March 1996 were computed with Equation (3.21), and $S_{j,k}$ were computed using these coefficients at different spatial scales with Equation (3.24). The plot of $S_{j,k}$ against position along the profile for different values of the scale parameters is shown in Figure 3.5 for reference. Subsequently, the values of B for the full beach profile data in March 1996 scale by scale were obtained by combining Equations (3.25), (3.26) and (3.27). Comparing the B values with the critical values as listed in Table 3.2 for the full length segment (421 observations) scale by scale, the change points in spatial wavelet variances for a specified scale can be identified at the first order if the B value was larger than the critical value. The identifying procedure was repeated until all the wavelet variances in the length of segments were uniform against the critical values.

Following the same procedure as described for spatial analysis, we obtained the average temporal spatial critical values. These values under dilations corresponding to $j = 1,2,\cdots 6$ of the

Daubechies's wavelet with two vanishing moments with changing segments in time series are listed in Table 3.3. These critical values will be used later to identify the change survey in temporal wavelet variance. For $j = 1$, the temporal scale is $2^1 = 2$ months, and so on. It is obvious that the critical values for identifying changes in temporal wavelet variance have a similar trend as that of the spatial ones.

3.5 The Discrete Wavelet Packet Transform

3.5.1 Introduction

The main advantage of the wavelet transform over other methods, such as Fourier analysis, is that it requires no assumptions of statistical stationarity. The obvious disadvantage of the DWT is that it provides a predetermined basis for the data set that does not depend in any way on the spatial/temporal variation of the original data. For one thing, the temporal scales of the beach elevation change for a fixed point along the profile are determined as an integer power of 2 multiple of the sampling interval. They are 2 months, 4 months... and so on. This principal disadvantage of the DWT was pointed out by Si (2003) who noted that the DWT does not resolve variation equally at all spatial frequencies. Lark (2004) also stated this problem in the context of soil variability. This is the reason that the discrete wavelet packet transform (DWPT) is becoming more widely used in signal analysis. Although it is not necessary to have uniform resolution in the frequency domain, a basis that is suitable to represent the specific features of beach profile data is needed.

A brief introduction to the DWPT will be presented in this section before using it in this thesis, since it has not been employed to analyse the variability of beach profiles before. For simplification, the notation for time series $f(t)$ is only used in the following when the methodology is introduced, but this is similarly applied to spatial variation as well.

3.5.2 The theory of the DWPT

For a given orthogonal wavelet function, we generate a library of bases called the wavelet packet basis. Each of these bases offers a particular way of coding time series, preserving global energy, and reconstructing exact features. The wavelet packets can be used for numerous different expansions of a given time series. The DWT basis for the given function is just one selection from the library of possible packet basis.

The DWPT procedure has some similarity with the discrete Fourier transform (DFT). Wavelet packet atoms are waveforms indexed by three naturally interpreted parameters: position, scale (as in wavelet decomposition), and frequency. For the Fourier transform, it is assumed that the amplitudes and phase of $f(t)$ for some frequency is the same for any t.

In the DWT, at each dilation of the basic wavelet, the wavelet and scaling function filters are applied only to the wavelet function coefficients generated at the previous dilation. This procedure is illustrated by the plot on the top of Figure 3.6, which presents the normal partition of frequencies. The function $f(t)$ is the time series of the beach elevations at given points along the profile, which is the input data labelled as $W_{0,0}$ in Figure 3.6. $G(\cdot)$, the transfer function of $\{g_l\}$, is a high-pass filter corresponding to the wavelet function, and $H(\cdot)$, the transfer function of $\{h_l\}$, is the low-pass filter corresponding to the scaling function.

In the corresponding DWPT, at each dilation of the basic wavelet, the wavelet and scaling function filters are applied to both the wavelet and the scaling function coefficients generated at the previous dilation so that the wavelet packet method is a generalization of wavelet decomposition that offers a richer signal analysis. This procedure is illustrated by the bottom plot of Figure 3.6, which shows the dilation to level three. This figure is an example of a wavelet packet basis. The transform that takes $f(t)$ to $W_{j,n}, n = 0, \cdots, 2^j - 1$ for any exponential scale j between 0 and J is called a DWPT. Any such transformation is orthonormal.

In theory, a signal might contain frequency content in each of the 8 frequency bands defines by the decomposition of exponential scale three, as shown in Figure 3.6. In practice, the strength of the frequency content in each of the band is likely to vary, and a good reconstruction of the data

might be possible with a subset of the bands. In this sense, the DWPT offers the advantage over the DWT of being able to resolve better the frequency band content of a given signal.

Each DWPT is associated with exponential scale j, and the j^{th} level DWPT yields transform coefficients that can be partitioned into 2^j vectors, namely $W_{j,n}, n = 0,\ldots,2^j - 1$. The DWPT effectively decomposes the frequency interval [0, 1/2] into 2^j equal individual intervals. The resulting standard frequency interval of the nodes in the DWPT basis (Percival and Walden, 2000) is

$$I_{j,n} = \left[\frac{n}{2^{j+1}}, \frac{n+1}{2^{j+1}}\right]. \tag{3.38}$$

where $I_{j,n}$ indicates the frequency interval in the n^{th} packet at exponential scale j of the DWPT. It should be noted that this standard frequency interval does not have any direct physical meaning. The frequencies should be decided by the basic sampling of signal, the wavelet function and the temporal scales (reciprocal of the standard frequency intervals).

3.5.3 The best basis algorithm

Many different orthonormal transforms can be extracted from a wavelet packet table taken out to some level as shown in Figure 3.6. For one thing, if the set $\{W_{3,0}, W_{3,1}, W_{2,1}, W_{1,1}\}$ from all of the wavelet packets in Figure 3.6 is selected this corresponds to the ordinary DWT. Other orthonomal basis could be selected from the table, for example $\{W_{2,0}, W_{3,2}, W_{3,3}, W_{1,1}\}$, which is a finer partition on some parts than in others. Every possible orthonormal transform is a disjoint dyadic decomposition, which by definition is a partitioning of the frequency interval [0, 1/2]. How to define which one of these many transforms is in some sense optimal for a particular time series? Coifman and Wickerhauser (1992) tackled this problem under the name of the 'best basis algorithm' with respect to an entropy-type criterion, which consists of the following two basic steps.

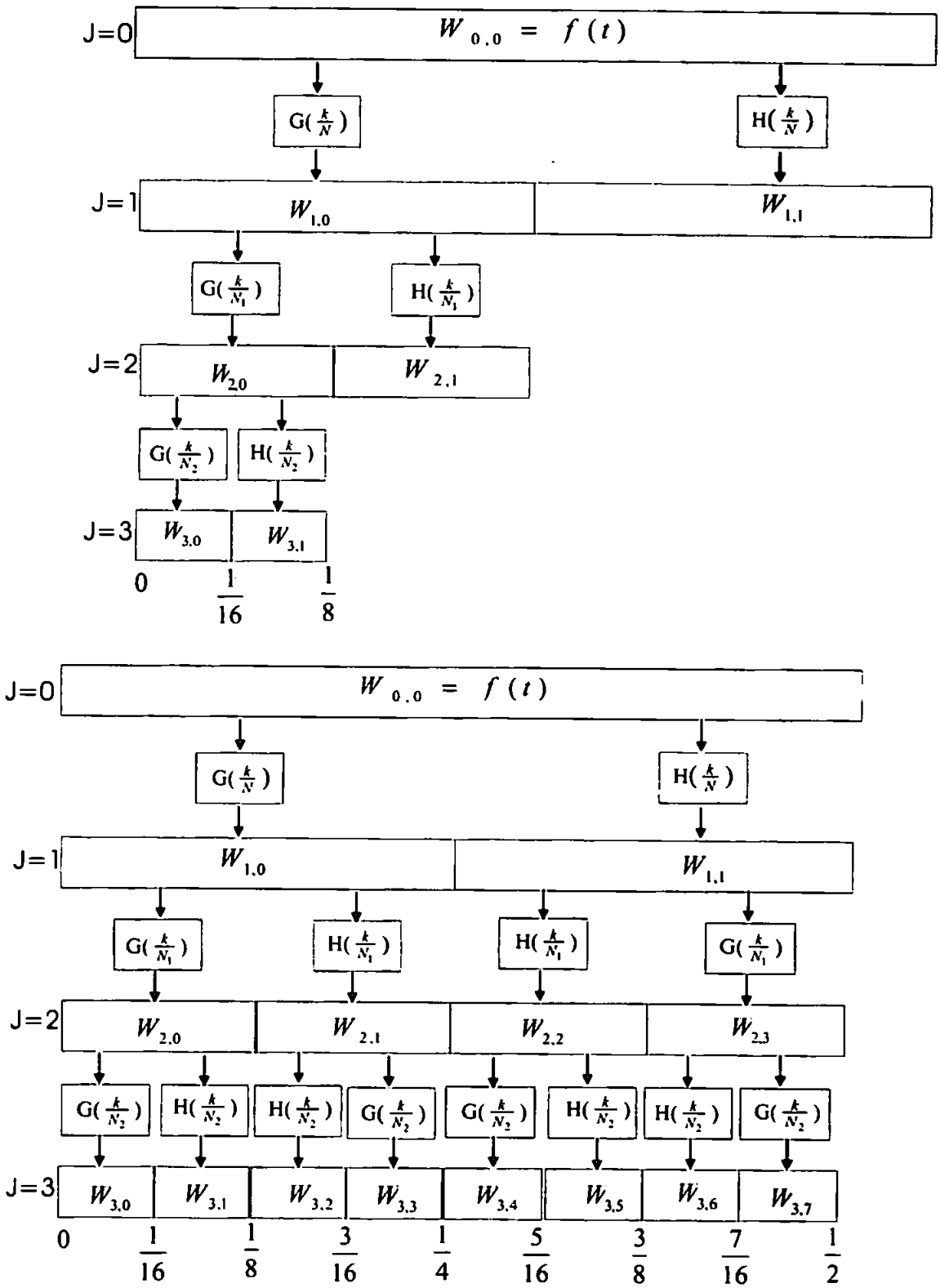

Figure 3.6 (Top) Flow diagram illustrating the analysis of W by the DWT. (Bottom) Flow diagram illustrating the analysis of W into $W_{3,0}, \ldots W_{3,7}$ by the DWPT.

1. Given a WP table to exponential scale J_0, then for every $(j,n) \in N$ it is associated with $W_{j,n}$ a cost $E(W_{j,n})$, where $E(\cdot)$ is an additive cost functional of the form

$$E(W_{j,n}) \equiv \sum_{i=0}^{N_j-1} E(W_{j,n,i}),$$

and $E(\cdot)$ is a real-valued function defined on $[0,\infty)$. In the following expressions, W is the signal and $W_{j,n,i}$ is the discrete wavelet coefficient in the location i of the nth packet at exponential scale j of W in an orthonormal basis.

Furthermore, the entropy **E** must be an additive cost function such that **E(0)** = 0 and

$$E(W) = \sum_i E(W_{j,n,i})$$

2. The 'optimal' orthonormal transform that can be extracted from the WP table is the solution of

$$\min_c \sum_{(j,n)\in c} E(W_{j,n}),$$

Classical entropy-based criteria match these conditions and describe information-related properties for an accurate representation of a given signal. Entropy is a common concept in many fields, though mainly in signal processing. The following example lists several different entropy criteria; many others are available.

1. The (nonnormalized) Shannon entropy, with the convention.

$$E(W_{j,n,i}) = -\sum_i W_{j,n,i}^2 \log(W_{j,n,i}^2)$$

2. The concentration in p_w norm entropy with $1 \le p_w$

$$E(W_{j,n,i}) = \sum_i \left|W_{j,n,i}\right|^{p_w} = \left\|W_{j,n,i}\right\|^{p_w}$$

3. The "log energy" entropy, with the convention $log0 = 0$

$$E(W_{j,n,i}) = \sum_i \log(W_{j,n,i}^2)$$

4. The threshold entropy, which is non-zero if the signal is larger than a threshold p_w, with

$$E(W_{j,n,i}) = \begin{cases} 1 & if\ |W_{j,n,i}| > p_w \\ 0 & otherwise \end{cases}$$

In this thesis, the Shannon entropy was used, since it is a widely used one. The best basis algorithm (Coifman and Wickerhauser, 1992; Wickerhauser, 1994) proceeds in the following way:

1. We mark all costs in the nodes at the bottom of the table. We start by examining this bottom row of nodes. One example of the cost is the value in Table 3.4.

2. We compare the costs of the sum of each pair of children nodes with their parent node and then do one of the followings:

(a) If the parent node has a lower cost than the sum of the cost of the children nodes, we mark the parent node.

(b) If the sum of the cost of children nodes is lower than the cost of the parent node, we replace the cost of the parent node by the sum of the costs of the children nodes.

3. We then repeat step 2 for each level as we move up the table. The end result is shown in Table 3.4.

4. Once we have reached the top of the table, we look back down the table at the marked node. The top-most marked nodes that correspond to a disjoint dyadic decomposition define the best basis transform.

Table 3.4 Final step of the best basis algorithm (Percival and Walden, 2000).

0.96							
0.28				0.68			
0.19		0.19		0.32		0.36	
0.12	0.12	0.12	0.12	0.32	0.0	0.28	0.28

3.5.4 Multi-scale analysis of the DWPT and the wavelet packet variance

Multiresolution analysis is a partition of a set of spatial data into components corresponding to the different scale parameters of the discrete wavelet transform. Like the DWT, the detail components corresponding to any wavelet packets can be obtained by conducting an inverse

transform of the corresponding coefficients so that the best basis can be reconstructed to represent the original data, $f(t)$.

When convolving the data with wavelet functions and scaling functions on finite-length signals, border distortion arises. In order to deal with the border distortion, data near the border should be treated differently. There are a few methods that include:

1. Zero-padding: This method iss used in the version of the DWT given in the previous sections and assumes that the signal is zero outside the original support. The disadvantage of zero-padding is that the discontinuities are artificially created at the border.

2. Symmetrization: This method assumes that signal or images can be recovered outside their original support by symmetric boundary value replication. This creates discontinuities in the derivatives of the data, but it is unlikely to lead to misleading results as long as the scale parameters are restricted to values less than or equal to half the shortest dimension of the sampling grid.

3. Periodic padding: This method assumes that the signal or image can repeat itself in period. Discontinuities might appear at the boundary, and the benefit of localization in wavelet analysis is lost if we generate coefficients near one boundary using values from the opposite boundary.

The wavelet packet variances are defined similarly to the wavelet variance. In the DWPT at exponential scale j there will be 2^j wavelet packet variances specified corresponding to the frequency interval. The variance of the DWPT in the n^{th} packet at exponential scale j is shown in Equation (3.39), in which $W_{j,n,i}$ denotes the discrete wavelet coefficient in the location i of the n^{th} packet at exponential scale j.

$$\sigma_{j,n}^2 = \frac{1}{2^j N}\sum_{i=1}^{N} W_{j,n,i}^2 . \tag{3.39}$$

3.6 Summary

In this chapter, wavelet transforms have been introduced first by comparison with Fourier transforms. To investigate the local variability of beach profiles, the methodology was narrowed to the discrete wavelet transform. Considering the relative small data series of beach profiles, the

adapted maximal overlap wavelet transform was introduced for using all the available data. The concept of wavelet variance and local wavelet variance component were introduced to investigate the magnitudes of beach elevation change clearly at different scales. To identify the most active zone of beach profile change and the depth of closure, B statistics were developed based on the wavelet coefficients. During the development of critical B values, the variogram was introduced.

However, use of the DWT requires that the sequence of spatial and temporal resolution is fixed as a dyadic sequence. This leads to an uneven sampling of frequency space, particularly at intermediate and low frequencies. This is the reason that the discrete wavelet packet transforms (DWPT) was introduced. It is expected the DWPT can fully solve the complex variability of beach profiles in both space and time.

Chapter 4. FIELD DATA AT DUCK AND PRELIMINARY STUDIES

4.1 General

Waves and currents interacting with bottom sediments produce changes in the beach and nearshore bathymetry. These changes can occur very rapidly in response to storms, or slowly as a result of persistent but less forceful seasonal variations in waves and current. Currently, there are only a few long-term surveys of the nearshore bathymetry in the world. Two well-known ones are the Coastal Research Station (CRS) at Lubiatowo, Poland, and the US Army Corps of Civil Engineers Field Research Facility (FRF) at Duck, North Carolina, USA. It has been acknowledged that the FRF data set is unparalleled with respect to high resolution in time and space of profile evolution so it is the main one used in this thesis to investigate the variability of beach profiles.

In this Chapter the field site at Duck will be described in brief and the previous work by others will be reviewed. Moreover, the wave conditions at Duck during the study period are investigated. The methods of data editing and interpolation based on the Duck data set are developed for later use, since the surveys are not regular either in time and space. Subsequently, the standard deviation of beach elevation in space and the EOF analysis are presented before the detailed wavelet analysis in **Chapter 5**. These provide a general impression of the beach profile changes during the period of study.

4.2 Data Set at the FRF, Duck, N.C., USA

4.2.1 Description of the FRF

The field research facility FRF is located along an approximately 1-km stretch of Atlantic Ocean barrier island beach in the village of Duck, as shown in Figure 4.1. In this section, an introduction of this site based on the information from the website http://www.frf.usace.army.mil/ is given. Some photos of this field site and the instruments used are shown in **Appendix A**.

The data set provides a good quality source of information on short, medium and long-term processes that affect coastal morphology. Since 1980 detailed surveys of the nearshore bathymetry have been conducted by the FRF. These data now cover twenty-three years and include hundreds of surveys at irregular intervals. They provide quantitative measures of the dynamic nature of the nearshore zone, including during storms when changes are most rapid. In addition, the natural long-term cycle of beach erosion and rebuilding, which may take many years, is well documented. These data are being used to refine theories of nearshore morphologic change and to develop and test numerical simulations of nearshore response to changing conditions. Apart from the long-term surveys, some short-term experiments, such as DUCK94 experiment, have also been conducted at Duck. The DUCK94 experiment was designed as fundamental to improved understanding of surf zone sediment transport.

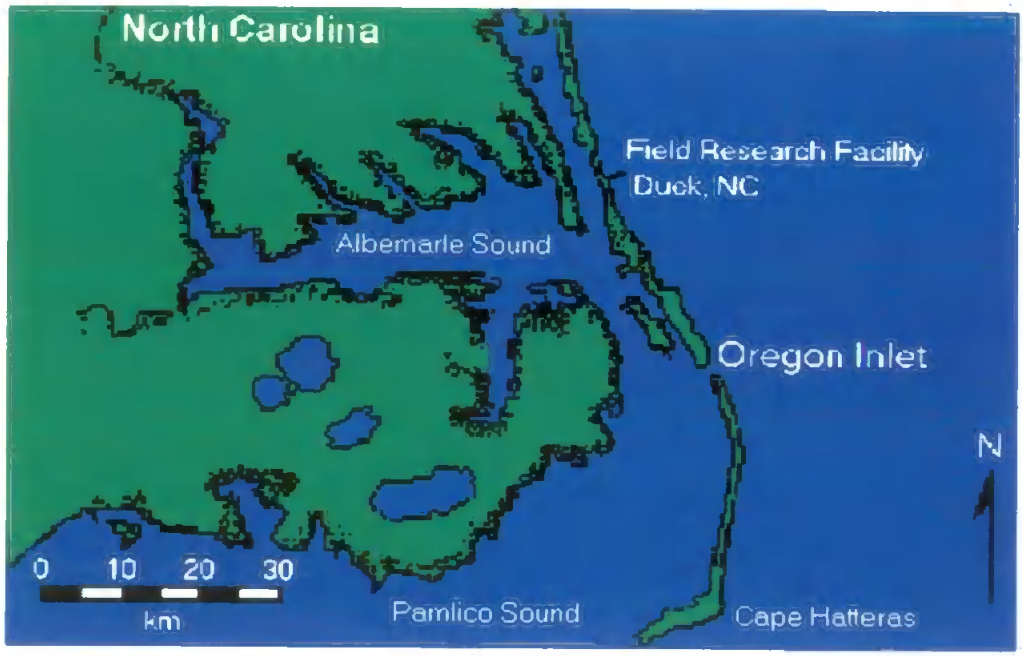

Figure 4.1 Geographic location of the FRF field site on the North Carolina coast.

The nearshore bathymetry at the FRF is characterized by regular shore-parallel contours, a moderate slope, and a barred surf zone (usually an outer storm bar in water depths of about 4.5m and an inner bar in water depths between 1.0 and 2.0m). This pattern is interrupted in the immediate vicinity of the pier where a trough runs under much of the pier's length, ending in a scour hole at the pier's seaward end where depths are up to 3.0m greater than the adjacent bottom.

The maximum variation of beach elevation occur just seaward of the shoreline. The sediment consists of a medium to fine sand mix. Mean grain size decreases from 1mm on the foreshore to 0.1-0.2mm offshore. The beach is microtidal with a tidal range between 0.7m (neaps) and 1.5m (springs). The beach foreshore is steep (1:12) and the bottom slope declines to 1:160 near 8-m depth.

The surveys are conducted over a series of perpendicular to the shoreline "profile lines" which extend from the dune to approximately 950m offshore. In addition, 4 of the 26 lines (58, 62, 188 and 190) are surveyed biweekly as part of a "4-line Survey." The locations are shown in Figure 4.2, together with the location of the FRF research pier. Miller *et al.* (1983) noted that profile lines 58 and 62 which are separated by 90m are located about 500m north of the research pier, while profile lines 188 and 190 are separated by 90m are located about 500m south of the research pier, in both cases minimizing the location influence of pier.

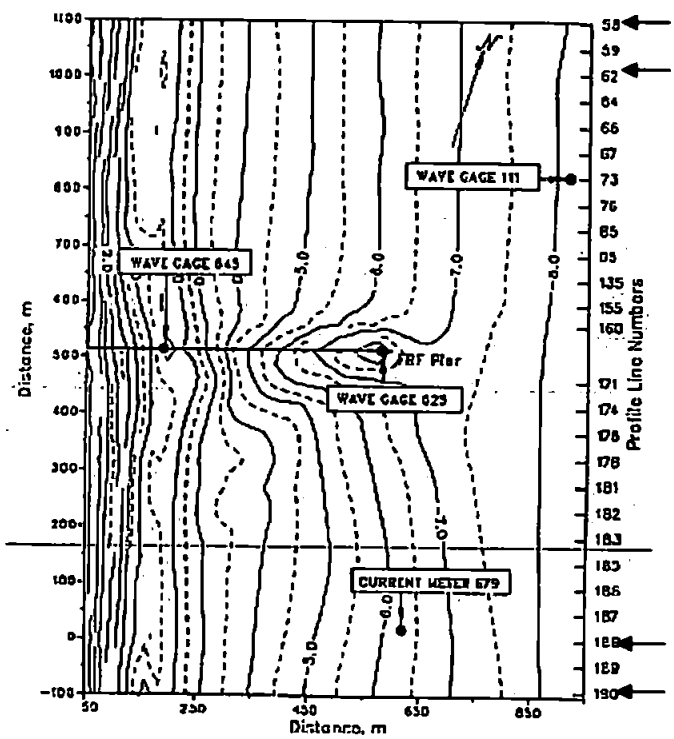

Figure 4.2 Locations of '4-line Survey' relative to the FRF research pier and bathymetry on September 9 1988.

All surveys were made using the Coastal Research Amphibious Buggy (CRAB), which consists of a tripod of 0.2m schedule-80 aluminium tubing, connected at the base by horizontal members 2.1m (7ft) above the ground, and an operations platform 10.7m (35ft) above the ground. An instrument to determine the CRAB's location and elevation is needed. From 1981-1991, two instruments were used: the Zeiss Elta-2s Electronic Survey System and the Geodimeter Auto-Tracking Survey System. The stated range of distance measurement of the Zeiss is 2km with a triple prism assembly as used on the CRAB. The distance accuracy is 2cm in the rapid measurement mode. The stated operating range of the Geodimeter is 5.5km with a single circular prism array. The distance accuracy is 10mm in the tracking mode. All profile elevation data are referred to the U.S. 1929 National Geodetic Vertical Datum (NGVD) to which elevation is customarily referenced at the FRF, and offshore distance is referenced to the FRF baseline. The NGVD and Mean Sea Level (MSL) datum at the FRF are nearly the same, with the relation given by MSL=NGVD+0.067m.

The wave data used in this study were collected from three different sets of instruments, as noted by the staff of the FRF (http://www.frf.usace.army.mil/frfdata.html). The first is an array of fifteen pressure gauges, collectively referred to as gauge 3111. Directional information was computed from these gauges using an iterative maximum likelihood estimator. The second type is a Baylor staff gauge (625) and a pressure gauge (641), both attached to the pier. The third is a Waverider buoy (630). All wave data is sampled at 2 Hertz, with five contiguous 34 minute records, for a total collection period of nearly 2 hours and 51 minutes. Wave height, H_{m0} is an energy-based statistic equal to four times the standard deviation of the sea surface elevations. Wave height reported from the pressure gauge has been compensated for hydrodynamic attenuation using the linear wave theory. Wave period is identified from the computation of a variance (energy) spectrum with 60 degrees of freedom calculated from a 34-min record. Peak wave period T_P is defined as the period associated with the maximum energy in the spectrum.

Wave height and period were typically recorded every 6hr but more frequently during some parts of the observation period, for which hourly values were recorded. Hourly values for the water level are available from a tide gauge located at the end of the research pier at the approximate 4-m depth contour.

4.2.2 Previous studies by other researchers on the data set at Duck

The Duck data set is widely recognized as being of high quality and suitable for studying coastal changes over a range of scales. This is evidenced by the fact that previous researchers have studied a range of phenomena. However, most of those studies have been based on the data set covering 12 years from 1981 to 1992. For example, the temporal and spatial scales of beach profile change at Duck were described by Birkemeier (1985) using the EOF with three and half years' profile data. The author identified the seasonal shift of sediment from the beach and inner bar to the offshore. The morphordynamics of bars was examined by Larson and Kraus (1994) using the field data from 1981 to 1991 of Duck. They suggested that the average spring and autumn profile shapes were almost identical and occurred as transitional states between the summer and winter profile shapes. More recently, Stive *et al.* (2002) studied the variability of shoreline evolution in terms of a range of different temporal and spatial scales using three data sets, and one of them was from Duck, where slight accretion was observed.

There are a few studies on the relationship between waves/storms and beach profiles based on the Duck data set. Lee *et al.* (1995) related the shoreline position, sediment volume and slope changes obtained from the profile data during ten and half years to storms to test the concept fair-weather/storm model, describing how the beach-near-shore profile undergoes long-term adjustments. It was suggested that the fair-weather/storm model may be a useful conceptual tool to examine medium- to long-term beach-nearshore profile behaviour. Subsequently, Lee *et al.* (1998) examined the medium-scale storm-driven variability of the beach in nearshore profiles at Duck, using the data from 1981-1991. The authors pointed out that given appropriate sequences, groups of storms can act as a large individual 'event'. The analysis of Lee *et al.* (1998) was extended by Birkemeier *et al.* (1999) to include data from 1981 to 1998 so that the importance and character of storm sequences in terms of duration, intensity, intervening time interval and profile response were examined. Larson *et al.* (2000) used the 11-year data on waves and profiles measured at Duck to study the covariation between waves and profile response. Their results suggested that the profile response showed higher correlation with the nearshore wave properties as compared to the offshore waves.

Sallenger *et al.* (1985) studied the storm-induced response of a nearshore-bar system using the data set at Duck during a fourteen-day period in October 1982. They noted that with the increase in wave height during the storm, the bar became developed and migrated offshore at rates up to 2.2 meter per hour. Based on intensive analysis of survey data from Duck, Larson and Kraus (1992) presented empirical predictive expressions describing the cross-shore movement of the linear nearshore bar.

Lippmann and Holman (1990) reported that the inner bar behaves in both an equilibrium and a sequential manner, depending on the incident wave conditions and antecedent morphology. Lippmann *et al.* (1993) investigated the influence of a possible outer bar on the behaviour of an inner bar, and determined the response of the bar system to the timing of episodic extreme wave events with the existence and amplitude of an outer bar at Duck offshore bar systems. Especially those with multiple bars provide natural coastal protection by dissipating wave energy. The authors suggested that the time series of monthly averaged statistics revealed episodic transitions between one and two bar configurations and was shown to contribute significantly to the non-stationary behaviour of bar system.

The observed bar behaviour at Duck during 16 years was explained by a simple heuristic model by Plant *et al.* (1999). They found that the characteristic bar response time is relatively long to the characteristic timescale of the forcing (waves). Ruessink *et al.* (2003) compared the interannual nearshore bar behaviour at Duck with other sites such as the Dutch coast using complex empirical orthogonal function analysis. They concluded that the evolution of bar amplitude with mean depth is similar for all sites and can be described empirically by a negatively skewed Gaussian function.

Non-linear methods were also employed in analysing the beach profile change at Duck by Southgate (1997) who indicated the possibility of much more dynamic behaviour with systems being maintained away from equilibrium and showing self-organised responses. More recently, fractal analysis techniques were applied to beach level time series collected at Duck by Southgate and Möller (2000). To compare with the fractal analysis results, the authors also carried out a spectral analysis using a fast Fourier transform.

4.2.3 Wave and storm conditions at Duck

Waves and storms are usually the main forcing conditions that drive beach profile changes. Therefore it is necessary to examine the wave conditions at Duck. The cumulative monthly wave directions were in the range from 69 to 88 degree, respectively in December and July during the period from 1987 to 1999. The mean was 76.9 degree. This result was summarised according to the 'wave rose' from the website http://www.frf.usace.army.mil/frfdata.html.

The summary of the severe wave conditions and general wave conditions are presented in this section. Table 4.1 lists the storms during the course of study, when the wave height exceeds 2m. I analysed the storm conditions from 1999 to 2003 and filled the items with 'under construction'. In addition, the extreme storms in this thesis were defined as those of which wave heights exceeded 4m.

Table 4.1 Storms at the FRF, Duck (the storm data from 1980 to 1998 come from the FRF website: http://www.frf.usace.army.mil/storms.html)

Storms at the FRF

- when the wave heights at the pier end exceeded 2 metres

1980
- Oct 24- 25
- Nov 24, 28
- Dec 27-29

1981
- Feb 11, 14
- Mar 8-9
- Aug 19-23
- Sep 4, 23
- Oct 11-16, 24, 29-31
- Nov 1-2, 12-15, 25-26
- Dec 5-6, 25

1982
- Jan 1, 26-27
- Feb 13, 17-19, 27- Mar 01
- Mar 16
- Apr 28
- May 12
- Aug 29
- Oct 10-13, 23-25
- Nov 19-25
- Dec 9, 12, 17-19

1983
- Jan 04, 10-12,21-22,27-29
- Feb 11-12, 14-15,18, 20-22, 26-27
- Mar 01, 12, 17-19, 24-27, 31- Apr 01
- Mar 24
- Jun 09
- Sep 15, 28-30 Tropical Storm **Dean**
- Oct 10-12, 20-22, 25
- Dec 12-13, 19-22,31

1984
- Jan 01, 11-15
- Feb 14-15, 23, 28

1985
- Jan 3-4
- Feb 12

- Mar 13
- May 31
- Sep 27, 29-30 Hurricane **Isidore**
- Oct 11-15 Hurricane **Josephine**, 17-18
- Nov 03, 20
- Dec 6

1986
- Jan 11, 23-25
- Feb 25
- Mar 7-8, 21-22
- Apr 18-21
- May 9-13
- Aug 17 Hurricane **Charlie's** eye made landfall 1530-1700
- Oct 10-12, 18-19
- Dec 1-3, 24

1988
- Jan 3, 7-8, 14,
- Feb 12, 28
- Mar 11
- Apr 8, 12-14, 19
- Jun 3-5
- Oct 4, 8
- Nov 1, 24
- Dec 4, 15-16

1990
- Feb 5
- Mar 6, 29
- May 22-23
- Oct 12-13 Hurricane **Lili** remained offshore
- Oct 25-27
- Nov 10, 17-19, 30
- Dec 8-9

1992
- Jan 3-5
- Feb 6-8
- Mar 26-27
- Apr 13, 28-30
- May 6-8, 19-20

- Mar 22-23
- Apr 14
- May 3
- Aug 2
- Sep 27 Hurricane **Gloria** passed offshore at 0230
- Oct 21-22
- Nov 4-5
- Dec 1-2

1987
- Jan 1-2, 17, 25-27
- Feb 16-18,
- Mar 10-16, 23-24, 30-31
- Apr 16, 25-28
- May 4-5
- Aug 14-15,
- Sep 4-5
- Oct 12-15
- Nov 11-12, 27-29
- Dec 29-30

1989
- Jan 4, 23-24
- Feb 17-19, 23-25
- Mar 7-11, 23-24,
- Apr 11,
- Sep 4-10 Hurricane **Gabrielle** well offshore
- Sep 21-22 Hurricane **Hugo**
- Sep 23-24, 27
- Oct 25-26
- Nov 23
- Dec 8-10, 13, 22, 23-25

1991
- Jan 7-9, 11-12
- Feb 23
- Mar 6-7, 29
- Apr 20-21
- May 18-19
- Jun 23
- Aug 18-19 Hurricane **Bob**, 48 km offshore Cape Hatteras
- Aug 25
- Sep 1-2, 20
- Oct 3, 16-17, 28- 1 Nov
- Nov 8-10
- Dec 19, 31

1993
- Jan 9-11, 16-17, 26-27
- Feb 1-4, 12, 26-28
- Mar 13(**Storm of the Century**), 18-19
- Apr 6-9, 27-30

- Sep 23 Tropical Storm **Danielle**
- Oct 4-6
- Dec 10-11, 12-16, 29

- Aug 31-01
- Sep Hurricane **Emily** 50 km offshore FRF at 0000 31st
- Oct 10-11, 26-27
- Nov 25-28
- Dec 16-18

1994
- Jan 3-4, 26-28, 30-31
- Mar 2-3
- May 4, 20-21
- Sep 3-5, 22
- Oct 3, 12-13, 14-17
- Nov 7, 10, 16-19 Hurricane **Gordon** never came close.
- Dec 8, 14-19, 22-24

1995
- Jan 15-16, 28-29
- Mar 2
- Aug 7-9, 15-20 Hurricane **Felix** remained offshore, 28
- Sep 19, 23, 29-30

1996
- Jan 7, 19, 27
- Feb 2-5, 16-17
- Mar 10-13, 27-30
- Aug 31Aug-2Sep
- Sep 31Aug-2SepHurricane **Edouard**: 400 km offshore
- Sep 5-6Hurricane **Fran**: landfall at Wilmington,NC at 2000 EST on 5th
- Oct 4-8, 22-24
- Nov 15-18, 22, 26
- Dec 14-16

1997
- Feb 8-9, 14
- Apr 1-2, 23-24
- May 27-28
- Jun 3-7
- Sep 4
- Oct 18-20
- Nov 6-7, 13-14
- Dec 27-28

1998
- Jan 27-29
- Feb 3-10, 16-18, 23
- Apr 4-5, 14, 22-23
- May 12-14
- Aug 26-28 Hurricane Bonnie, FRF landfall
- Dec 14, 16

1999 under construction
- Jan 2-3, 31
- Feb 1, 22
- Mar 26-27
- Apr 29,30
- May 1-3,14-17
- Aug 30,31
- Sep 1-5, 15-16, 21-22
- Nov 11-12
- Dec 19-20

2000 under construction
- Jan 13-14, 24-25
- Mar 17-24
- Apr 18-20, 25, 26
- May 29-31
- Aug 30
- Sep 5-8
- Oct 1-2, 27
- Nov 27
- Dec 2-5

2001 under construction
- Jan 13-14, 26
- Feb 22
- Mar 22
- Apr 26, 27
- May 6
- Sep 15, 30
- Oct 1, 14
- Nov 7, 17
- Dec 9

2002 under construction
- Jan 3-5
- Feb 2
- Mar 2

2003 under construction
- Feb 16-18
- Mar 14, 18-21
- Apr 12, 16

- Apr 3
- Sep 8, 10
- Oct 16
- Dec 7, 12
- Sep 19

The monthly standard deviations of wave height and wave period during the 22 years were calculated to show the general annual variation in wave conditions, as displayed in Figure 4.3. It shows that the smallest standard deviation is in July and the largest one is in February. Figure 4.4 shows that the standard deviations of wave periods during the 22 years are smallest in July and largest in September. At Duck the wave height exhibits clear seasonality, with lower waves occurring during the summer and higher waves in the winter, whereas the mean period remains fairly constant throughout the year. During the 22 years from July 1981 to September 2003 with the 95% confidence interval the mean wave height is (1.03 ± 0.04)m and period is (8.68 ± 0.09)s.

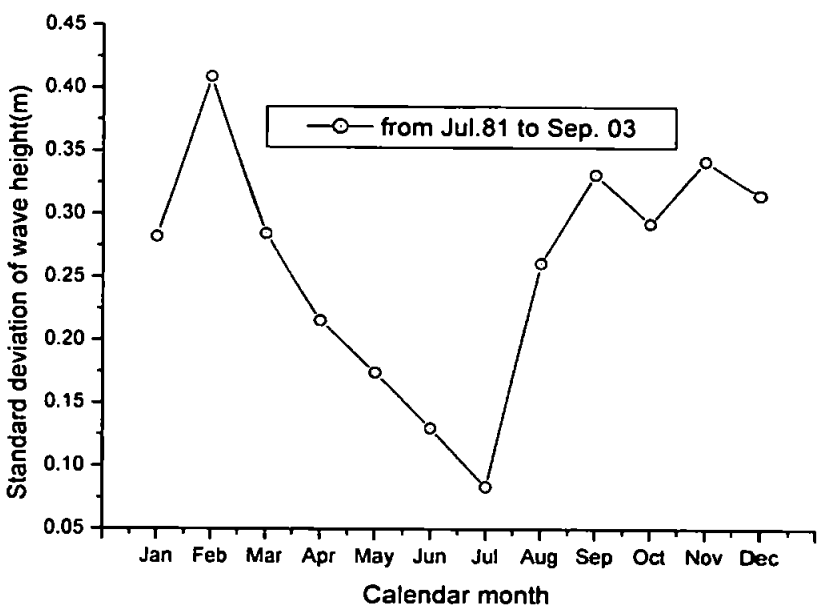

Figure 4.3 Standard deviation of wave heights during the 22 years.

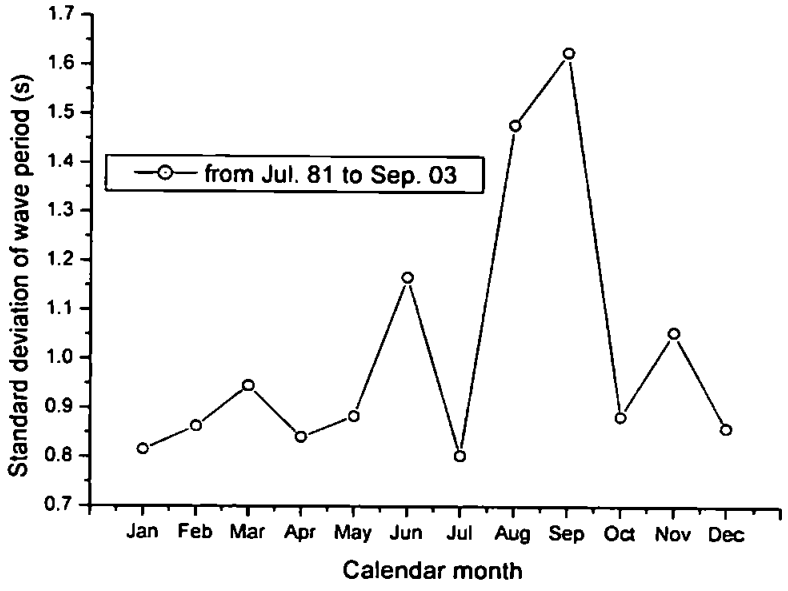

Figure 4.4 Standard deviation of wave periods during the 22 years.

4.2.4 Sediment transport and DoC

Capobianco *et al.* (1995) investigated the qualitative relationships between sediment transport components and profile change in the medium and long term by considering 11 years of data at Duck. Their main conclusion was the verification of the conceptual fair-weather-storm model. Thornton and Humiston (1996) examined the bar formation at Duck within the framework of the energetic-based sediment transport model developed from the earlier work of Bagnold (1954). Plant *et al.* (2004) investigated the prediction skill of nearshore profile evolution models based on DUCK94 experiment. They criticized the existing sediment transport model. The longshore sediment transport rates were presented by Miller (1999) during storms in November 1995 and March and April 1996 at Duck.

The DoC has been studied with the Duck data set by previous workers. Stauble and Cialone (1996) argued that the seaward of 5-m, 6-m depth most sample distributions remained unchanged throughout the study in DUCK94 experiment, which was an indication of the DoC. Moreover Larson and Kraus (1994) also suggest that the DoC is around 4-m water depth by observing the 11-year Duck data set. Capobianco *et al.* (1997) argued that the DoC at Duck is time-dependent by investigating the DoC at different time intervals. Moreover, they also argued that the DoC is scale-

scale dependent with respect to the different change criteria. Using the data from July 1981 to July 1993, Nicholls *et al.* (1998) examined the characteristics and interpretation of the DoC at Duck. Both the studies by Capobianco *et al.* (1997) and Nicholls *et al.* (1998) were developed from the work by Hallermeier (1981), which is an analytical DoC from the extreme wave heights. Most recently, Schwartz and Birkemeier (2004) also discussed the problem of profile closure at Duck.

4.2.5 Problems of beach profile data and the pre-processing

As in any experiment or field survey, there are inevitably errors in the Duck surveys. There are three error sources in beach profile survey, which are operational errors, instrument errors, and external errors. Operational errors include operator errors and limitation of the survey procedure. Instrument errors result from limitations of instruments or devices with which measurements are taken. External errors arise from variations in natural phenomena such as temperature, humidity, wind, and gravity. Those errors were discussed by the FRF staff, who published the error analysis in the FRF website (http://www.frf.usace.army.mil/frfdata.html). Operation errors of the Zeiss survey system resulted from improper levelling of the instrument, mis-aiming the instrument at the centre of the prism cluster while taking the measurement, an error in positioning the instrument in coordinate space (particularly in elevation), and movement of the tripod during the survey. Incorrectly aiming the instrument also resulted in an error but only on individual points. The details of the survey methods, error determination and correction, and survey accuracy were discussed by Howd and Birkemeier (1987) and Lee and Birkemeier (1993).

Errors affecting single points were found and removed in this thesis by a procedure which is presented in this section. Techniques for pre-processing the DUCK data have been developed with the data from DUCK94 experiment. When investigating the standard deviation of elevation in the time series for given offshore distances, it was found that there are obvious spikes in the dune zone for a few beach profiles. However, these spikes in standard deviations have no physical meaning. It is suggested that some of the points in the profile data sets are outliers, due to the error-sources described. One way to detect erroneous points is to compute the slope between successive observations. An outlier might give rise to implausibly large slopes.

To check the influence of slope distribution on the accuracy of interpolation, the basic procedure is to look for comparisons between successive observations where the absolute slope exceeds some threshold τ. When this happens we chose which point to delete as erroneous by 1) deleting point x_i, and then predicting point x_{i+1} by cubic spline interpolation from all the other data and 2) following the same procedure after deleting point x_{i+1}. We obtain the point with the smallest prediction error.

In order to select a threshold absolute slope τ for general use the mean-square error of prediction under a cross-validation method (predicting each value after removing it from the data) was computed for data edited using different thresholds (τ =1.0, 0.5, 0.3, 0.2 and 0.1). Mean square errors of beach elevation that describe the spatially variability of the smooth interpolated surface from the surveyed data were computed after cutting off slopes with different thresholds. Cutting off the slope means deleting one of the two adjacent points between which the slope is large. If the slope between two points is greater than a criterion value, the check procedure is carried out twice separately for the two points named x_i and x_{i+1}. The mean square errors are compared between deleting x_i and x_{i+1}. If the mean square error is smaller when x_i is deleted than the mean square error when x_{i+1} is deleted, point x_{i+1} will be kept in the data set. The point x_i is considered as abnormal, which might come from measure error in experiment.

One typical curve of them is illustrated in Figure 4.5, which displays the relationship between the thresholds of cut-off slopes and mean square errors of beach elevation (PL=200) from 20 surveys in the DUCK94 experiment. The figure illustrates that as the thresholds decrease the mean square error becomes smaller until the threshold is 0.3. However, beyond this threshold the relevant mean square error increases again as the thresholds decrease. The reason for the mean square error goes up with the thresholds of 0.1 and 0.2 is that the survey sampling in the dune zone is relatively sparse. The foreshore slope is around 1/12 at Duck (Lee *et al.*, 1998). However, if we would set the threshold at 1/12, it will result in losing some significant data. By compromising, one of the two points will be deleted if the slopes between them are greater than 0.3 in this thesis before doing further analysis.

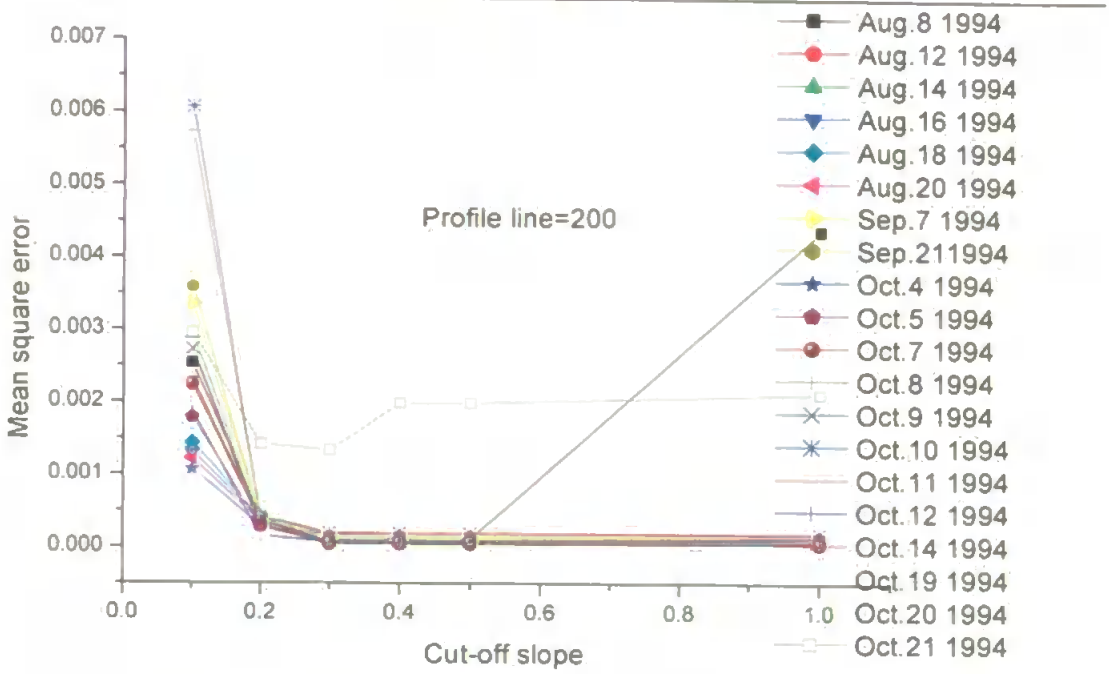

Figure 4.5 Cut-off slope vs. mean square error for the profile line 200 in the DUCK94 experiment.

4.2.6 Techniques of interpolation

Data collected from the FRF at Duck are not absolutely regular. However, regular data are needed for wavelet analysis by scale. The field data at Duck are dense and locally very smooth, so an appropriate interpolation will have little effect on the variation. On this basis it was decided to interpolate the data to regular spacing.

There are a number of interpolation techniques available, such as: linear interpolation; polynomial interpolation; rational function interpolation and cubic spline interpolation. Among these methods, cubic spline interpolation can fit the raw data most smoothly. The normal cubic spline interpolation (Press *et al.*, 1992) was initially employed to interpolate the field data set. However, the interpolator might overly smooth the observations (Plant *et al.*, 2002). By analysing the standard deviations of beach elevation at given offshore distances, we concurred with the findings of Plant *et al.* (2002) that the error of interpolation is highest where sampling is sparse, such as along the dune line (x-75m). An advanced cubic spline interpolation method was used, which computes a cubic spline interpolant consistent with the concavity of the data. The subroutine

CSON (in the IMSL Library, 1994) was used to interpolate the irregular data of surveyed beach profiles after filtering some bad data as discussed in the above section.

In this thesis, the investigation is focused on profile lines 58, 62, 188 and 190 since they are surveyed with high temporal frequency. The surveys used in this thesis span from July 1981 to September 2003. To maximize the number of usable surveys and to include as much offshore information as possible, the data were filtered within the range from 70m to 910m offshore. The surveyed data were interpolated onto a regular 2m spaced resolution to take advantage of the high resolution of survey in space. In addition to the spatial interpolation, the unequally spaced time series was interpolated linearly to provide measurements of beach levels at intervals of one calendar month. Therefore there are 267 surveys and each survey has 421 observation points in space along the profile line 62. The calendar months corresponding to the 267 surveys from July 1981 to September 2003 are listed in **Appendix A** for later reference.

4.3 Basic Statistical Analyses and EOF Analysis

4.3.1 Basic statistical analyses of beach profile change

Storms tend to move beach sand rapidly offshore, and sand moves onshore during fair-weather. Usually there are more storms during autumn and winter compared with spring and summer. At Duck, the profile varies from unbarred to triple-barred, though a double-barred profile with a narrow well-defined inner bar and a broad outer bar was often identified, as stated by Howd and Birkemeier (1987) and Lee and Birkemeier (1993). To have a general idea of the variability of beach profiles at Duck, it is necessary to present some basic statistics of the data.

First of all, the mean profile of the profile lines 58, 62, 188 and 190 during the period from July 1981 to September 2003 was calculated and shown in Figure 4.6. The standard deviations of beach elevation of the four profile lines over the survey period were computed and shown in Figure 4.7 against offshore distance. In Figure 4.7 there are two obvious positive peaks of the standard deviation along cross-shore located 120m and 260m offshore. The mean shoreline (MSL) during the 22 years is located 120m where the average elevation is zero. Figure 4.6 shows that

these four profile lines behave similarly in the long-term although the standard deviations for the profiles located south of the pier differ from those located north of the pier. In this thesis one representative profile line 62 are investigated in detail. The standard deviations show strong spatial non-stationarity, a strong motivation for the choice of wavelet analysis.

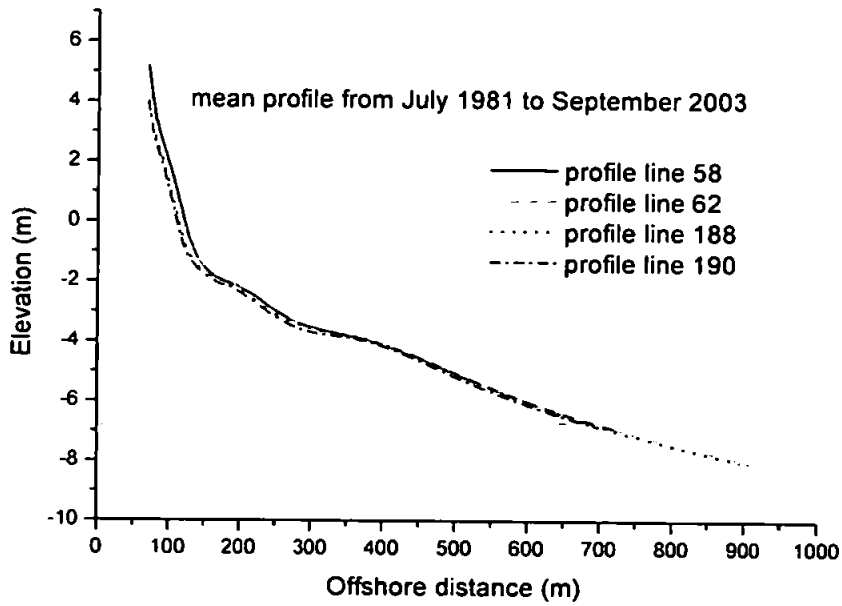

Figure 4.6 Mean profiles at Duck from July 1981 to September 2003.

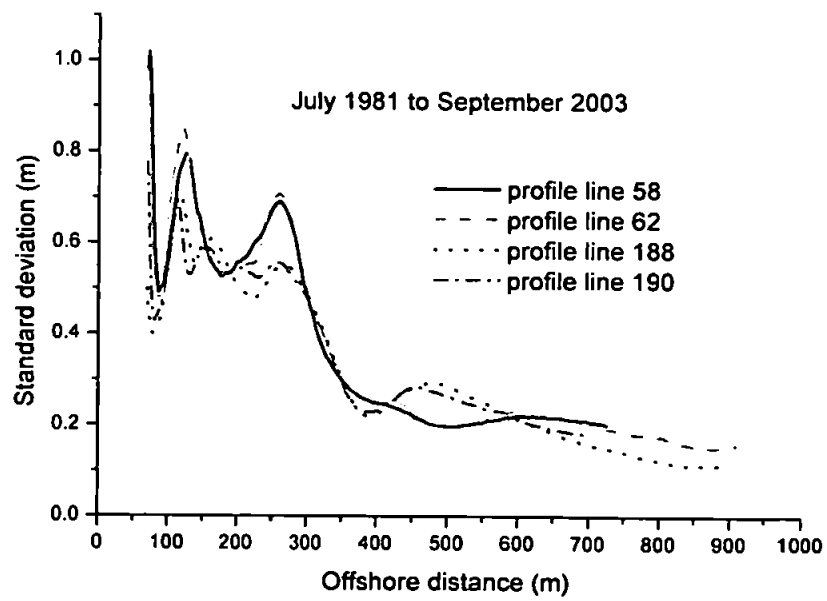

Figure 4.7 Standard deviations of beach elevation against offshore distance.

4.3.2 Results of the EOF analysis

The EOF analysis was conducted before the wavelet analysis because it is an established technique for studying the variability of beach profiles. The analysis was performed on the data with respect to the mean record of 22 years. The input data are the matrix with 421x267 in rows and columns, which represent the spatial and temporal series, respectively. A symmetric matrix was calculated using Equation. (2.1) with the input matrix of 421 by 267. Subsequently, EOF was conducted. Results of the EOF analysis based on the correlation matrix of the locations for profile line 62 are shown in Figure 4.8. These are the eigenvectors with the first three largest eigenvalues. The corresponding first three temporal eigenvectors are displayed in Figure 4.9.

The two figures can be easily explained by first determining the effect of positive and negative weightings on the different eigenvectors. The first eigenvector accounts for 35.3% of the variance in the data from the mean function. When the first temporal weighting is positive, the beach profile has one bar, usually located around 260m offshore. According to the temporal weightings shown in Figure 4.9 the first eigenvector has larger positive weightings during the period from September 1994 to November 1995 with the largest in April 1995. During this period, only one bar is identified which is located between 190m and 300m offshore. Figure 4.10 shows that the bar on the beach profile in April 1995 is around 260m offshore, whereas one of the two peaks in the first spatial eigenvector is located at 260m offshore, as indicated in Figure 4.8. This consistency again provides evidence that the first eigenvector characterizes the bars.

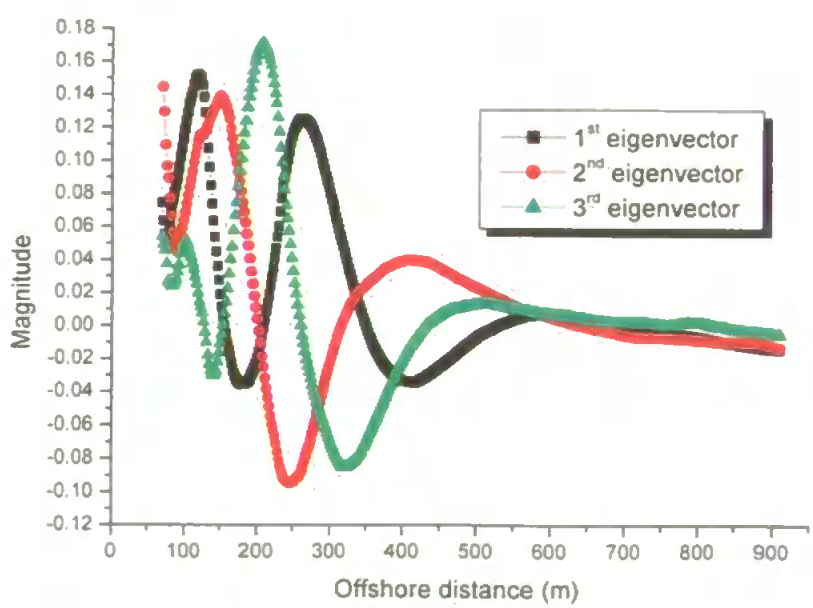

Figure 4.8 The first three spatial eigenvectors of profile line 62.

When the weighting is negative, the first eigenvector describes an inner bar just seaward of the shoreline and a well-defined outer bar. The two negative peaks of the first temporal weightings are in September 1983 and September 2000. These two profile configurations are also displayed in Figure 4.10. It can be identified in Figure 4.10 that the beach profile in September 2000 has two bars and a deep trough between the two bars, with the inner bar located 178m and the outer bar located 410m offshore. In addition, the two negative peaks of the first spatial eigenvector can be identified at 182m and 410m offshore from Figure 4.8. It can be concluded that the first eigenvector describes the change from one bar to two when the temporal weightings change from positive to negative.

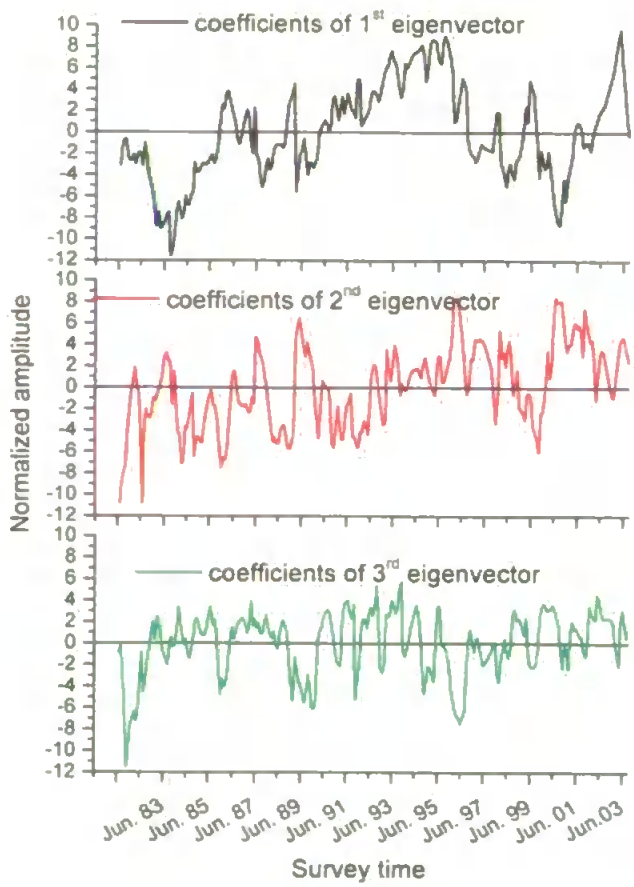

Figure 4.9 Weightings of the first three eigenvectors of profile line 62.

The second eigenvector also describes the bar movement in beach profiles. It accounts for 25.3% of the variance from the mean beach function. As illustrated in Figure 4.9, the weightings

from surveys in May 1989 and March 1996 are two positive peaks, and weightings from the surveys in July 1982 and October 1999 are two negative peaks. Those four profile configurations are shown in Figure 4.11. It can be seen from Figure 4.11 that when the weightings are positive the beach profiles have one bar with significant bar height, and when the weightings are negative the beach profiles have one or two bars in the surf zone.

In all, the combination of the first two eigenvectors account for 60.6% of the variance in the 22 years, whereas Birkemeier (1985) explained that the first two eigenvectors accounted for 64.8% of the variance. The difference is a weak indication of the non-stationarity of beach profile changes in time series. However, as Birkemeier (1985) also found, the first two eigenvectors can explain the bar movement, which actually is the essential movement of the beach profiles.

The third eigenvector accounts for 15.3% of the variance from the mean beach function, which is not very significant when compared with the first two. By observing Figure 4.9, it is found that the temporal weightings of the third eigenvector have a weaker annual periodicity. Hence the third eigenvector is responsible for the seasonal migration of bars. This result is much clearer when studying the data set for a shorter period. Birkemeier (1985) argued that the third eigenvector has well-defined annual cycles by investigating the three and half year Duck data. However, the eigenvectors beyond the first three become difficult to explain especially when the time series of data are longer. The eigenvalues and the corresponding percent of variances are summarised in Table 4.2 for the first five eigenvalues, which accounted for 87.6% of the variance in data set.

Table 4.2 Results of EOF

Eigenvector	Eigenvalues	Percentage variance accounted for	Accumulated percentage variance
1	0.047	35.3%	35.3%
2	0.034	25.3%	60.6%
3	0.02	15.3%	75.9%
4	0.009	6.6%	82.5%
5	0.007	5.1%	87.6%

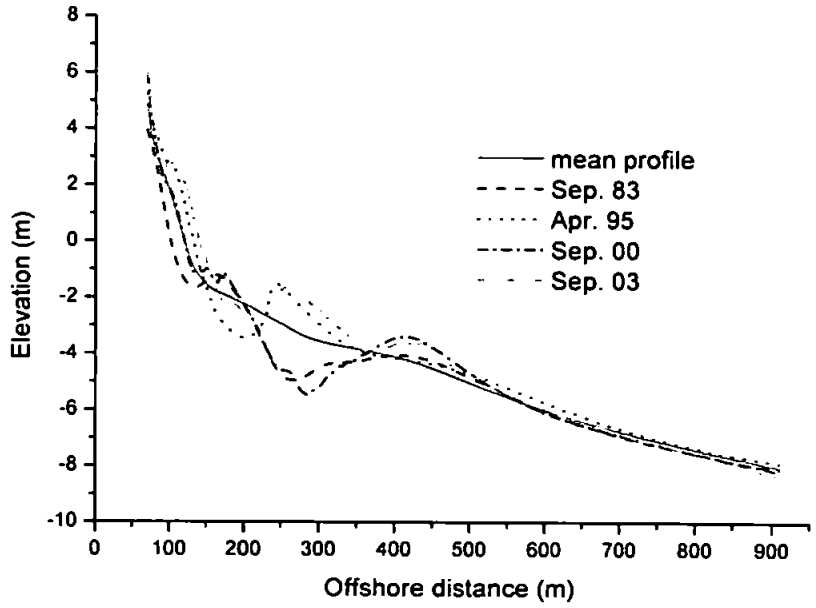

Figure 4.10 Typical profiles with changes from one bar to two bars.

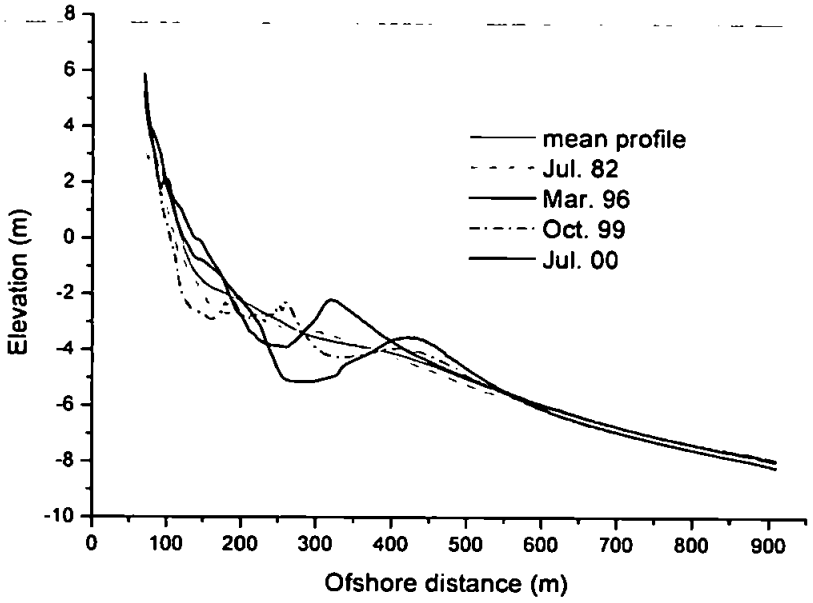

Figure 4.11 Typical profiles in the second eigenvector.

Altogether, the first three eigenvectors account for 75.9% of the overall variability of beach profiles. They explain the bar migration from different aspects. It should be noted that in the previous works most of the authors limited their studies to the first three eigenvectors since the other eigenvectors are much more difficult to interpret. Finally, we emphasise again the stationary assumption of the EOF analysis. For details, please refer to the discussion of EOF in **Chapter 2**.

Chapter 5. SPATIAL ANALYSES OF BEACH PROFILE CHANGES AT DUCK

5.1 Introduction

In this chapter, the field data sets at Duck are analysed using the methodology in **Chapter 3**. The results from one representative profile, line 62, are presented and discussed in detail.

In Section 5.2.1, the variance of the profile is divided among six spatial scales using the AMODWT. The overall variance of each surveyed profile during the course of study is presented over six scales. The predominant variances at particular scales are compared with the temporal weightings in EOF analysis. In Section 5.2.2, the local variation of the profile at different spatial scales is presented. The advantage of wavelet analysis over the EOF analysis is shown. In Section 5.2.3, an effort is made to link the profile changes at larger spatial scales to the wave conditions. In Section 5.2.4, the contours of spatial wavelet standard deviations in the temporal-spatial plane at six scales are presented. In this way, the general spatial variability of the profile during the course of study is investigated. Meanwhile, the infrequent beach profile response to severe storms is identified by the separated contours in deep water. In Section 5.2.5, both the most active zone of the profile changes and the DoC are investigated by identifying the change points in spatial wavelet variance.

The principal conclusions from the results using the DWT/AMODWT in Section 5.2 are summarised in Section 5.3. In response to some limitations of the DWT/AMODWT in studying the beach profile changes both in space and time, the results from the DWPT are presented in Section 5.4 to further identify the scale (frequency) contents at which the profile changes happen. This **Chapter** concludes with a summary.

5.2 Spatial Analyses of Beach Profiles

5.2.1 Variability of beach profiles at several spatial scales

Prior to doing the wavelet analysis the mean profile was subtracted from the profile data to eliminate the profile shape effect on the results. As noted in **Chapter 4**, there are 267 surveys (months) of profile line 62 therefore 267 separate wavelet transforms were conducted on the 421 data across the beach profile to investigate the variability in space. The local variation in the cross-shore direction is partitioned among six spatial scales in a dyadic sequence of multiples of the basic sampling interval (2m). Since each wavelet is a high-pass filter, the resulting detail components in physical spatial scale intervals are 4-8m, 8-16m...and 128-256m. For convenience, the lower limit is referred to in what follows. The spatial AMODWT coefficients $\tilde{d}_{j,t}$ and the relevant wavelet variances $\tilde{\sigma}_j^2$ of all of the beach profiles in the study period were computed using Equations (3.21) and (3.18) separately as described in **Chapter 3**. The overall spatial wavelet variances of beach elevation at all scales are shown in Figure 5.1, plotted against the survey time. The Y-axes in the subplots of Figure 5.1 are not in the same scales to reveal the largest variance at different spatial scales clearly. It can be seen that the wavelet variances of beach profiles are dominated by the coarser scales of 128m and 64m.

Figure 5.1 shows that the profile in May 1996 has the largest wavelet variance at the spatial scale of 128m. By referring to the temporal weightings of Figure 4.9 in the EOF analysis, it is found that the largest weighting of the second eigenvector is for May 1996. From this comparison, it is clear that wavelet analysis also can identify the profile with the largest variance during the course of study. Another peak of wavelet variances at this spatial scale in Figure 5.1 is identified in September 2000, when the temporal weighting of the first eigenvector in the EOF analysis has a negative peak as indicated in Figure 4.9. In order to investigate the common features with larger wavelet variance at the spatial scale of 128m, the configurations of the first four beach profiles having largest wavelet variances are displayed in Figure 5.2. The profiles are from March 1996, September 2000, August 2000 and February 1996, ordered in decreasing variance. It should be noted that July 2000 is another positive peak at the temporal weightings of the second EOF

eigenvector. It is clear that the bars on the four surveys in Figure 5.2 are quite significant both in height and width. For one thing, the bar height of March 1996 was over 1.5m above the mean level. The profile in August 2000 and September 2000 had a deep trough and a quite wide outer bar.

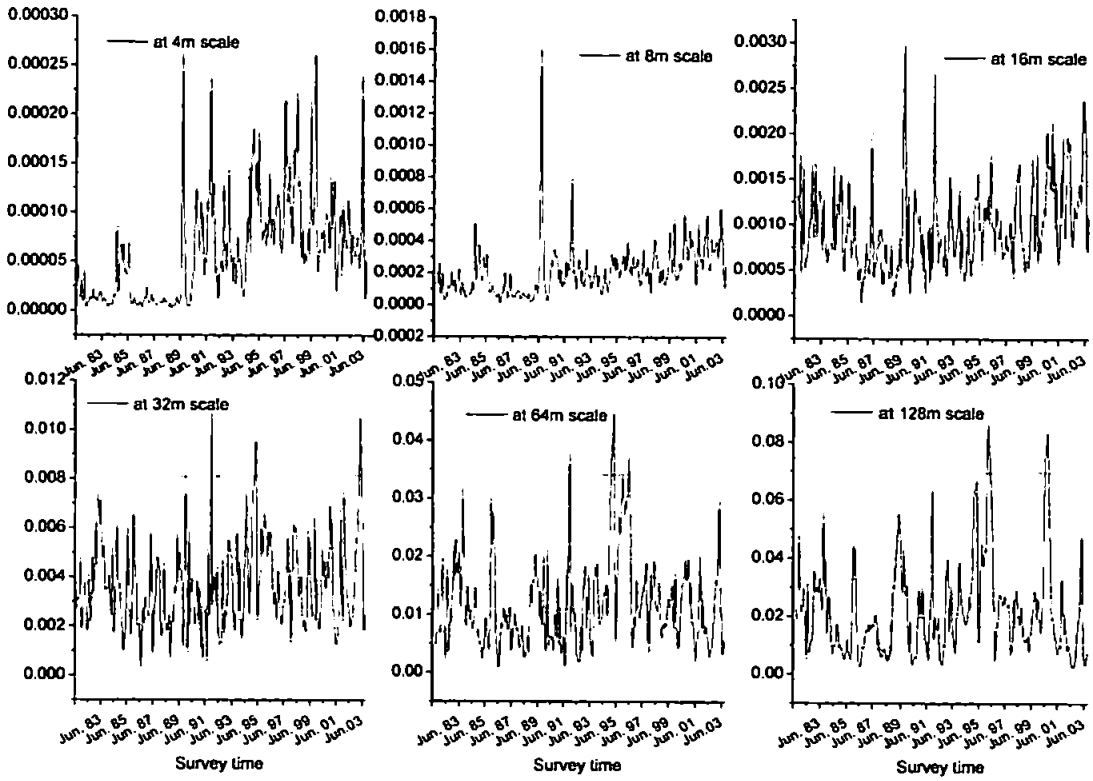

Figure 5.1 Wavelet variance at all spatial scales during survey period (Y axes are not in the same scales).

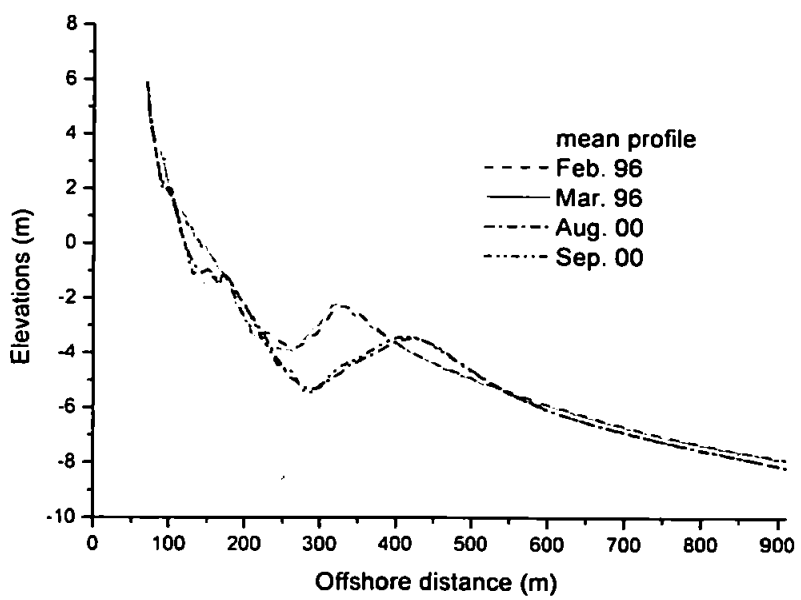

Figure 5.2 The four surveys with the largest wavelet variance at the spatial scale of 128m.

Similarly, it is found that the profile in April 1995 has the largest wavelet variance at the spatial scale of 64m as exhibited in Figure 5.1. In addition, by referring to the temporal weightings of Figure 4.9 in the EOF analysis, it is also found that profile in April 1995 is a positive peak at the temporal weightings of the first eigenvector. The profile that has the second largest spatial wavelet variance at the spatial scale of 64m is identified in March 1995. The plot of the four profiles, April 1995, March 1995, December 1991 and June 1996, with the largest spatial wavelet variances at the spatial scale of 64m is shown in Figure 5.3. These four surveys also have significant bar crests; however, the four bars on these four profiles in Figure 5.3 are much narrower and further landward compared with the bars on profiles shown in Figure 5.2. According to the previous studies, bar crests might move 100m even 200m offshore during storms. For one thing, the bar crest was moved 165m offshore due to the severe storms in November 13-15th in 1981 (Birkemeier, 1985). Thus it can be seen that the changes in the wavelet variances at the spatial scales of 128m and 64m can account for the bar migration, just as the combination of the first two eigenvectors in the EOF analysis does.

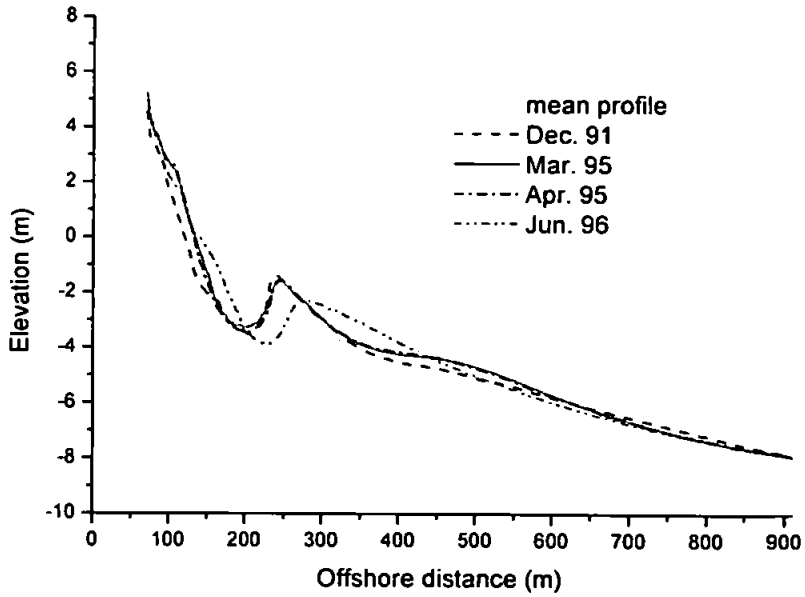

Figure 5.3 The four surveys with the largest wavelet variance at the spatial scale of 64m.

Figure 5.1 shows that during the course of the study the largest spatial wavelet variance at the spatial scale of 32m occurs in December 1991, when the profile has an obvious inner bar just beyond the shoreline. The four profiles with the largest spatial wavelet variances at the spatial scale of 32m are displayed in Figure 5.4, which are from December 1991, April 2003, April 1995 and March 2003. By examining all of the surveys with relatively larger wavelet variance at the spatial scale of 32m, it is found that all of the four beach profiles change significantly in the portion between 110m and 200m along the profile. Therefore, it can be conjectured that the spatial wavelet variances at the spatial scale of 32m can characterize the spatial dimensions of the elevation changes in the portion just seaward of the shoreline.

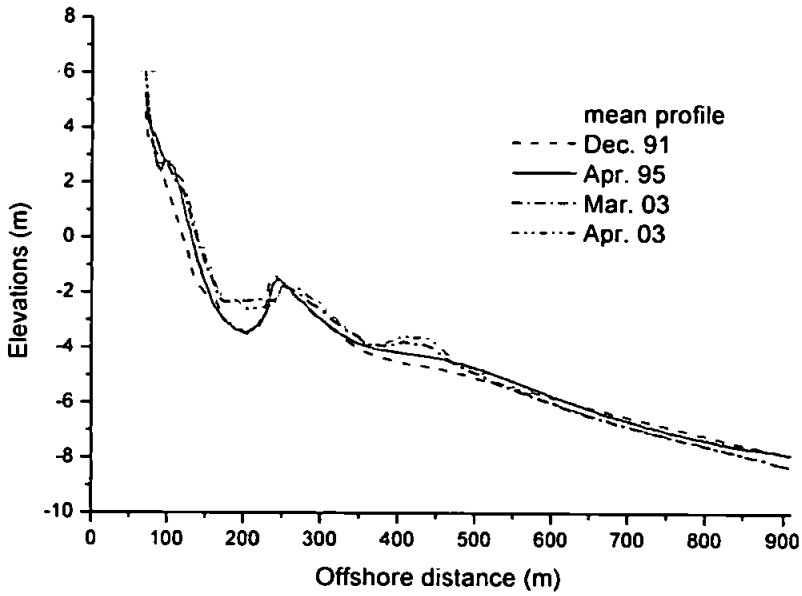

Figure 5.4 The four surveys with the largest wavelet variance at the spatial scale of 32m.

The largest spatial wavelet variance at the spatial scale of 16m is in August 1989, and the second, third and fourth largest spatial wavelet variance are December 1991, September 1989 and April 2003. The four profiles are displayed in Figure 5.5 with the mean across 22 years. In comparison with the profiles with larger variance at the coarser scales, it is found that the four profiles of the largest variance at the spatial scale of 16m have much larger variation in the dune zone and in the region around shoreline. Therefore, the variance at the spatial scale from 4m to

16m can capture some of the elevation changes in the surf zone and the spatial scales define the dimensions of them.

In comparison with the EOF analysis presented in **Chapter 4**, wavelet techniques can be used to identify the different spatial patterns of beach profile changes as does the EOF analysis. Further potential of the wavelet techniques and their superiority over the traditional EOF is demonstrated by tracing the specific surveys that correspond to the largest wavelet variance at different spatial scales.

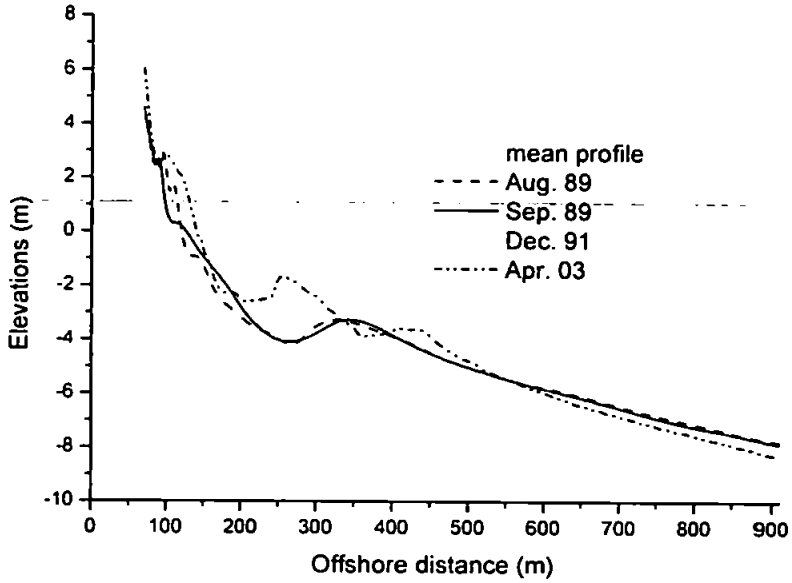

Figure 5.5 The four surveys with the largest wavelet variance at the spatial scale of 16m.

In general, the coarser scales can capture the large beach profile changes in space, and the changes in the steep dune zone can be captured by the finer scales. First, the wavelet variances at coarser scales of 128m and 64m characterize the elevation changes of bar. This result shows that the maximum positive (accretion) elevation changes are typically related to the formation and migrations of bars. Second, the spatial wavelet variances at the spatial scales of 32m and 16m characterize the elevation changes in the portion just seaward of shoreline. Third, some smaller changes in the surf zone can be captured by the spatial scales from 4m to 8m. These conclusions based on the case studies will be investigated further in the following sections. However, the results do illustrate that wavelet techniques are much more powerful than the EOF, since the EOF analysis

does not partition the components of variation by spatial scales, and different components of different scales appear to characterize better the variation of beach elevation in different zones.

Since the profiles having larger variance at the spatial scales of 128m and 64m manifest a profile configuration with well pronounced bars and/or troughs, the surveys with smaller variance are expected to have smooth profile shape without spectacular bed-forms. This inference can be validated by Figure 5.6 that displays the ten profiles having smallest wavelet variance at the spatial scale of 128m. It is obvious that these profile configurations are quite smooth and most of them are surveyed in summer. During summer with low waves, the outer bar moved slightly onshore simultaneously with flattening, to finally disappear. Meanwhile, the deep trough was also filled with sediment and so flattened.

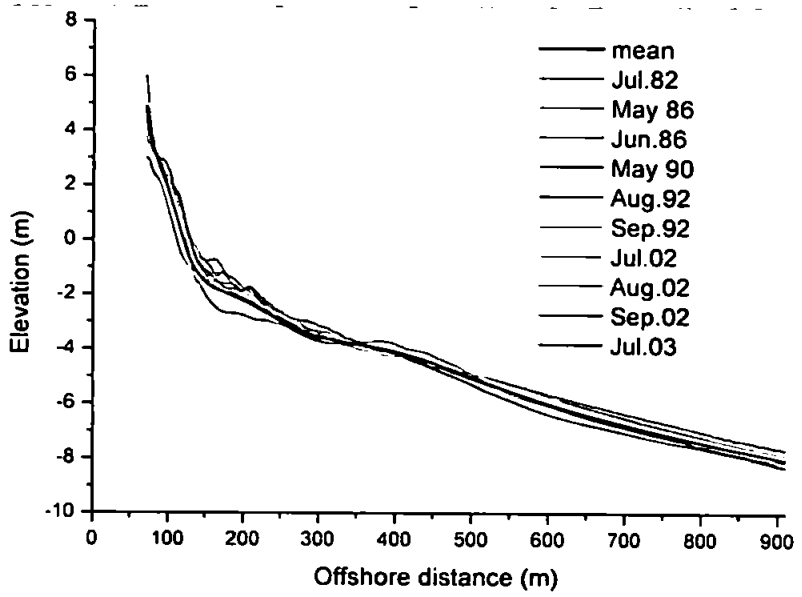

Figure 5.6 The ten surveys with smallest wavelet variance at the temporal scale of 128m.

5.2.2 Multi-scale analysis of beach profile change in space

The profile in March 1996, as shown in Figure 5.2, was used to show how readily the wavelet analysis decomposes the beach profile variation into different scales. The spatial wavelet coefficients $D_{j,k}$ were calculated using the DWT and the wavelet coefficients were reconstructed to detail components scale by scale. The detail components were plotted against offshore distances

as shown in Figure 5.7. By this multiresolution analysis, the beach profile changes were divided to a range of spatial scales so that changes at different positions along the profile can be characterized well by different spatial scales.

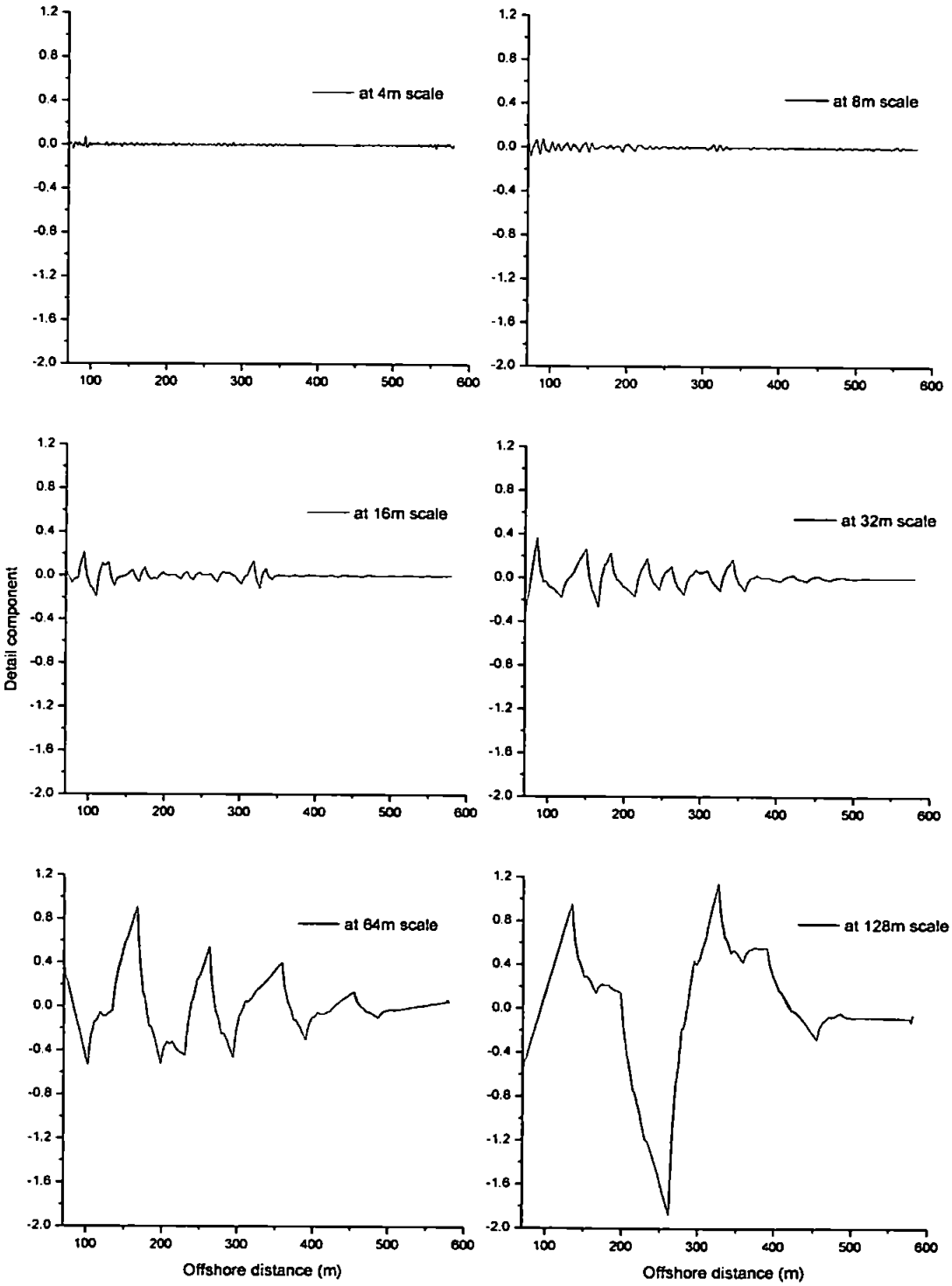

Figure 5.7 The detail components of the profile in March 1996.

The locations where variation from different scales affects the profile are vividly shown in Figure 5.7, which cannot be identified by other statistical methods. It also can be seen that the variation of this profile from the mean is mainly at the spatial scale of 128m. The details at the spatial scale of 128m clearly show that the negative peak corresponds to the trough (220-270m) and the positive peak corresponds to the bar (270-400m) in this profile, as seen in Figure 5.2. However, in this multi-scale analysis the variation beyond 582m offshore cannot be analysed because the DWT requires that the input data is an integer power of 2. In what follows the AMODWT analysis was used to take full advantage of the profile data from 70m to 910m offshore.

To explain the localization of the variation of beach profiles at different spatial scales, we focus on the profiles with the largest wavelet variance at the spatial scales of 128m, 64m, 32m and 16m as identified from Figure 5.1. For one thing, the surveys in March 1996 and April 1995 correspond to the significant peaks at the spatial scale of 128m and 64m respectively. In addition, another profile in March 1992 with smaller variances is also presented to compare with the characteristics of the profiles with larger variances. The wavelet variance at the spatial scales of 8m and 4m will not be investigated specifically since they contribute less to the overall variance as shown in Figure 5.1.

Figure 5.8 shows the accumulated components of the AMODWT spatial wavelet variances of beach elevation in March 1996, plotted against offshore positions. Each layer of the graph corresponds to one of the spatial scales, and at any position the thickness of the layer shows the size of the wavelet variance component at that scale and location. On the whole, the contribution of wavelet variances at the spatial scale of 128m is largest landward of 450m, and there is almost no variance of beach elevation seaward of 450m. However, the spatial wavelet variances between 125-150m are dominated by the spatial scale of 64m. The wavelet variance components at the spatial scales of 16m and finer is much obvious landward of 100m. The results indicate that the significant spatial scale at which profiles vary differs across the beach profile although the total variance is mostly dominated by the spatial scale of 128m.

Figure 5.9 shows the accumulated components of the spatial wavelet variances of beach elevation in April 1995, plotted against offshore distance. The overall wavelet variance of the survey in April 1995 is slightly smaller than that of March 1996. Moreover, the components of

spatial wavelet variances at the spatial scales of 64m are much larger around 140-200m than those of March 1996 as shown in Figure 5.9. This result can be explained by the deep trough located in this area. Apart from the dominant variances at the spatial scales of 128m and 64m, the relatively large variance component at the spatial scale of 32m around 230m offshore captures the narrow bar crest. It also can be seen that there are no significant variance components seaward of 400m at all spatial scales.

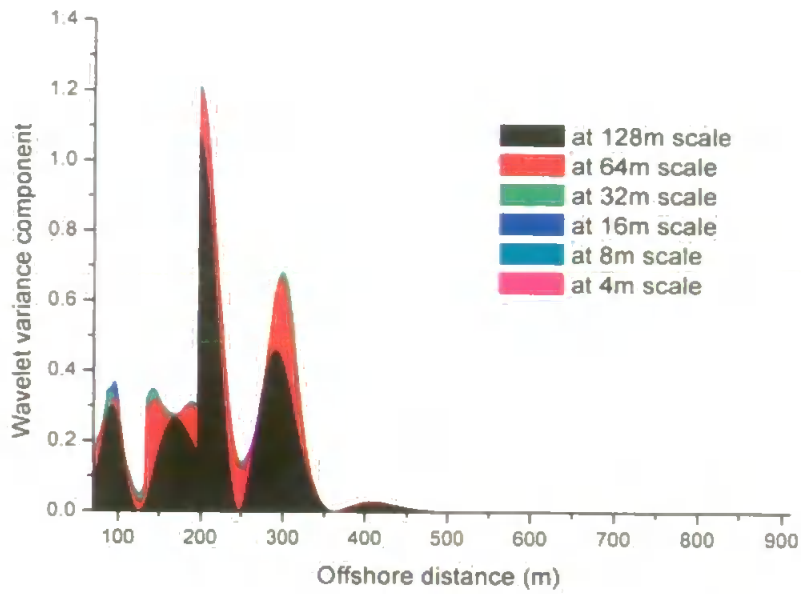

Figure 5.8 Accumulated wavelet variance component ($\tilde{d}_{j,k}^2 / 2^j$) for the profile in March 1996 (MSL intercepts at120m).

Figure 5.10 shows the accumulated components of the spatial wavelet variances of beach elevation in December 1991. Although the variance of beach elevation is mainly at the spatial scale of 128m, the wavelet variance components at the spatial scale of 32m can be identified clearly from Figure 5.10. The obvious region of the profile that has significant variance at the spatial scale of 32m is in the region from 196m to 238m offshore with two peaks at 204m and 230m, where the deepest trough and the highest bar crest are respectively.

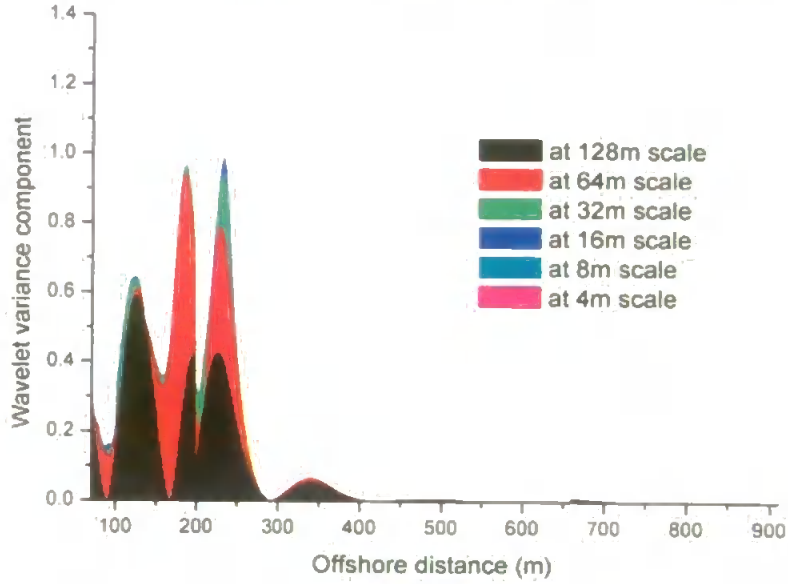

Figure 5.9 Accumulated wavelet variance component ($\tilde{d}^2_{j,k}/2^j$) for the profile in April 1995 (MSL intercepts at120m).

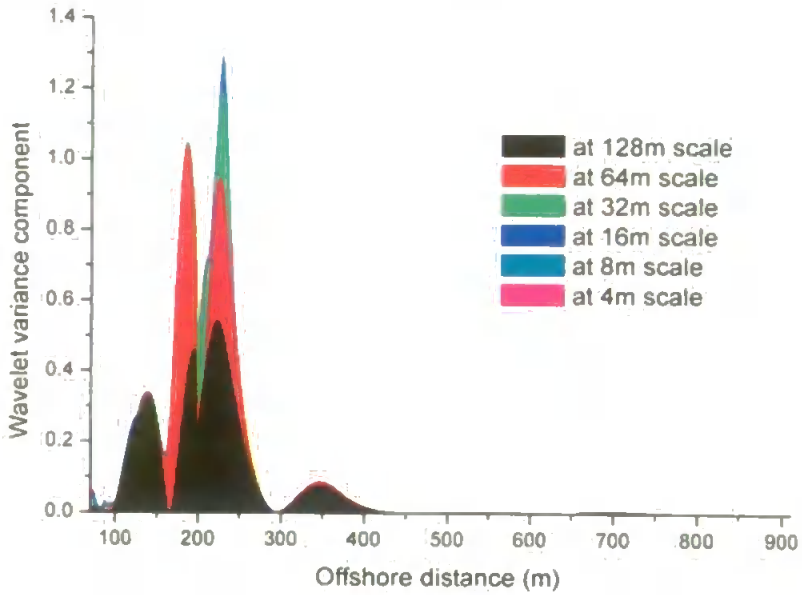

Figure 5.10 Accumulated wavelet variance component ($\tilde{d}^2_{j,k}/2^j$) for the profile in December 1991 (MSL intercepts at120m).

Figure 5.11 shows the accumulated components of the spatial wavelet variances of beach elevation of the survey in August 1989. A striking feature from Figure 5.11 is that the overall variance of beach elevation in August 1989 was quite small compared with those of the above three

profiles. This result is not surprising since the profile in August is usually rebuilt by the milder summer waves. Another conspicuous feature in Figure 5.11 is that the wavelet variance components around 100m landward are dominated by the finer scales, especially by the spatial scale of 16m. This can be seen clearly from the enlarged part of the dune zone as shown in the right plots of Figure 5.11. This result indicates that the wavelet variance at the spatial scale of 16m can characterize better the profile changes in the dune zone since this zone is quite narrow and steep. Moreover, it is seen that even in such a narrow region 70m-150m the contribution of variances from different spatial scales is different. This result shows the complex character of beach profile changes in space.

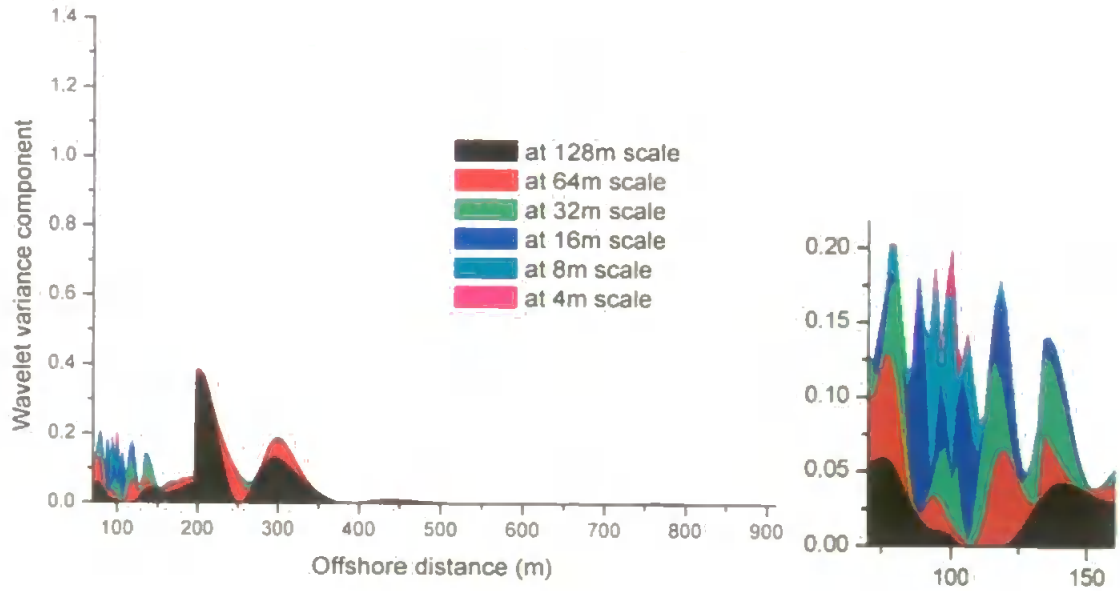

Figure 5.11 (Left) Accumulated wavelet variance component ($\tilde{d}^2_{j,k}/2^j$) for the profile in August 1989 (MSL intercepts at120m). (Right) Enlarged plots in the dune zones.

Figure 5.12 shows the accumulated components of the spatial wavelet variances of beach elevation of the profile in March 1992. The overall wavelet variance of beach elevation of the survey in March 1992 is close to that of August 1989; however the dominant spatial scales that contribute most to the beach profile changes are different. This difference is associated with the month that the profile was surveyed. It can be seen from Figure 5.12 that in March 1992 the

dominant spatial scales at which significant change of beach elevation occur are 128m and 64m. It is obvious that the profile in March 1992 presented a winter bar form whilst the profile in August 1989 was typical summer one. Moreover, the wavelet variance component at the spatial scale of 32m shows its maximum around 130m offshore where is the deepest point of the trough. The bar crest is located at 210m where the variance mainly comes from the spatial scale of 64m. This smaller spatial scale captures the steep bed-form seaward of the shoreline.

The five representative case studies of spatial variances of beach elevation indicate that wavelet analysis can be used to both identify the local variation of beach profiles and partition the variances into a range of spatial scales. In this way, the smaller scale changes that are usually shadowed by larger scales can be identified. Generally speaking, the wavelet variance components of beach elevation at a range of spatial scales in the five surveys clearly show the spatial non-stationarity of beach profile changes, as we expect. It is also found that when the overall variance is large the proportion of variance at coarser spatial scales is often the largest, and vice versa.

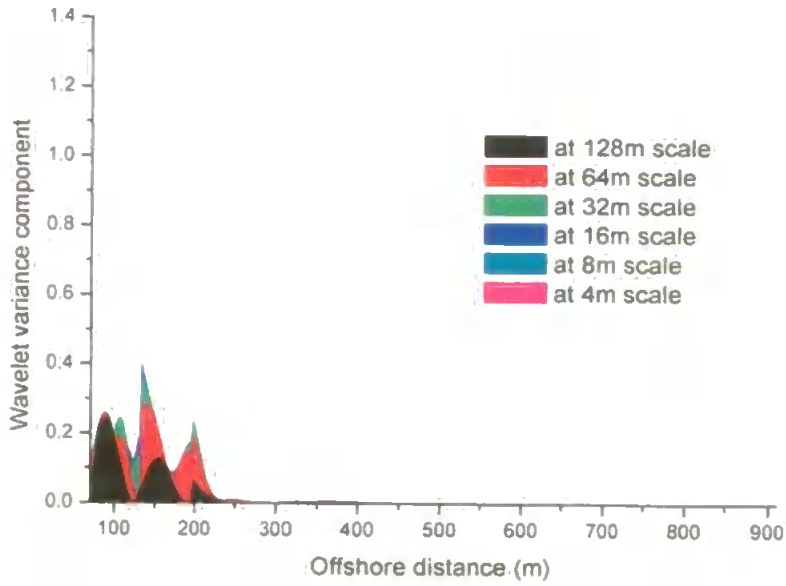

Figure 5.12 Accumulated wavelet variance component ($\tilde{d}_{j,k}^2 / 2^j$) for the profile in March 1992.

In addition, there are a few obvious features in Figures 5.8-5.12. The significant variance of the profile in March 1996 was in the region from 200m to 350m with the maximum at 210m offshore. The significant variance of the profile in April 1995 was in the region from 100m to 280m with the

maximum located 240m offshore, while the significant variance of the profile in March 1992 was in the region from 70m to 180m with the maximum at 130m offshore. It is apparent that the spatial wavelet variance components of beach elevation are almost down to zero seaward of 450m at all scales for the profile in March 1996. Similarly, there is no significant variance seaward of 400m for the profiles in April 1995 and December 1991. In addition, no obvious variance can be identified seaward of 370m from the profile in August 1989 and seaward of 300m from the survey in March 1992. These results suggest that wavelet variances might be a means to identify the DoC of beach profiles. This will be investigated further in Section 5.2.4.

5.2.3 Seasonal patterns of beach profile changes

Some tentative conclusions, which have to be further substantiated, have been drawn from the above case studies of the variability of beach profiles in space. On the whole, most of the surveys with the largest wavelet variance of beach elevation at the spatial scale of 128m and 64m are in February, March and April. On the other hand, the surveys with the largest wavelet variance at the spatial scale of 16m are in August. These results indicate the scale-dependent characteristic of beach profile changes might be related to the seasonal wave conditions.

During late autumn and winter beach profiles experience high-energy waves or storms, so usually the dimension of beach profile change is large and the variation of beach elevation is significant. In consequence, the wavelet variances of profiles are larger at the coarser spatial scales in late winter and early spring (February, March and April). During spring and summer, the weather is calm so that beach profiles respond to mild waves. Therefore, the beach elevation changes are smaller in magnitude and the spatial dimensions of changes are smaller in late summer and early autumn spatial scales. This is supported by the wavelet variance components of the survey in August 1989. In addition, the variances at the finer scales are more obvious in the dune and surf zones than those of the other zones, because beach profiles in the surf zone experience a few kinds of varied forcing conditions, such as small waves as well as storms. However, in deep water beach profiles will only respond to strong storms.

To validate this seasonal pattern of beach profile changes that resulted from the above case studies, the overall wavelet variances of beach profiles during the 22 years were averaged into

calendar months at all spatial scales and shown in Figure 5.13. It is obvious that the overall average wavelet variance increases as the spatial scale increases. It can be seen that at the spatial scale of 128m the largest monthly average wavelet variance is in February and the smallest is in August. It also can be seen from Figure 5.13 that at the spatial scale of 64m the average wavelet variance is largest in December and the smallest in August. The overall trend at these two coarser scales is that the variance is small in June, July and August and large in December, January, February and March.

The average monthly wavelet variance at the spatial scale of 32m shows a slight difference from that of 128m and 64m, which may be due to some delay. Figure 5.13 also shows that the average wavelet variance at the spatial scale of 16m is largest in April and smallest in November. In addition, the average wavelet variance at the spatial scale of 8m and 4m shows an inverse temporal structure from that of 128m and 64m, because the largest wavelet variance at the two finer scales is in summer (August) and the smallest is in winter. Due to the small wavelet variance at the smaller spatial scales, they are not discussed further.

It is interesting to find that the shape of the monthly wave height plot (Figure 4.3) is extremely similar to the wavelet variance at the spatial scales of 128m and 64m. This may indicate that on average the deterministic pattern of beach profile changes responds to the seasonal wave conditions. However there are still some small scale beach profile changes that cannot be explained by a simple correlation with the wave heights. This conclusion supports the contention that the beach profile change is a highly non-linear dynamic system that cannot be explained simply by the wave conditions.

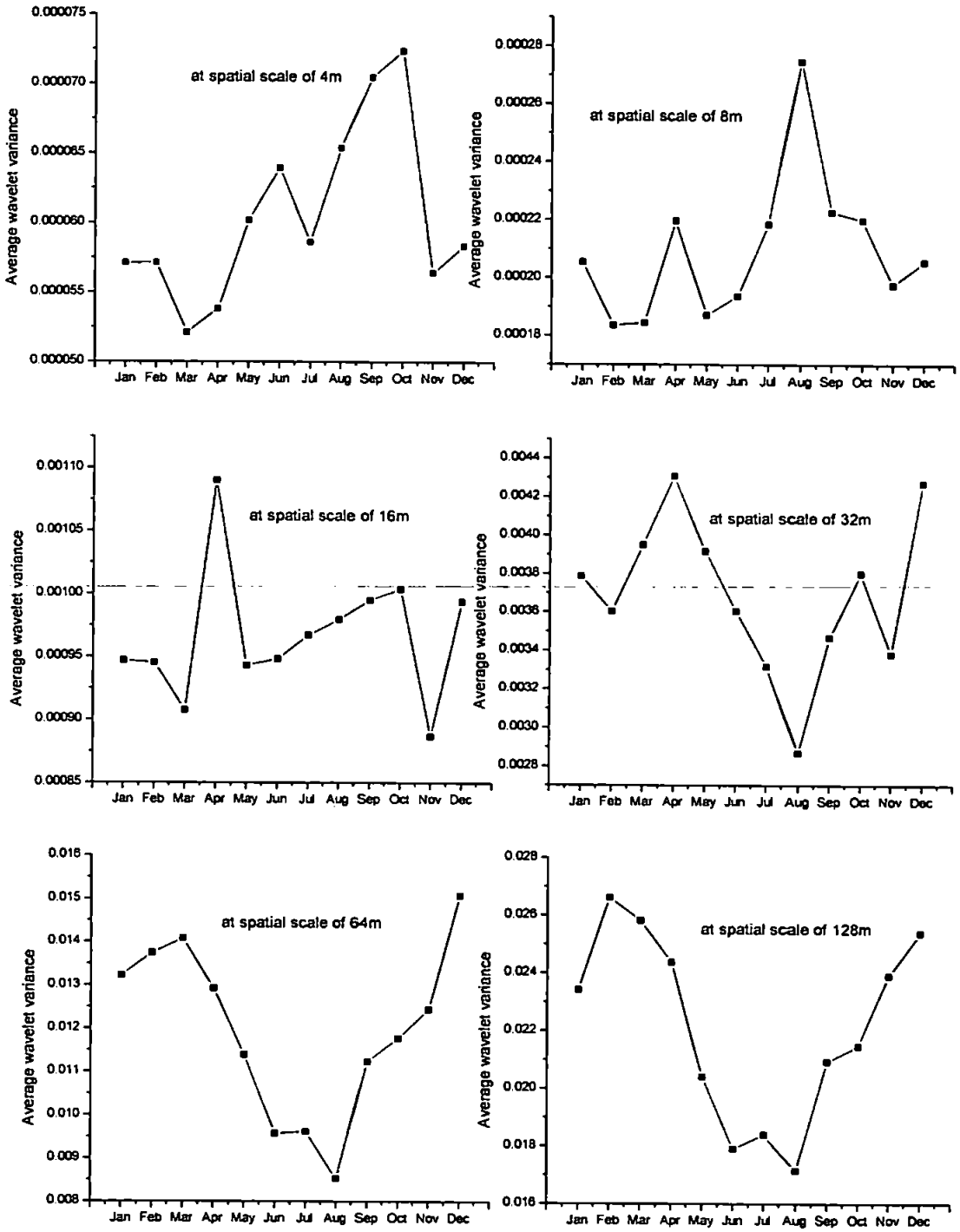

Figure 5.13 Monthly average wavelet variance across 22 years at all spatial scales.

5.2.4 Contours of the spatial wavelet standard deviations of beach elevation

In Section 5.2.2, a few case studies have been conducted to study the variability of beach profiles over a wide range of spatial scales. In addition to the case studies, the spatial variability of beach profiles was related to the seasonal forcing conditions by investigating the monthly average wavelet variances during the 22 years. To investigate the deterministic patterns at different spatial scales of beach profile changes further during the course of study, the spatial wavelet standard deviation (SD) of beach elevation was studied. This kind of study aims to identify the extraordinary events as well as the general (average) deterministic patterns of beach profile changes.

The spatial wavelet SD components of beach elevation of each survey were computed using Equation (3.23).The contours generated from the spatial SD components among all of the surveys were plotted on the space/time plane scale by scale. In the following plots, the vertical axis (space) is the offshore distance and the horizontal axis (time) is the month when the profile was surveyed. The darker contours denote the larger wavelet SD components, and vice versa.

Figure 5.14 shows the contours at the spatial scale of 4m during the course of the study. The maximum spatial SD at this spatial scale is 0.1. It can be seen from Figure 5.14 that most of the contours are distributed landward of 200m with the maximum in the dune zone. Moreover, the region with the largest SD is around the 48th month (June 1985) located 70m-120m offshore. This result suggests the large change of elevation in the dune zone in June 1985. Another two regions with larger SD in the same portion along the profile are around the 110th month (August 1990) and 198th month (December 1997). It is obvious that the contour patches with larger SD are centred in the dune zone at the spatial scale of 4m.

Figure 5.15 shows the contours at the spatial scale of 8m. The maximum spatial SD at this scale is 0.14. Generally speaking, the contours at this scale are distributed in a wider portion along the profile than that of spatial scale of 4m. There are a few regions with larger wavelet SD in the dune zone around the 24th, 96th and 260th months, which are in June 1983, June 1989 and February 2003. Apparently, most of the significant wavelet SD of beach elevation at the spatial scale of 8m is still identified during the period from June to August. Two similar regions centred in the 148th survey (October 1993) and 235th (January 2001) are observed from Figure 5.15. Both of them are located at 100m-180m offshore.

Figure 5.16 shows the contours at the spatial scale of 16m. The maximum spatial SD at this scale is 0.26, which is much larger than those of the two finer scales. Also, the distribution of the contours extends offshore further. There are three regions with relatively larger SD located 190m-290m during the course of study, which contrasts with the smaller SD at the two finer scales. In addition to the above features in Figure 5.16, the SD in the dune zone still has a significant contribution at the spatial scale of 16m.

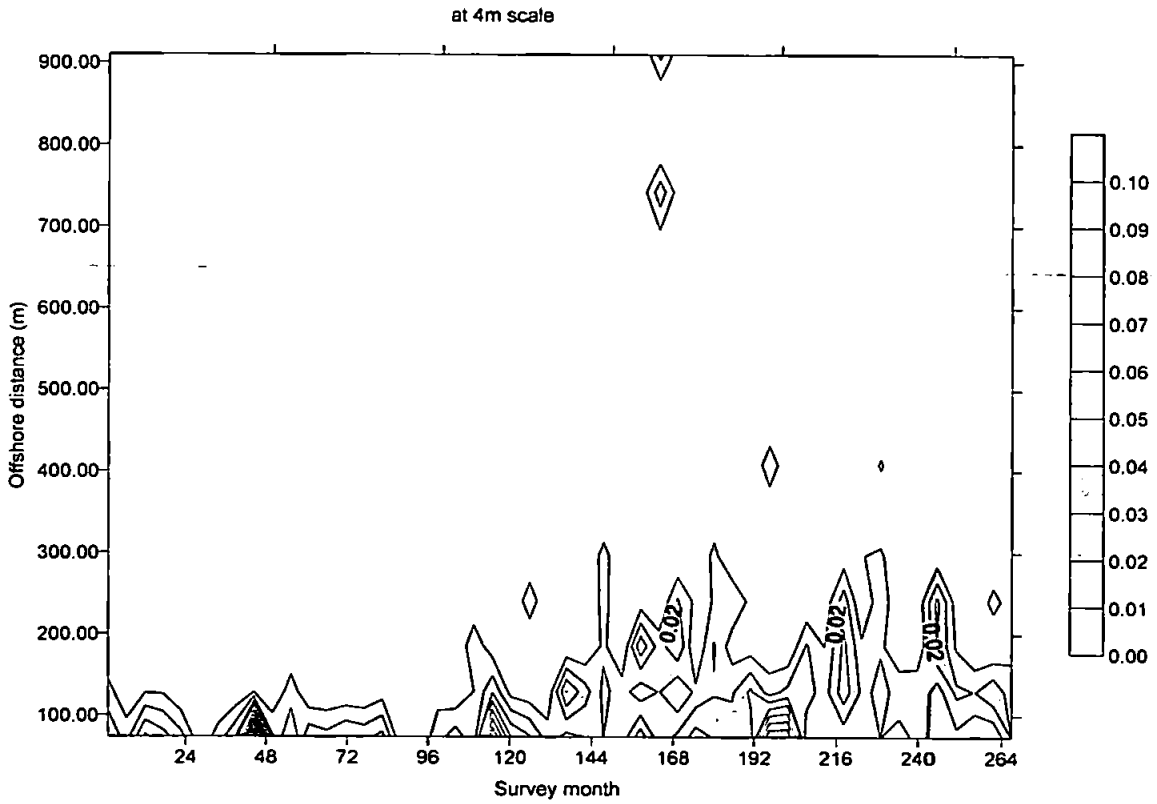

Figure 5.14 Contour of wavelet SD at the spatial scale of 4m during the course of the study.

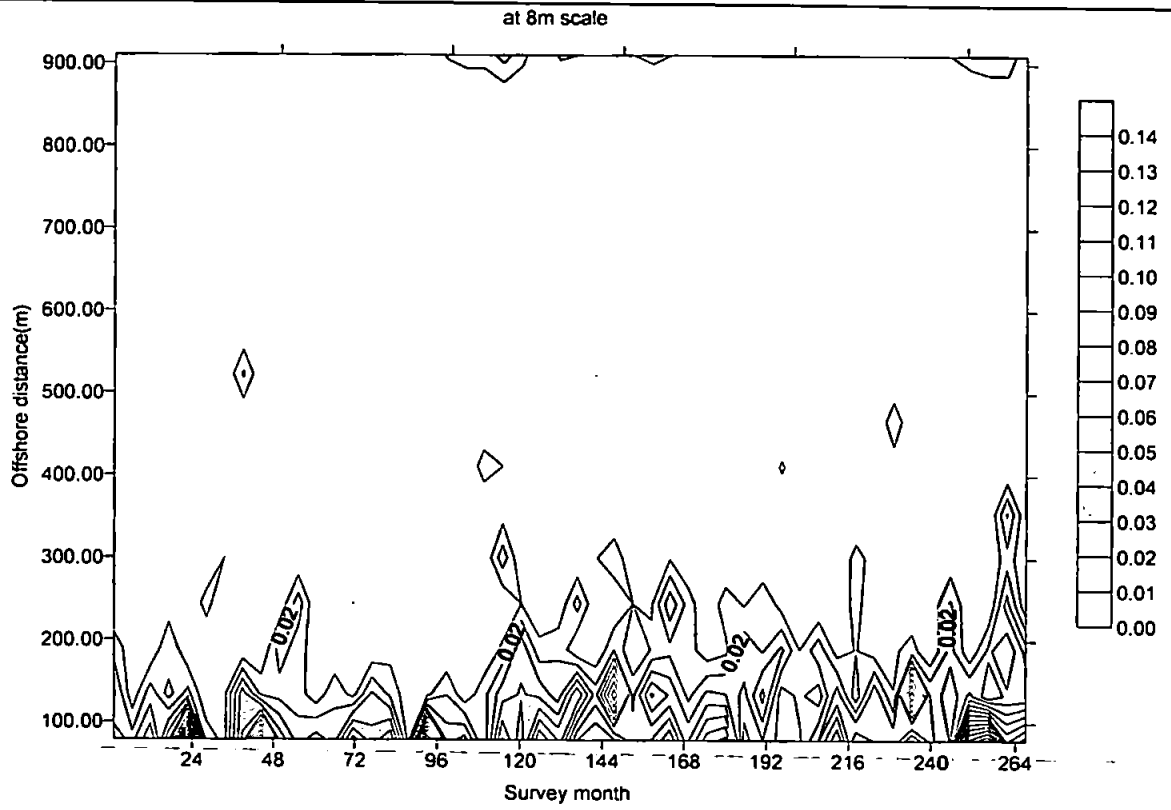

Figure 5.15 Contour of wavelet SD at the spatial scale of 8m during the course of the study.

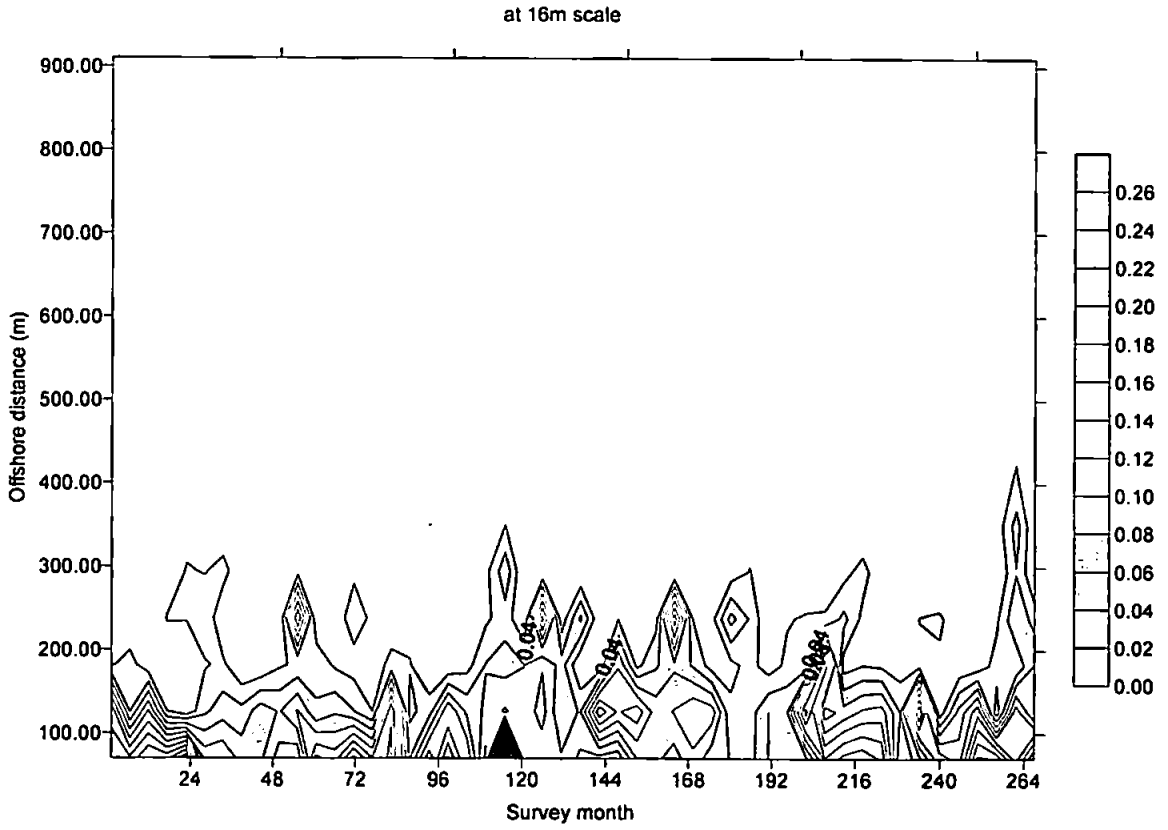

Figure 5.16 Contour of wavelet SD at the spatial scale of 16m during the course of the study.

Figure 5.17 shows the contours at the spatial scale of 32m. The maximum spatial SD at this scale is 0.45, which is almost twice of that of spatial scale of 16m. It also can be seen that the SD in the dune zone has become less significant in comparison with those of the three finer scales. The three patches on the contours of wavelet SD at the spatial scale of 16m are still present at this scale. Also, the large wavelet SD in the dune zone around the 24th (June 1983) is still present.

Figure 5.18 shows the contours at the spatial scale of 64m for the period of the study. It can be seen that the maximum spatial SD at this scale is 0.7. The region of the largest SD is centred in the 128th month (February 1992) located at 150m-290m offshore. A small separate contour of SD is centred in the 228th survey (June 2000) around 400m offshore. This can be explained by the severe storms on 29th May 2000 with wave heights up to 5.0m and wave periods up to 10s. During the storms, sediment was transported offshore resulting in the formation of a distinct outer bar, which grew in size. In consequence, the volume of sediment on the upper shoreface increased abruptly.

Figure 5.19 shows the contours at the spatial scale of 128m for the period of the study. The maximum spatial SD at this scale is as same as that of spatial scale of 64m. It can be seen that the contours at the spatial scale of 128m extends to 400m offshore. A number of contours in Figure 5.19 are identified in a narrow region around 230m offshore, therefore they are related to the movement of the inner bar. The dense contours from 70m to 150m are related to the sediment transport between dune zone and shoreface. Apart from these dense contours in the surf zone, there are two obvious contours of SD around 700m offshore (in deep water). One is around the 142nd survey (April 1993), and another is the 228th survey (June 2000), which has been discussed at the spatial scale of 64m. The wave conditions presented in **Chapter 4** show that there was a very severe storm on March 13, 1993 (the storm of century) with wave heights up to 4.6m and periods up to 12.19s. In addition, there was a storm surge of 1.3m in height.

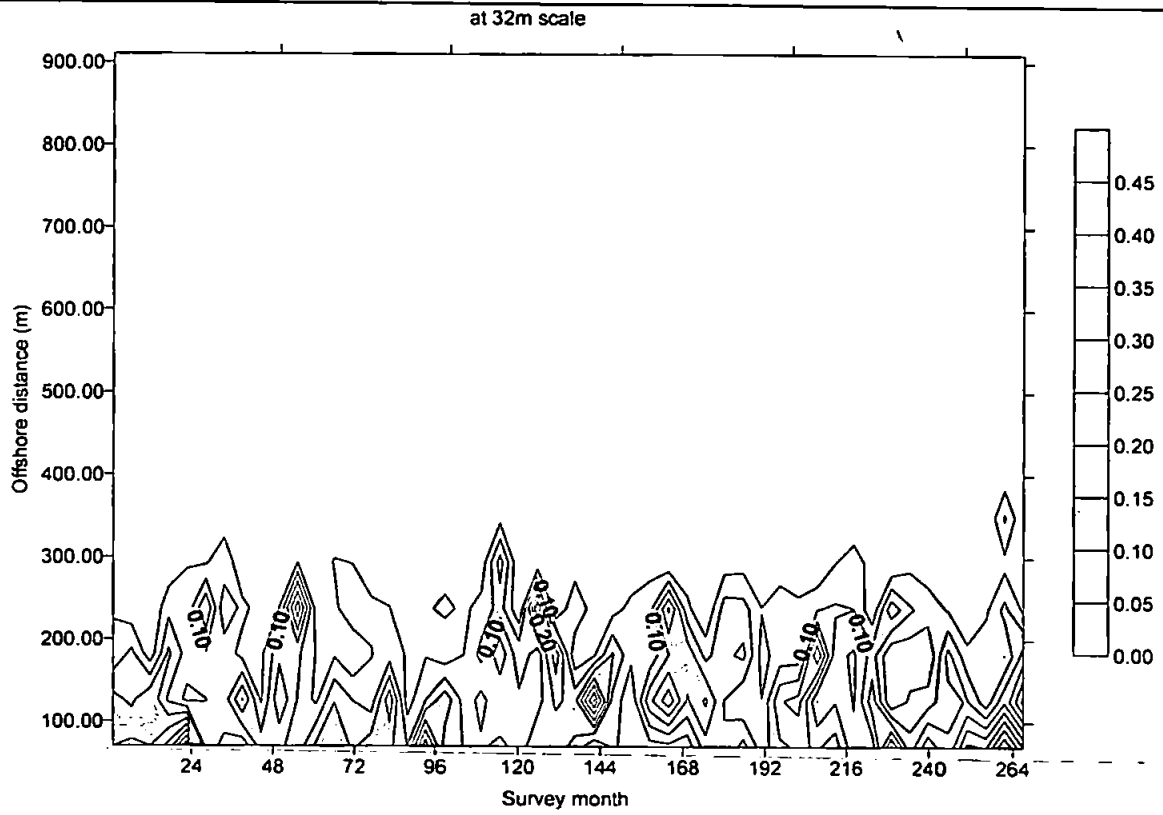

Figure 5.17 Contours of wavelet SD at the spatial scale of 32m during the course of the study.

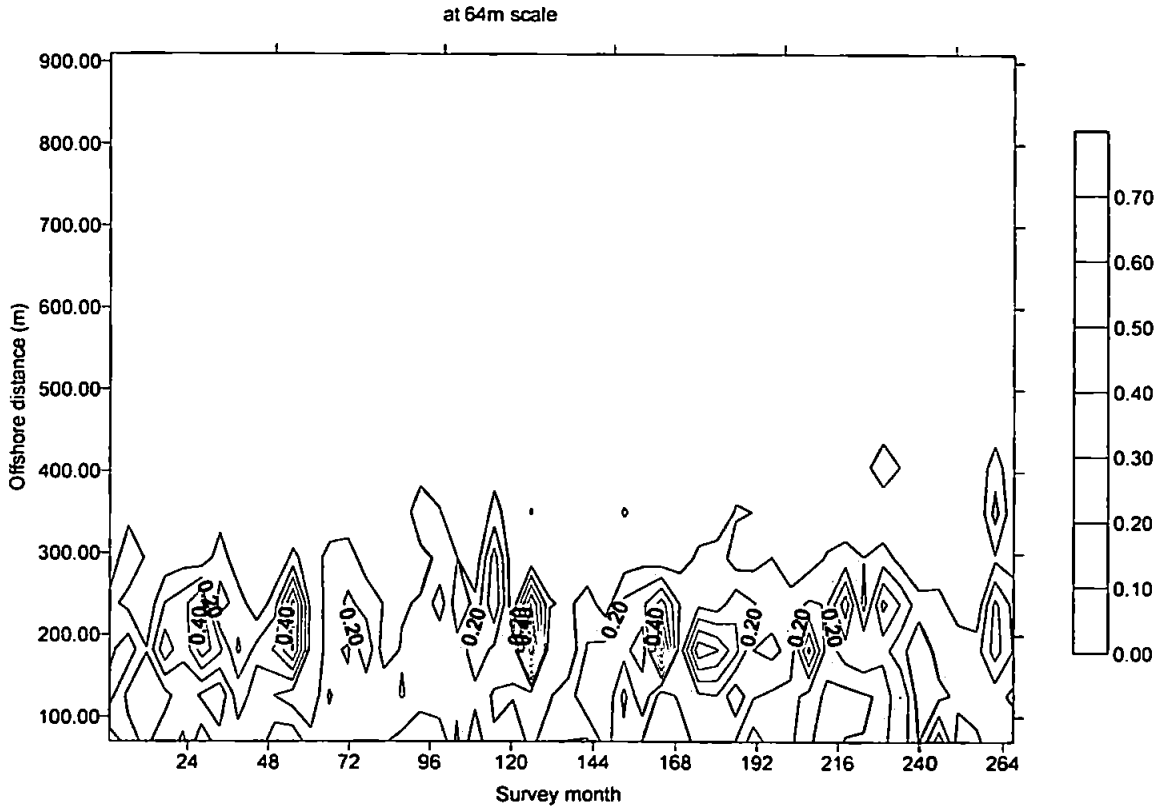

Figure 5.18 Contour of wavelet SD at the spatial scale of 64m during the course of study.

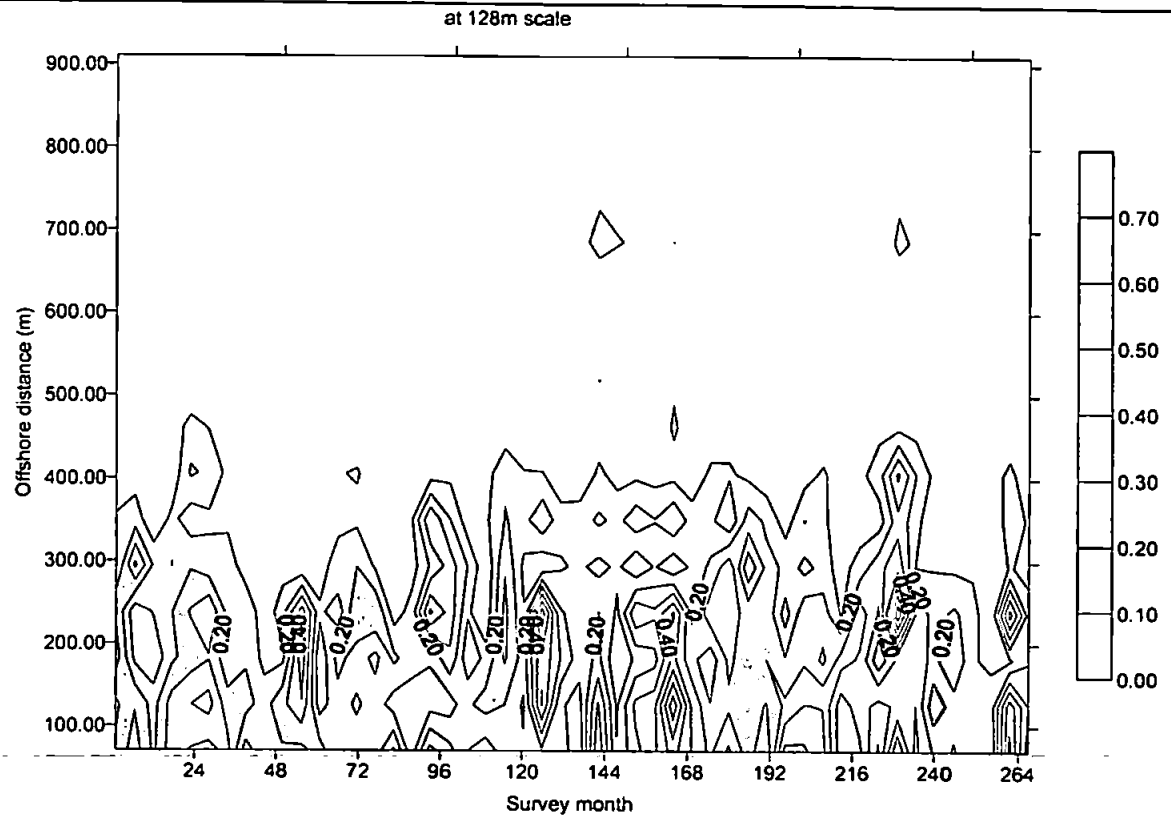

Figure 5.19 Contours of wavelet SD at the spatial scale of 128m during the course of the study.

So far, the features of the contours of spatial wavelet SD of beach elevation have been identified scale by scale so that both the general pattern of beach profile changes and the infrequent individual events have been interpreted. All the six sets of contours at different spatial scales almost have no contours seawards of 500m during the course of the study. The contours in the region from the shoreline to about 300m offshore are especially dense, which illustrates that the sediment transport is most active in this zone. This result is in agreement with the findings of previous work such as Lee *et al.* (1998) who observed the vertical range of the profile envelop during 1981-1991 at Duck. Moreover, the maximum wavelet SD of beach elevation increases with the spatial scales. This result further emphasizes that when the beach elevation changes are in larger magnitudes in vertical the spatial dimensions of the changes are also larger.

In addition to the common features of the contours, the scale-dependent characteristic of the beach profile changes is also quite obvious. It is found that the contours of the wavelet SD at the spatial scale of 4m and 8m are quite similar and the dense patches on them are centred in the dune zone. The dense patches in the dune zone at the spatial scale of 4m, 8m, 16m and 32m cannot be

found at the spatial scales of 64m and 128m. This result indicates that beach elevation changes in the dune zone can be well captured at the spatial scale smaller than 32m. This finding can be verified by the configuration of beach profiles that the slope in the dune zone is quite steep at Duck, such as example is shown in Figure 5.11.

It is also found that the contours of wavelet SD of beach elevation at the spatial scale of 64m and 128m are also quite similar. The dense patches of contours at these two spatial scales are centred in the later autumn or winter surveys located in the region from 180m to 270m offshore. Therefore the wavelet variance from these two coarser scales reflect the larger change of beach profiles during later autumn and winter, which is usually related to the offshore movement of the bar. The bar migrations are also the key characteristic of beach profile changes, which also has been evidenced by the case studies in Section 5.2.2.

Meanwhile, the effect of the infrequent extraordinary events, such as the extreme single storm or storm groups, on the profile can also be identified at different spatial scales from the contour of wavelet SD, such as the century storm on March 13, 1993.

5.2.5 Identifying change points in spatial variance of beach elevation

All the above results show that the local variance components of the profile are quite indicative of the most important changes along the profile. Thus, to quantify these changes, locations of significant change in spatial wavelet variance were identified at each spatial scale against the critical values listed in Table 3.2 following the procedure developed in **Chapter 3**.

The identified change points in the wavelet variance were plotted on the contours of SD at the same spatial scales. The marks 1, 2, 3, 4 and 5 on the plots are the ranked orders of identified changes in the spatial wavelet variance. Therefore, the points on the plots marked with a '+ 1' are the locations where the largest change in variances along the profile at each survey is identified. According to the methodology in **Chapter 3**, the lower orders denote the most significant change in the wavelet variance; therefore the changes in the first three orders are discussed.

Figure 5.20 shows shaded contours of spatial wavelet SD with points of significant changes in spatial wavelet variances at the spatial scale of 4m. The first order changes in wavelet variances at

the spatial scale of 4m are identified in the region from 120m to 280m offshore and concentrated at 160m offshore, as shown in Figure 5.20. It also can be seen that the identified change points in wavelet variances in the second order are scattered in a broad range from the dune zone to very deep water. The results indicate the non-uniformity of variance at the spatial scale of 4m along the profile.

Figure 5.21 shows shaded contours of spatial wavelet SD with points of significant change in spatial wavelet variances at the spatial scale of 8m. The distribution of changes in wavelet variance at the spatial scale of 8m is quite similar to that of 4m in that the changes in the wavelet variance identified in the first order are also centred at 160m offshore. However it can be seen from Figure 5.21 that the distribution of the first order changes is concentrated in a narrower region than that of from spatial scale of 4m.

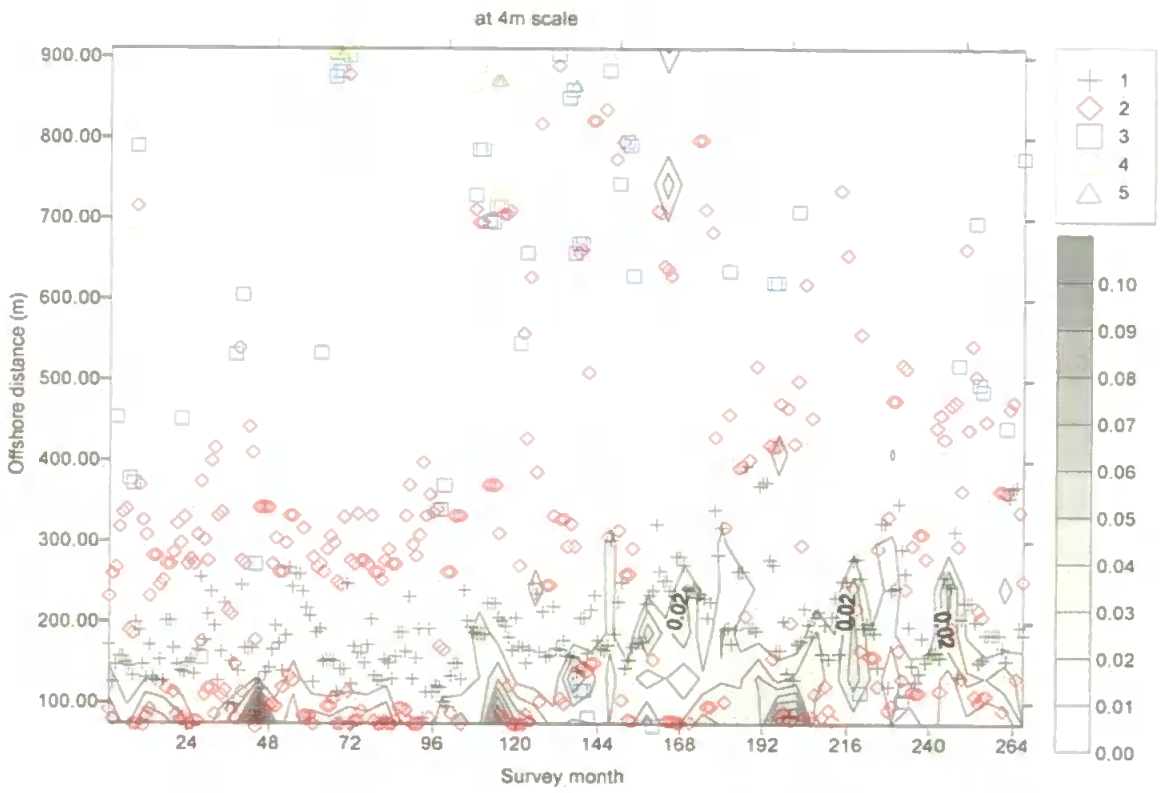

Figure 5.20 Distribution of change points in the wavelet variance at the spatial scale of 4m.

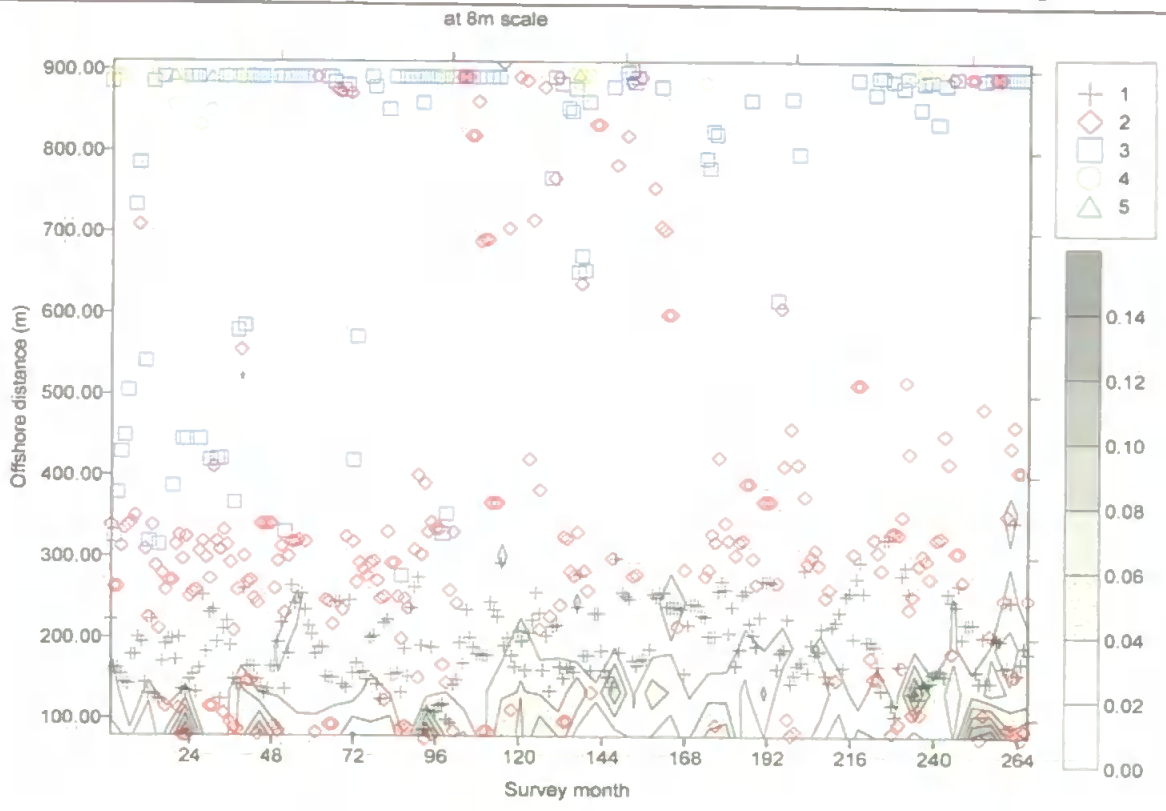

Figure 5.21 Distribution of change points in the wavelet variance at the spatial scale of 8m.

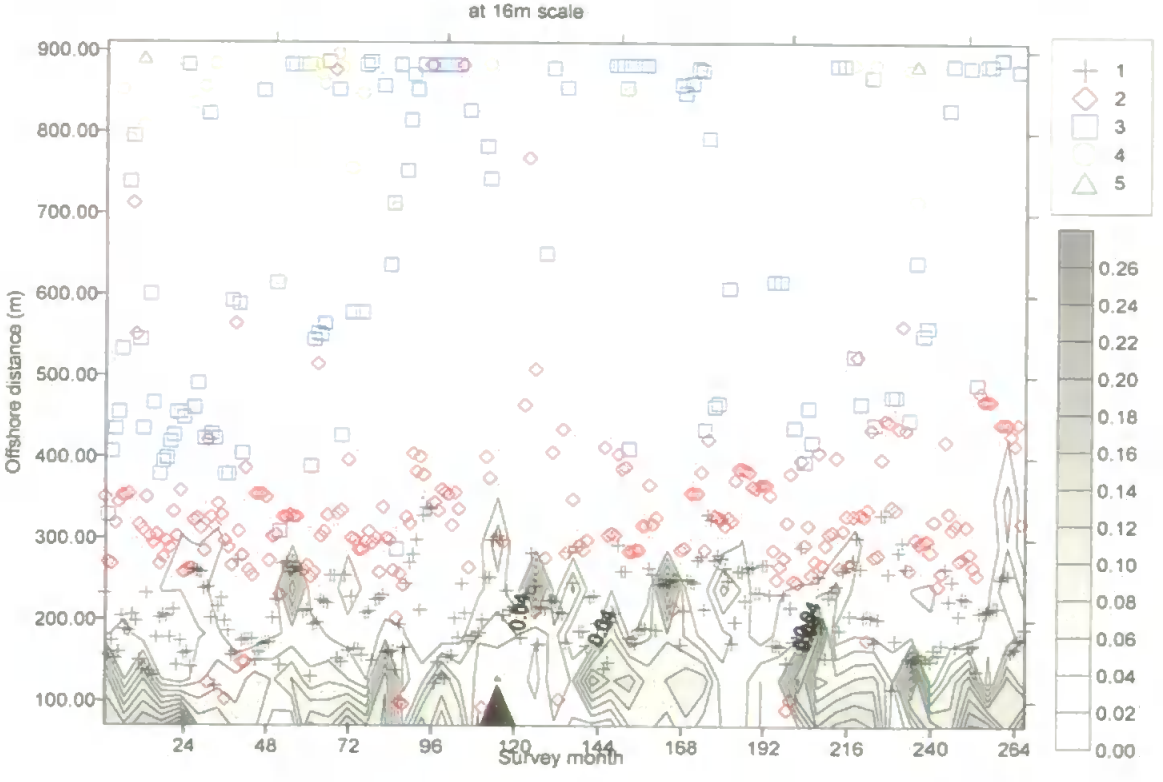

Figure 5.22 Distribution of change points in the wavelet variance at the spatial scale of 16m.

Figure 5.22 shows shaded contours of spatial wavelet SD with points of significant change in spatial wavelet variances at the spatial scale of 16m. It can be seen from Figure 5.22 that the changes in the wavelet variance identified in the first order are centred at 175m offshore. Comparatively, the distribution of second order changes in the spatial wavelet variance is more concentrated at this spatial scale.

Figure 5.23 shows shaded contours of spatial wavelet SD with points of significant change in spatial wavelet variances at the spatial scale of 32m. It can be seen from Figure 5.23 that the changes in the wavelet variance identified in the first order are also centred at 260m offshore. It is also found that the second order change in the wavelet variance is distributed in a narrow region centred at 390m offshore. Another conspicuous feature in Figure 5.23 is that the identified changes in the spatial wavelet variance at the third order are in the region from 400m to 600m offshore, which may be related to infrequent winter storms.

Figure 5.24 shows shaded contours of spatial wavelet SD with points of significant change in spatial wavelet variances at the spatial scale of 64m. It can be seen from Figure 5.24 that the changes in the wavelet variance identified in the first order at the spatial scale of 64m are also centred at 260m offshore. It is found that the identified changes in the spatial wavelet variance at the second order are in a narrow region centred at 410m offshore.

Figure 5.25 shows shaded contours of spatial wavelet SD with points of significant change in spatial wavelet variances at the spatial scale of 128m. It can be seen that the distributions of the identified change points in the wavelet variance in both the first and second order are quite similar to that of at the spatial scale of 64m. The identified points at this spatial scale are much more concentrated than those of the finer scales. Figure 5.25 also demonstrates that change points in the wavelet variances at the second order are in the portion from 400m to 500m offshore. It also shows that the variances are almost uniform seaward of 500m since there are no change points marked on the plot. In order to clarify, the histogram of the distribution of all points identified by changes in wavelet variances at the spatial scale of 128m is shown in Figure 5.26, which shows there are two peaks located at 260m and 410m along the profiles.

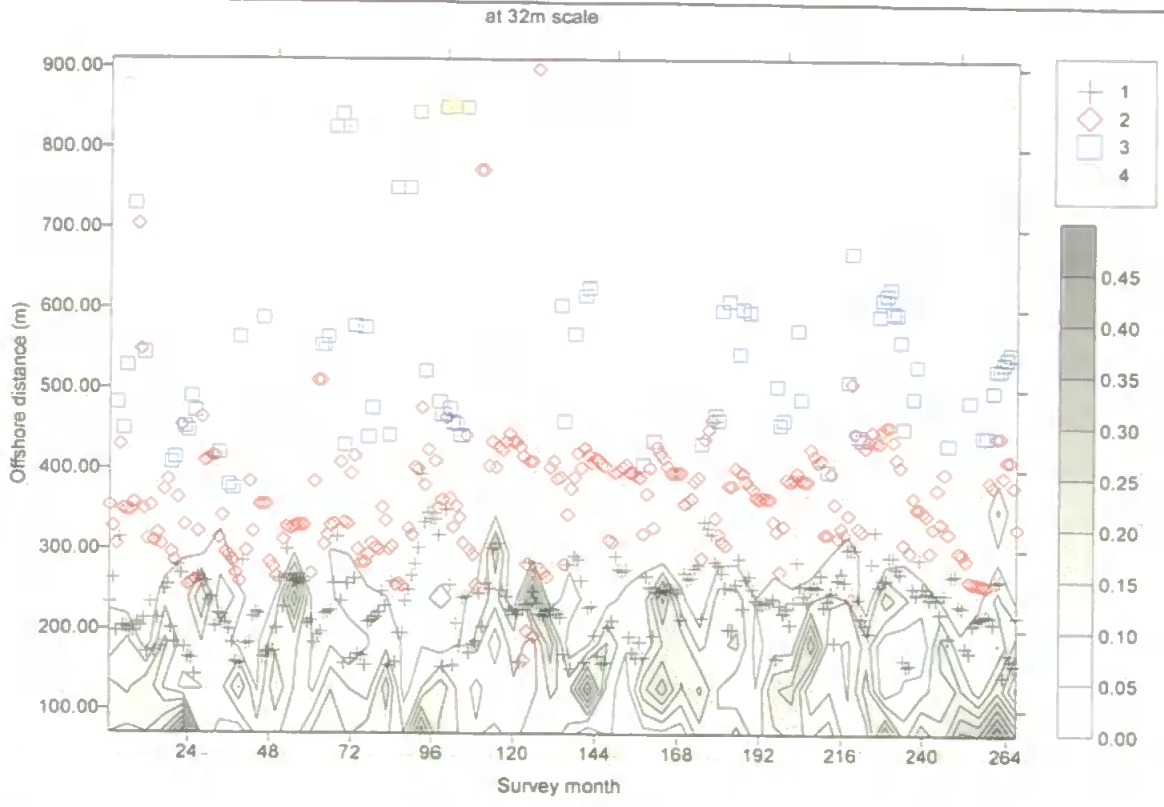

Figure 5.23 Distribution of change points in the wavelet variance at the spatial scale of 32m.

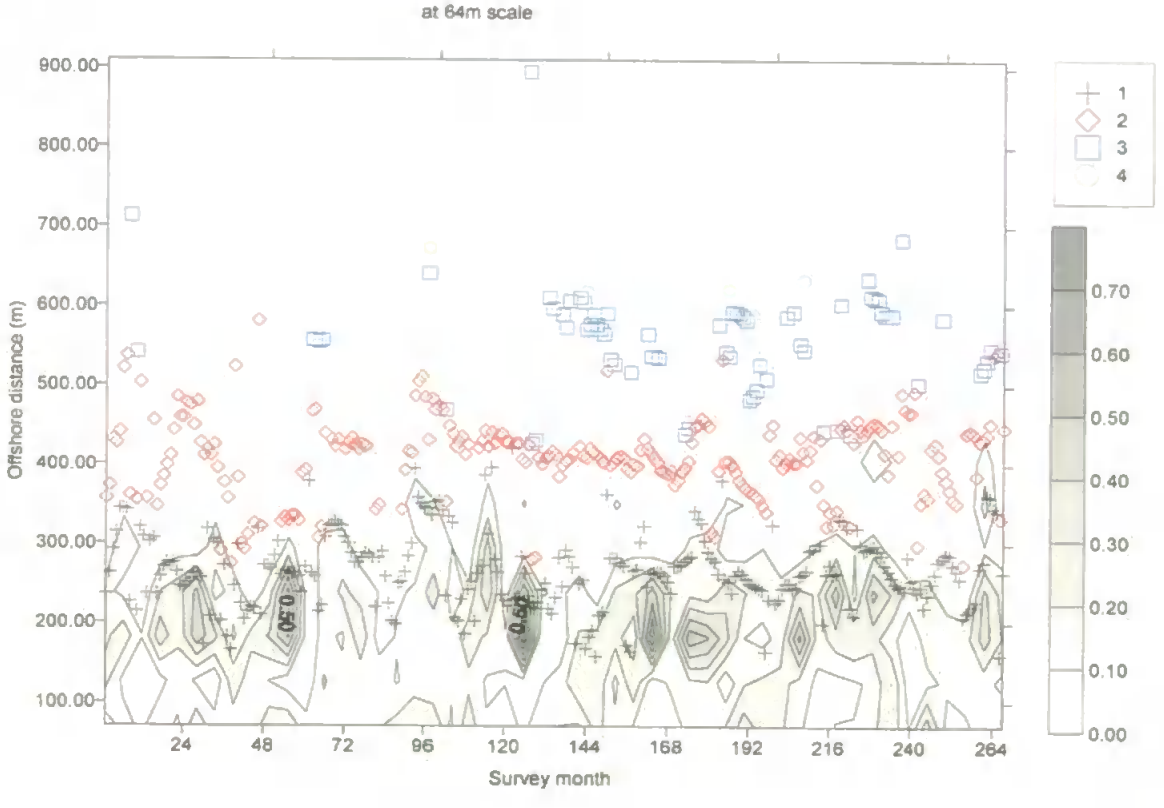

Figure 5.24 Distribution of change points in the wavelet variance at the spatial scale of 64m.

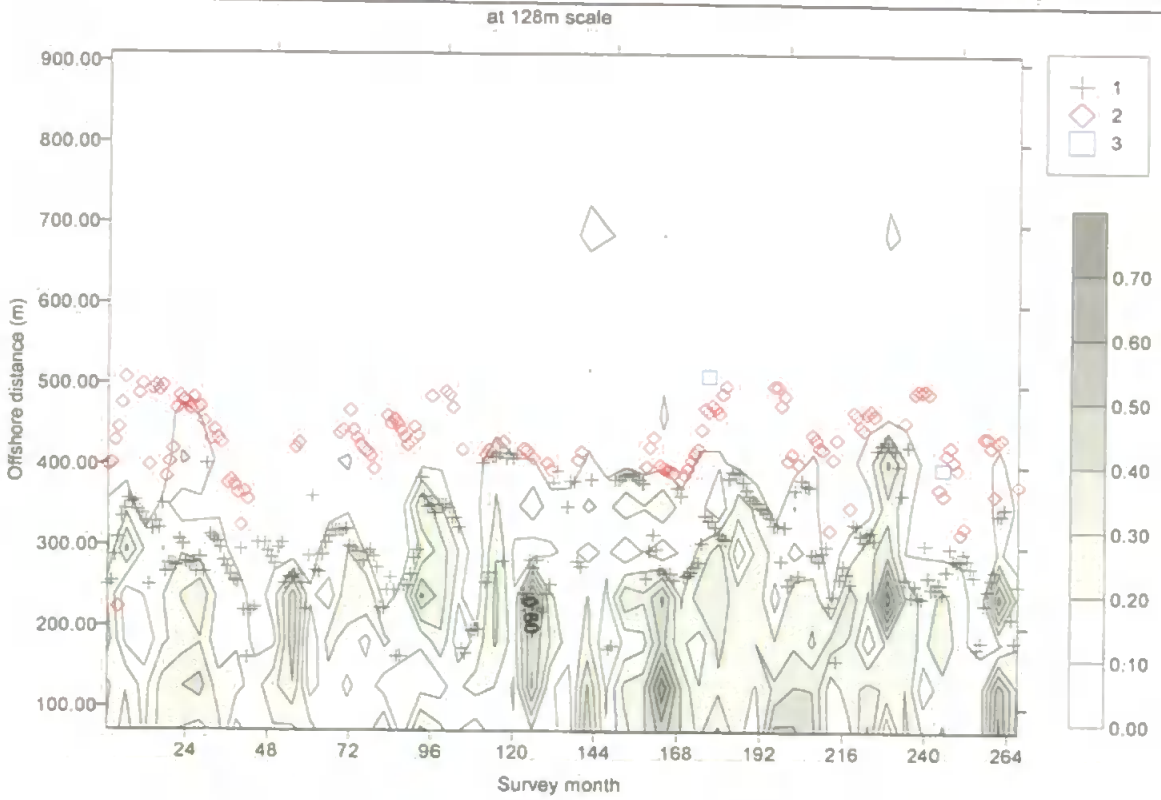

Figure 5.25 Distribution of change points in the wavelet variance at the spatial scale of 128m.

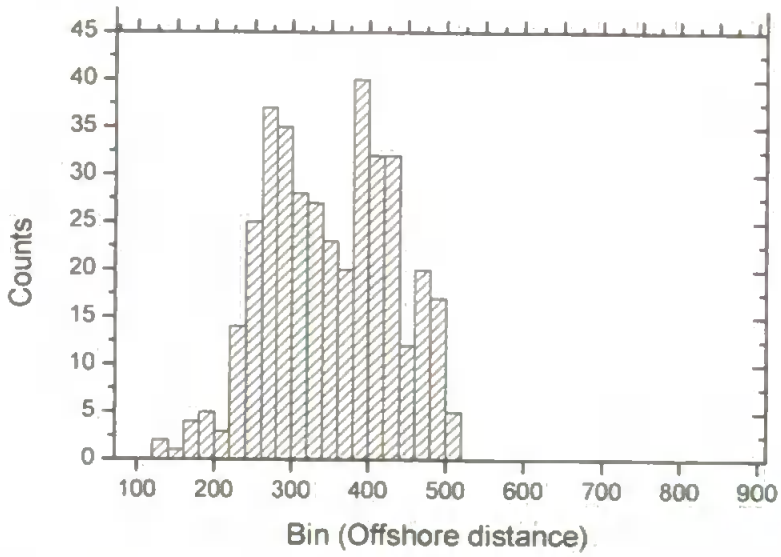

Figure 5.26 Histogram of identified changes in wavelet variance at the spatial scale of 128m against cross-shore position.

As shown in Figures 5.20-5.22, the change points in spatial wavelet variance at finer scales in the first order are mostly concentrated from 160m to 175m along the profile, although the distribution seems fairly erratic. This distribution might reflect the bar migration during the course

of study. In general, the change points in spatial wavelet variance at the spatial scales of 32m, 64m and 128m are identified in the first order centred at 260m offshore and those of identified in the second order are located 410m offshore. According to the previous studies, the transitional bar appears frequently around 260m and the beach elevations do not change much seaward of 410m (about at 4-m depth) at Duck. On the other hand, the 4-m depth corresponds to the seaward limit of offshore movement of the outer bar crest (Larson and Kraus, 1994; Nicholls *et al.*, 1998). Therefore, it is natural to match the bar migration and the DoC point with these two changes in spatial wavelet variances.

The identified change points in the wavelet variance at the spatial scale of 128m are specified with the three example survey profiles discussed in Section 5.2.2, because the wavelet variance components at coarsest scales are easy to observe directly. The identified changes in the wavelet variances at the spatial scale of 128m from the 177th survey (March 1996) are located at 332m, 466m and 510m offshore in the first order, second and third order, respectively, as shown in Figure 5.25. These identified change points in the spatial wavelet variance are in agreement with Figure 5.8, where the components of spatial wavelet variance are shown. The changes in the wavelet variance at the spatial scale of 128m from the 166th survey (April 1995) are located at 266m and 392m offshore in the first and second order respectively. Those sharp changes in the spatial wavelet variance components can be observed in Figure 5.9 also. The change in spatial wavelet variance at the spatial scale of 128m from the 129th survey (March 1992) is identified at 218m offshore, which can also be found in Figure 5.12.

In general, it can be concluded that the most significant change of beach elevation (bar migration in the surf zone) and the closure point (no significant variation seaward of this point) can be obtained by identifying the change points in spatial wavelet variances at the coarsest scale. However, if following the identified change points in spatial wavelet variance at finer scales, it is difficult to define the general DoC for all the surveys because the critical values of B, as shown in Table 3.2, are much tighter at finer scales. However, these results do support the contention that the DoC of beach profiles is also scale-dependent. If following the change points in spatial wavelet variance at coarse scales, the results are in agreement with Larson and Kraus (1994).

The procedure described in **Chapter 3** provides a new statistical methodology for identifying and classifying features of morphologically significant locations along the profiles, which could be an alternative to the equation of Hallermeier (1981). The concluding remark for the investigation is that the DoC of beach profiles is a relative concept in coastal morphology. The practical employment of it in coastal engineering depends on the scale of interest.

5.3 Principal Conclusions from the AMODWT Results

Wavelet transforms have been employed to study the variation of the profile line 62 surveyed at Duck. The AMODWT has been used to adapt to our relatively smaller data set as well to estimate the variance with higher efficiency. First of all, the wavelet variances from the AMODWT at a range of spatial scales were investigated and compared with the results from the EOF analysis. In comparison with the EOF analysis the usefulness of wavelet techniques to study the multi-scale variability of beach profiles has been established. Generally, wavelet techniques allow us to explore and quantify the non-stationary behaviour of beach variability more effectively than with the EOF method.

This spatial analysis of variance, using wavelet techniques, provides an insight into the relative importance of variations along the profile at different spatial scales. The wavelet decomposition also provides a natural means of investigating fluctuations in the beach level variability along the profile. This allows locations at which beach profile changes and the scales of those changes to be identified. Some key findings from the spatial analysis are:

- Firstly, multiresolution analysis using the wavelet transform gives a quantitative estimate of the relative importance of different spatial scales to the overall variability of the beach profile. The larger variances from the spatial scales of 128m and 64m characterize the profiles with obvious bed-forms, such as bars and troughs (Figure 5.2) whilst the smaller variances indicate a smooth profile without spectacular bed-forms (Figure 5.6).
- Secondly, the wavelet variance components show that the contributions from different scales at different parts of the profile are different, which suggests that the morphological evolution of the profile as a whole is dependent upon different processes along the profile.

The results also provide evidence of the scale-dependent character of beach profile changes.

- Thirdly, the spatial wavelet variances at spatial scales of 128m make a large contribution to the variation of beach profiles overall. These results are to be expected from the consideration that the primary agent for morphological evolution is the incoming waves. When there are high-energy waves, the changing portion of the beach profile is wide and the spatial scale at which elevation changes occur is also larger. Additionally, variances coming from finer scales are more obvious in the dune and surf zones than those of other zones, because beach profiles in the surf zone experience small waves as well as storms, however in deep water beach profiles will only change in response to strong storms. The results provide new quantitative evidence to support the contention that the variation of beach profiles in space is not statistically stationary.
- Fourthly, analysis of the changes in variances of individual spatial components indicates that this provides a useful measure for defining the DoC of beach profiles. The zone in which the changes in beach elevations are not significant would be expected to coincide with a measurable change in the spatial variance. The DoC identified by the change in spatial wavelet variances at the spatial scale of 64m and 128m is more consistent with the findings of Larson and Kraus (1994) than with the results of Nicholls *et al.* (1998), which is acknowledged as providing a conservative estimate. In general, by identifying the changes in spatial wavelet variance at different scales, the scale-dependent DoC is justified. The procedure described in this thesis provides a statistical method for identifying the most active zones as well the DoC.

5.4 Analysis of the Spatial Variability with DWPT

5.4.1 General

In the above sections, the spatial variability of beach elevation of profile line 62 at Duck were analysed using the DWT. The complicated variations of beach profiles in space have been

decomposed into several scales, and some promising results are obtained. The results have exhibited that the wavelet technique is a powerful tool for studying the variability of beach profiles. However, the obvious disadvantage of the DWT is that it provides a predetermined basis for the data set that does not depend in any way on the spatial/temporal variation of the original data. The temporal or spatial scales of beach elevation changes are fixed as the dyadic sequence $2^j x_0, j = 1,2,3...$, where x_0 is the sampling interval in time or space.

In this section, the analysis is repeated but using the DWPT and the selected best basis rather than the AMODWT. The non-dimensional standard frequency intervals are shown in Equation (3.38), and the spatial scales referred to in this thesis are multiples of the basic sampling rates with the reciprocal of the upper limit of the frequency interval. Daubechies's (1988) wavelet with two vanishing moments was employed to do the DWPT analysis. The Shannon entropy function, introduced by Coifman and Wickerhauser (1992), was used in the best basis algorithm in this thesis since it is a most widely used criterion. The beach profile data were extended symmetrically in order to deal with the border distortion as well as to preserve the local character of the variability of beach profiles. Multiresolution analysis was performed on the extended data.

5.4.2 Spatial scale analysis using the DWPT

Three representative surveys of profile line 62 were investigated using the DWPT and compared with the results from the DWT in the following. The full set of wavelet packets were generated by six dilations and the best basis was selected from the DWPT. Table 5.1 lists all the wavelet packets for the profile in March 1996 $W_{j,n}; j = 1,2,...6$. The best basis was denoted by shaded cells. Figure 5.27 shows the best basis selected from the DWPT of the survey in March 1996, ordered in increasing spatial scales from bottom to top. The sum of the components on the eight packets in the best basis reconstructs the original variation as shown in the top plot of Figure 5.27.

Two packets in the normal DWT were decomposed again in the best basis, where $W_{1,1}$ was decomposed to $W_{2,2}$ and $W_{2,3}$, and $W_{5,1}$ was decomposed to $W_{6,2}$ and $W_{6,3}$. Figure 5.27 indicates that the beach profile changes can be better captured by the spatial interval of 4-5.3m and 5.3-8m

respectively along the profile than the interval of 4-8m in the DWT. Moreover, the variance in the interval of 64-128m in the DWT can be better resolved by two intervals 64-85.3m and 85.3-128m. Figure 5.27 shows that the variation at the spatial scale of 64-85.3m explains the presence of the first bar crest well.

Similarly, the detail components in the best basis of the survey in April 1995 were computed and displayed in Figure 5.28. The components denoting variation of beach elevation at the spatial scale of 85.3m are identified in the best basis. It can be seen that the first and third significant positive peaks at the spatial scale of 85.3m coincide with the locations of the two bar crests as illustrated on the top most plot.

Figure 5.29 shows the detail components in the best basis of the profile in March 1992. As found in the AMODWT analysis, this profile has an obviously smaller overall variation than those of in March 1996 and April 1995. However, Figure 5.29 displays many more packets in the best basis in comparison to those of the other two surveys. It can be seen that the variance at the spatial scale of 8-16m in the DWT was decomposed to two components, 8-10.66m and 10.66-16m. The changing between strong and weak periodicity of the detail components at the spatial scale of 10.66m along the profile shows strong intermittent character of beach elevation changes. Similarly, the detail components at the spatial scale of 21.3m characterize much of the two bar crest in March 1992.

Table 5.1 DWPT packets for the profile in March 1996 with shaded cells denoting the best basis.

(1,0)	(2, 0)	(3, 0)	(4, 0)	(5, 0)	(6, 0)
					(6, 1)
				(5,1)	(6, 2)
					(6, 3)
			(4, 1)	(5, 2)	(6, 4)
					(6, 5)
				(5, 3)	(6, 6)
					(6, 7)
		(3, 1)	(4, 2)	(5, 4)	(6, 8)
					(6, 9)
				(5, 5)	(6, 10)
					(6, 11)
			(4, 3)	(5, 6)	(6, 12)
					(6, 13)
				(5, 7)	(6, 14)
					(6, 15)
	(2, 1)	(3, 2)	(4, 4)	(5, 8)	(6, 16)
					(6, 17)
				(5, 9)	(6, 18)
					(6, 19)
			(4, 5)	(5, 10)	(6, 20)
					(6, 21)
				(5, 11)	(6, 22)
					(6, 23)
		(3, 3)	(4, 6)	(5, 12)	(6, 24)
					(6, 25)
				(5, 13)	(6, 26)
					(6, 27)
			(4, 7)	(5, 14)	(6, 28)
					(6, 29)
				(5, 15)	(6, 30)
					(6, 31)
(1, 1)	(2, 2)	(3, 4)	(4, 8)	(5, 16)	(6, 32)
					(6, 33)
				(5, 17)	(6, 34)
					(6, 35)
			(4, 9)	(5, 18)	(6, 36)
					(6, 37)
				(5, 19)	(6, 38)
					(6, 39)
		(3, 5)	(4, 10)	(5, 20)	(6, 40)
					(6, 41)
				(5, 21)	(6, 42)
					(6, 43)
			(4, 11)	(5, 22)	(6, 44)
					(6, 45)
				(5, 23)	(6, 46)
					(6, 47)
	(2, 3)	(3, 6)	(4, 12)	(5, 24)	(6, 48)
					(6, 49)
				(5, 25)	(6, 50)
					(6, 51)
			(4, 13)	(5, 26)	(6, 52)
					(6, 53)
				(5, 27)	(6, 54)
					(6, 55)
		(3, 7)	(4, 14)	(5, 28)	(6, 56)
					(6, 57)
				(5, 29)	(6, 58)
					(6, 59)
			(4, 15)	(5, 30)	(6, 60)
					(6, 61)
				(5, 31)	(6, 62)
					(6, 63)

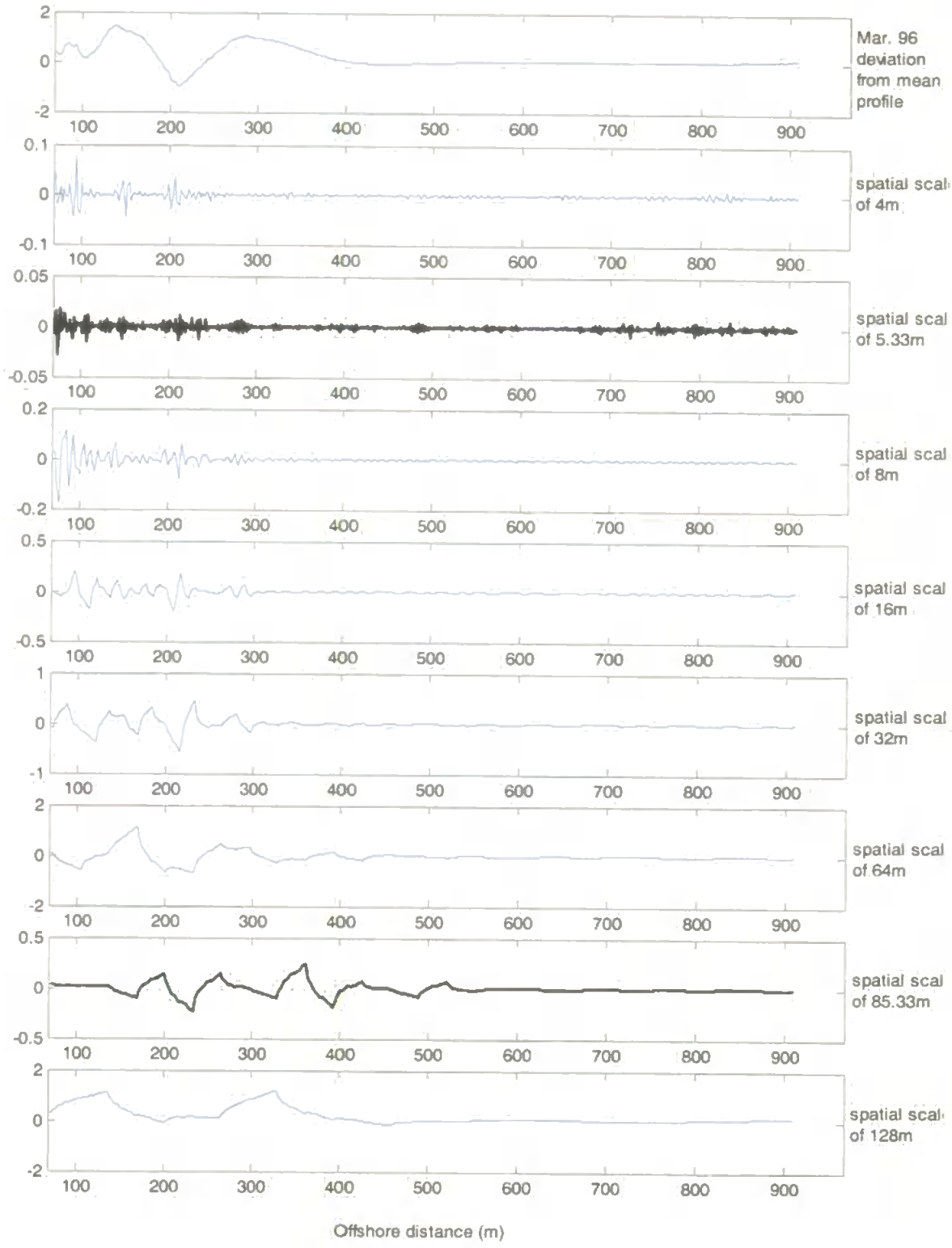

Figure 5.27 Reconstruction of the detail components in the best basis from the DWPT of the profile for March 1996 against cross-shore.

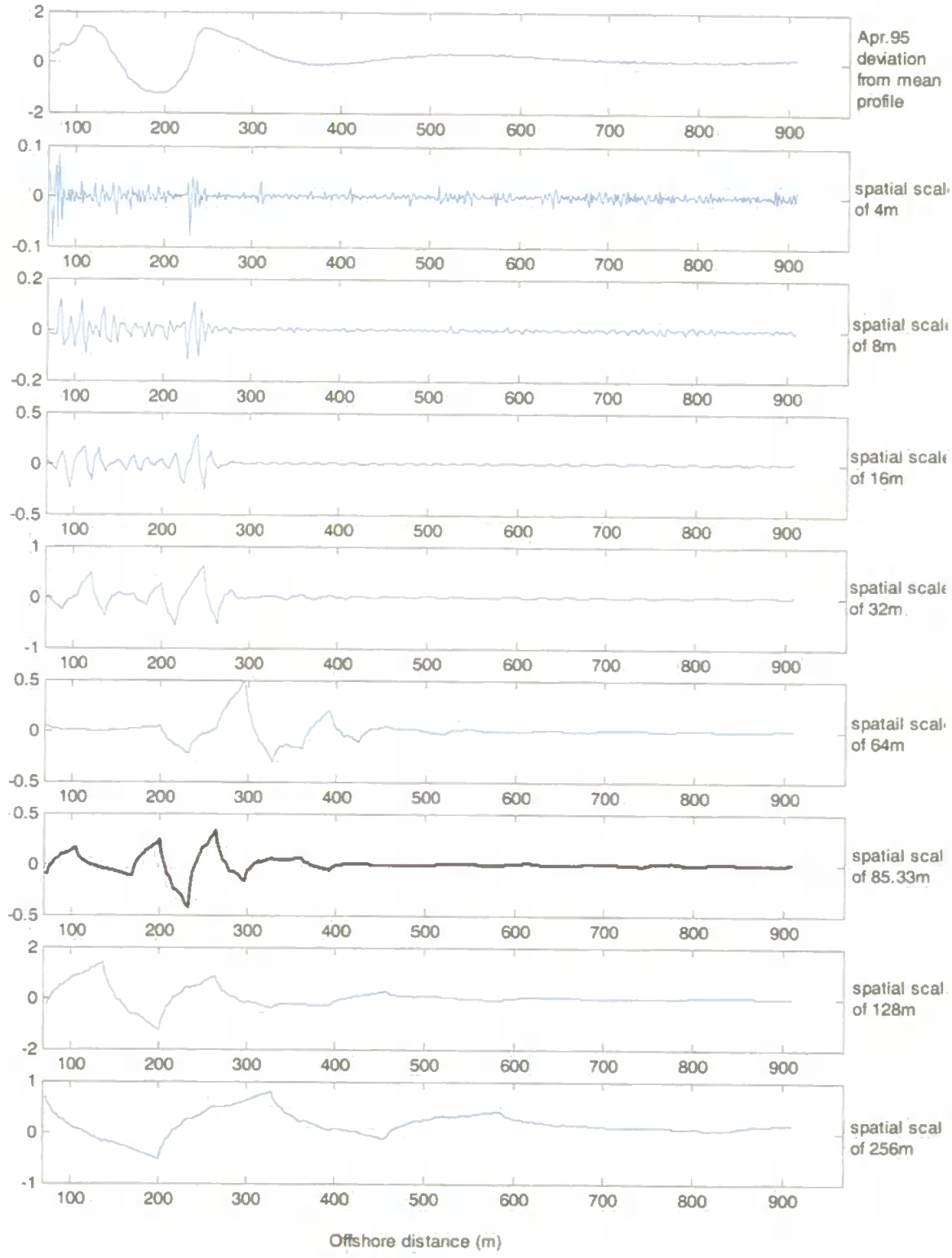

Figure 5.28 Reconstruction of the detail components in the best basis from the DWPT of the profile for April 1995 against cross-shore.

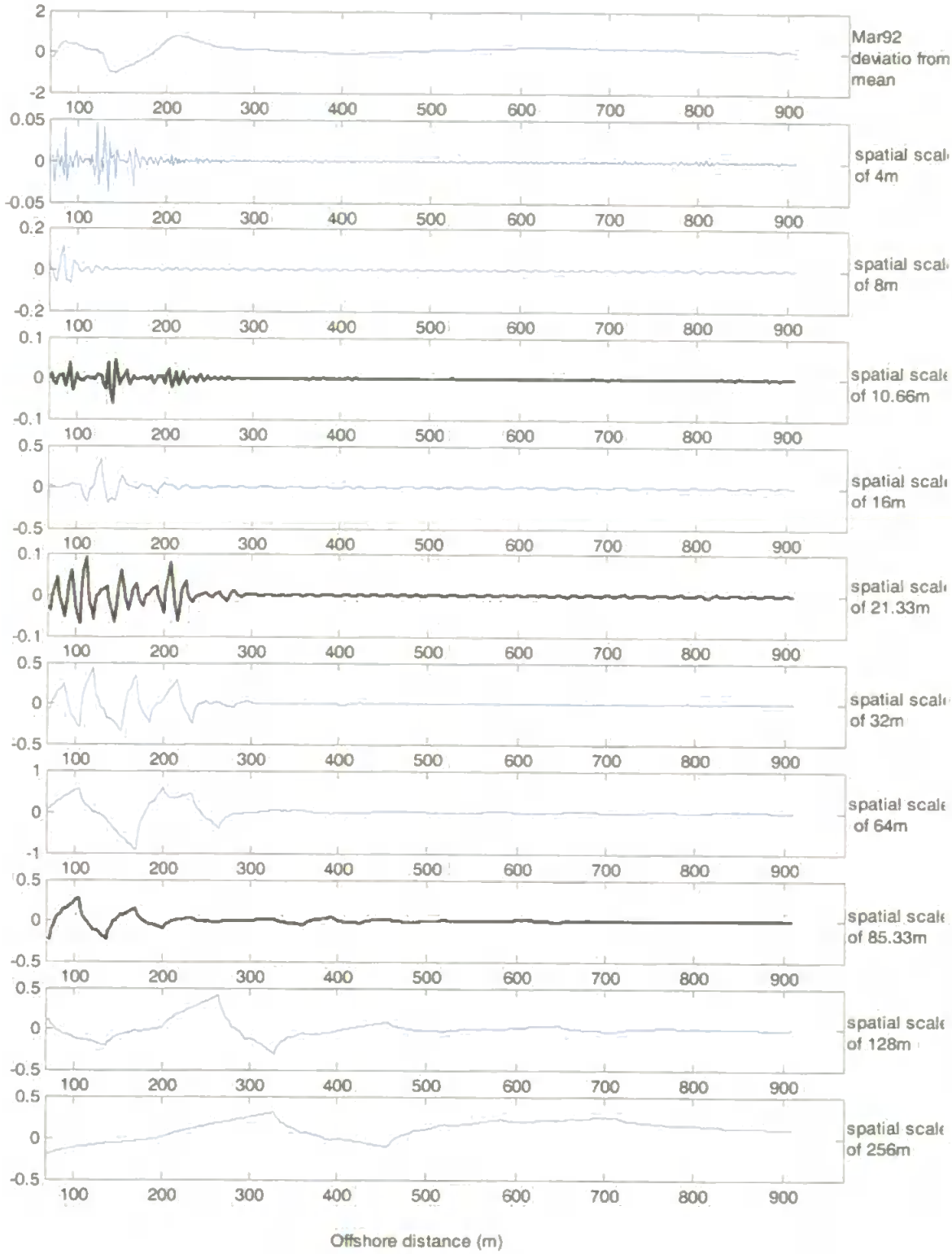

Figure 5.29 Reconstruction of the detail components in the best basis from the DWPT of the profile for March 1992 against cross-shore.

The spatial wavelet packet variances from the best basis of the surveys in March 1996, April 1995 and March 1992 were computed using Equation (3.39) in order to obtain the relative importance of the packets at different scales. The plots are displayed together with those from the DWT in Figure 5.30, Figure 5.31 and Figure 5.32, respectively for the purpose of comparison. As noted above, the spatial scales in these three figures are multiples of the reciprocal of the upper limit in the frequency intervals, since the spatial scales are usually used to describe the variation of beach profiles in coastal engineering.

The predominance of the variance at the spatial scale of 128m and 64m is the common feature of the three figures, which is consistent with the results from the DWT. The variance at the spatial scale of 85.3m in the best basis is another common feature among them, although the contributions from these scales are not as significant as the spatial scale of 128m and 64m. In the previous studies using the AMODWT, the variances at these two coarser scales have been related to the bar migration by comparison with the temporal weightings in the EOF analysis. It is concurred that the length of inner bars at Duck has a mean of 95m with maximum and minimum of 280m and 35m, respectively (Larson and Kraus, 1994). It is obvious that the mean bar width is close to the spatial scale of 85.3m, therefore, the variance at the spatial scale of 85.3m provides further support for the conclusion that most of the variance explains the bar migrations and the dimensions of the bar are defined by the predominant spatial scales.

Moreover, there are some differences in the best basis among the three profiles due to the various beach profile configurations. From this point of view, the DWPT provides a more detailed analysis into the variability of each surveyed profile. In consequence, the understanding of the beach profile variability is refined.

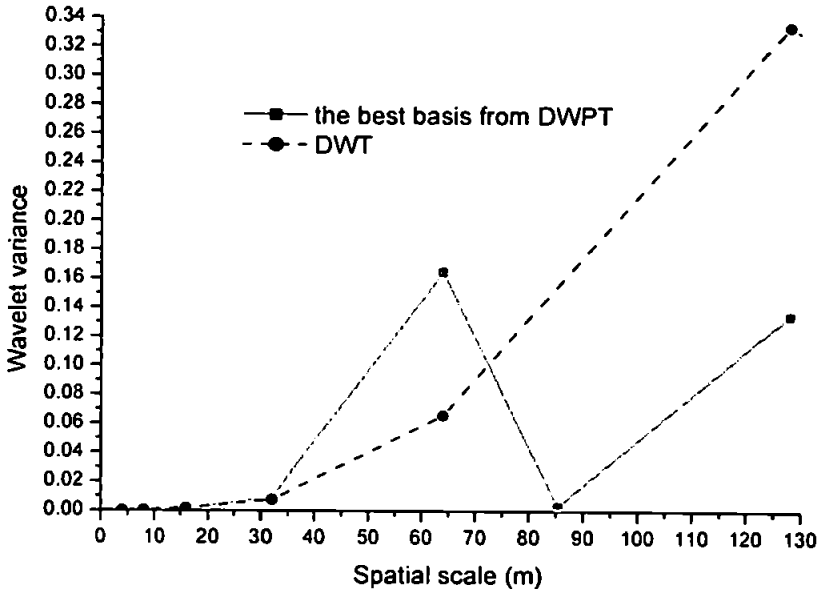

Figure 5.30 Spatial wavelet variance at different spatial scales in the best basis of the profile for March 1996.

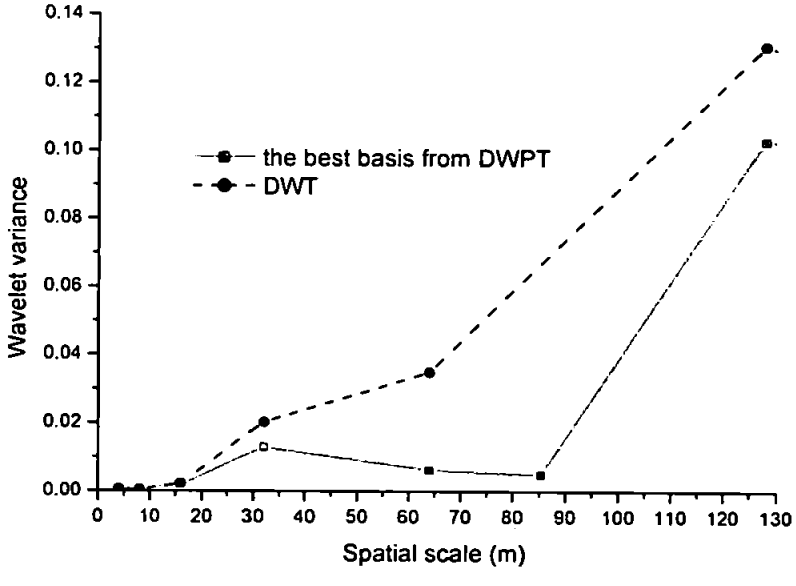

Figure 5.31 Spatial wavelet variance at different spatial scales in the best basis of the profile April 1995.

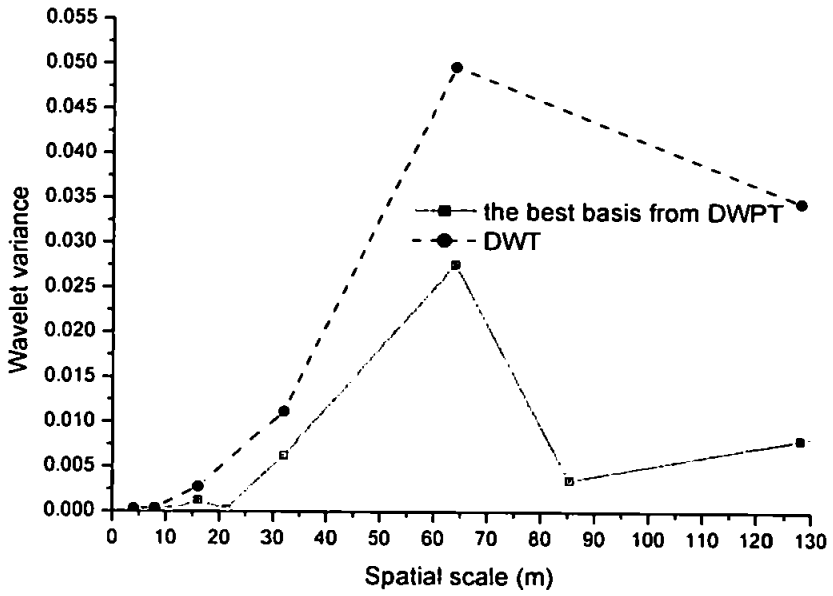

Figure 5.32 Spatial wavelet variance at different spatial scales in the best basis of the profile for March 1992.

On the other hand, the bases in the best basis from the DWPT are not much larger than that of from the DWT, implying that spatial scales of beach profile changes are not so complicated. However, the conclusions from the AMODWT that the coarser scales characterize the bar/trough are substantiated further.

5.5 Summary

In this chapter, the variation of beach profiles has been investigated over a wide range of scales in time using the wavelet transforms with emphasis on the AMODWT. The most important contributions from the study on the data set at Duck using wavelet techniques are as follows:

1. Providing powerful quantitative evidence for the non-stationary nature of beach profile changes in both time and space.
2. Successfully characterizing the main spatial patterns of beach profile change. The scale-dependent spatial patterns are explained by the site character and seasonal wave conditions. In addition, the effects of extreme events are revealed.
3. The DoC is investigated using a new statistical method in coastal engineering. The results indicate a strong scale-dependency.

Chapter 6. TEMPORAL ANALYSES OF BEACH PROFILE CHANGES AT DUCK

6.1 Introduction

In Section 6.2, the temporal variability of particular beach elevations is studied. In Section 6.2.1, the locally temporal variation of the beach elevations at the shoreline is divided among six temporal scales and the long-term trend is identified. Another two particular points in the time series are studied similarly. It is followed by much physical interpretation for the three particular points along the profile. A particular concern about the temporal variability of the different zones along the profile is shown in Section 6.2. The contours of temporal wavelet standard deviations in the spatial-temporal plane are presented in Section 6.3. The general temporal variability along the profile is well captured by the contours at different scales. Also in this section, some physical explanation is given to the extraordinary response in deep water. The results of change points in temporal variances are presented in Section 6.4. Further investigation of temporal variability of beach elevations with the DWPT is presented in Section 6.5.

6.2 Multi-scale analysis of beach profile change in time

6.2.1 Local variation and long-term trend

A similar approach to the spatial analysis in Section 5.2 was performed to investigate the temporal scales of the changes of beach elevation at specified locations along the profile line 62 using the wavelet technique. As noted in **Chapter 4**, there were 421 observations in space series along the profile; therefore 421 separate wavelet transforms on beach elevations in time series of 267 months were conducted. The results from a few representative observations of beach elevation along the profile are shown in detail to demonstrate the multi-scale analysis in time series of wavelet transforms. The first observation is located at 120m offshore which is at the mean shoreline of the profile line 62 over 22 years, and the second was chosen from the peak of the SD of beach elevation in Figure 4.7, which is located 260m offshore. In addition, the variability of

beach elevation in time series of the point located 410m offshore, where the elevation change is not significant and sometimes one outer bar is identified, is studied. The evolution of the three points during the course of study of 22 years is displayed in Figure 6.1.

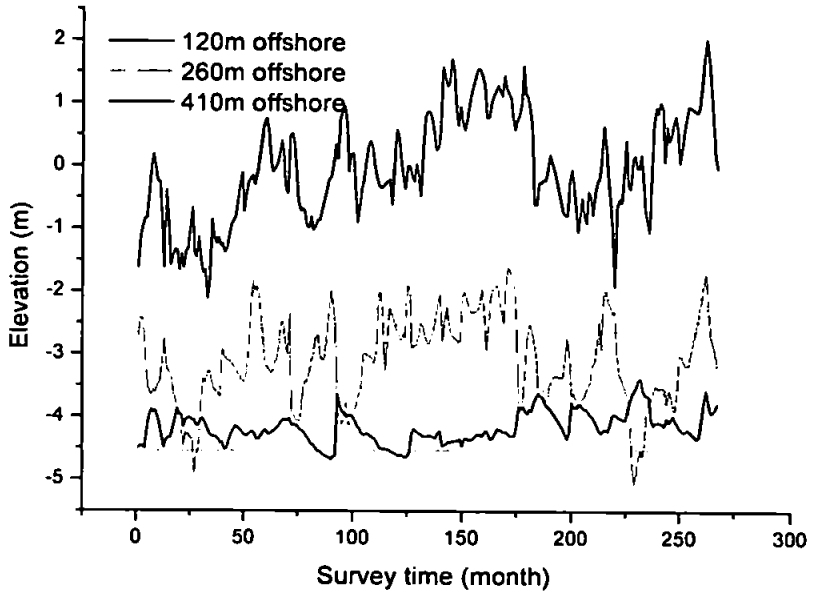

Figure 6.1 Evolution of the three points during the course of the study.

Since the incoming wave energy is dissipated in the surf zone, the long-term trends should reflect the response of the shoreline to changes in the prevailing wave climate, i. e., the trends represent the long-term forced behaviour. Therefore, multiresolution analysis of the temporal variability of beach profiles using the DWT was carried out on the observations at 120m offshore during the course of study. The detail components and approximations at different temporal scales were obtained by doing the inverse transform of the DWT as described in **Chapter 3**. The top plots in both Figure 6.2 and Figure 6.3 are the beach elevation during the course of study.

Figure 6.2 shows the detail components of beach elevation against the survey time at the temporal scales of 2 months, 4 months...and 64 months, which is denoted by d1, d2 ...and d6 on the plots. The detail components characterize the local variation in time series which happens at different temporal scales. For example, the variation of beach elevation in the 9th month (March 1982) is predominantly involved at the temporal scale of 16 months, which is denoted as d4 on the plot as shown in Figure 6.2.

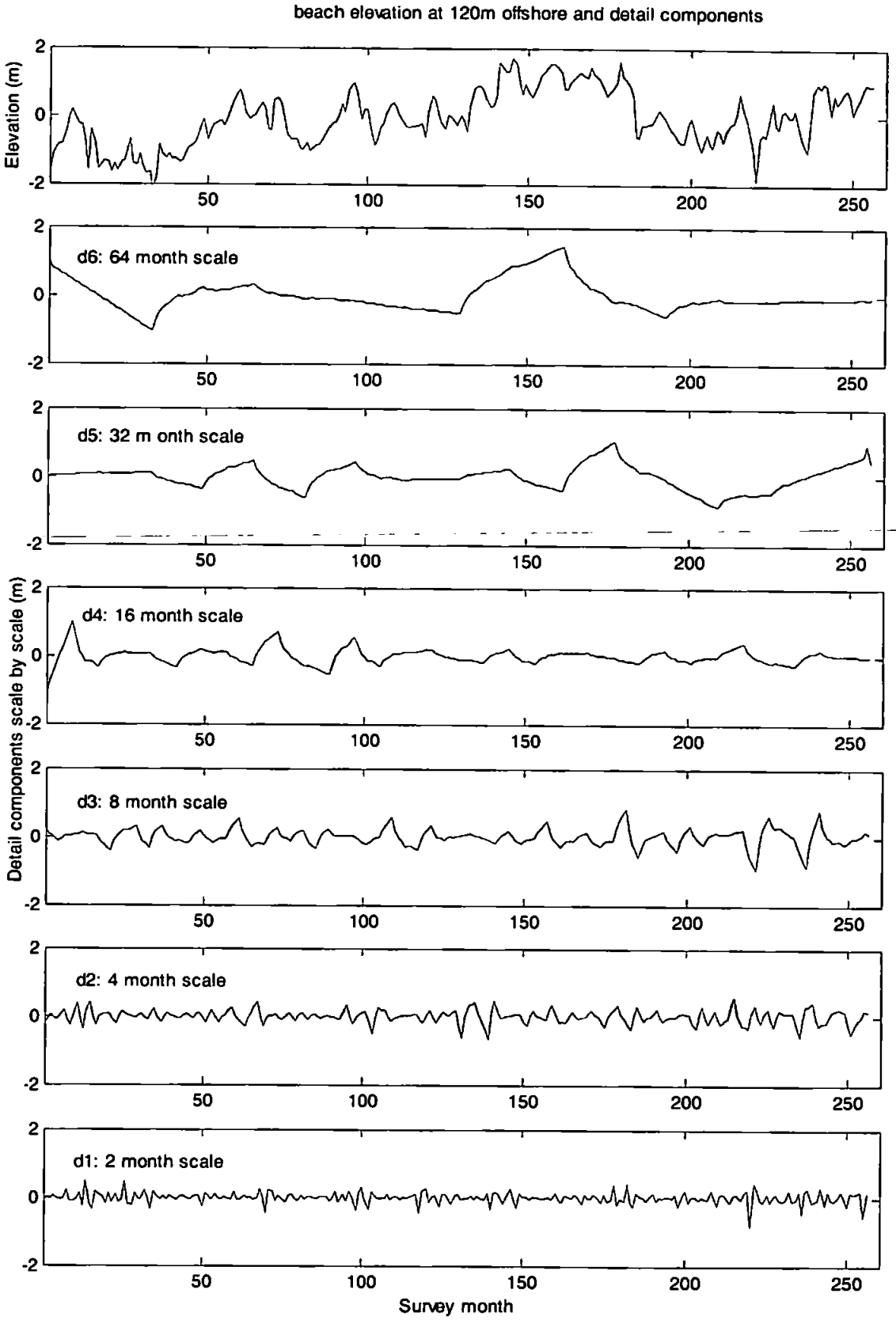

Figure 6.2 The detail components of beach elevation 120m offshore at different temporal scales.

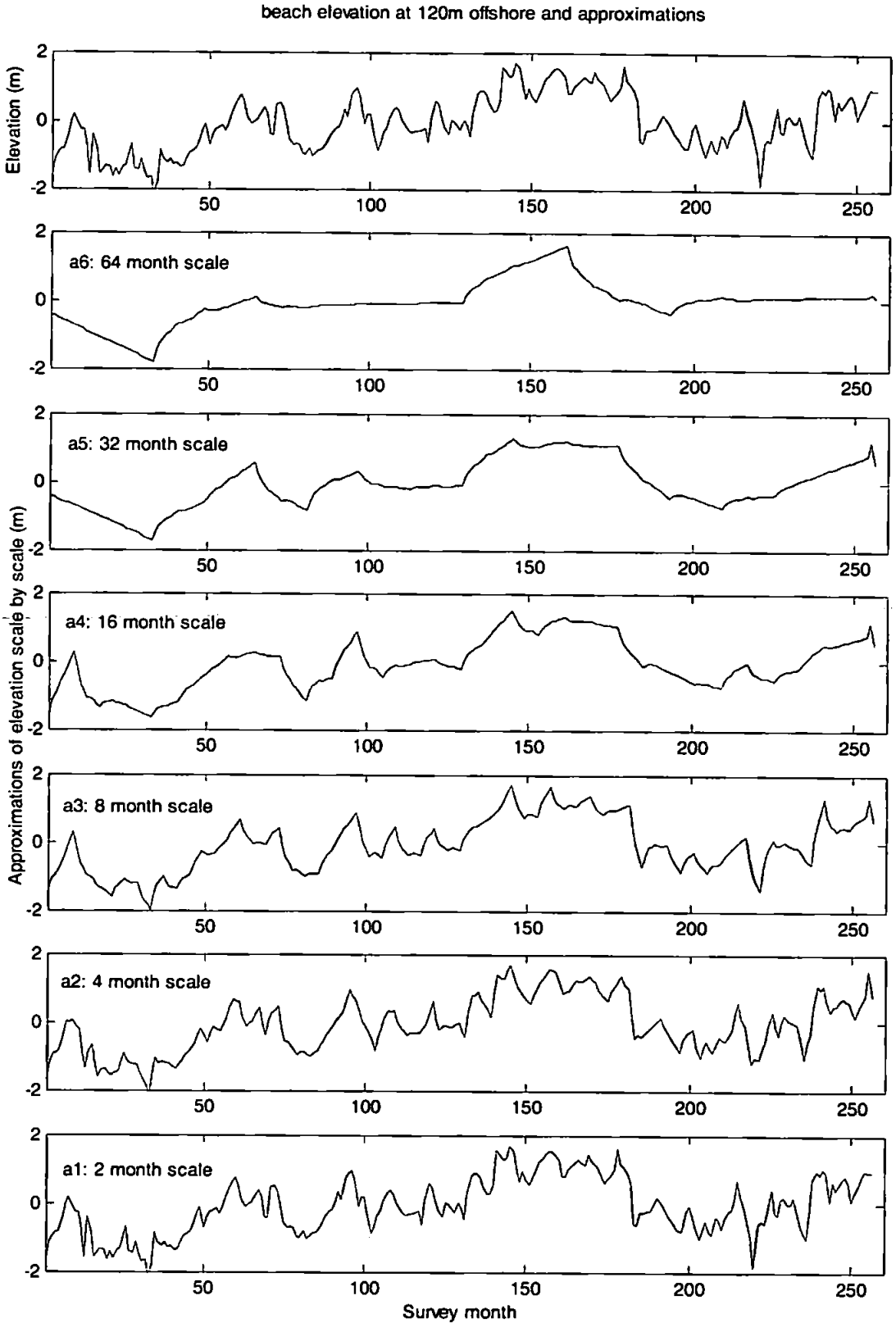

Figure 6.3 The approximation of beach elevation at 120m offshore at different temporal scales.

The approximation components at different scales by subtracting the corresponding detail components from the original beach elevations are shown in Figure 6.3 during the course of study, where a1 denotes the approximation components at the temporal scale of 2 months. The long-term

trend becomes gradually clear in the approximation components with the increasing of the temporal scales. This result indicates that wavelet transforms provide a powerful tool to identify the long-term trend of the variability of beach profiles by filtering out the short-term fluctuations which might correspond to events such as storms or storm groups.

6.2.2 Wavelet variance components of three observations

The temporal wavelet variance components of beach elevation at 120m, 260m and 410m offshore were computed. The accumulated components were plotted against the survey time and shown in Figure 6.4, Figure 6.5 and Figure 6.6. Each layer of the graph corresponds to one of the temporal scales, and at any month the thickness of the layer shows the size of the wavelet variance component at that scale and the month that the profile was surveyed.

Figure 6.4 shows that the wavelet variance components are distributed over a wide range of temporal scales from 2 months to 64 months. However, it can be seen from Figure 6.4 that the dominant wavelet variance scales differ over the course of the study. It can be observed from Figure 6.4 that the wavelet variance components during the period from August 1984 to June 1986 is mostly at the temporal scale of 32 months, while around December 1987 the variance is dominated by the temporal scale of 16 months. Moreover, it is found that the wavelet variance component around June 2000 is dominated by the temporal scale of 64 months. The temporal wavelet variance components at all scales during the period from June 1998 to December 2001 are quite significant during the survey time. Figure 6.4 shows that the variance during the period from June 2002 to September 2003 is quite obvious at the temporal scale of 64 months. In all, the temporal variance components at the various temporal scales change in the time series, revealing the beach elevation changes are highly non-stationary at the point on the shoreline.

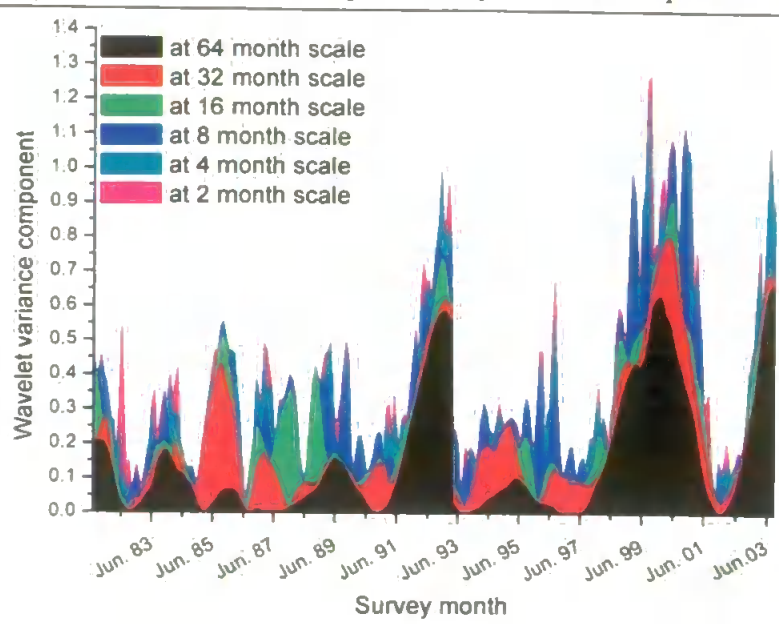

Figure 6.4 Accumulated wavelet variance at 120m offshore during the course of the study.

Figure 6.5 shows the accumulated components of the temporal wavelet variance of beach elevation against the survey time at 260m offshore where there is usually a transitional bar. The point located at 260m is often identified as the first order change in spatial wavelet variance in Section 5.2.5. In general, the largest wavelet variance components of beach elevation at 260m offshore are at the temporal scales of 16 months and 8 months during the course of study, even though at times other temporal scales dominate.

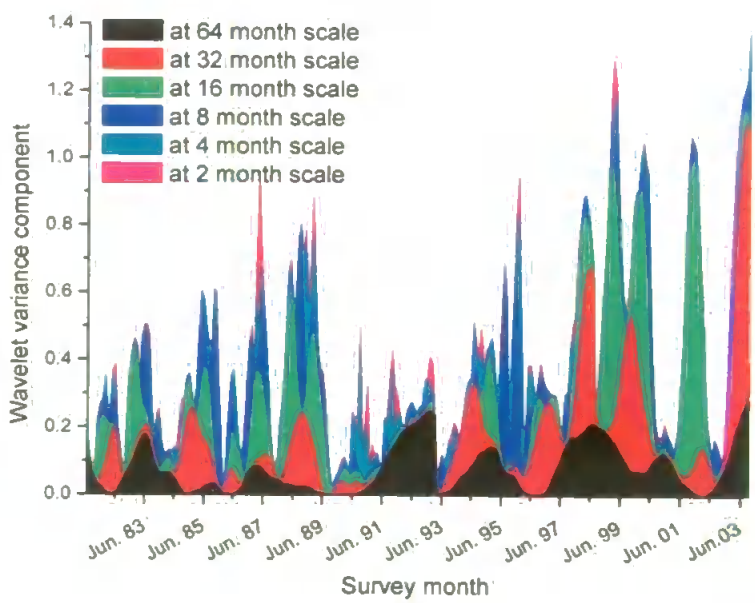

Figure 6.5 Accumulated wavelet variance at 260m offshore during the course of the study.

These variance components shown in Figure 6.5 display the intermittency of beach elevation change at this observation. For example, the variance in October 1990 is dominated by the component at the temporal scale of 4 months. At this observation point, it also can be seen that the component of temporal wavelet variance at all scales is also largest during the period from June 1998 to June 2001, which is similar to that of at 120m offshore, as displayed in Figure 6.4. Moreover, the variance during the period from June 2002 to September 2003 is quite significant at the temporal scale of 32 months. In short, the variance of beach elevation at this observation is mainly at the temporal scales of 16 and 8 months in a descending order. The larger variance at temporal scale of 16 months suggests a strong interannual variation of beach elevation at this point. Ruessink *et al.* (2003) argued that the return period of the bar north of the pier at Duck amounted to 5.9 years. However, Figure 6.5 illustrates that the six-year periodicity is quite weak and intermittent at 260m offshore, where a transitional bar is often present. The variance at the temporal scale of 8 months reflects the annual period of beach profile changes, which might be related to the annual signature of the wave conditions at Duck (Larson and Kraus, 1994).

Figure 6.6 shows that the components of the wavelet variance at all scales during the survey time at 410m offshore are much smaller than those of 120m and 260m offshore as shown in Figure 6.4 and Figure 6.5. The analysis of wavelet variance components illustrates the relatively small change of beach elevation in deep water. Moreover, the variance during the period from June 2002 to September 2003 is quite obvious at the temporal scale of 8 months. It can also be seen from Figure 6.6 that the temporal wavelet variance components at finer scales contribute much to the overall variances.

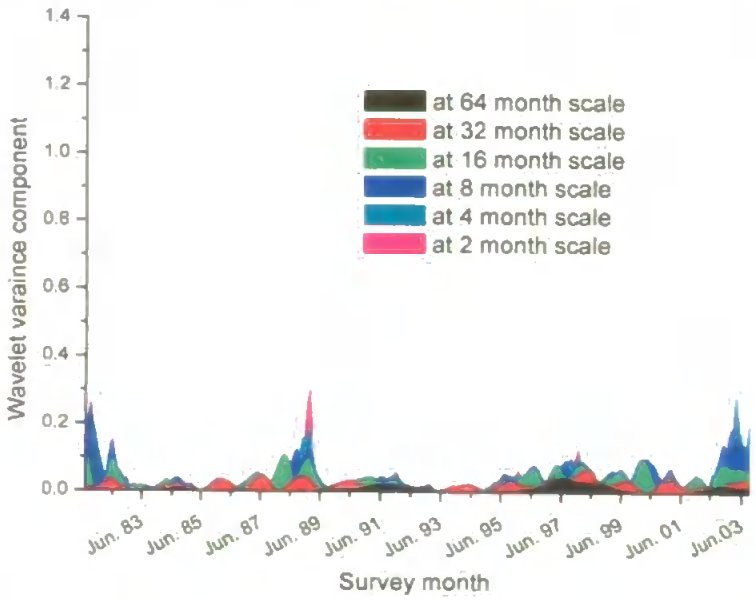

Figure 6.6 Accumulated wavelet variance at 410m offshore during the course of the study.

These analyses at three positions show that the temporal variance at given points along the profiles is the combination of variance components at several temporal scales with one or two dominant ones. Since the dominant scales change during the course of study for a particular location, the temporal wavelet variance components provide strong evidence for the spatial non-stationarity of the beach profile changes. The three case studies also show that during a particular period the dominant temporal scales vary along the profile. For one obvious period from June 2002 to September 2003, the dominant temporal scales are 64 months, 32 months and 8 months for the three observations located at 120m, 260m and 410m offshore respectively.

6.2.3 Physical interpretation on the typical wavelet variance components of the three observations

There are a few periods when the wavelet variance is relatively large in Figure 6.6, which could be explained by extreme events. One such period is between the end of 1988 and the beginning of 1989. The profile configurations from September 1988 to March 1989 are displayed in Figure 6.7, which shows the profile evolution during winter with considerable offshore sediment transport. It can be seen that there was a bar in September 1988 located around 190m

offshore and the bar crest gradually moved offshore till February 1989 the bar crest was situated around 280m offshore. The bar migration from September 1988 to February 1989 is a typical beach profile response to the severe winter waves.

Figure 6.7 also illustrates another obvious phenomenon that the bar crest moved further to 380m offshore and a wide trough formed in March 1989. The bar moved around 100m offshore in a month due to the storms in late February 1989 and March 1989. On February 25th, 1989 the wave height was up to 4.09m and with wave period of 11.13s and on March 11th, 1989 the wave height was 4.23m with wave period of 12.19s. These intense short-term phenomena explain why the wavelet variance at the temporal scale of 2 months was largest in February 1989 as indicated in Figure 6.6.

Another striking period illustrated in Figure 6.6 is from August 2002 to August 2003, when the wavelet variance component is relatively large. The most significant contribution in this period is from the temporal scale of 8 months, which contrasts with early 1989 when the variance at the temporal scale of 2 months is quite large. The result can be interpreted by the unusually calm weather during the winter of 2002. Therefore, the annual beach response is more conspicuous during this period. In all, these two special periods shown in Figure 6.6 are explained by different weather conditions corresponding to different temporal scales.

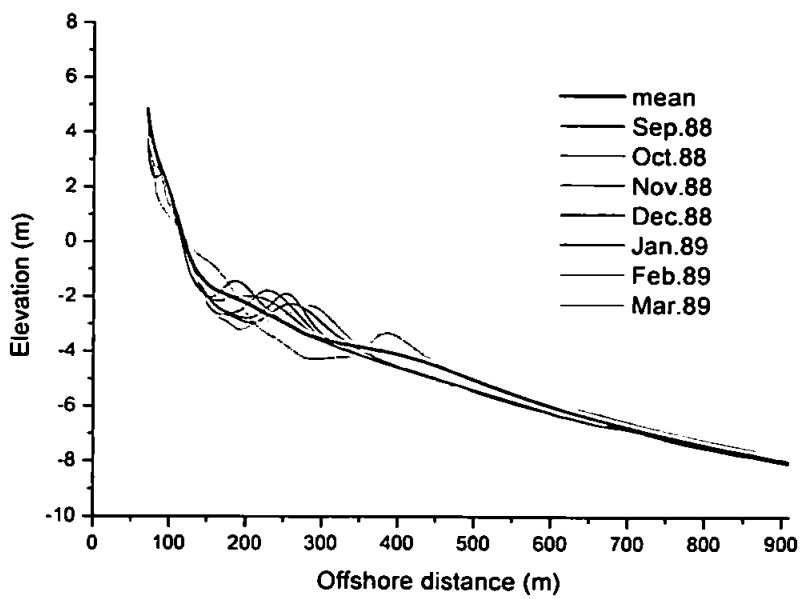

Figure 6.7 Bar migration from September 1988 to March 1989.

The temporal wavelet variance components at 120m offshore are very large from December 1989 to December 1995 as shown in Figure 6.4. Therefore, a detailed discussion is given below. It is obvious that the annual cycle is much more apparent during this period of study. Meanwhile, the temporal wavelet variance components at 260m offshore also display a weaker annual cycle during these six years. On the other hand, the variance during this period is quite small at 410m offshore (mean water depth of 4.17m). The studies by previous researchers have demonstrated that the active zone of sediment transport is in the region seaward of 4m water depth. Therefore, this period shows the general seasonal change of beach profiles.

Figure 6.8 shows a typical shoreline change after a mild summer during the six year period. It can be seen in July 1993 that the dune zone is obvious above the mean elevations and almost no apparent bar crest. Therefore, wave energy would not be dissipated much when waves were propagating onshore from upper shoreface to inshore. Consequently, the shoreline was vulnerable to any forcing conditions. This can explain that the variance was quite large at 120m offshore but quite small at 410m offshore from the profiles in July 1993, August 1993 and September 1993. After three months deposition of the sediment from the dune zone, till October 1993 an inner bar formed as seen in Figure 6.8. Subsequently, the bar moved offshore slightly, which can be observed from the profile in November 1993.

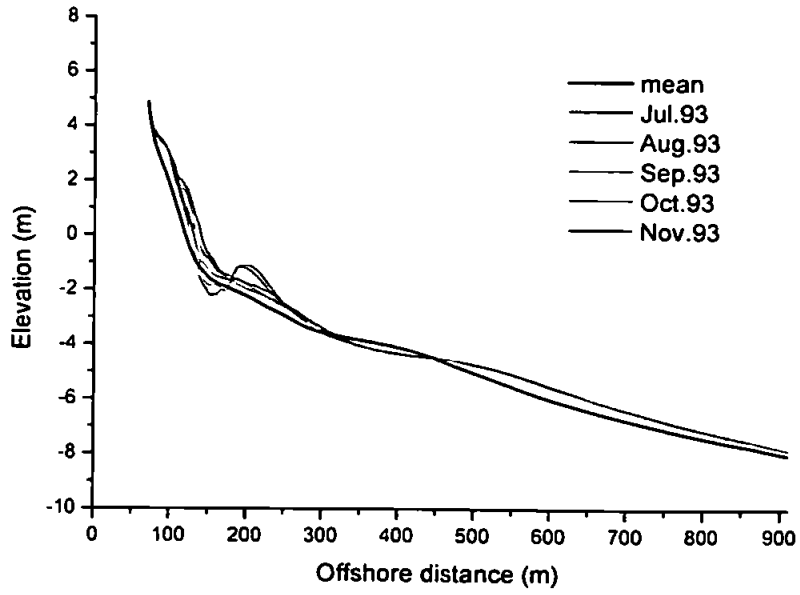

Figure 6.8 Typical summer beach profile change.

The three representative observation points also illustrate that in 2002 the temporal wavelet variance components are small. These results indicate that the beach profile change must have been quite small. The profile configurations of the surveys from May 2002 to January 2003 are shown in Figure 6.9. It can be seen that during this short period although an inner bar can be identified it was quite small. Apparently, the beach elevation at 410m offshore did not change much during this period. On the other hand, the observation end point that is located at 910m offshore was substantially below the mean in January 2003. The mean water depth at this observation was 8.03m, whilst in January 2003 the water depth was 8.36m. These results reveal an unusual onshore sediment transport during later autumn and winter. Moreover, Figure 6.9 shows an obvious node at 358m during this short period. Between the node and the point at 410m offshore the beach elevations of these surveys were slightly under the mean profile. These can be attributed to the calm winter in 2002.

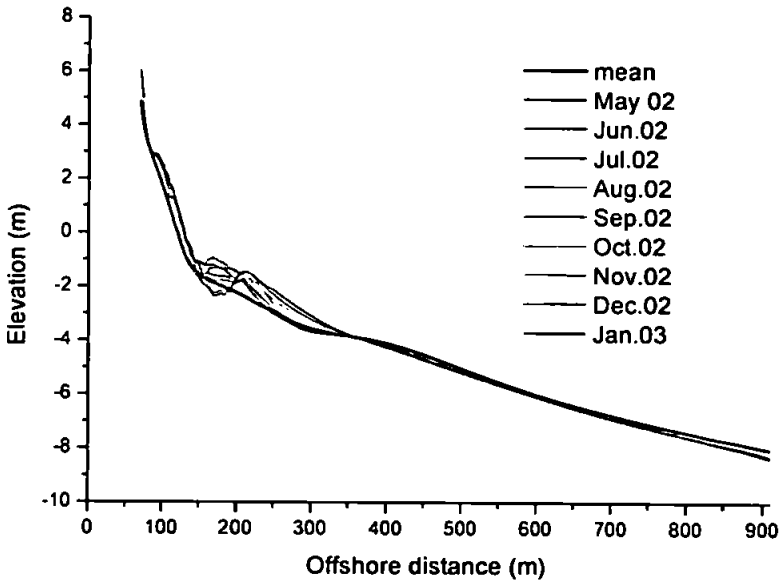

Figure 6.9 Beach profile changes in a mild winter of 2002.

6.3 Scale-dependency of beach profile changes in time

In Section 6.2, the temporal scales of beach profile changes have been studied on three representative observation points along a profile. Some common features and individual characters have been distinguished. To compare the variability of beach elevation at different locations along the profile, the wavelet correlation coefficients between the three time series at different scales were computed using Equation (3.20). The correlation coefficients among the three points were plotted in Figure 6.10 against the temporal scale.

The correlation between the changes of beach elevation at 120m and 260m decreases when the temporal scale increases from 2 months to 8 months. The possible explanation is that the extreme events affect the beach profile changes in a period less than 8 months. On the other hand, the correlation increases steeply from -0.197 to 0.861 when the temporal scale increases from 8 months to 64 months, which suggests that in the long-term the changes at 120m are highly correlated with those of 260m.

The correlations between the changes in beach elevation at 120m and 410m show a different pattern at the longest temporal scale. The correlation coefficient at the temporal scale of 64 months is -0.486, which strongly indicates the sediment exchange at these two observations. The larger correlation at the temporal scale of 2 months between the observations of 260m and 410m offshore may imply that when there are extreme events these two observation points behave in a more similar way than do the two observations at 120m and 260m. Moreover, the correlation between 260m and 410m is negative at the temporal scales larger than 4 months. This result implies that sediment is transported between them at this temporal scale. That is, the sediment transported offshore from 260m will deposit at 410m and the sediment transported onshore will accrete again at 260m in the temporal interval of 4-8 months. In addition to this short term sediment transport, the larger negative correlation between these two points indicates the migration of bars at longer terms.

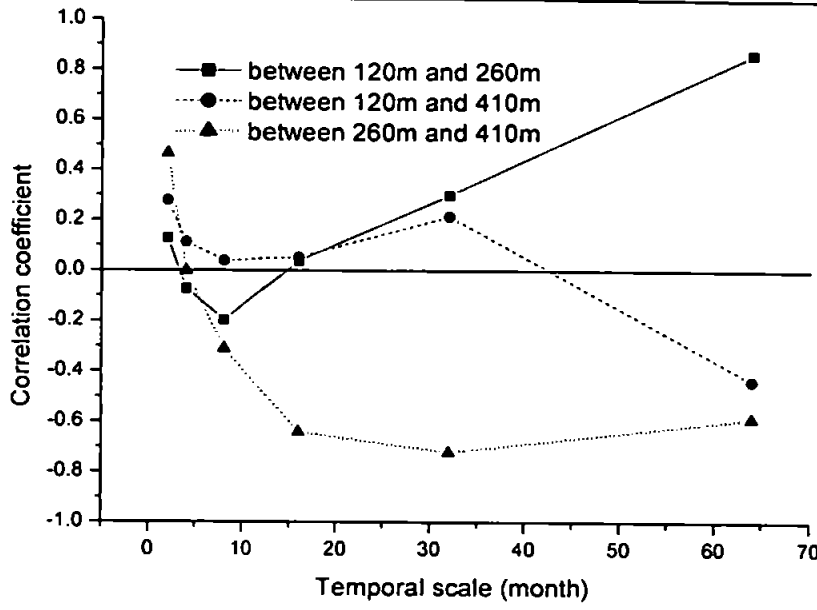

Figure 6.10 Correlation among the three points at different temporal scales.

The beach profile was divided into nine regions as listed in Table 6.1 in order to investigate the space-dependency of temporal wavelet variance along the profile further. Subsequently, the average wavelet variance of these regions at different scales were computed and shown in Figure 6.11. To distinguish the variability more specifically, R1 denotes the dune zone, R2 and R3 denote the inner bar zone, R4 and R5 is defined as the outer bar zone and R6 to R9 is defined as the upper shoreface.

Figure 6.11 shows that the overall average wavelet variance decreases when the observation points move towards the upper shoreface. However, the pattern of variance in region R1, the dune zone, is apparently different from those of other regions. It also can be seen from Figure 6.11 that the maximum variance at this temporal scale is located in the region of R2.

It also can be seen from Figure 6.11 that the maximum average wavelet variances at the temporal scales of 16 and 32 months are in the region of R3. Generally, sediment eroded from the dune zone is often transferred past the shoreline and deposited just seaward of the shoreline. However, the average wavelet variance at the temporal scale of 64 months is largest in the dune zone and larger than the variance at other finer scales in the region of R6. Therefore, a possible explanation is that at the temporal scale of 64 months (64-128 months, in average 6 years) there is

exchange of sediment between the dune zone and the upper shoreface. This interpretation is consistent with the argument of Wright *et al.* (1991) that the onshore-offshore exchange of sediment over years to decades is not confined to the average surf zone, where most beach profile studies have occurred, but extends across the shoreface.

Table 6.1 Regions across the beach profile

R1	R2	R3	R4	R5	R6	R7	R8	R9
Dune zone	Inner bar zone		Outer bar zone		Upper shoreface			
70-120m	122-220m	222-320m	322-420m	422-520m	522-620m	622-720m	722-820m	822-910m

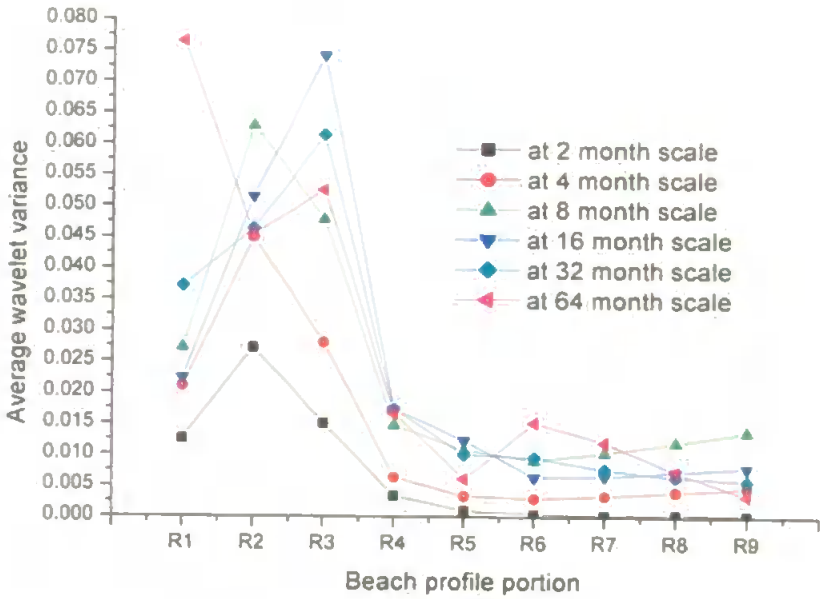

Figure 6.11 Average wavelet variance in different portion along the profile with an interval of 100m.

The temporal wavelet variances of beach elevation were plotted scale by scale for all the given points along the profile as shown in Figure 6.12 in order to give a general overview of the wavelet variance. The shapes of the plots of the wavelet variance at the temporal scale of 64, 32 and 16 months are similar to that of the SD of beach elevation shown in Figure 4.7. This similarity shows the consistency of wavelet analysis with traditional statistical analysis, while the different shapes at

the temporal scale of 8, 4, and 2 months again illustrate the strengths of wavelet techniques that can characterize the short term variation of beach elevation that can be shadowed by long-term trend.

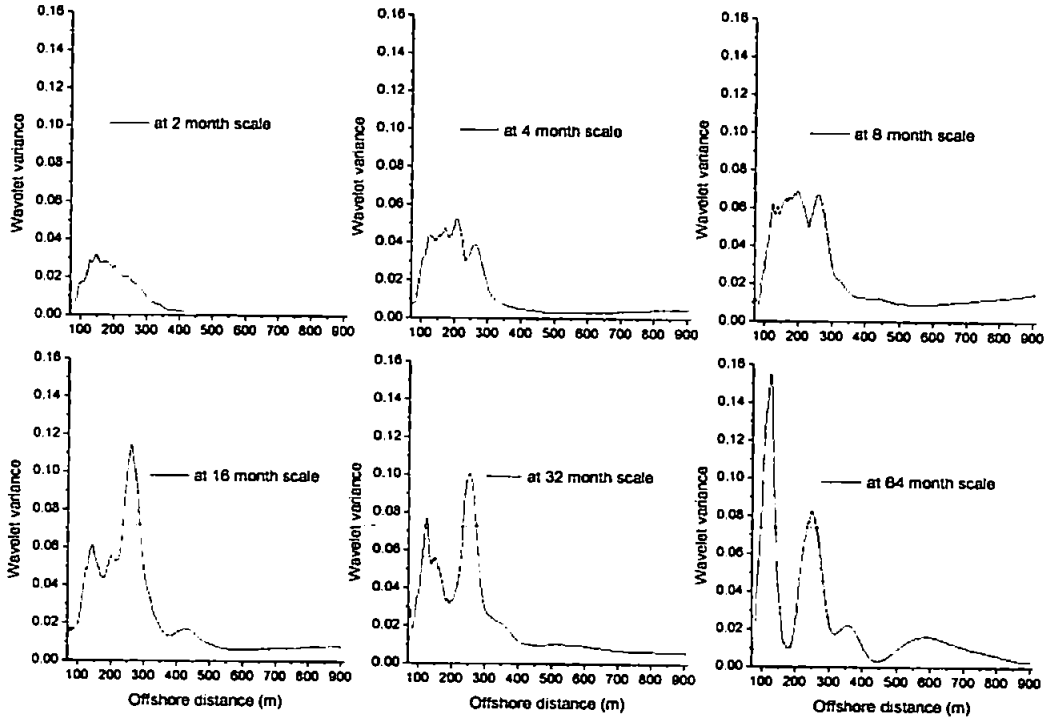

Figure 6.12 Wavelet variance at all temporal scales against cross-shore position.

It is seen that all of the peak variances of beach elevation at the temporal scales of 16, 8 and 4 months are around 260m offshore, where inner bars usually occur. This figure further substantiates that change in the beach profiles seaward of 400m is negligible, indicating "closure" for the data set, which is consistent with the results from the spatial analysis presented in Section 5.2.4. The fact that the wavelet variance at a given point has similar order of magnitudes at different scales, as shown in Figure 6.12, give an overall view that the variances come from a combination of temporal scales, indicating the different coastal morphodynamic at different portions of the profile. Moreover, it can be seen that the dominant temporal scales vary with the locations along the profile. This explains the different temporal patterns of beach profile changes at different locations along the profile.

6.4 Contours of temporal wavelet standard deviations of beach elevation

The variability of the profile in time over a wide range of scales has been studied at three representative observation points along the profile in the above sections. To generalize the main patterns of beach profile changes during the course of study at different temporal scales, the temporal wavelet SD components of beach elevation at each observation along the profile were computed using Equation (3.23).

The contours generated from the temporal wavelet SD of all the beach elevations along the profile are illustrated in the space-time plane scale by scale. In what follows, the horizontal axis denotes the offshore distances and the vertical axis denotes the months that the points along the profile were surveyed. The larger magnitudes are denoted by darker contours.

Figure 6.13 displays the contours at the temporal scale of 2 months along the profile. The maximum temporal SD component of beach elevation is 0.7. There are two regions of larger SD on the contour located at 160m, which are centred in the 36th (June 1984) and 90th month (February 1989) separately. The interpretation is that the profile in June 1984 had an inner bar centred at 160m. In contrast, the profile in February 1989 had an apparent trough centred 160m offshore whilst it had a conspicuous bar located 246-354m.

Moreover, the beach elevations seaward of 360m in February 1989 were substantially below the mean profile, which explains the large SD shown in Figure 6.13. This beach profile responded to the storm group during the February 1989 and March 1989. That means another storm in March 1989 occurred before the sediment transported to the upper shoreface during the storm in February 1989 had enough time to transport back to the surf zone. Therefore the SD is also relatively large in the upper shoreface region. Another striking peak of SD in Figure 6.13 is located in the region from 420m to 500m centred in the 232nd month (October 2000), when an outer bar was identified around 410m offshore.

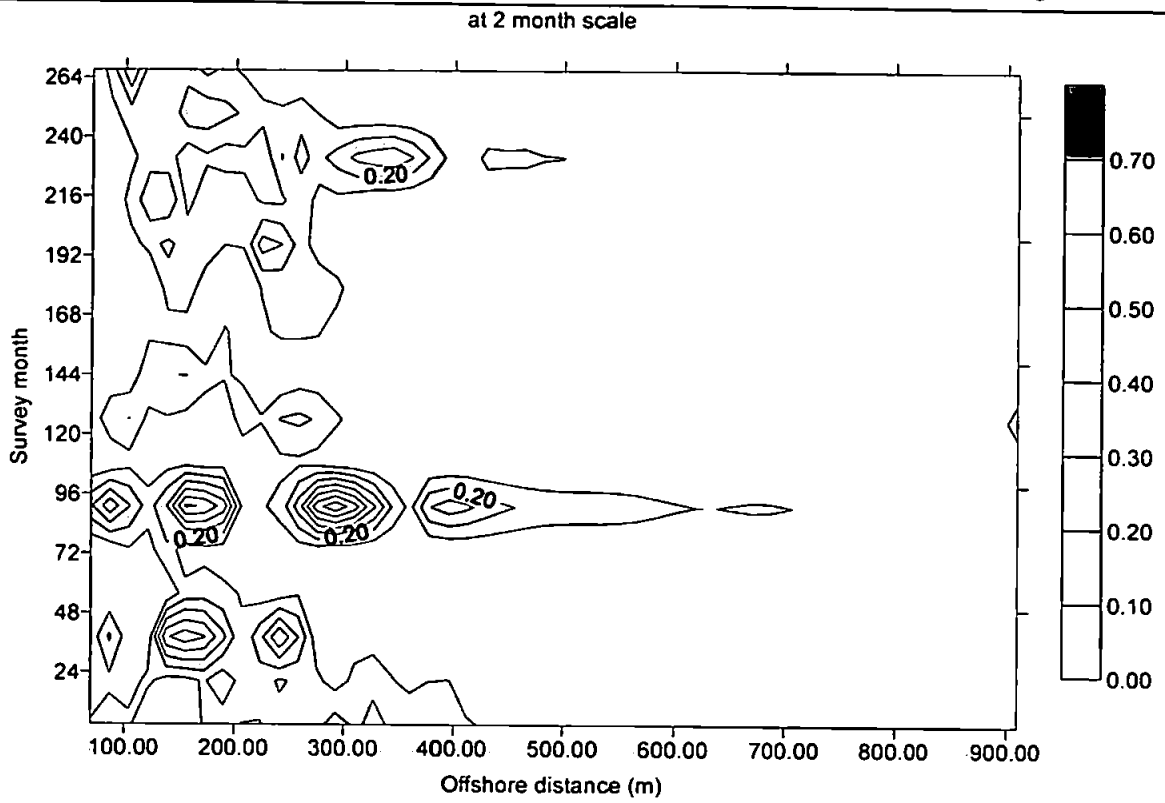

Figure 6.13 Contour of wavelet SD at the temporal scale of 2 months along the profile.

Figure 6.14 displays the contours at the temporal scale of 4 months along the profile. The maximum temporal SD component of beach elevation is 0.5. The feature centred in the 90th survey (February 1989) on the contour is similar to that of at the temporal scale of 2 months. Moreover there is another patch located 190m offshore, where an inner bar located in the region 180m-224m offshore was identified in October 1996 (the 184th survey). Another striking patch on the plot is centred in the 204th survey (June 1998) during the period from April 1998 to August 1998 (the 202nd to 206th survey) when two bars were identified, with one situated 400m offshore. In addition, the contour of wavelet SD at the temporal scale of 4 months shows the sediment transport in deep water during the period from June 2002 to September 2003 (the 228th to 267th survey), which may be related to the calm winter.

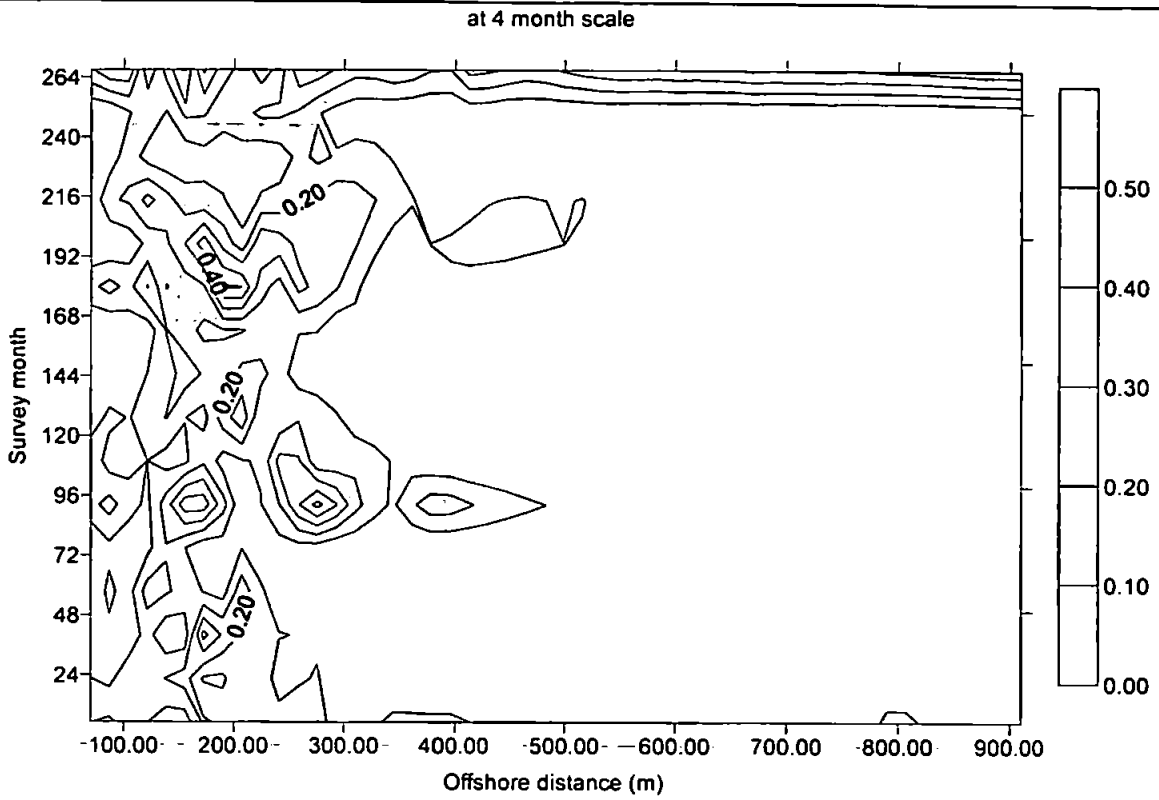

Figure 6.14 Contour of wavelet SD at the temporal scale of 4 months along the profile.

Figure 6.15 displays the contours at the temporal scale of 8 months along the profile, where the maximum temporal SD component of beach elevation is 0.7. Apparently, the patch, related to February 1989 (the 92nd survey) at the temporal scale of 8 months, is not as striking as at the two finer scales. There are two patches around the 58th month (April 1986). The patch located 180m offshore explains the presence of a deep trough whilst another patch located 240m offshore explains the existence of an inner bar in April 1986 (the 58th survey).

In addition to the sediment transport in deep water during the period from June 2002 to September 2003 as identified on the contour at the temporal scale of 4 months, another similar process is identified at the temporal scale of 8 months during the period from July 1981 to August 1982 (the 1st to 14th survey). The adapted wavelet filters of Cohen *et al.* (1993) might introduce bias due to the edge effect of wavelet transforms, which is the possible explanation for this patch since the forcing conditions are normal during this period.

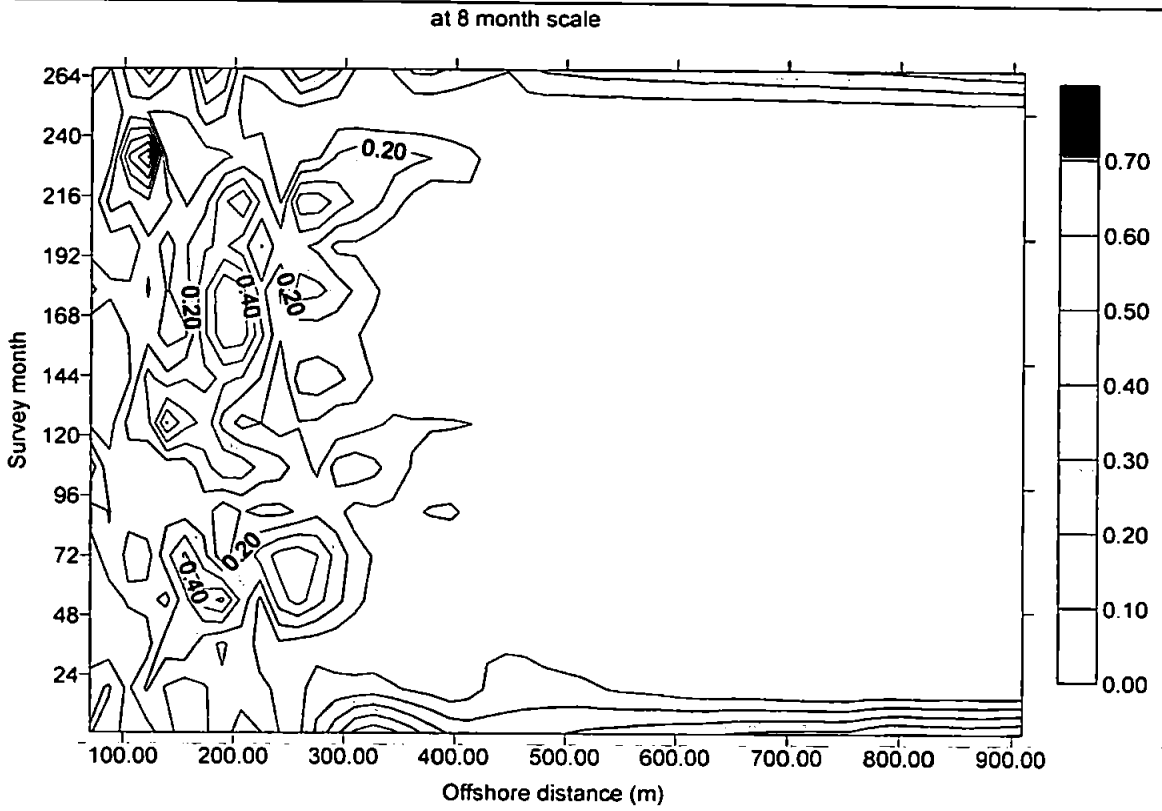

Figure 6.15 Contour of wavelet SD at the temporal scale of 8 months along the profile.

Figure 6.16 displays the contours at the temporal scale of 16 months along the profile, where the maximum temporal SD component of beach elevation is 0.8. In comparison with the above two temporal scales, it is found that the contour patch with SD of 0.4 at the temporal scale of 16 months moves further offshore from October 1996 to June 1998. This result can explain that the bar crest in the surf zone was shifted further offshore due to the storms. Moreover, it can be seen from Figure 6.16 that the patch of contours identified at the temporal scale of 8 months during the period from July 1981 to August 1982 still holds at the temporal scale of 16 months.

Figure 6.17 displays the contours at the temporal scale of 32 months along the profile. The maximum temporal component of SD is 0.7. In terms of the distribution of the large SD, the overall contour at the temporal scale of 32 months is quite different from those of the finer scales as discussed above. A striking feature on this figure is the peak in SD during the period from February 1987 to February 1989 with a region extending further to 680m offshore. As a matter of fact, both February 1987 and February 1989 were marked as storm groups by Lee *et al.* (1998), who defined storm groups as at least two storms within a period of less than 39 days both with wave

height $H_{m0} > 4$ m. Another large patch on this contour is related to the storm group in August 1999 when the maximum wave height was up to 6.1m on August 31 1999. This patch of contours extends to 910m offshore. The two apparent large patches provide strong evidence that the beach profile changes over longer periods usually involves larger portions of the beach profiles.

In addition, there are two very narrow patches on the contours in Figure 6.17. One is around the 144th survey (June 1993) from 500m to 650m offshore, which might be the consequence of the storms in March 1993. Another is around the 177th survey (March 1996) from 500m to 620m offshore corresponding to the storm on March 1996. Referring to the results in Section 5.2.1, the survey in March 1996 has the largest wavelet variance at the spatial scale of 128m.

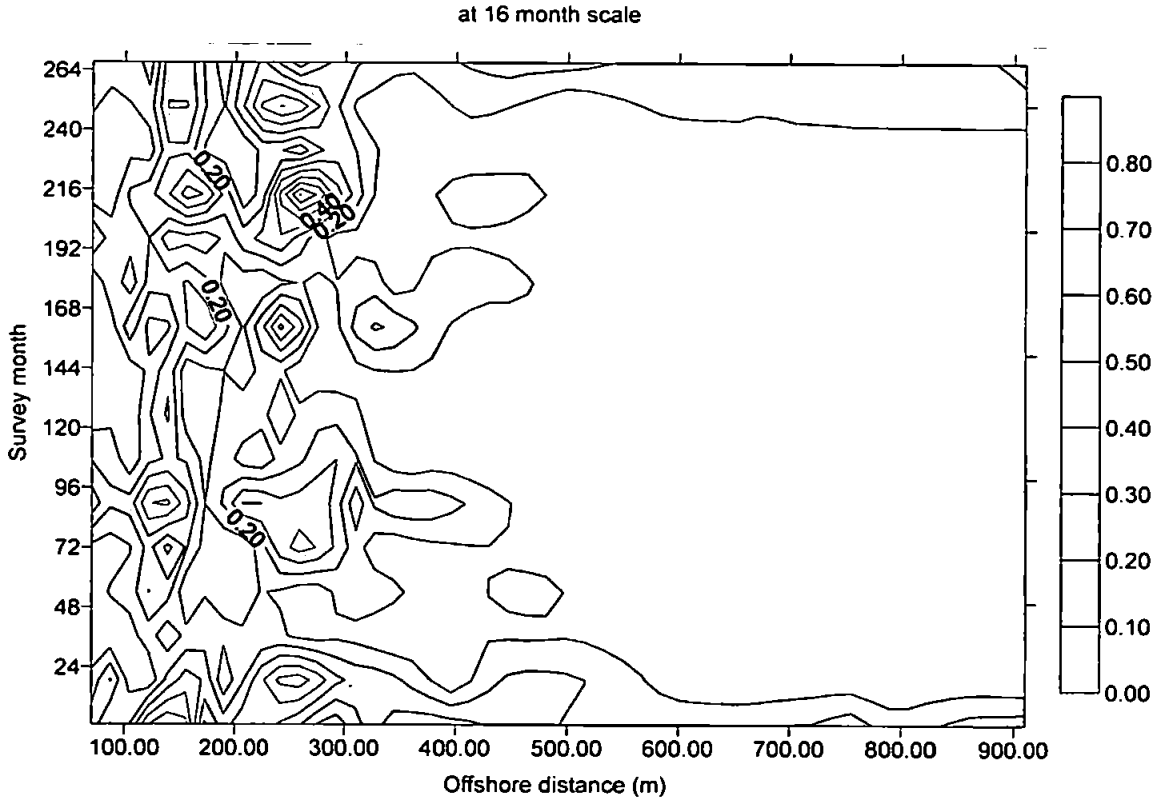

Figure 6.16 Contour of wavelet SD at the temporal scale of 16 months along the profile.

Figure 6.18 displays the contours at the temporal scale of 64 months along the profile. The maximum temporal SD component of beach elevation is 0.7. The region of the largest SD is centred at 120m offshore during the period from the 216th (June 1999) to 267th month (September

2003). This result again highlights that beach elevation change near the shoreline involve in large temporal scales.

In addition, there are a few striking patches located 460m-800m offshore in Figure 6.18. One representative patch spans from the 80th to 156th survey, which is during the period from February 1988 to June 1994. During this period there were three intensive storm groups occurred in February 1989, December 1989 and October 1991 (Lee *et al.* 1998). The Halloween storm in October 1991 was most remarkable since its energy was unusually high and the wave period was up to 24s. Another representative patch includes the 177th survey, which has been discussed for the contour at the temporal scale of 32 months. The difference is that the patch spans longer in time and wider in space along the profile.

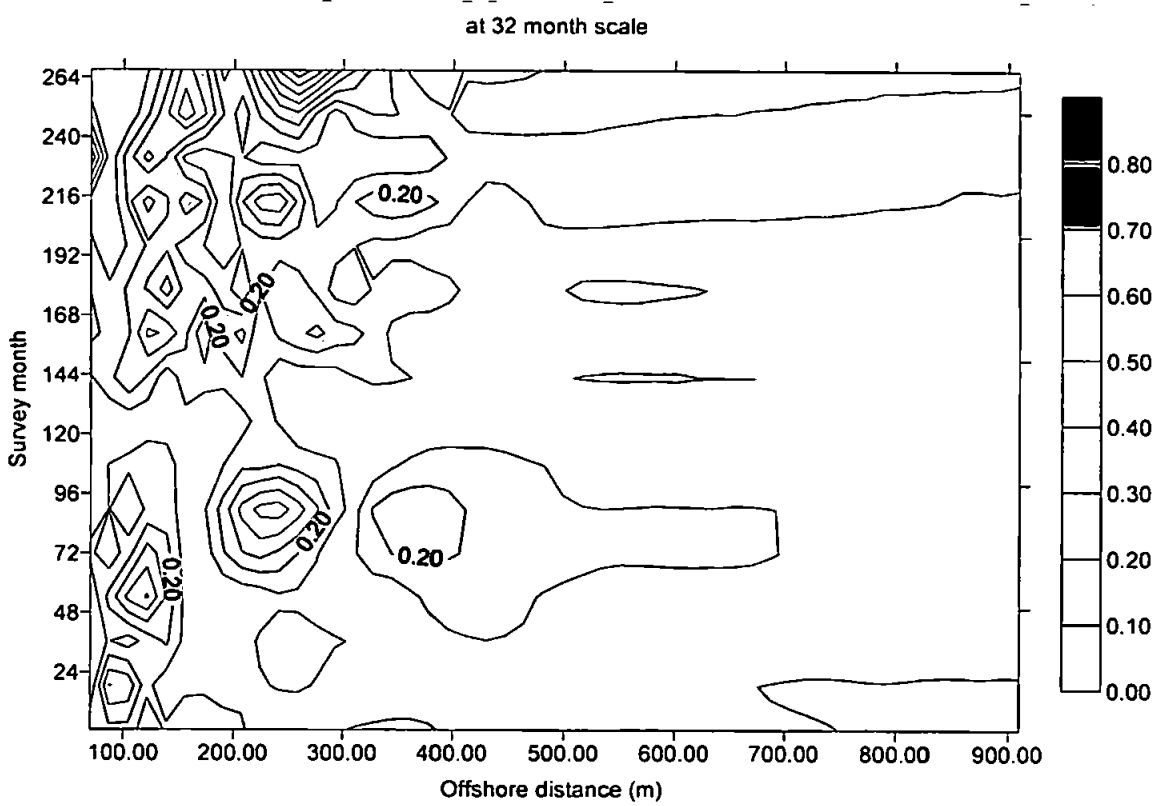

Figure 6.17 Contour of wavelet SD at the temporal scale of 32 months along the profile.

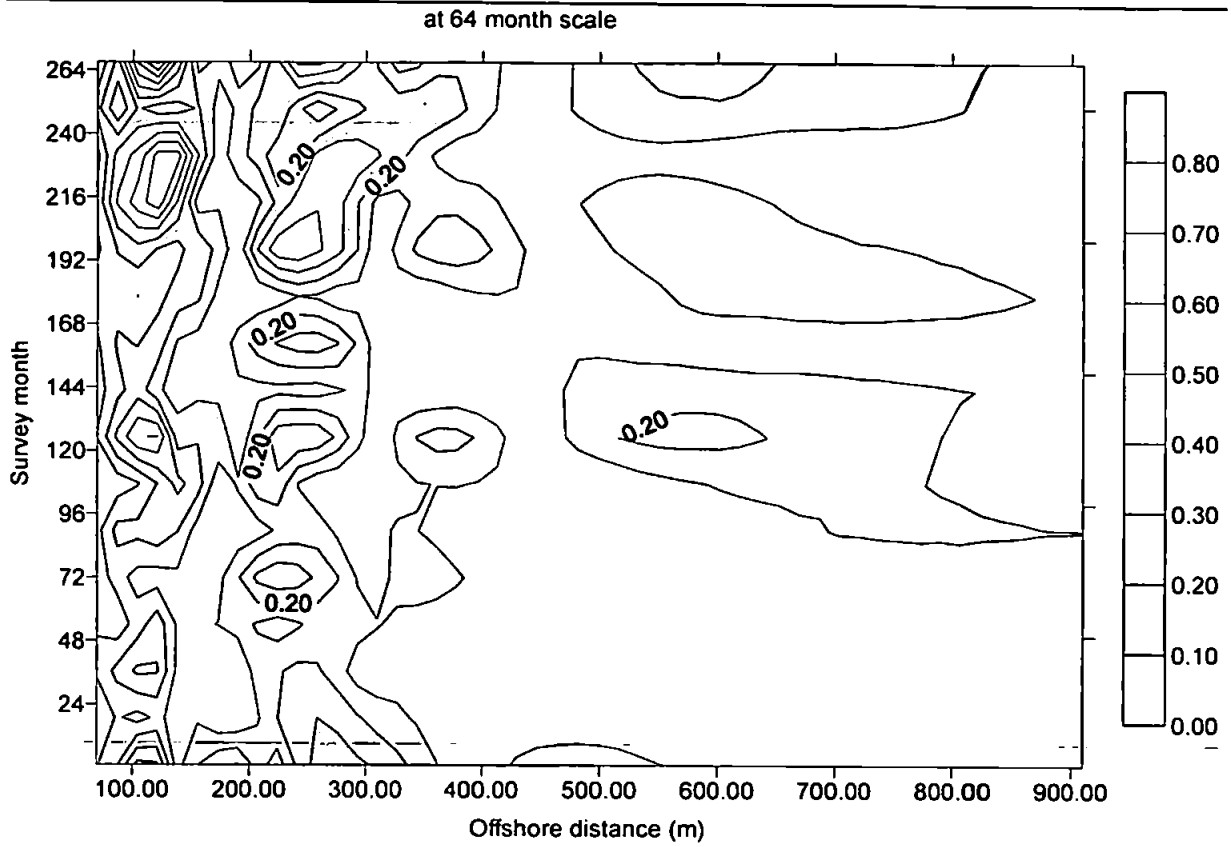

Figure 6.18 Contour of wavelet SD at the temporal scale of 64 months along the profile.

The analyses above show that changes in beach elevation along the profile contain different temporal patterns. For example, the striking feature that is located 400m-700m offshore along the profile in February 1989 on the contour of temporal scale of 2 months has no equivalent at the temporal scale of 8 months. This result again illustrates the nature of scale-dependency of beach elevation changes in time series. Moreover, the distribution of patches on the contour of temporal scale of 8 months is much more regular than other scales. It can be concluded that the overall beach profile changes shows a strong annual period since the 8 month scale is referred to the temporal interval 8-16 months.

By analysing the contours of temporal wavelet SD, some extreme storm events have been identified. However, not all the beach profile response to storms can be distinguished by observing the contours of SD of beach elevation at a range of temporal scales. The first reason is that the onshore feed of sediment is not significantly affected by individual storms during the fair weather conditions. Another explanation is that beach profile change depends much on the antecedent profile configuration before the storms.

The comparison of the contours at all temporal scales implies that the maximum wavelet SD component of beach elevation does not vary greatly among different temporal scales. This result is quite different from that of spatial pattern analysis in Section 5.2.4 where the maximum component of wavelet SD increases significantly with the spatial scales. No temporal scales contributing predominantly to the overall variance illustrate again the much more complicated variability of beach profiles in the time series.

6.5 Identifying changes in temporal wavelet variance of beach elevation

As in the case for the spatial analysis, the time at which changes in temporal wavelet variances occur can be identified according to the procedure described in **Chapter 3**. The critical values to identify the changes in temporal wavelet variance at different scales are listed in Table 3.3. Figures 6.19-6.23 display the identified changes in temporal wavelet variance scale by scale, where the different marks from one to nine denote the orders that the changes in temporal wavelet variance are identified.

The identified changes in the wavelet variance at the temporal scale of 2 months are shown in Figure 6.19. It can be seen that most of the identified changes in temporal wavelet variance happen seaward of 400m (deep water), and the changes usually happen in winter. This result is not a surprise. In general, the occurrence of severe storms that move sediment offshore (in deep water) is in winter. If much sediment is transferred offshore due to extremely severe storms, the temporal wavelet variance components of the observations in deep water might have a sharp change from the general seasonal trend. For example, in the portion from 700m to 910m across profiles, changes in wavelet variance at the temporal scale of 2 months are identified in the 124^{th} survey (October 1991) when there were severe storms with wave height up to 5m and wave period up to 20s.

Most of the changes in the wavelet variance at the temporal scale of 4 months are also located seaward of 400m, as shown in Figure 6.20. The difference is that the most of the changes in variance at this temporal scale are identified in summer. Moreover, the overall orders of identified changes in the wavelet variance decrease from nine to four as the temporal scales increase from 2

months to 4 months. The reason is that the critical values B at finer scales are stricter than those of the coarser scales as shown in Table 3.3.

The number of the identified changes in temporal wavelet variance becomes less as the temporal scale increases. Figure 6.21 depicts the contour of the temporal SD and the change months in wavelet variance at which significant change occurs at the temporal scale of 8 months. It can be seen that the changes in temporal variance located seaward of 750m are identified in the 8th and 253rd survey, which are in February 1982 and July 2002. This result indicates that at most parts of beach profiles the temporal variance at the temporal scale of 8 months is uniform.

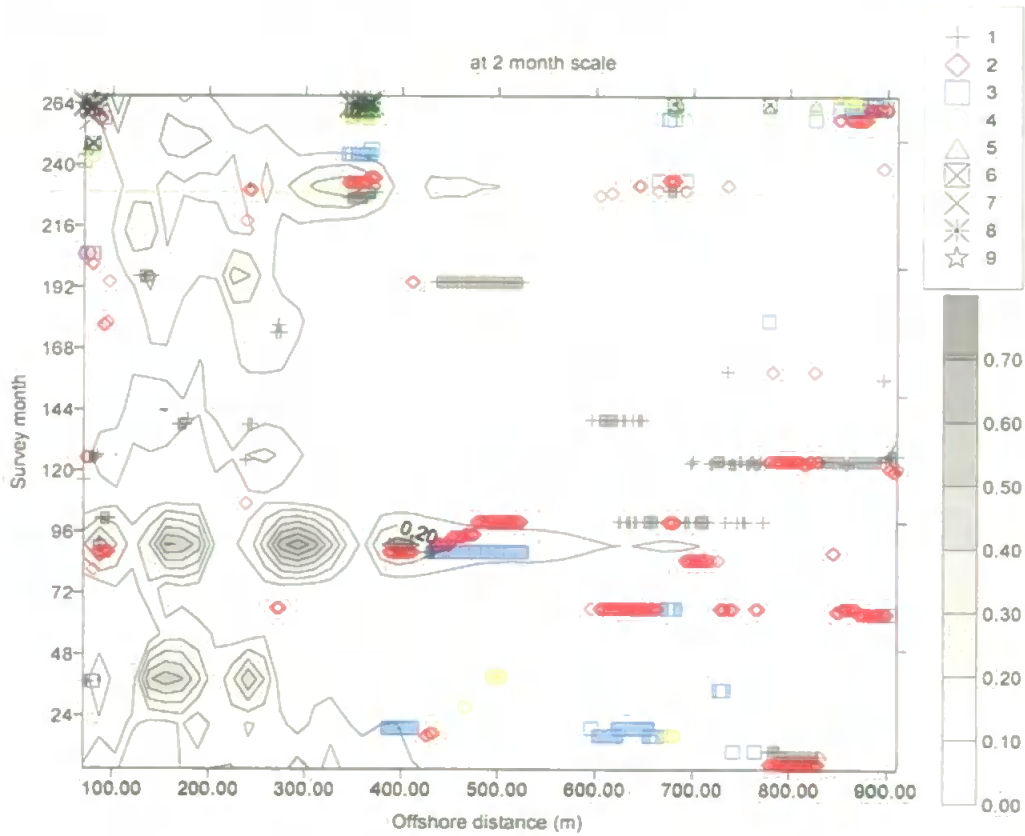

Figure 6.19 Distribution of changes in temporal wavelet variance at the temporal scale of 2 months.

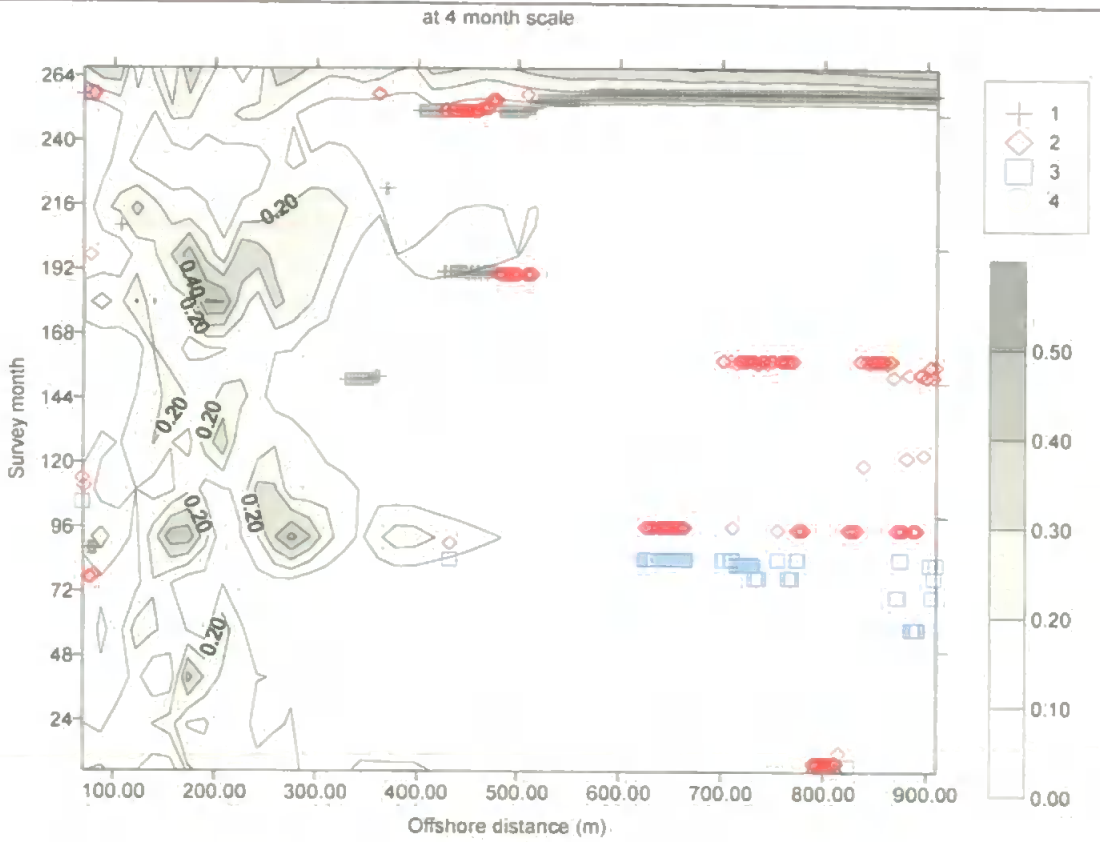

Figure 6.20 Distribution of changes in temporal wavelet variance at the temporal scale of 4 months.

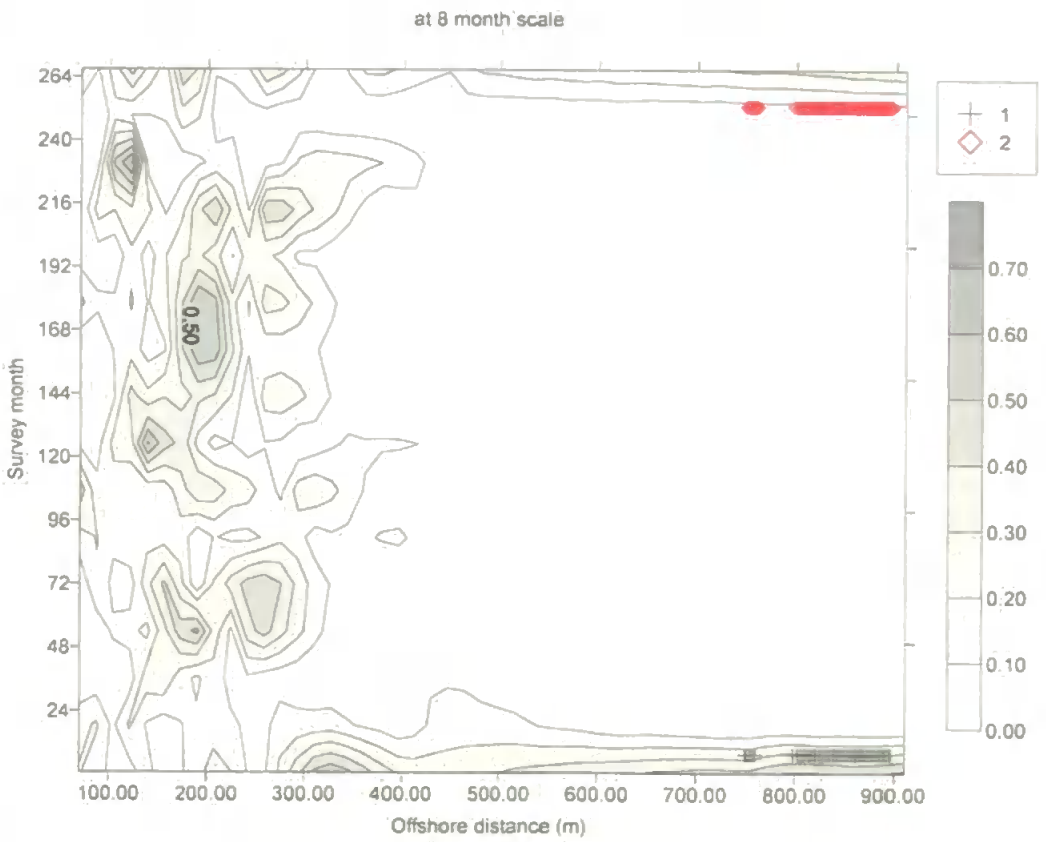

Figure 6.21 Distribution of changes in temporal wavelet variance at the temporal scale of 8months.

A similar trend is found in the variances of part of the profiles at the temporal scales of 16, 32 and 64 months. The significant changes in wavelet variance at the temporal scale of 16 months and 64 months are shown in Figure 6.22 and Figure 6.23. The distribution of identified changes in temporal variance at the temporal scale of 32 months is not displayed in this thesis because there is only one identified change in wavelet variance. The change identified at 72m offshore in the 160th survey is in October 1994. This change is overlooked since the point is close to the boundary of this study. The change might be due to the edge effect of wavelet transforms as described in **Chapter 3**. The uniformity of temporal wavelet variance at the coarser scales demonstrates that the beach profiles are highly correlated over these longer temporal scales.

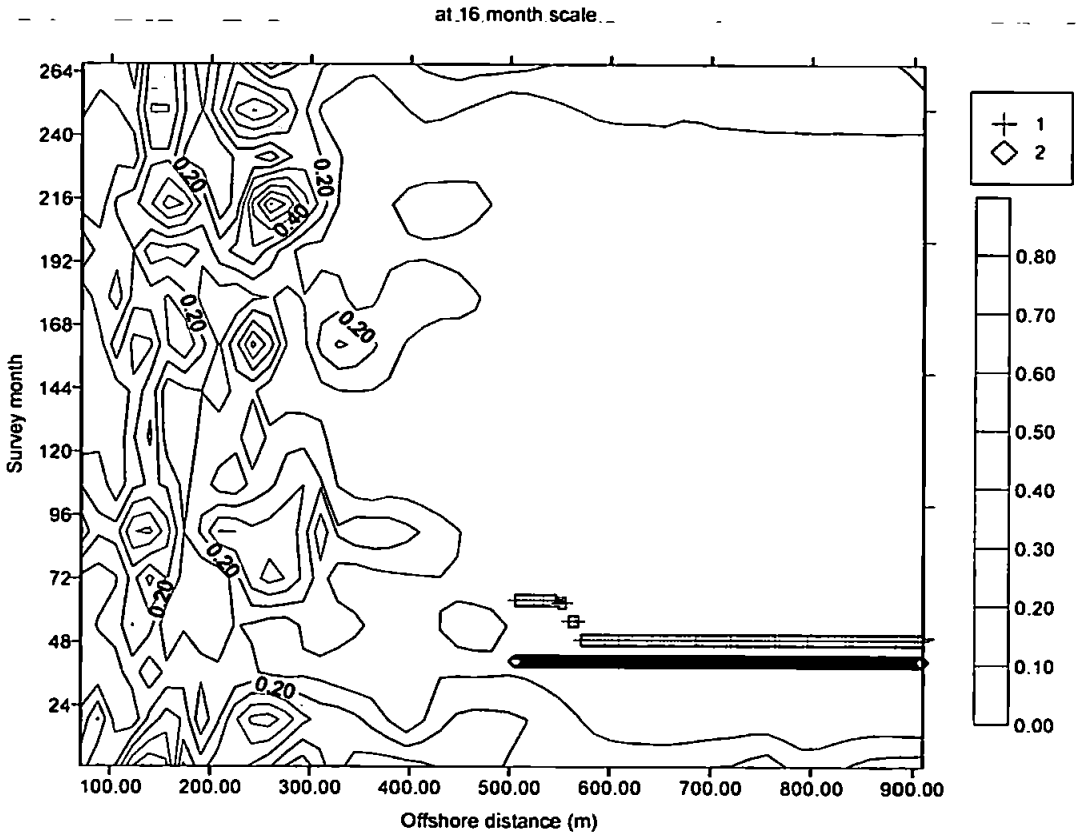

Figure 6.22 Distribution of changes in temporal wavelet variance at the temporal scale of 16 months.

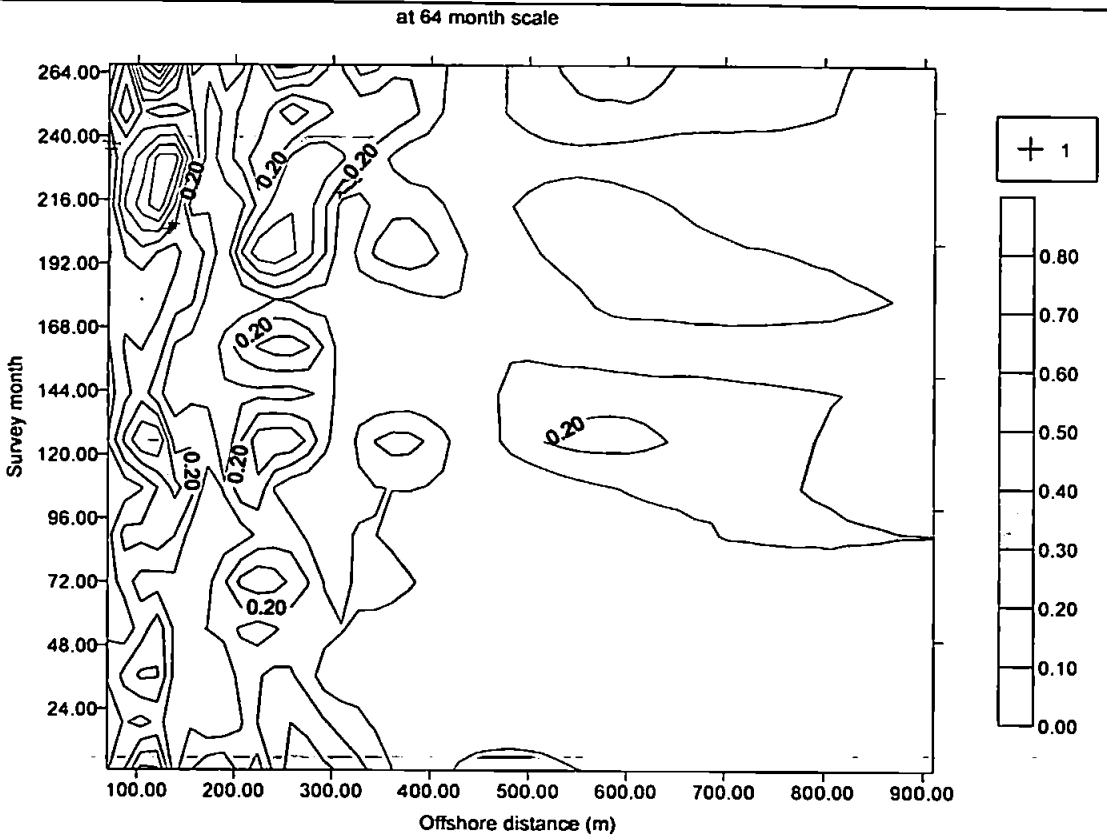

Figure 6.23 Distribution of changes in temporal wavelet variance at the temporal scale of 64 months.

The identified change points in temporal wavelet variance can be interpreted further by examining the beach elevations during the course of the study at different scales. Figure 6.24 shows the evolution of beach elevation during the course of study from 350m to 850m offshore with an interval of 100m. As one example, the detail components at the temporal scale of 4 and 8 months are shown in Figure 6.25 for the beach evolution at 650m offshore. The detail components at the temporal scale of 4 months show an apparent change in the 92nd month (February 1989). The spike on the plot of the temporal scale of 4 months interprets the change point in Figure 6.20. The much smoother plot of the temporal scale of 8 months explains there is no change in temporal variance at 650m in Figure 6.21.

In all, the identified changes in temporal wavelet variance show a strong scale-dependency. The many changes at the temporal scale of 2 and 4 months can be explained by the short term storms, which have no long-term effect as indicated by the few changes at the coarser scales. The spatial distribution of the changes in temporal variance shows that most of the abrupt changes in variance

of beach elevation are in seaward of 400m. These results demonstrate again that the unusual severe storms or storm groups affect the profile in deep water (upper shoreface) whereas the waves during mild weather cannot affect the upper shoreface of the profile.

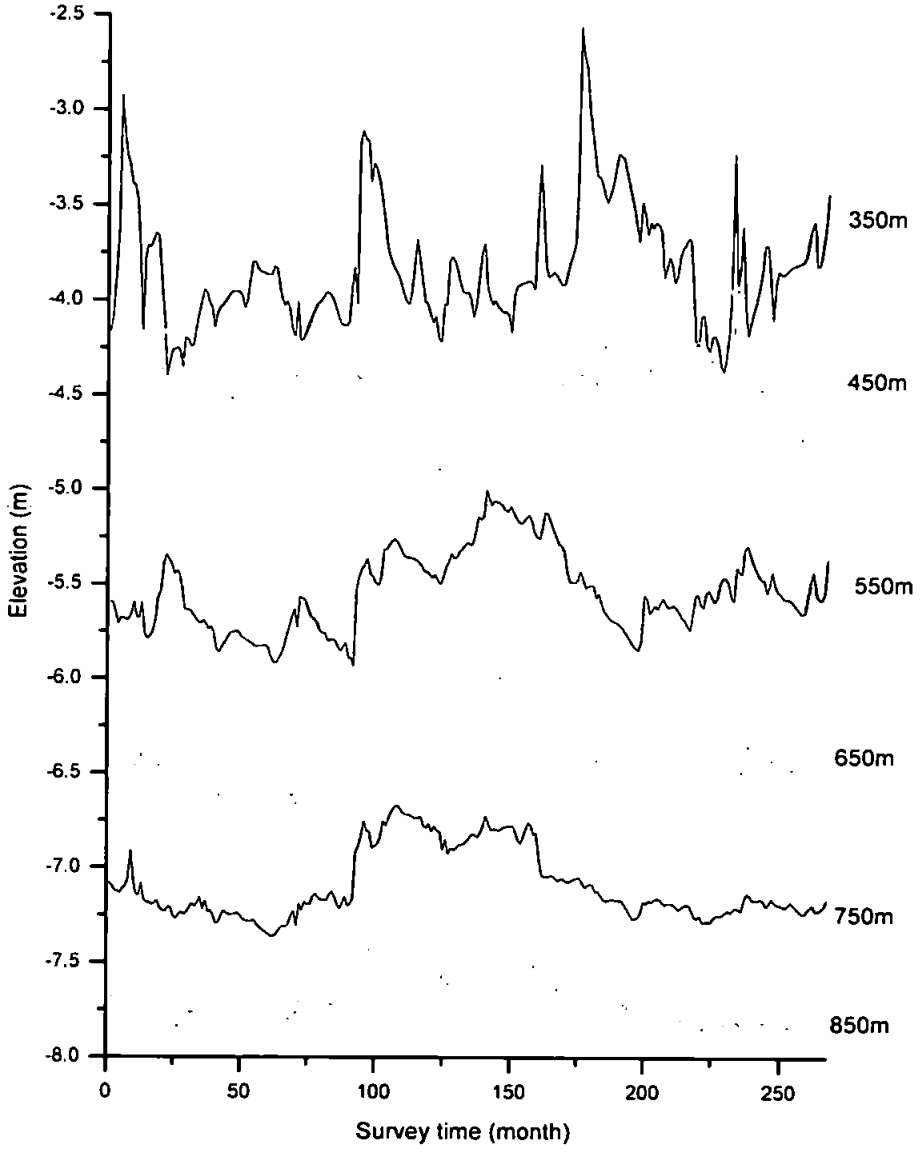

Figure 6.24 Beach elevations at different locations along the profile during the course of the study.

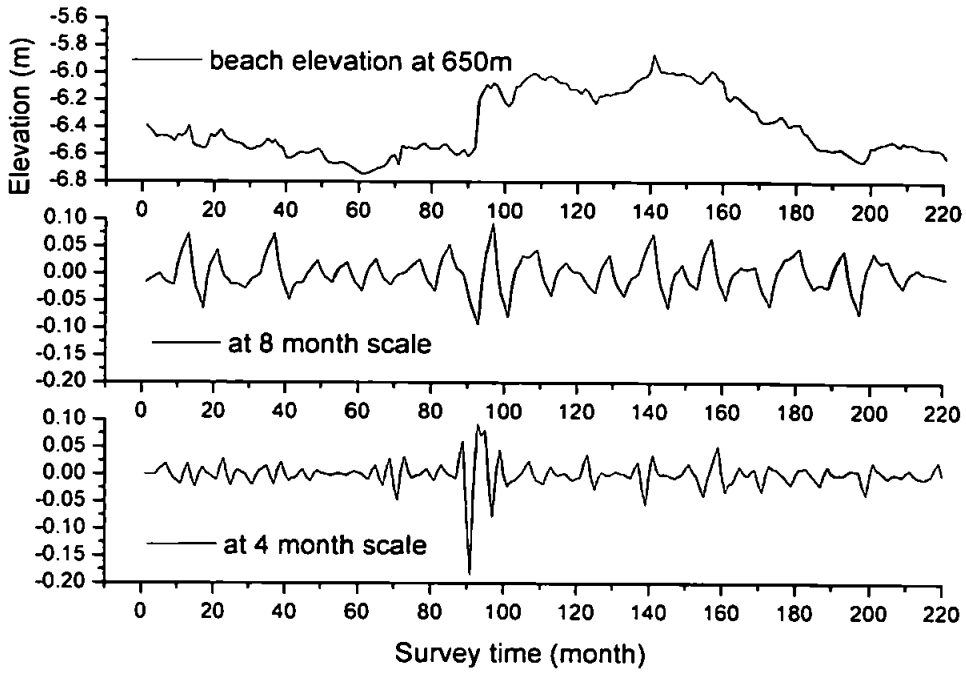

Figure 6.25 Detail components at the temporal scale of 4 months at 650m offshore.

6.6 Principal Conclusions from the AMODWT Analyses

In an analogous way, the second wavelet analysis was applied to the temporal variation of beach levels at fixed locations along the profile. In what follows are some findings:

- The results on the whole provide strong support for the contention that variations of beach profiles are statistically non-stationary in time.
- The detail components in the DWT capture the local variation in time series which happens at different temporal scales, and the approximation components at higher scales can indicate the long-term evolution of beach elevation. This provides information about the dominant time scales of beach elevation changes at particular locations along the profiles.
- The temporal scales contrast with those from the spatial analysis in that they do not show the clear dominance of a few scales. The result shows that there are no clearly defined temporal scales of variation that dominate consistently during the course of study. Rather, there is a strong pattern of intermittency at most temporal scales, which is clear at locations across the length of the profile.

- However the wavelet analysis at the three representative locations along the profile does indicate that different temporal scales have a different balance of influence on the overall variance as one moves along the profile.
- The contours of wavelet SD at different temporal scales provide much more general information about the beach profile changes at all observation points along the profile. The significant change in beach elevations occurs at the temporal scale over 4-16 months. Moreover, the contours of wavelet SD of beach elevation support the contention that the changes of beach elevation occurring over a longer time period usually involve a larger portion of beach profiles.
- The relatively larger number of changes identified in temporal wavelet variance at finer scales seaward of 400m has been explained by the irregular occurrence of extreme single storms or storm groups that have obvious impact in deep water.
- The few identified changes in the wavelet variance at the temporal scales of more than 8 months illustrate the long-term uniformity of beach profile changes.

So far, by analysing the variability both in space and time using the AMODWT, the basic temporal patterns of beach profile line 62 at Duck have been identified and some exceptional events have been explained. Due to the localized nature of wavelets, wavelet analysis is well suited for investigating non-stationary time or space series. This property makes them extremely useful as a tool for analyzing coastal data.

6.7 Temporal Analysis with the DWPT

6.7.1 Temporal scale analysis using the DWPT

Similar analyses to the spatial scale analysis are carried out to study the beach elevation changes in time series using the DWPT. The time series of beach elevation at three fixed points along the profile line 62 at Duck were examined with wavelet packets obtained by six dilations of the wavelet. For information of the evolution of the three points during the course of study, please refer to Figure 6.1.

Table 6.2 DWPT for the point at 120m offshore with shaded cells denoting the best basis.

(1,0)	(2, 0)	(3, 0)	(4, 0)	(5, 0)	(6, 0)
					(6, 1)
				(5,1)	(6, 2)
					(6, 3)
			(4, 1)	(5, 2)	(6, 4)
					(6, 5)
				(5, 3)	(6, 6)
					(6, 7)
		(3, 1)	(4, 2)	(5, 4)	(6, 8)
					(6, 9)
				(5, 5)	(6, 10)
					(6, 11)
			(4, 3)	(5, 6)	(6, 12)
					(6, 13)
				(5, 7)	(6, 14)
					(6, 15)
	(2, 1)	(3, 2)	(4, 4)	(5, 8)	(6, 16)
					(6, 17)
				(5, 9)	(6, 18)
					(6, 19)
			(4, 5)	(5, 10)	(6, 20)
					(6, 21)
				(5, 11)	(6, 22)
					(6, 23)
		(3, 3)	(4, 6)	(5, 12)	(6, 24)
					(6, 25)
				(5, 13)	(6, 26)
					(6, 27)
			(4, 7)	(5, 14)	(6, 28)
					(6, 29)
				(5, 15)	(6, 30)
					(6, 31)
(1, 1)	(2, 2)	(3, 4)	(4, 8)	(5, 16)	(6, 32)
					(6, 33)
				(5, 17)	(6, 34)
					(6, 35)
			(4, 9)	(5, 18)	(6, 36)
					(6, 37)
				(5, 19)	(6, 38)
					(6, 39)
		(3, 5)	(4, 10)	(5, 20)	(6, 40)
					(6, 41)
				(5, 21)	(6, 42)
					(6, 43)
			(4, 11)	(5, 22)	(6, 44)
					(6, 45)
				(5, 23)	(6, 46)
					(6, 47)
	(2, 3)	(3, 6)	(4, 12)	(5, 24)	(6, 48)
					(6, 49)
				(5, 25)	(6, 50)
					(6, 51)
			(4, 13)	(5, 26)	(6, 52)
					(6, 53)
				(5, 27)	(6, 54)
					(6, 55)
		(3, 7)	(4, 14)	(5, 28)	(6, 56)
					(6, 57)
				(5, 29)	(6, 58)
					(6, 59)
			(4, 15)	(5, 30)	(6, 60)
					(6, 61)
				(5, 31)	(6, 62)
					(6, 63)

Table 6.2 lists all packets from DWPT for the beach elevation of the point located at 120m offshore $W_{j,n}; j = 1,2,...6$. The best basis is denoted by shaded cells. It can be seen there are 20 wavelet packets in the best basis, which means that variations at this point can be divided into 20 frequency intervals. Similar analysis shows that in the best basis there are 16 packets and 10 packets for the time series of beach elevation at 260m and 410m offshore respectively. They are substantially more than the 7 packets in the corresponding DWT. That is, the temporal variations of beach elevation at given points have a more complicated frequency content (temporal scales) than the DWT can resolve. It is found that the number of packets in the DWPT decreases as the observation point moves from the shoreline to the upper shoreface along the profile.

Figure 6.26, Figure 6.27 and Figure 6.28 show the reconstruction of the beach elevations located 120m, 260m and 410m offshore on the packets in the best basis, plotted against the survey time. The reconstruction shows the local variations in time at the point at different temporal scales as well indicates the temporal scales of the variations. The labels on the Y axes are the lower limit of the temporal scales, so the plot labelled by 2 months exhibits the beach elevation changes in the temporal scale interval of 2-4months. They are ordered in increasing temporal scales from left to right and from top to bottom.

It is seen from Figure 6.26 that the detail components in the best basis at the temporal scale of 42.7-64 months explain most of the beach elevation changes during the 1st to 160th month. The components at the temporal scales of 32-42.7 months explain the much variation during the period from the 160th to 267th month. These two components together explain the variance contribution from the temporal interval 32-64 months in the normal DWT. It is obviously that the normal DWT analysis is insufficient. This result shows the temporal intermittency of beach elevation changes at 120m offshore. Apart from this, the components at the temporal scale of 64 months display predominance.

Moreover, the intermittency of beach elevation changes in time at this point is much more evident from the packets in the best basis in Figure 6.26, such as at the temporal scales of 7.5-8 months and 7.1-7.5 months. In addition, the detail components at the temporal scales of 5.3-6.4 months capture well the variation around the 33rd (March 1984) and 220th survey (October 1999),

especially the last one. This component captures well the steep change of beach elevation at 120m offshore from the 215th to 220th survey (May 1999 to October 1999), which can be seen from Figure 6.1. The storms with wave heights up to 6.1m from August 3, 1999 to September 5, 1999 were a significant factor for the changes. Another factor was that before the storms the profile had a deep trough 240m landward. Therefore, when there were storms the dune zone was eroded.

Figure 6.27 shows that the components at the temporal scale of 16-18.3 months explain much of the overall variation of beach elevation located 260m offshore. However, the detail components are not uniformly large during the course of study. The fluctuations are small from the 120th to 170th month (from June 1991 to August 1995), which is a good representation of the beach elevation changes at 260m offshore shown in Figure 6.1. On the other hand, these small fluctuations during this period can be seen almost regular from the detail components at the temporal scale of 25.6-32 month.

In addition, the detail components in the best basis at the temporal scales of 64-128 months explain another significant variation at 260m offshore. However, the other components in the best basis show that the underlying temporal variation is quite intermittent. Among these components, the details at the temporal scale of 21.3 months and 32 months are smaller from the 1st to 150th month (July 1981 to December 1993) while they contribute much to the overall variation from the 150th to 267th month (December 1993 to September 2003). Especially, the fluctuations of beach elevation at 260m offshore from 216th to 262nd month (June 1999 to April 2003) shown in Figure 6.1 are well characterized at the temporal scale of 32-42.7 months. Therefore, the DWPT results provide a better quantitative means of identifying the intermittency of beach profile changes. As well, the significant fluctuations during different periods can be identified.

Figure 6.28 shows the reconstruction of the beach elevation at 410m offshore on the packets in the best basis during the course of study. It is found that the detail components at the temporal scale of 18.3-21.3 months capture well the significant variation from the 90th to 93rd survey (February 1989 to May 1989) at 410m offshore in Figure 6.1. Previously the exceptional beach elevation changes in February 1989 have been identified and discussed on the contours of temporal wavelet SD. The largest contribution for the variation is at the temporal scale of 18.3 months. One possible explanation is that the recovery period of the sediment induced by the storms is around 18.3-21.3

months at this point. It is also found that the best basis at the temporal scales of 2 months and 4 months also contribute much to the variation during the period from the 90th to 93rd survey (December 1988 to March 1989). The possible explanation is that the effect of storms on beach profiles is at a few different temporal scales.

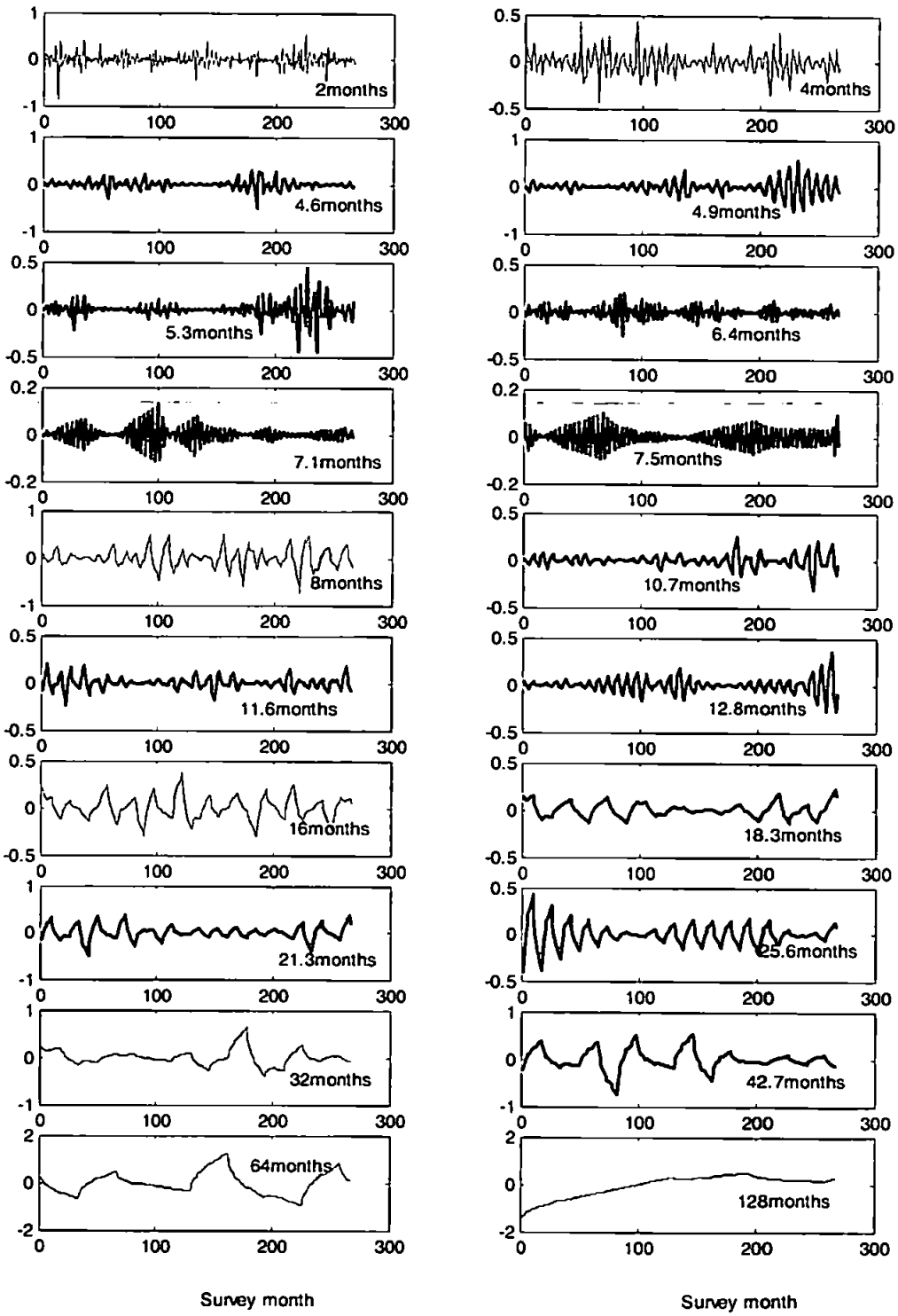

Figure 6.26 Reconstruction of the detail components in the best basis from the DWPT at 120m offshore during the course of the study.

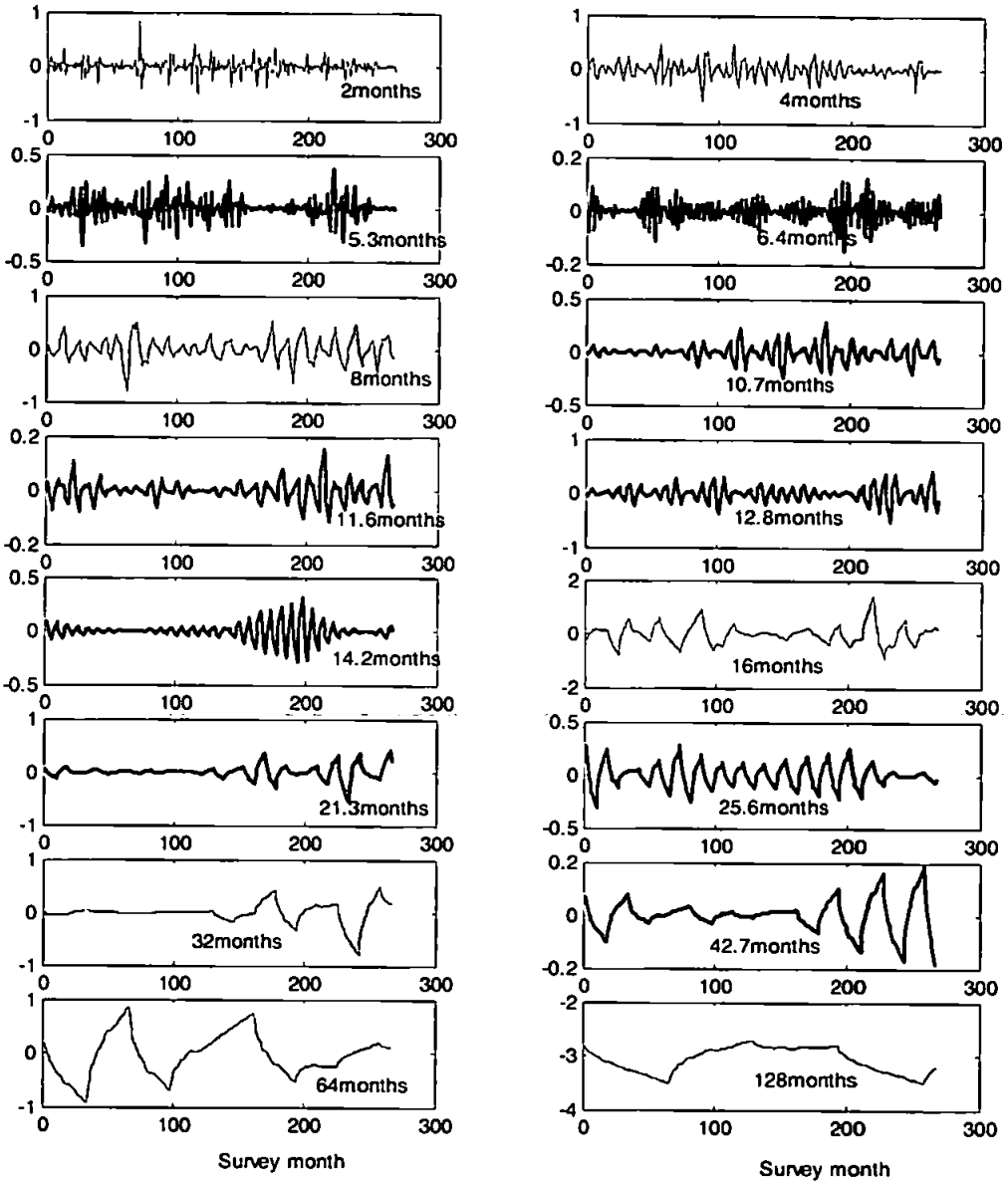

Figure 6.27 Reconstruction of the detail components in the best basis from the DWPT at 260m offshore during the course of the study.

Moreover, the detail components at the temporal scale of 16 months in Figure 6.28 characterize well the peak of beach elevation changes at 410m offshore in Figure 6.1. The peak occurred in the 185th month (November 1996). In contrast, this fluctuation is not obvious in the detail components at the temporal scale of 21.3 months, which characterizes well the peak in the 231st month (September 2000) shown in Figure 6.1. The profile in November 1996 had one inner bar and outer bar and between them the elevation at 290m was on the average; whilst the elevation at 290m was almost 2m below the average (a deep trough) in September 2000. These results suggest that

although the beach elevations at 410m offshore might exhibit various peaks during the course of study the presence and absence of them could have different temporal patterns due to the different fluctuation of neighbouring points.

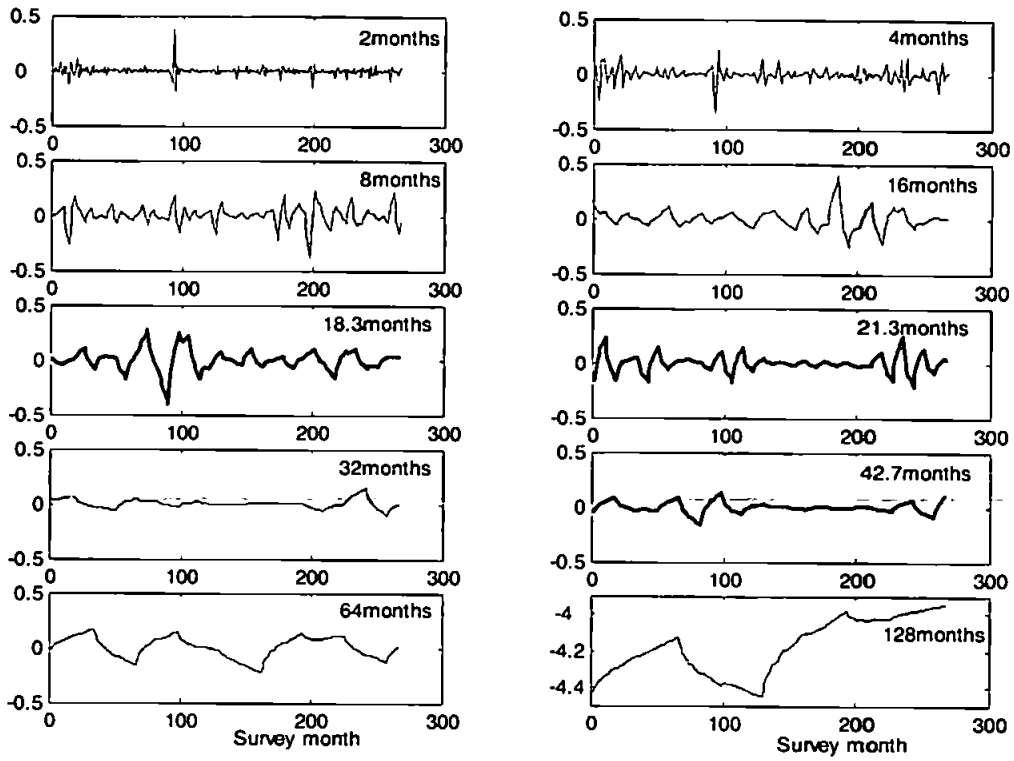

Figure 6.28 Reconstruction of the detail components in the best basis from the DWPT at 410m offshore during the course of the study.

Subsequently, the temporal wavelet packet variances in the best basis at the three particular points were computed in order to seek the dominant temporal scales at which the beach elevation changes. The frequency intervals were also inversed to the corresponding temporal scales. Figure 6.29 shows the distribution of wavelet packet variances in the best basis of the point located 120m offshore, plotted against the temporal scales. It is obvious that the variance at the temporal scale of 64 months is the largest. The second largest wavelet packet variances occur at the temporal scale of 42.7 months. These results indicate that at the shoreline, beach elevation changes occur over longer timescales.

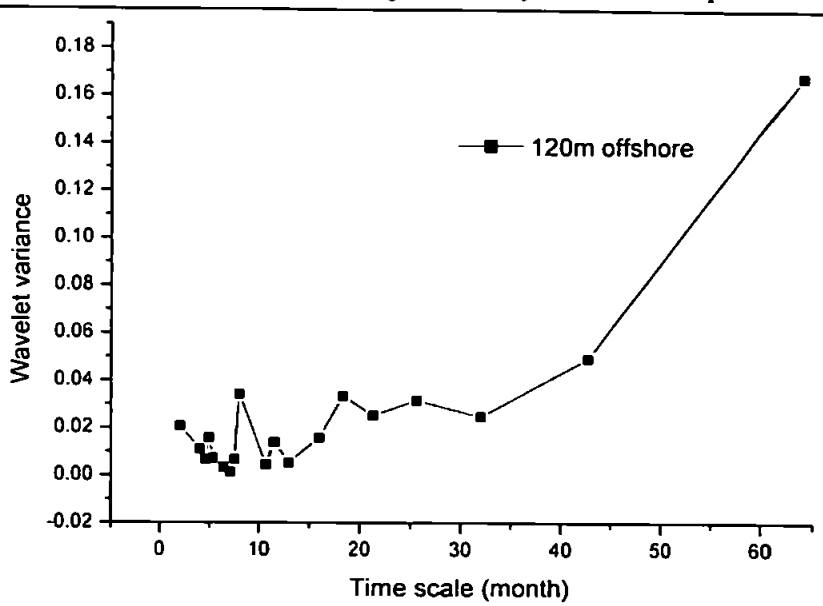

Figure 6.29 Temporal wavelet variance at different scales in the best basis at 120m offshore.

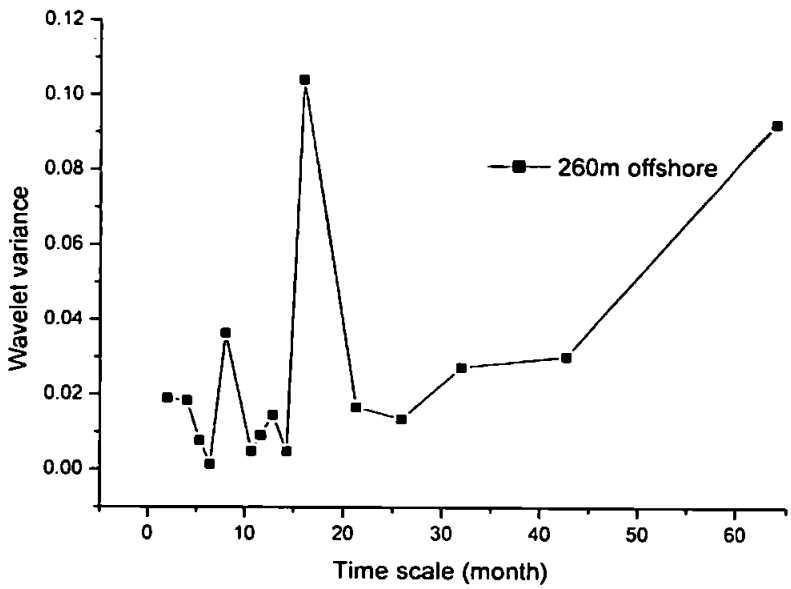

Figure 6.30 Temporal wavelet variance at different scales in the best basis at 260m offshore.

Figure 6.30 and Figure 6.31 show the distribution of the wavelet packet variances on the best basis of points at 260m and 410m offshore, respectively. Compared these two figures with Figure 6.29, the variances are distributed in fewer scales and the overall wavelet variances become smaller when the points move farther offshore. Moreover, there is a striking peak in Figure 6.30 that corresponds to the variance at the temporal scale of 16 months (range in 16-18.3 months). This result indicates that at 260m offshore the predominance is the interannual variation, which contrasts with the main forcing conditions, seasonal wave conditions. It further supports the contention that

the beach profile changes are not only the direct result from the forcing conditions (Southgate and Möller, 2000).

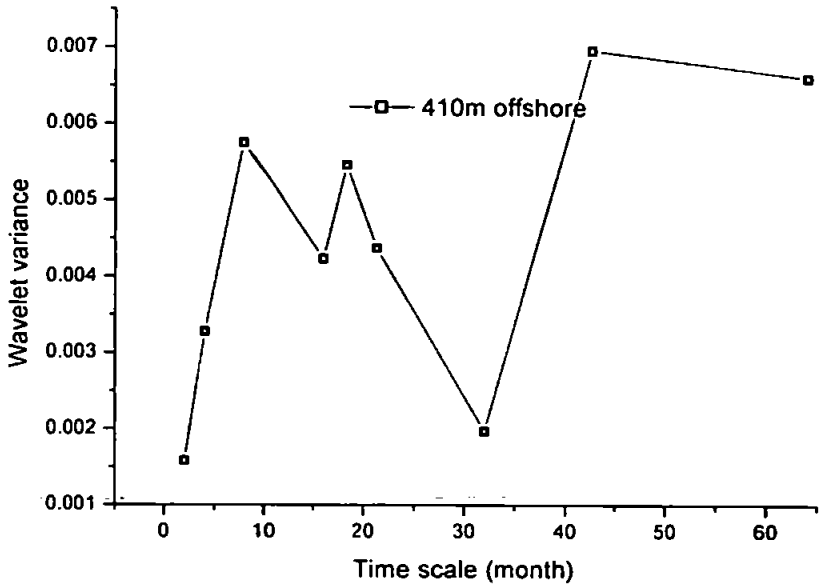

Figure 6.31 Temporal wavelet variance at different scales in the best basis at 410m offshore.

The distribution of wavelet packet variances explains the complicated temporal scale content and large magnitudes of beach elevation changes in the surf zone. Also, the relatively simpler temporal scale content and smaller magnitudes of beach elevation changes in the upper shoreface zone are illustrated. Moreover, the distribution of variances at different points again shows the dominant temporal patterns of beach elevation vary along the profile.

In all, the multiresolution analysis of beach elevation at fixed points using the DWPT reveals many more temporal scales of beach elevation changes than the DWT analysis can resolve. This is because the scales in the DWT are limited to the integer power of two whilst the beach elevation changes are quite complex in time. It is obvious that the DWPT is more powerful to study the temporal variability of beach profiles than the DWT.

6.7.2 Discussions and Conclusions

The variability of beach profiles in both time and space has been studied further using the DWPT. The DWPT with best basis selection allows us to achieve a decomposition of data on a

basis with a partition of the frequency interval that best captures complex and localized spatial and temporal variation of beach profiles.

Three particular surveys of profile line 62 at Duck were studied using the best basis from the DWPT to further identify the spatial scales, at which beach profile changed. The results indicate that the spatial scales of the variation of beach profiles are not fully identified using the DWT. The variances at the spatial scale of 85.3m in the best basis selected from the DWPT might explain the average movement of the bar, considering that the mean width of the inner bar at Duck is 95m (Larson and Kraus, 1994). This finding refines the results from the DWT analysis that the bar migrations at Duck might involve the spatial scales over 128m and 64m.

The time series of beach elevation at three fixed points along the profile line 62 have been investigated using the best basis from the DWPT to provide further insight into the temporal scales of beach profile changes. The best basis from the DWPT provides more frequency (time scales) contents, at which beach elevation changes, than the DWT does. The beach elevation changes at 120m offshore also show the most complex frequency (time scales) contents among the three points along the profile. It verifies that both the magnitudes and the range of scales of beach elevation changes vary along the profile.

In summary, the DWPT provides a more accurate way to quantify the complex beach profile changes.

6.8 Summary

In this chapter, the variation of beach profiles has been investigated over a wide range of scales in time using the wavelet transforms with emphasis on the AMODWT. The most important contributions from the study on the data set at Duck using wavelet techniques are as follows:

1. Providing powerful quantitative evidence for the non-stationary nature of beach profile changes in both time and space.
2. The intermittency of beach profile changes in time series is vividly illustrated. Apart from the intermittency, the main periods and long-term trend of beach profile change are identified by the wavelet approximation components.

3. The dominant temporal scales of beach profile changes vary within different zones along the profile.
4. The primary correlation in different zones is studied over a range of temporal scales. The correlation between different zones again shows the scale-dependency.

The all-around scale analyses employing wavelet techniques provide detailed information of beach profile changes in both time and space at Duck. The results are expected to satisfy the concerns of interest in the variability at different scales in coastal engineering. An important implication is that the changes of beach profile over years and decades are not simply the cumulative results of small temporal scales. On the other hand, at smaller temporal scales, the storm and storm groups play an important role on the beach profile changes.

Chapter 7. RESULTS FROM THE DATA SET AT LUBIATOWO

7.1 General

In this chapter, the wavelet transforms introduced in **Chapter 3** will be applied on the data set at the Coastal Research Station (CRS), Lubiatowo in Poland with the aim of demonstrating the general value of the methodology developed on the Duck data set. This site has a multi-bar shore, which is different from the two bar system at Duck. This data set is not as large as that at Duck; its advantage for wavelet analysis is that the sample points are regularly spaced along the profiles. On the other hand, the wave conditions at this site are not recorded in detail as at Duck, which makes it harder to interpret the results from wavelet analysis.

First of all, the field site at Lubiatowo is described together with the morphological data collected. Subsequently, the previous works by other researchers based on this data set are reviewed. Due to the few surveys in time series, the temporal variability of beach profiles will not be studied in this thesis, and effort is focused on the spatial variability of beach profiles. Characteristic features of the spatial patterns are examined quantitatively using the wavelet techniques and the patterns are related to the underlying physical site characteristics at Lubiatowo.

7.2 Site and Data at the CRS Lubiatowo, Poland

7.2.1 Description of the site and data set at Lubiatowo

Situated on the open sea beach about 80km northwest of Gdańsk, the Coastal Research Station (CRS) of the Polish Academy of Sciences' Institute of Hydro-Engineering (IBW PAN) was established in 1969-1970 on the premises of a century-old coast-guard station. The CRS is a unique establishment of its kind in Europe. Figure 7.1 shows its topographical location. The bottom part of Figure 7.1 shows the shoreline and baseline of survey as well as the distribution of the survey

lines alongshore. The natural conditions occurring at the Lubiatowo beach are typical for the whole Polish coast.

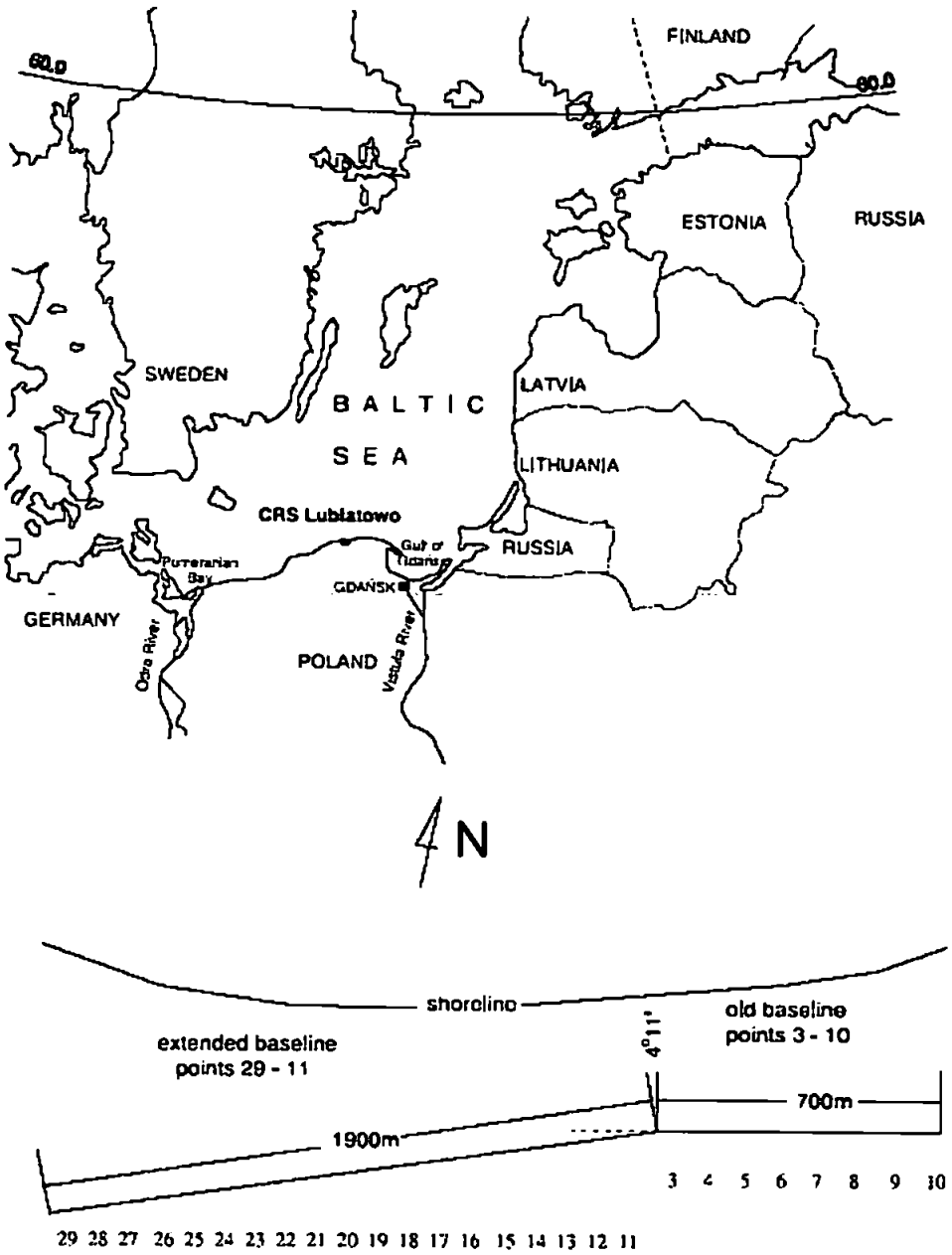

Figure 7.1 Location of CRS on the Baltic Coast (Różyński, 2003a).

The coast at the CRS Lubiatowo consists of fine sand with average grain size diameter D_{50}=0.22mm and is featured by multiple, predominantly four, longshore bars. A dune strip forms the onshore boundary. In all, there are 27 observation points equally spaced every 100m, covering the longshore stretch of 2600m. The range of cross-shore measurements varies from 600m up to about 1500m, depending on weather conditions during records, and usually covers about 1000m.

The spacing of records across profiles is kept constant at approximately 10m. Profile lines 4, 5, 6 and 7 are most intensively surveyed from 16th May 1987 to 21st June 2000. Therefore, they will be used in this thesis. The surveys document long-term phenomena reasonably well but they cannot resolve the impact of individual events.

Long-term bathymetric surveys show that the nearshore zone at the CRS Lubiatowo is characterized by multiple, usually four longshore bars and a mild average beach slope of $1-1.5\%$. The bars are very stable in the sense that they do not migrate; rather they oscillate about their average locations (Pruszak *et al.* 1997, 1999). The first innermost bar is situated about 120-170m from the baseline, with the water depth over the crest of the bar being 1m, the 2nd bar is located between 220-300m and the water depth at its crest is 2m, the 3rd bar is located between 400-500m and the water depth of its peak is 3-3.5m finally the 4th is located between 600-800m and the water depth of its peak is 4-5m.

For average storms the significant wave height outside the surf zone, at a depth of 20m, usually reaches 2-2.5m with periods of 5-7s. As the waves propagate onshore their energy is dissipated, so for water depths of 2-3m the average wave height is 0.5-1m with periods of 4-5s (Pruszak *et al.* 1999). Closer to the shoreline, the height of wave during storms reduces to 0.3-0.5m. These figures demonstrate how much energy is dissipated during the travel of wave trains to the shore.

7.2.2 Previous studies by other researchers on the data set at Lubiatowo

Previous studies on coastal morphology at the CRS Lubiatowo were summarized by Różyński (2003b). I will give a brief review of the previous work before reporting the wavelet analysis. Ostrowski *et al.* (1992) tackled the problem of shoreline change using measurements of shoreline position from 1983 to 1990 at Lubiatowo. Pruszak (1993) analysed the beach profile changes using EOF and investigated the equilibrium profile using Dean's (1991) method. The author introduced the concept of a seabed equilibrium profile varying in time. Apart from the analysis of shoreline evolution, Pruszak *et al.* (1997) studied the bar parameters using traditional statistical tools. They argued that the sediment movement is not negligible in the outermost section of the profile. The

DoC at Lubiatowo was investigated by Różyński *et al.* (1999) who suggested that the annual DoC extends further offshore than Duck due to the complex multibar system.

Różyński *et al.* (1999) argued that the second bar is the most conspicuous bed-form in multi-bar profiles with a maximum bar height up to 2.5-3m and it undergoes the strongest morphodynamic changes. The POP method was employed by Różyński and Jansen (2002) to study the pattern of nearshore bed topography. They argued that the bed evolution is slow enough to be grasped by annual records. Różyński (2003a) evaluated the importance of interactions among multiple longshore bars at Lubiatowo employing CCA. The author indicated that it is impractical to use records of more than one beach profile at a shore featured by high alongshore uniformity, because the geometric resemblance produces unrealistic and artificial method skills, clouding actual bar interaction. Pruszak and Różyński (2001) examined the periodic structure of the long-term trend of the shoreline at the CRS Lubiatowo using Fast Fourier Transforms and a spectral analysis.

Considering the non-stationarity of the variability along cross-shore, the profile was divided into a few segments by Pruszak and Różyński (1998) to investigate the variability of multibar profiles by random sine functions. Różyński *et al.* (2001) used the SSA method to analyse the temporal and spatial variation in shoreline position at the CRS Lubiatowo. In addition, the authors tried to identify the forced and self-organized response of the shoreline. They justified the use of increasingly sophisticated techniques by arguing that the shoreline is a highly nonlinear system so that it could exhibit chaotic or self-organised behaviour. The very latest study on this data set is the long-term shoreline response by Różyński (2005) using the multichannel singular spectrum analysis.

These previous works are important to provide basic understanding of the beach topography at the CRS Lubiatowo. The non-stationarity of the beach profile changes at this site also has been recognized. However the study on this respect is insufficient. Hence, it is expected that an alternative study based on wavelet techniques will provide further insight into the variability of beach profiles at Lubiatowo.

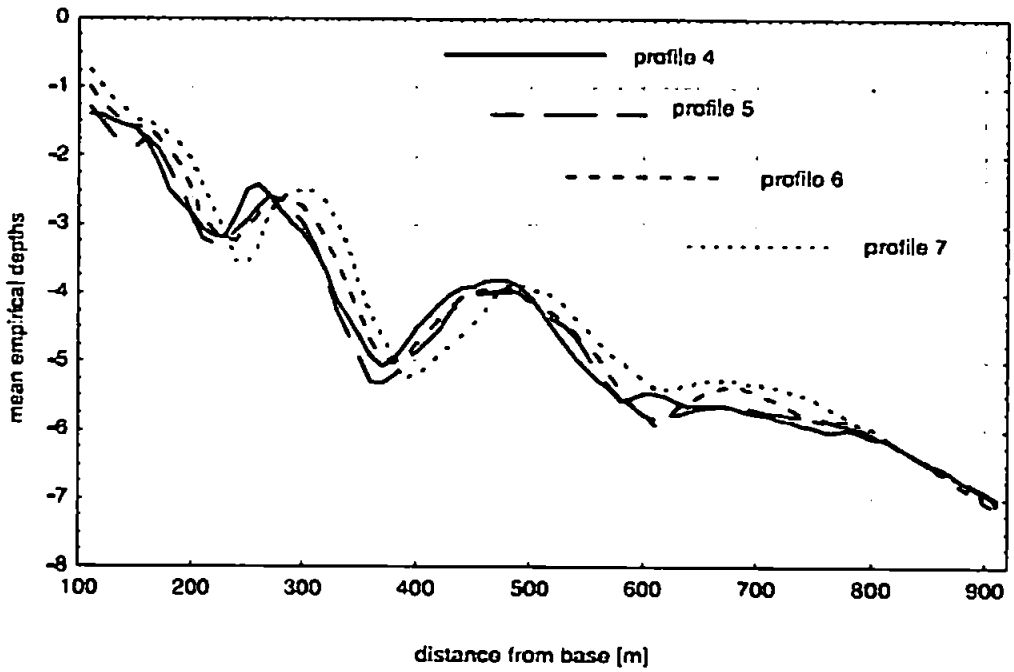

Figure 7.2 Mean empirical profiles 4, 5, 6 and 7 (Różyński, 2003a).

7.3 Spatial scale Analysis on the Data Set at Lubiatowo

7.3.1 General analysis of Profiles 4, 5, 6 and 7 using wavelet transforms

An assumption that these four profiles behave similarly had been justified from the previous study by Różyński (2003a) on the mean profiles, as shown in Figure 7.2. Since most of the survey began from at 100m from the baseline, the mean profiles in Figure 7.2 were calculated from 100m also. Therefore in this thesis it is focused on the variability of representative one, Profile 4. The AMODWT was conducted to a scale exponent of 4 on beach profile data for all the surveys after subtracting the mean profile calculated over the 22 surveys. Subsequently, the spatial wavelet variances of beach elevation were computed scale by scale.

The spatial wavelet variances of beach elevation were computed using Equation (3.18) to investigate the general pattern at different spatial scales of beach profile change during the period of study at Lubiatowo. The wavelet variances of profile 4 at different spatial scales within surveys from May 1987 to June 2000 are shown in Figure 7.3. It is obvious that the variance at the coarsest scale, 160m, is not always the largest component of variance for this profile. This is in

contrast to the results of the Duck data set, in which the variance contribution from the coarsest scale, 128m, is the largest for all the surveys of profile line 62. For one thing, it can be observed that the contribution from the spatial scale of 80m is the largest among all spatial scales in June and August 1990 (the 38th and 40th month on the plot). In addition, unlike the Duck data set, the survey that has the largest variance from the coarsest scale does not have the largest overall variance among the surveys. It can be seen that the survey in August 1990 (the 40th month) has the largest overall wavelet variance whilst the survey in April 1988 (the 12th month) has the largest variance from the spatial scale of 160m.

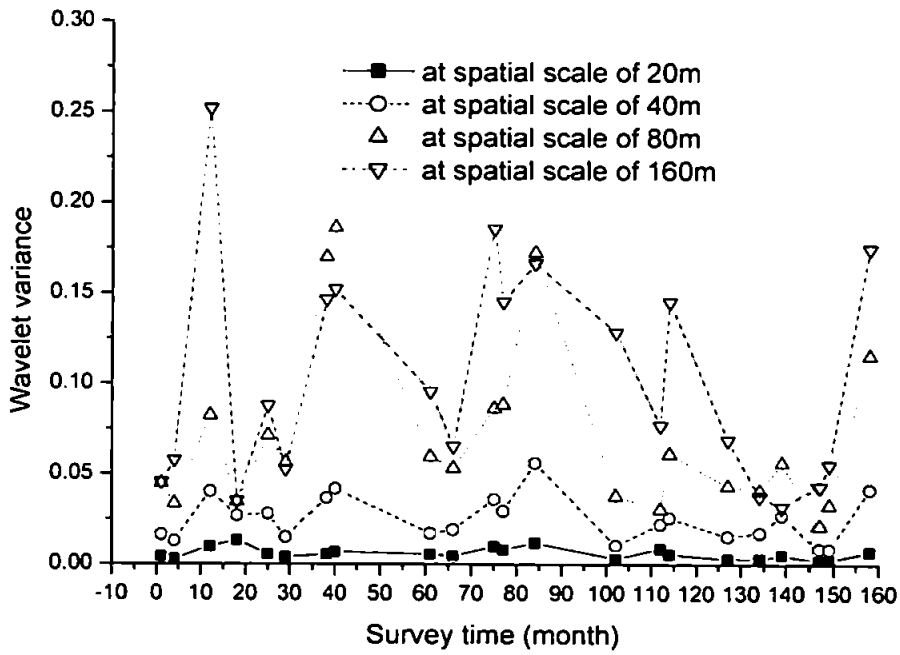

Figure 7.3 The variance at different spatial scales within surveys from September 1993 to June 2000.

Taking the advantages of the localized character of wavelet coefficients, the local components of wavelet variance were computed. Since the basic sampling is uniform with an interval of 10m, the components of wavelet variance are expected to provide much more localized information on variation of beach elevation than those of the Duck data set does. Therefore it is worthwhile to investigate the wavelet variance components of beach elevation survey by survey. The components of wavelet variance for all the 22 surveys of profile 4 at different spatial scales are given in the

Appendix from Figure A1 to A22, where the corresponding original profile configuration and the mean profile are also presented together. The mean profile in those figures is denoted by the dotted line. It is obvious that the wavelet variance components are distributed across the whole profile and do not fall to negligible values at either end of the study. These results are different from those of the Duck, where in the upper shoreface the variance of beach elevation is negligible. Therefore, with the present data the DoC cannot be identified by the wavelet variance.

It can be seen from Figures A1 to A22 that the most significant contribution of beach profile change landward of 700m is at the spatial scale of 80m. This phenomenon is especially apparent in the surveys of June 1990, August 1990 and April 1994, as shown in Figures A7, A8 and A13 in Appendix. The troughs deviating largely from the mean are the common morphological feature of these figures. For one thing, both of the troughs between the first and second bar and between the third and fourth bar are quite deep on the profile configuration in April 1994. It also can be seen in Figure 7.3 that the largest variance component at the spatial scale of 40m is in April 1994 (the 84th month) among the 22 surveys. In connection with Figure A13 this suggests that the variance at the spatial scale of 40m describes the deviation of the steep bed-form from the mean profile. In contrast, in the portion of troughs the profiles only deviate little from the mean in July 1999 and September 1999. In consequence, their variances at the spatial scale of 80m are quite small.

Though the previous work by other researchers has been used to argue that bars at Lubiatowo do not migrate, their oscillation still can be captured by the wavelet variance at the spatial scale of 160m. One representative survey is in April 1988, as shown in Figure A3, where the deviation of the second and third bar crests from the mean profile can be seen and the wavelet variance component at the spatial scale of 160m is significant. This figure again illustrates that the changes of the troughs between bars can be characterized well by the spatial scale of 80m.

In general, when there are four bars on the profiles the wavelet variance components at the spatial scales finer than 160m are very small seaward of 700m. It can be seen from Figures A17 to A21 that the fourth bar is not very apparent on the profiles during the period from November 1997 to September 1999. The total wavelet variances of these surveys are small but the variance components at most spatial scales are more or less uniform across the whole profile from the shore to the deep water. However, the fourth bar is conspicuous on the profile in June 2000 and the

dominant wavelet variance components seaward of 700m is still at the coarsest spatial scale, 160m. This phenomenon can be explained by the huge winter storms in January and February 2000 (Różyński, 2003a). Due to the huge waves, the sediment was transported offshore and deposited in the deep water, which resulted in the formation of a fourth bar.

It can be concluded from the analyses above that the variances from the spatial scale of 20m and 40m together characterize some spatial patterns of beach profile changes at Lubiatowo, such as the steep slopes. It also can be concluded that the variances at the spatial scale of 80m characterize the general beach profile change, especially the changes of troughs. Moreover, it can be argued that the variance at the spatial scale of 160m can be used to characterize some very big bed-forms, such as outer bars, which form during extreme high waves in deep water.

The breakpoint mechanism and infragravity waves are the two leading explanations for bar generation whilst O'Hare and Huntley (1994) proposed that the bar formation is due to the coupling of short wave breaking and long waves. It is interesting to note that for average storms the significant wave height outside the surf zone, at a depth of 20m, usually reaches 2-2.5m with the wave period of 5-7s. Using the linear wave theory, this corresponds to a wavelength $L_0 = 1.56T_p^2 \approx 76m$ (where T_p is the wave period) in the deep water. As the waves propagate onshore their energy is dissipated, so in the water depth of 2-3m the average wave height is 0.5-1m with period of 4-5s. According to the shallow water equation, the wavelength in the water depth of 2-3m is $L = \frac{\sqrt{gd}}{T_p} \approx 1.1m$ (where d is the water depth) on average. The fact is that the wavelength in deep water is only half of the largest bed-forms, which is not in conflict with the bar generation due to the infragravity waves. Usually the periods of infragravity waves are up to 20s. From another point of view, the spatial scales in wavelet analysis negate the bar generation results from the infragravity waves. Alternatively, the mechanism of the bar generation at this site might be due to the wave breaking, which supports the argument of Pruszak *et al.* (1997).

7.3.2 Contours of the wavelet SD of beach elevation of Profile 4

The wavelet SD of beach elevation of each survey was computed using Equation (3.23). The contours of the components of the wavelet SD of beach elevation in all surveys are illustrated scale by scale in this section. Since the surveys started and ended at different positions, the surveys were trimmed to a common rectilinear grid, and then the contours of wavelet SD at different spatial scales were plotted. To maximize the number of usable surveys and to include as much offshore information as possible, the minimum and maximum co-ordinates offshore were set to 100m and 890m on Profile 4. With the same length of data along the profile the relationship between successive surveys at different spatial scales can be investigated. Table 7.1 lists the series number corresponding to the surveys after trimming.

Table 7.1 The surveys of Profile 4 filtered in the range of 100m-890m offshore.

1	August 14, 1987
2	October 5, 1988
3	May 24, 1989
4	August 14, 1990
5	May 21, 1992
6	July 20, 1993
7	October 16, 1995
8	August 14, 1996
9	October 6, 1996
10	November 5, 1997
11	June 26, 1998
12	November 23, 1998
13	July 4, 1999
14	September 8, 1999
15	June 21, 2000

The contours among the 15 surveys of spatial wavelet SD components of beach elevation are shown in Figure 7.4, Figure 7.5, Figure 7.6 and Figure 7.7, corresponding to the spatial scales from 20m to 160m. The darker areas denote the larger SD. It can be observed that the maximum SD rises from 0.85 to 4 as the spatial scales increase from 20m to 160m. On the whole, the SD increases with the spatial scales, as shown in those figures. In comparison with the spatial contours of SD at Duck, it is obvious that the contours at Lubiatowo are distributed across the whole profile. That is, there is significant spatial variation offshore.

These results are strong evidence that the larger change in beach elevation involves larger portions of the profiles. In addition, it is clear that the variation of beach elevation in different regions can be best captured by different spatial scales. The components of the wavelet SD of beach elevation are the largest around the 4th survey (August 14, 1990) at all spatial scales. The components of the wavelet SD of beach elevation are quite small around the 13th survey (July 4, 1999).

Moreover, the dominant morphological features in the region from 100m to 200m offshore are at the spatial scales of 40m and 80m, especially at 80m as shown in Figure 7.5 and Figure 7.6. It is generally observed at the CRS that the innermost bar is situated about 120-170m from the baseline. Therefore it is possible that the variation of the innermost bar is associated with spatial scale 80m. The components of wavelet SD of beach elevation in the region from 200m to 300m along cross-shore are the largest at nearly every scale. It has been observed at the CRS Lubiatowo that the second bar is usually located 220-300m from the baseline. Therefore it can be inferred that the second bar is associated with the largest variation of beach elevation among the four bars. The result indicates that the second bar is situated in the area of the most frequent wave breaking. This finding from wavelet analysis is in agreement with Pruszak *et al.* (1997) that the second bar is the most conspicuous bed-form of a multi-bar profile and the one undergoing the strongest morphodynamic change.

The wavelet SD components at the spatial scales of 20m and 40m are quite small in the region from 400m to 500m as shown in Figure 7.4 and Figure 7.5; while the SDs are slightly larger at the spatial scales of 80m and 160m as displayed in Figure 7.6 and Figure 7.7 compared to those in the region of from 200m to 300m. Since the third bar is usually identified 400-500m from the

baseline at the CRS, it can be concluded that the variation of the third bar involves larger spatial scales than the other two do but smaller changes in beach elevation.

It also can be seen that in the region from 600m to 800m the wavelet SD components are small at the spatial scales of 20m, 40m and 80m whilst they are quite large at the spatial scale of 160m. This result indicates that the variation of the fourth bar also involves the largest interval in space along the profile at the CRS. It can be concluded that the evolution of the outermost bar is associated with the largest spatial scales caused by extreme storm conditions when waves break in the deep water.

Moreover, in comparing with the wavelet SD at all scales, it can be found that the variability of the third bar is the smallest in general. That the variability of the third bar is the smallest among the four can be explained by the following two reasons. First of all, when there are high energy waves or storms the third bar is sheltered by the fourth bar since the fourth bar is situated in deepest water, which can be explained by the wave conditions at site. Różyński (2003a) pointed out that the average surf scaling coefficient, $\varepsilon_s = \left(H_b \cdot \omega^2\right)/\left(g \cdot m^2\right)$, falls in the range from 1000 to 3000, which indicates that the coast at Lubiatowo is highly dissipative. High energy waves or storms can dissipate much energy when they propagate onshore over the fourth bar and in consequence beach elevations around the fourth bar change significantly. On the other hand, the first and second bars undergo all kinds of waves, storms and currents so the variations around these two bars, especially the second bar, are significant.

So far, the variability at different scales has been assigned to different portions along the profile by investigating the contours of wavelet SD of beach elevation of the 15 surveys of Profile 4 at the CRS. First, the variation of the innermost bar is well captured by the wavelet variance at the spatial scale of 80m. Second, the contours of wavelet SD of beach elevation at all scales indicate that in the portion of the second bar the beach elevation changes most significantly. Third, the changes of beach elevation in the portion of the third bar are not large in magnitude but involve larger spatial scales. Fourth, the change of the outermost bar entitles large variation of beach elevation in vertical as well as involves over larger spatial dimensions along the profile.

The results have been limited to the multiples of integer power of 2 with the basic sampling of 10m so that the spatial scales are at 20m, 40m, 80m and 160m. To investigate the structure of the

spatial variability of beach profiles further study with the DWPT on this data set is presented in Section 7.4.

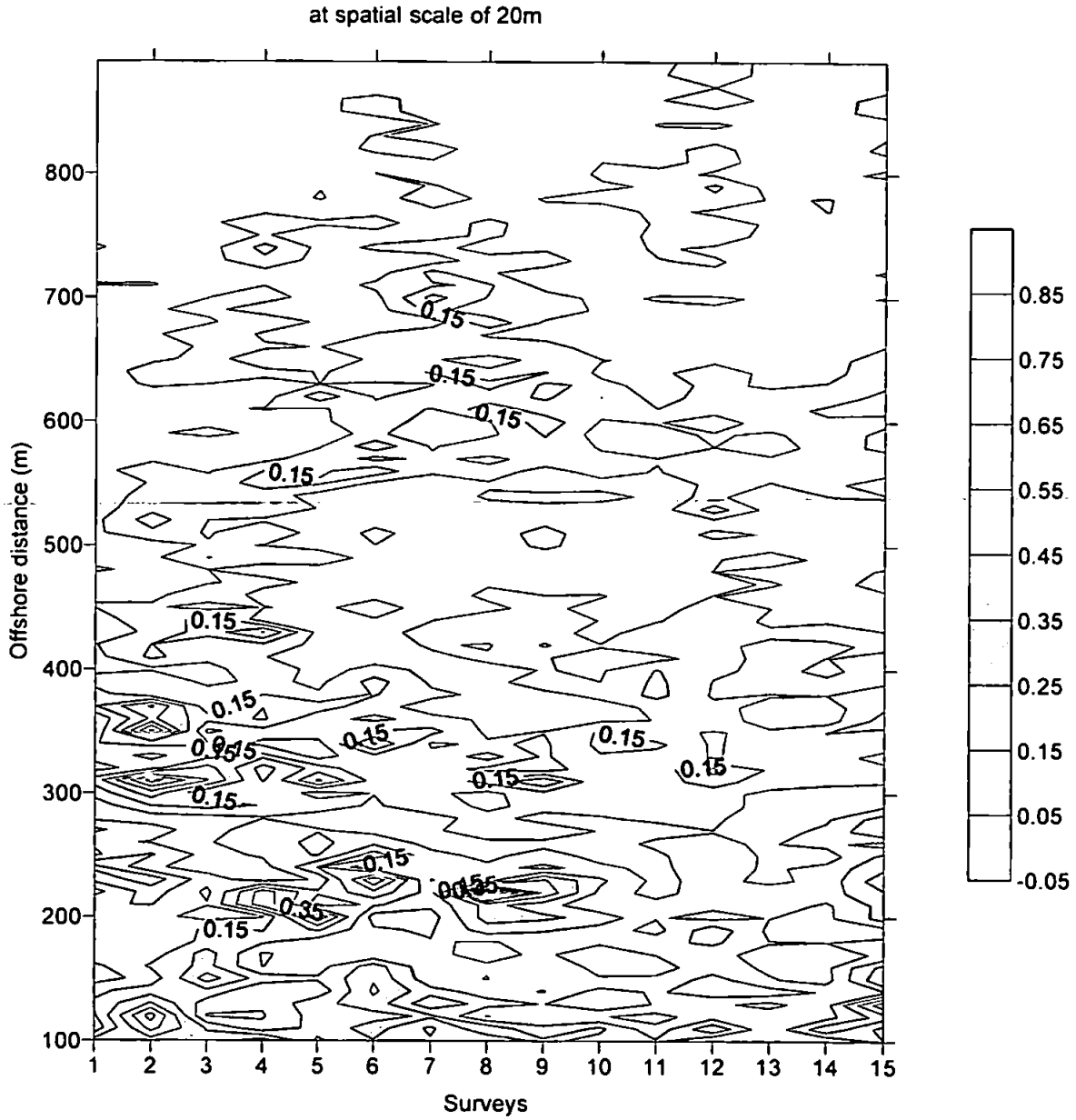

Figure 7.4 Contour of wavelet SD in successive surveys at the spatial scale of 20m.

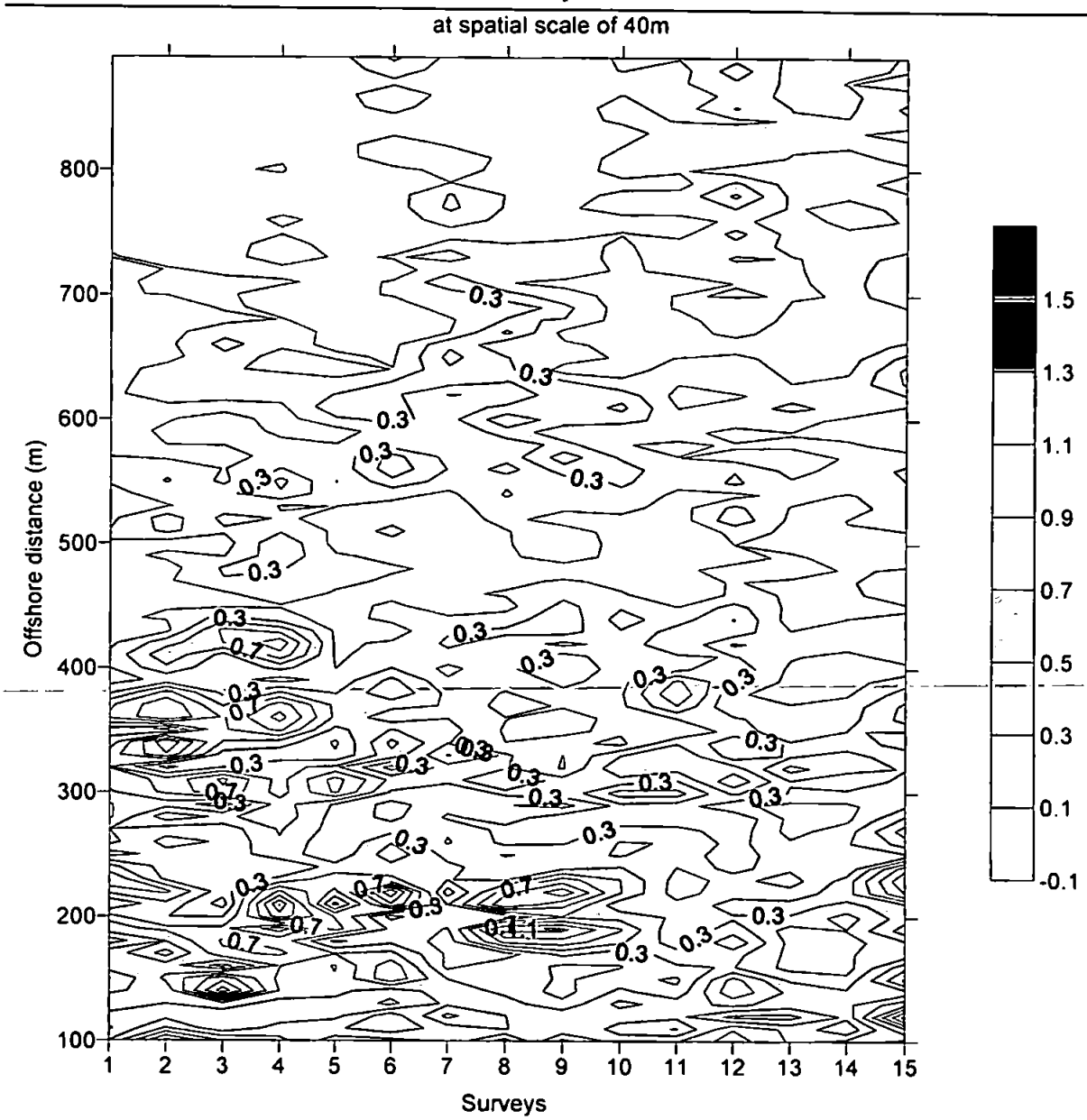

Figure 7.5 Contour of wavelet SD in successive surveys at the spatial scale of 40m.

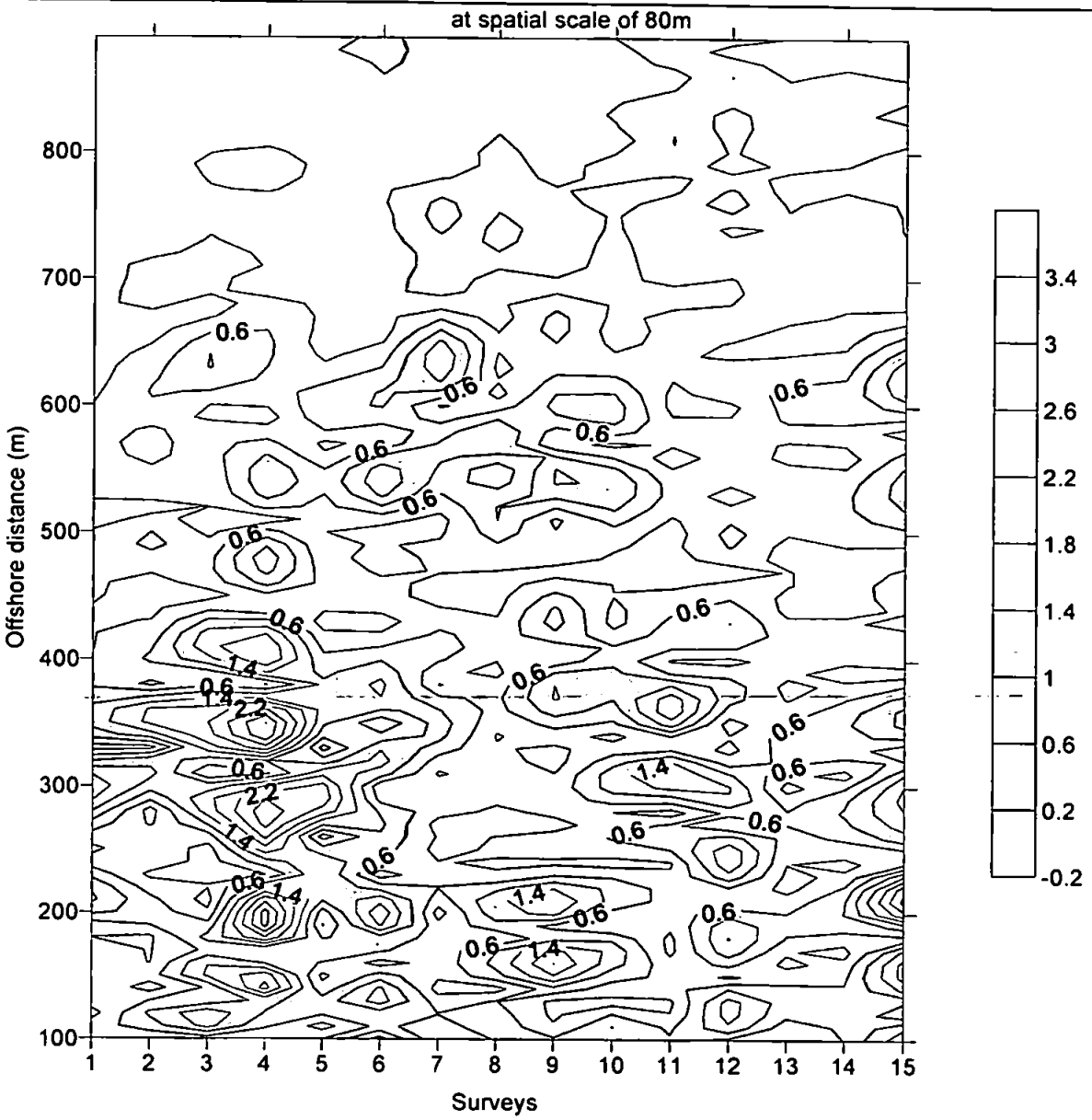

Figure 7.6 Contour of wavelet SD in successive surveys at the spatial scale of 80m.

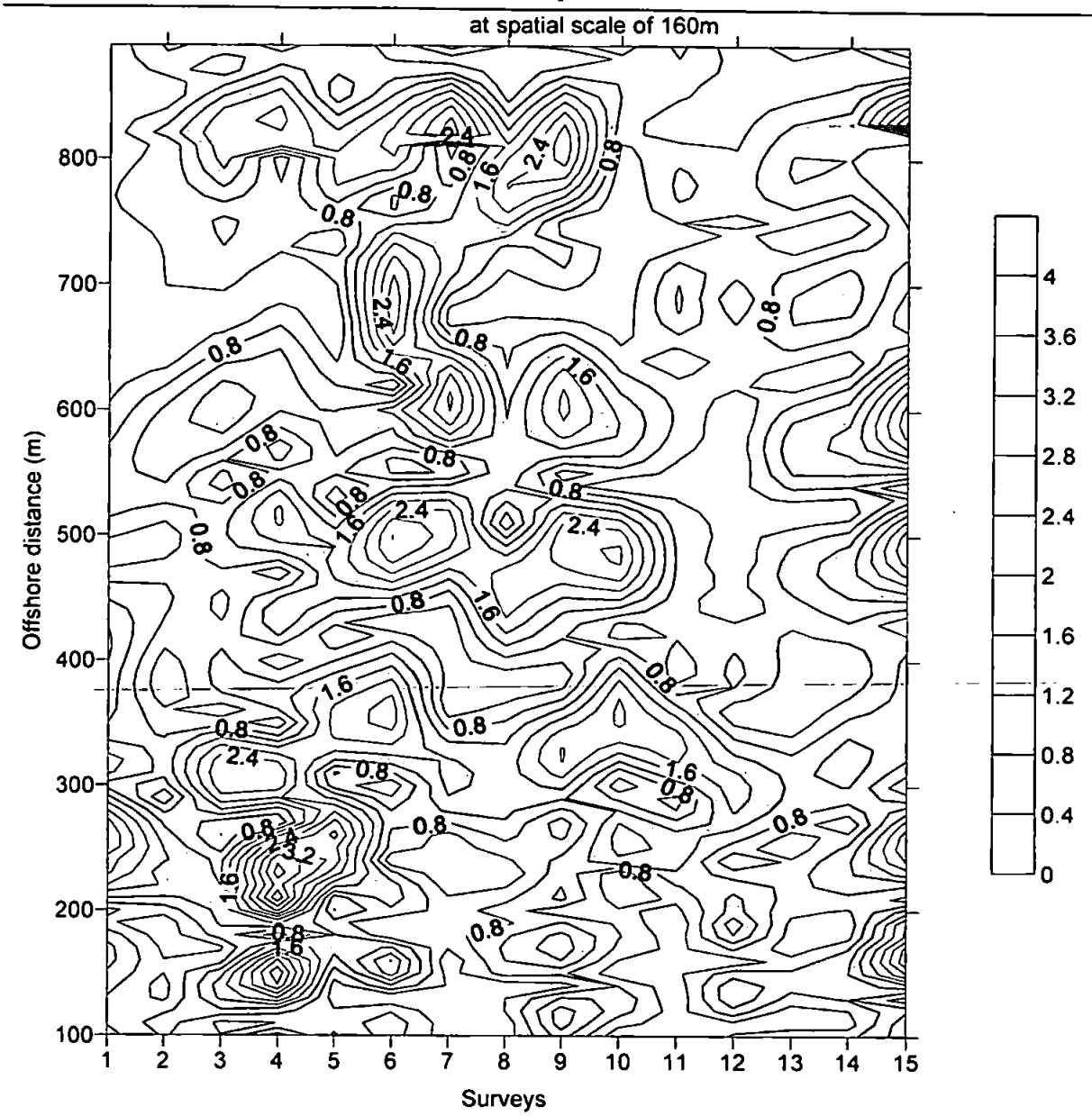

Figure 7.7 Contour of wavelet SD in successive surveys at the spatial scale of 160m.

7.4 Analyses of the Spatial Variability with the DWPT

The DWPT was conducted on all the 22 surveys of Profile 4 at Lubiatowo. The best bases selected from the DWPT of the 22 surveys are listed in Table 7.2 to deepen the investigation of the spatial patterns of beach profile change during the course of study. It is found from Table 7.2 that the deviation of beach elevation of the survey on 5th October 1988 has the most complicated spatial scale components whilst the survey on 30th September 1993 has the most simple spatial

Table 7.2 Records for the best basis of Profile 4 based on 10m interval:

May87	Aug87	Apr88	Oct88	May89	Sep89	Jun90	Aug90	May92	Oct92	Jul93	Sep93
(4,0)	(4,0)	(4,0)	(4,0)	(4,0)	(4,0)	(4,0)	(4,0)	(4,0)	(4,0)	(4,0)	(2,0)
(4,1)	(4,1)	(4,1)	(4,1)	(4,1)	(4,1)	(4,1)	(4,1)	(4,1)	(4,1)	(4,1)	
(4,2)	(3,1)	(4,2)	(3,1)	(4,2)	(4,2)	(4,2)	(4,2)	(3,1)	(3,1)	(3,1)	
(4,3)		(4,3)		(4,3)	(4,3)	(4,3)	(4,3)				
(2,1)	(3,2)	(3,2)	(3,2)	(3,2)	(2,1)	(2,1)	(3,2)	(2,1)	(2,1)	(3,2)	(2,1)
	(3,3)	(3,3)	(3,3)	(3,3)			(4,6)			(4,6)	
							(4,7)			(4,7)	
(1,1)	(1,1)		(3,4)	(1,1)	(1,1)	(1,1)	(1,1)	(1,1)	(1,1)	(1,1)	(1,1)
			(4,12)								
			(4,13)								
			(4,14)								
			(4,15)								

Apr94	Oct95	Aug96	Oct96	Nov97	Jun98	Nov98	Jul99	Sep99	Jun00
(4,0)	(4,0)	(4,0)	(4,0)	(4,0)	(3,0)	(4,0)	(4,0)	(4,0)	(4,0)
(4,1)	(4,1)	(4,1)	(4,1)	(4,1)		(4,1)	(4,1)	(4,1)	(4,1)
(3,1)	(4,2)	(4,2)	(3,1)	(3,1)	(3,1)	(3,1)	(4,2)	(4,2)	(4,2)
	(4,3)	(4,3)					(4,3)	(4,3)	(4,3)
(3,2)	(2,1)	(2,1)	(4,4)	(2,1)	(3,2)	(2,1)	(2,1)	(2,1)	(4,4)
			(4,5)						(4,5)
(4,6)			(3,3)		(3,3)				(3,3)
(4,7)									
(3,4)	(1,1)	(2,2)	(1,1)	(1,1)	(1,1)	(2,2)	(1,1)	(1,1)	(1,1)
(3,5)									
(2,3)		(2,3)				(2,3)			

scale components. Moreover, according to the study of wavelet variance components it has been found that the survey on 14th August 1990 has the largest overall wavelet variance. Therefore, we

focus our study on these three surveys to investigate the spatial scales that beach elevation change involves with the DWPT. For reference, the spatial scales, which are the multiples of the basic sampling interval (10m) of the reciprocal of the upper limit of the frequency intervals, are listed in Table 7.3.

The top-left plots on Figure 7.8, Figure 7.9 and Figure 7.10 show the original profiles surveyed in October 1988, August 1990 and September 1993 respectively, and the other plots are the components obtained by the decomposition on packets in the best basis. The reconstruction components are ordered by increasing spatial scales from left to right and from bottom to top.

Obviously the variation of beach elevation in the survey in October 1988 from the mean profile is distributed in a few dominant spatial scales though there are 11 packets in the best basis, as shown in Figure 7.8. It can be seen that the variation of beach elevation in the region from 200m to 400m along the profile is distributed at such a few spatial scales as 21.3m, 40m, 53.3m and 160m. Figure 7.8 demonstrates that the elevation changes at the spatial scales of 21.3m, 40m and 53.3m are much smaller than the change at the spatial scale of 160m. However, the variances at the spatial scale of 40m capture the elevation changes slightly landward of 400m where there was a trough between the second and third bar in October 1988. The changes of the second, third and fourth bar are captured well at the spatial scale of 160m. It can be seen from Figure 7.8 that the change of the first bar is projected strongly onto the spatial scale of 24.6m as well as the spatial scale of 80m.

Table 7.3 Spatial scales corresponding to the packets in the best basis from the DWPT:

Scale Exponential 1		Scale Exponential 2		Scale Exponential 3		Scale Exponential 4	
Packet	Spatial scale (m)	Packet	Spatial scale (m)	Packet	Spatial scale (m)	Packet	Spatial scale (m)
(1,0)	40	(2,0)	80	(3,0)	160	(4,0)	320
						(4,1)	160
				(3,1)	80	(4,2)	106.7
						(4,3)	80
		(2,1)	40	(3,2)	53.3	(4,4)	64
						(4,5)	53.3
				(3,3)	40	(4,6)	45.7
						(4,7)	40
(1,1)	20	(2,2)	26.7	(3,4)	32	(4,8)	35.6
						(4,9)	32
				(3,5)	26.7	(4,10)	29.1
						(4,11)	26.7
		(2,3)	20	(3,6)	22.9	(4,12)	24.6
						(4,13)	22.9
				(3,7)	20	(4,14)	21.3
						(4,15)	20

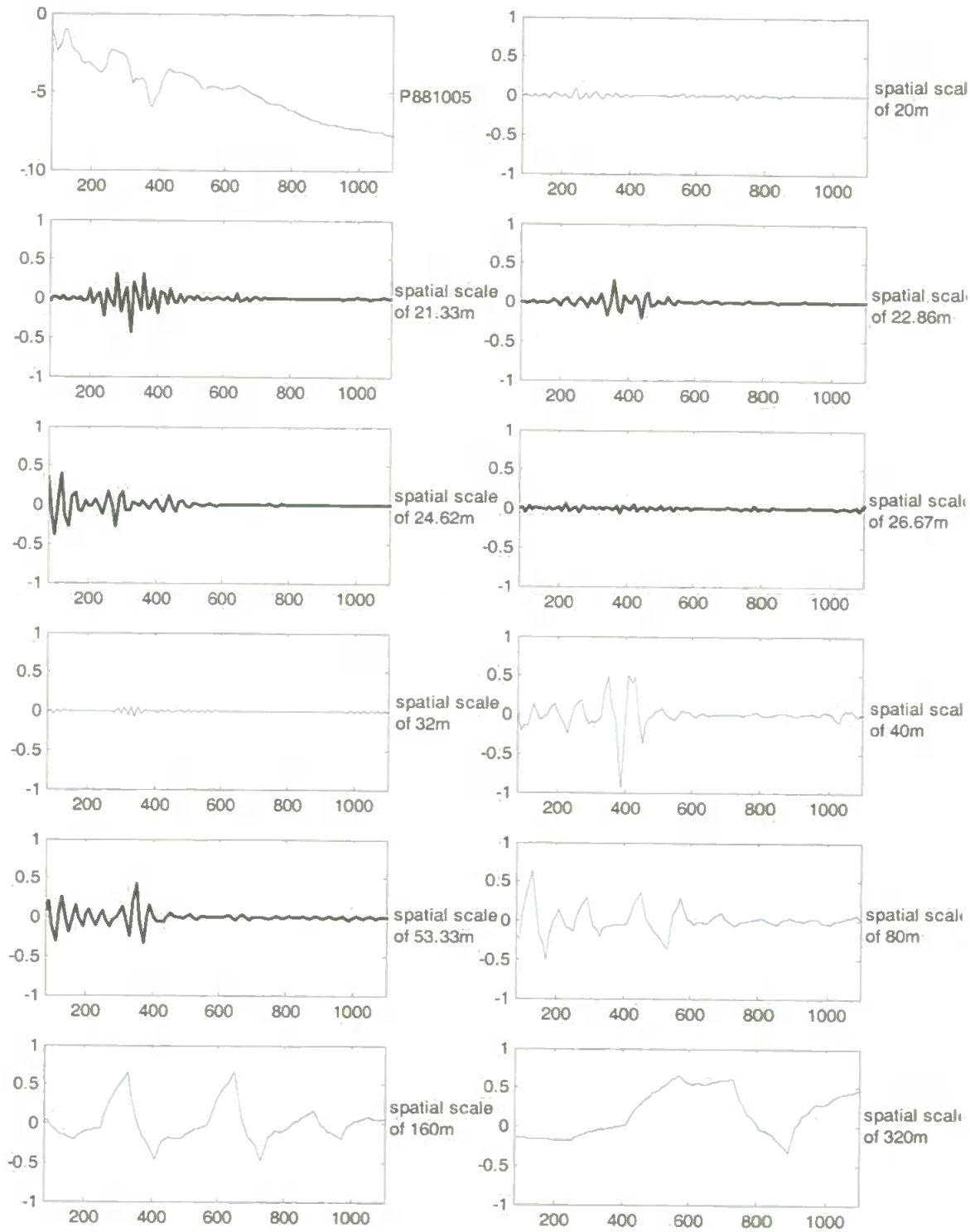

Figure 7.8 Reconstruction of the details on the best basis of the survey in October 1988.

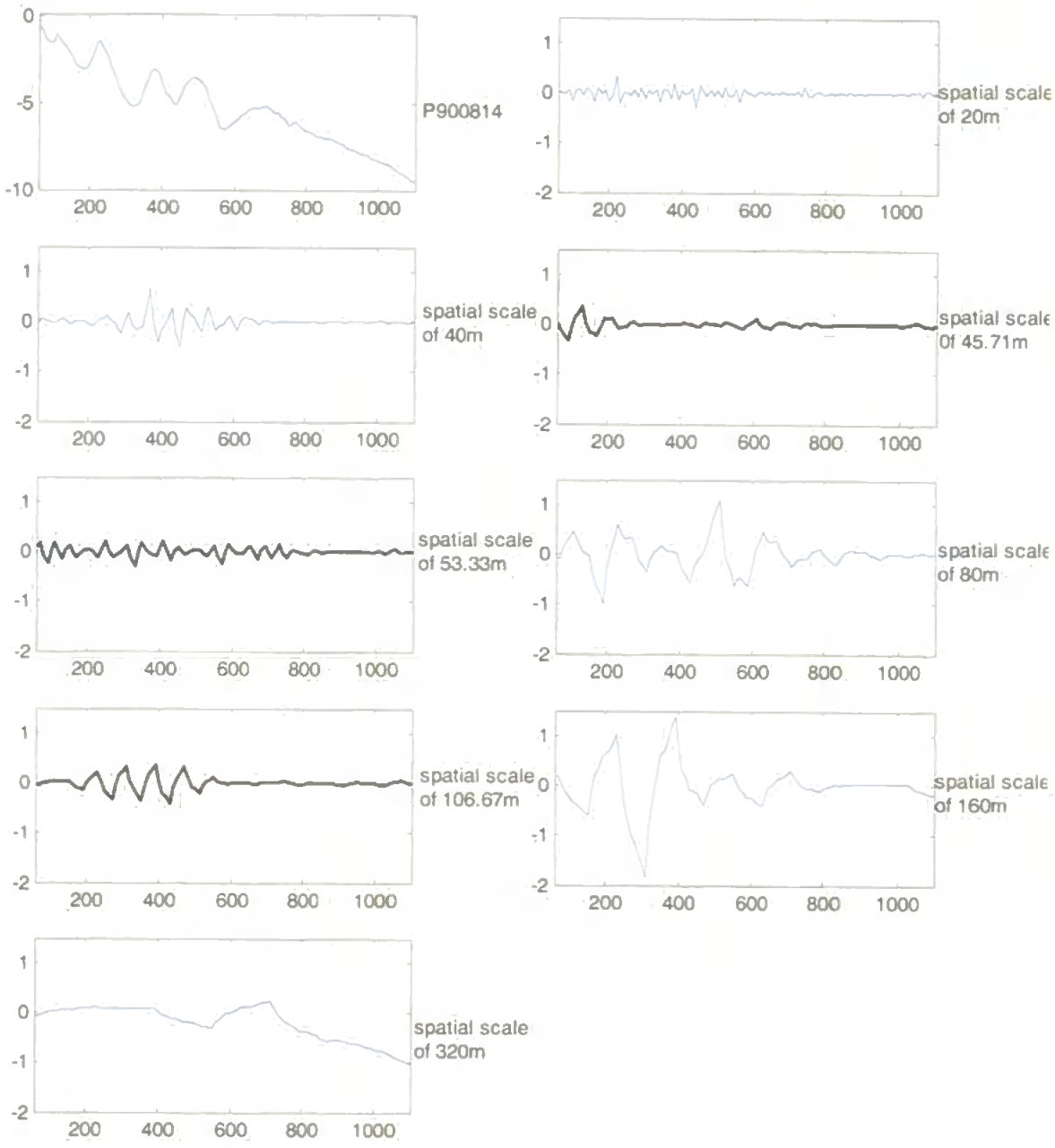

Figure 7.9 Reconstruction of the details on the best basis of the survey in August 1990.

It can be found from Figure 7.9 that the magnitudes of beach elevation changes of the survey in August 1990 are larger than in October 1988 but the distribution of the spatial scales are relatively simple with only 8 packets in the best basis. It can be observed from Figure 7.9 that the variation at the spatial scale of 106.7m contributes much to the region from 200m to 500m along the profile surveyed in August 1990. In addition, the elevation changes in the region of the trough between the first and second bar can be captured at the spatial scale of 80m as indicated in Figure 7.9. In

general, the survey in August 1990 illustrates that beach profile changes are distributed as a relatively simple spatial structure but with large amplitudes.

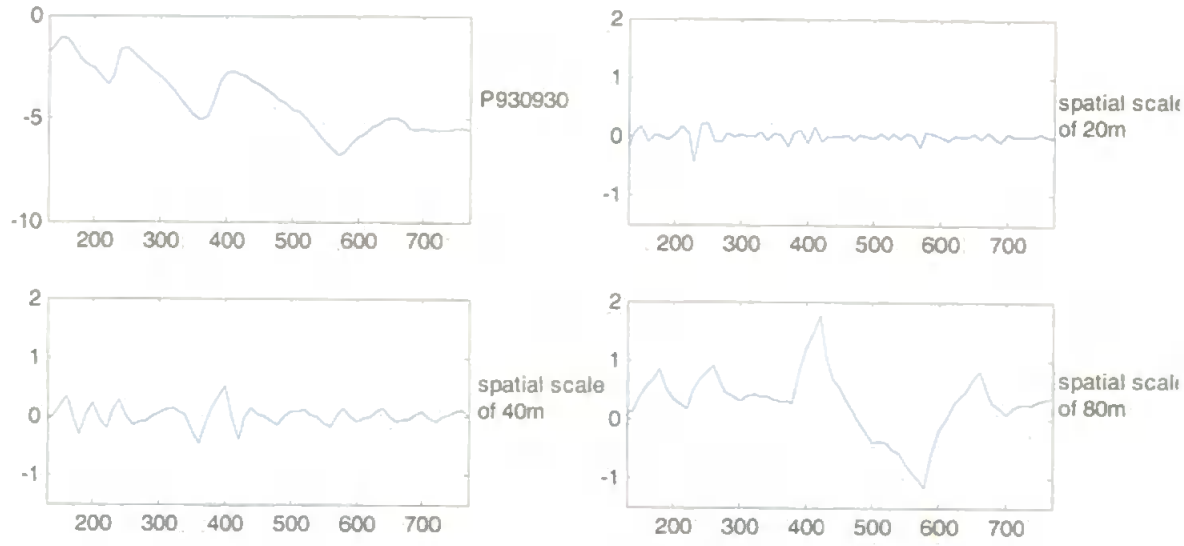

Figure 7.10 Reconstruction of the details on the best basis of the survey in September 1993.

Figure 7.10 illustrates the simplest nature of spatial scales in the best basis from the survey in September 1993. There are only three packets in the best basis, which is even less than the normal DWT. That is the variation of beach elevation in this survey can be captured well only by spatial scales of 20m, 40m and 80m. The trough between the second and third bar is captured by the packet at the spatial scale of 40m while the trough between the third and fourth bar is captured by the packet at the spatial scale of 80m.

The overall wavelet variances from different spatial scales on the best basis for the surveys in October 1988 and August 1990 are presented in Figure 7.11 and Figure 7.12 respectively. They are expected to illustrate better the relative importance of spatial scales that contribute to the beach profile change in different surveys. For comparison, the variances in the two figures were plotted in the same dimensions. It is obvious that the variance of the profile in October 1988 at the spatial scale of 40m is only smaller than the variance at the spatial scale of 160m. However, the second largest variance is at the spatial scale of 80m for the profile in August 1990, and also there is a significant contribution from the spatial scale of 106.7m, which is not included in the profile in October 1988. These results exhibit that in general the beach profile changes in October 1988 is

characterized by a range of small spatial scales whilst the beach profile change in August 1990 is characterized by a few large spatial scales.

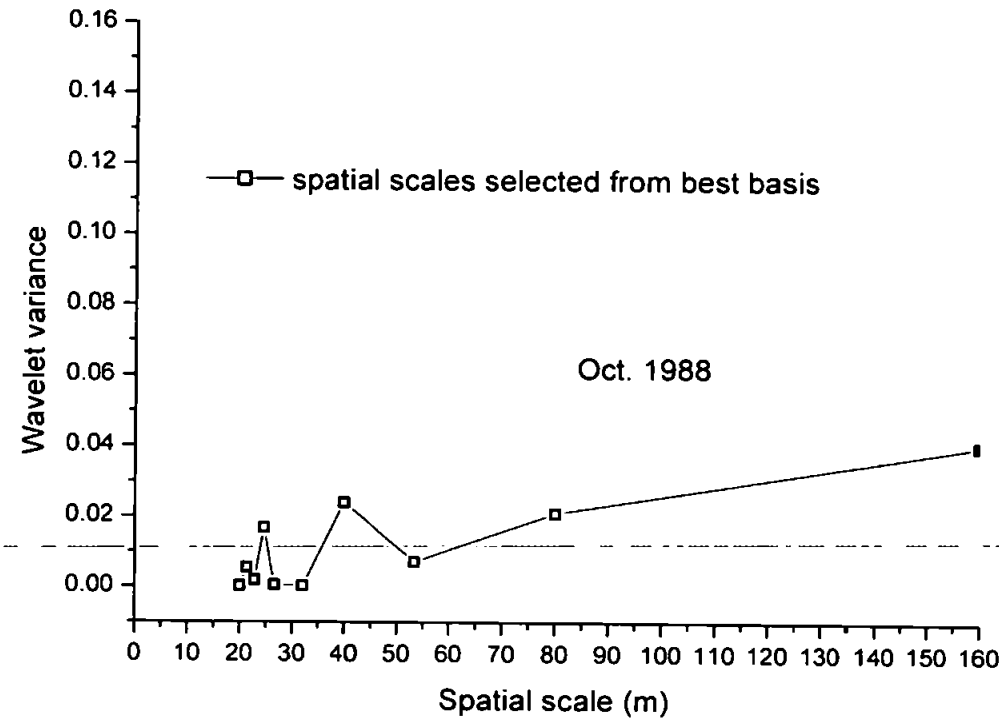

Figure 7.11 Wavelet variances at the spatial scales on the best basis of survey in October 1988.

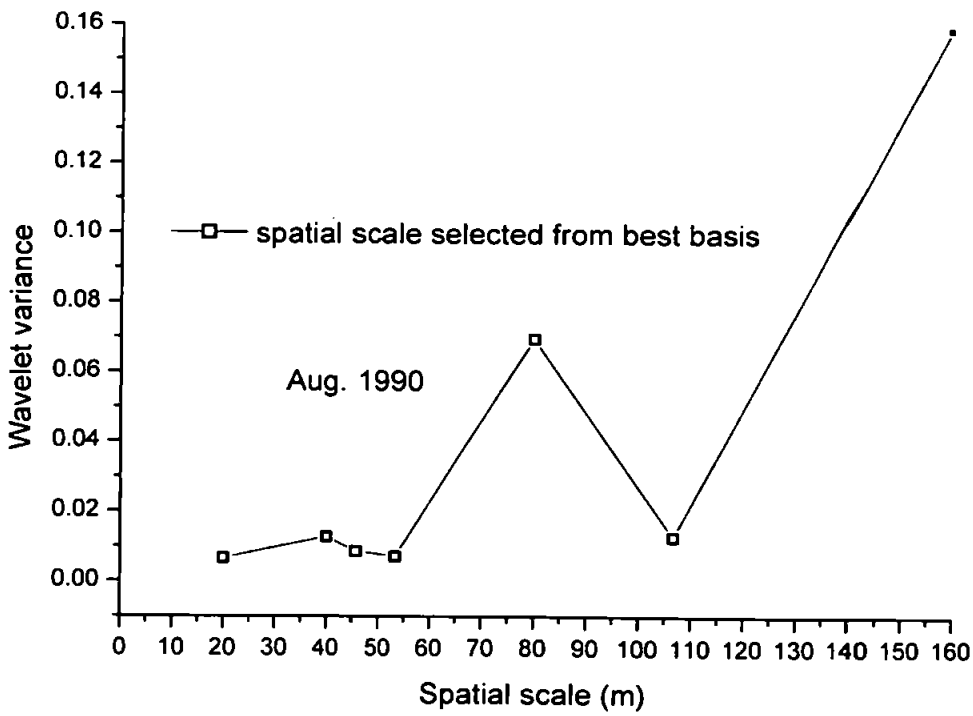

Figure 7.12 Wavelet variances at the spatial scales on the best basis of survey in August 1990.

7.5 Summary of the Results from the Data Set at Lubiatowo

In the above sections, the wavelet techniques have been applied to the data set at Lubiatowo to analyse the spatial variability of beach profiles. There are a few key findings from studying the data set.

- The variance at the coarsest scale, 160m, is not always the largest component of variance for this profile and the survey that has the largest variance from the coarsest scale does not have the largest overall variance among the surveys. These results are in contrast with those of the Duck data set.
- The variances at the spatial scales of 20m and 40m together are related to the beach profile change of the steep portion. The general beach profile changes can be characterized by the spatial scale of 80m. Moreover, there are occasions when the variation involves the large spatial scale at 160m.
- The distribution of the contours in the deep water is different from that of Duck data set, which has an apparent DoC.
- The results from the contours of wavelet SD characterize the different patterns of the elevation change in the zones of different bars. First, most of the elevation changes around the innermost bar are from the wavelet variance at the spatial scale of 80m. Second, the contours of wavelet SD at all scales indicate that the beach elevation changes in the portion of the second bar are the largest. Third, the amplitudes of changes in beach elevation in the portion of the third bar are not significant but involve larger spatial scales. Fourth, the variation of the outermost bar is large as well as involves the largest spatial scales.
- In conjunction with the average storm conditions, the bed-forms defined by the spatial scales from wavelet analysis suggest that the bar at this site is generated by wave breaking, which agrees with Pruszak *et al.* (1997).

- The DWPT analysis indicates that even though most of the variability of beach profiles in space can be characterized by the normal DWT in some cases the DWPT can specify the nature of beach profile changes in space better at Lubiatowo.

In all, it can be concluded that the variance at the spatial scale of 80m can characterize the general variability of beach profiles at Lubiatowo. In particular, the deviation of the troughs between the bars can be well characterized at the spatial scale of 80m. The larger deviations of the troughs than the bars from the mean characterize the multi-bar system at Lubiatowo where the bars do not migrate much. Moreover, when the bars/troughs on the profile are quite wide along the profile the variance at the spatial scale of 160m can characterize part of the elevation changes.

In general, it is found that the structure of the spatial scales at Lubiatowo is more complex than Duck due to the multi-bar character at Lubiatowo. However, due to the different forcing environments the bar crests at Lubiatowo do not migrate much onshore or offshore. At Duck, there are only one or two bars, when there are storms the bar crest can move 100m even 200m offshore. That is the reason most of the beach profile changes can be characterized by one or two larger spatial scales. The final conclusion from this study is that the most important spatial scales that contribute to beach profile change are determined by the site characteristic of the data set.

Chapter 8. CONCLUSIONS AND FUTURE WORK

8.1 Conclusions

8.1.1 Conclusions from the Duck data set

In this work, the variability of beach profiles in both time and space at Duck has been studied intensively using the wavelet techniques. The wavelet decomposition also provides a natural means of investigating fluctuations in the beach level variability along the profile. This allows locations at which the variability of the profile changes to be identified and the scales of those changes to be identified. Multiresolution analysis using the wavelet transforms gives a quantitative estimate of the relative importance of different spatial scales to the overall variability of the beach profile.

Though this work is not concerned with the prediction of beach profiles, the detailed investigation of the variability of beach profiles have a number of implications for prediction. Some key findings from the spatial analysis are:

- The components of wavelet variance show that the contributions from different scales at different parts of the profile vary along the profile, which suggests that the beach morphological evolution as a whole is dependent upon different processes along the profile. The results also provide evidence about the scale-dependent character of beach profile changes.
- The spatial wavelet variances at the coarsest spatial scale make the largest contribution to the overall variance of the profile. In conjunction with the results of EOF, these results are expected from the consideration that the primary agent for morphological evolution is the incoming waves. When there are high-energy waves, on sandy beaches the large waves will create a wider surf zone. Thus, the coarser scales can characterize the wider zone and the spatial wavelet variances at these scales describe the larger changes in beach elevation. In this way, the spatial wavelet variances at the coarser scales reflect the dominant processes, which usually involve the bar migration at Duck.
- Variances at the finer scales are more obvious in the dune and surf zones than those of other zones, because beach profiles in the surf zone experience small waves as well as

storms, however in deep water beach profiles will only change in response to extreme storms.

The scale-dependent variance across all 22 years in given calendar months provides some insight into the relationship between the beach profile changes and the wave conditions. They are:

- The average monthly wavelet variances at the coarse spatial scales in a year appear to be correlated with the average monthly wave heights. These variances explain the strong seasonal beach response to the wave heights.
- The average monthly variances at the finer scales show different patterns from the monthly wave heights. It supports the contention that beach profile change cannot be fully explained by the wave heights.
- Only the infrequent events can have significant impact on the upper shoreface.

Analysis of the changes in spatial variance components provides a useful measure for defining the DoC of beach profiles. Even though the DoC is a disputed concept in coastal engineering, the procedure described in this work provides a statistical method for identifying changes in wavelet variance quantitatively. The zone in which the changes in beach elevation are not significant would be expected to coincide with a measurable change in the spatial variance. The DoC identified by the change in spatial wavelet variances at the spatial scale of 128m is more consistent with the findings of Larson and Kraus (1994) than with the results of Nicholls *et al.* (1998), which is acknowledged as providing a conservative estimate. The concluding remark is that the DoC is scale-dependent. The changes in variances also indicate the most active zones where the variance is the most significant and different from the other zone.

The results from the temporal wavelet analysis contrast with those from the spatial analysis, in that they do not show the clear dominance of a few scales. The intermittency of beach profile changes is much stronger in time than in space. The temporal variances provide information about the dominant time scales of the beach profile changes at particular locations along the profile. The key findings from the temporal analysis:

- There are no clearly definite temporal scales of variation that dominate consistently during the course of study for a given observation point. Rather, there is a strong pattern of intermittency at most temporal scales, which is clear at locations across the length of the profile. This finding is different from Birkemeier (1985) and Ruessink *et al.* (2003) who suggested a three and half year cycle of beach profiles and 5.9 years return period of the bars respectively at Duck.
- The wavelet variance components at the three locations along the profile indicate that different temporal scales have a different balance of influence on the overall variance as one moves along the profile. This reflects that the forced response and self-organised response have a different balance along the profile, which is consistent with Southgate and Möller (2000). The forced response usually refers to the linear response of profiles from the forcing conditions, such as waves. However, self-organised response refers to nonlinear processes so that beach profile can take the form of repeated patterns at definite temporal and spatial scales without depending on the forcing conditions. In the surf zone, beach profile changes display stronger interannually self-organized response since the main forcing conditions are the seasonal waves. However, around the shoreline, the self-organized response occurs at temporal scales smaller than one year due to the storm surges. On the other hand, the elevation changes around the shoreline in long-term show stronger forced response due to the wave conditions.
- The contours of wavelet SD have shown the general temporal variability of beach elevation along the profile during the period of study. The most important contribution is that some infrequent beach profile responses to extreme storms/storm groups have been well identified. That not all the beach responses to storms are identified shows that the beach profile before the storms has a substantial effect of the beach profile evolution.
- The DWPT analysis shows that the beach profile changes in time series are much more complicated than the DWT/AMODWT can resolve. The DWPT shows that the observations have more frequency/scale contents in shallow water than in deep water. This relatively few frequency contents explain the physical process that in the upper zone beach profiles only respond to high waves that break in deep water. However, in the surf zone the

beach profiles respond to a complex nonlinear interaction of all kinds of waves and currents, so the frequency/scale contents in this zone are distributed across a broad range of temporal scales.

- The temporal variance from the DWPT shows closer information on the time scales that beach elevations change. At the point 120m offshore, the largest variance component is at temporal scales greater than 64 months, which provides evidence for the existence of long–term trends of the shoreline. By contrast, at 260m a large proportion of the variance is at the temporal scale interval of 16-18.3 months. The variation at this temporal scale interval corresponds to the interannual variability of the sandbars at Duck (Plant *et al.*, 1999; Lippmann *et al.*, 1993) since the transitional bar is always present at 260m.
- Few changes in temporal wavelet variances at the temporal scale of 8 months and larger scales again indicate that there is a long-term trend of the beach profile evolution.
- The highly negative wavelet correlation between the point 120m and 410m at the temporal scale of 64 months indicates that there could be sediment exchange between the dune zone and outer bar zone in the long-term. This is in agreement with Wright *et al.* (1991).

8.1.2 Conclusions from the Lubiatowo data set

In this thesis, the concerns on the beach morphology at Lubiatowo are on the spatial variability. The key findings from the spatial scale analysis using the wavelet techniques are:

- The beach is highly variable along the whole profile, which is illustrated by the wavelet variance components in deep water for most of the surveys. This implies that the survey should extend further offshore to identify the DoC.
- That the second bar is the most conspicuous bed-form is illustrated by the larger wavelet SD components at all spatial scales on the contours. This finding is consistent with Pruszak *et al.* (1997).
- On average, the bed-forms at Lubiatowo can be defined in the spatial interval of 80-160m even though at times the spatial scale larger than 160m dominates. The deviation

of the steep bed-form from the mean, especially the trough between the first and the second bar, can be captured in the spatial scale interval of 40-80m.

- The prevailing spatial scales contributing to the largest variance of the profile suggest that the bar generation is due to the wave breaking at this site, which agrees with Pruszak *et al.* (1997). This result from another point supports the contention that the beach at Lubiatowo is highly dissipative.

In comparison with the results of Duck, the advantage of the DWPT for spatial scale analysis is more obvious due to the complex beach morphology at Lubiatowo with multiple bars. The wavelet packets in the best basis varying from three (the profile in September 1993) to eleven (the profile in October 1988) for the different profiles shows the wide range oscillations along the profile of the elevations from the mean.

8.1.3 Final comments

The conclusions from the two different data sets have been summarized above, from which the different set characterization can be found. The following are the common features of the results from the wavelet analyses:

- The wavelet variance components characterize the magnitudes of beach profile changes in elevation at given points at different scales. Meanwhile, the prevailing spatial scales define the horizontal dimensions of the main bed-forms, such as the bars and troughs, along the profiles. It is mainly reflected in the bar migration at Duck and the changes of elevation of troughs at Lubiatowo.
- Though the explicit interpretation is not given about the beaches response to waves, the results in this thesis indicate a strong relationship between waves and beach profiles. This is consistent with their site characterization. Both Duck and Lubiatowo are wave dominated.

8.2 Future Work

Predictability will be low where variability is large (van Rijn *et al.*, 2003). Therefore, investigation of the variability is essential to the future prediction of beach profiles. This work has demonstrated that the wavelet techniques are very useful for analysing the non-stationary time/space series of beach profile data. Wavelet analyses help us to understand the multi-scale variability of beach profiles. It is believed that the prediction of beach profiles can be improved greatly by taking into account the variability at different spatial and temporal scales. These results suggest how much the variation from other scales should be included when predicting beach profiles at specifically temporal scales. If we want to predict the evolution of a beach profile over the long term (e.g. 50 years) then we may be less concerned about short-term variations, which may be harder to model. Also, in space, the variability at specific scale exploits how much the beach can be predicted at different zones along the profile. The results indicate that the prediction in the outer bar zone would be easier than the shoreline zone.

Meanwhile, there are many other systems that show strong non-stationarity in coastal engineering. These complex phenomena have not been fully investigated, so it is expected that wavelet techniques will throw more light on these problems. In summary, there are some research strategies for the future work:

1. The long-term trend of the shoreline can be studied further using wavelet techniques and compared with the results from other techniques, such as the SSA.
2. The relationship between the wave conditions and beach profile changes needs to be studied further using the wavelet correlation at different scales. As well, other weather conditions at sites can also be related to the beach profile changes using wavelet techniques. It is expected that a full recognition of the relationship between different forcing conditions and the beach profile response in a wide range of temporal scales will contribute much to the beach profile prediction using the process-based models.
3. Even though beach profiles behave similarly at these two sites studied, both the longshore and cross-shore variability of beach morphology could be examined simultaneously using the two-dimensional MODWT in the future. This kind of study is expected to reveal the degree of similarity among different zones at different scales.

The spatial variability at different scales provides us with information on the intervals of surveys and the most important locations in space and time when measurements should be conducted more intensively in field site surveys later. As for Duck, in the upper shore zone the survey can be considered with sampling rate of 10-20m in space annually, corresponding to the little contribution of wavelet variance from the smaller spatial scales. However, in the surf zone the survey can be conducted more intensively in space and time. The different temporal patterns along the profile are good indications for the coastal management, in which beach nourishment is an important component. Whole-profile nourishment and bar nourishment are two main nourishment strategies (Capobianco *et al.*, 2002). The nourishment period can be referenced to the predominant temporal patterns along the profile. The specific locations for bar nourishment can be referenced to the spatial variability also. The main temporal patterns of the elevation changes around the bars suggest the nourishment period of the bars. It was found in this thesis that the transitional bars at Duck have a strong periodicity of 16-18.2 months, indicating the period of the bar nourishment at this site. The scale-dependent depth of closure can provide insight into the siting of coastal structures of different dimensions by considering the relative stability of beach profiles.

References:

Aminti, P., Pruszak, Z. and Zeidler, R. B., 1995. Multiscale shore variability at two coasts. *Proceedings of Coastal Dynamics' 95*, pp. 617-628.

Akaike, H., 1973. Information theory and extension of the maximum likelihood principle. In: *Second International Symposium on Information Theory*, pp.267-281.

Aubery, D. G., 1979. Seasonal patterns of onshore/offshore movement. *Journal of Geophysical Research*, 84: 6347-6354.

Bagnold, R. A., 1954. Experiments on the gravity-free dispersion of large spheres in Newtonian fluid under shear. R. Soc. London, A225: 49-63.

Barnett, T. P., Preisendorfer, R., 1987. Origins and levels of monthly and seasonal forecast skill for United States surface air temperature determined by canonical correlation analysis. *Monthly Weather Review*, America Meteorology Society, 115: 1825-1850.

Birkemeier, W. A., A. M. ASCE, 1985. Time scales of nearshore profile changes. *Proceedings of 19th Coastal Engineering*, Vol. 3, pp. 1507-1521.

Birkemeier, W. A., Nicholls, R. J. and Lee, G. H., 1999. Storms, storm groups and nearshore morphology change. *Proceedings of Coastal Sediments '99*. pp. 1109-1122.

Bodge, K. R., 1992. Representing equilibrium beach profiles with an exponential expression. *Journal of Coastal Research*, 8(1): 27-55.

Bosboom, J., Aarninkhof, S. G. J., Reniers, A. J. H. M., Roelvink, J. A., Walstra, D. J. R., 1997. UNIBEST-TC 2.0, Overview of model formulations. Report H2305, Delft Hydraulics, Delft, The Netherlands.

Bosch, E.H., Oliver, M. A. and Webster, R., 2004. Wavelets and the generalization of the variogram. *Mathematical Geology*, 36: 147-186.

Brampton, A. H., Coastal Group, HR Wallingford, 1992. Beaches-the natural way to coastal defence. *Coastal Zone Planning and Management*, pp. 221-229.

Bruun, P., 1954. Coastal erosion and the development of beach profiles. Beach Erosion Board, U. S. Army Corps of Eng., Tech. Memo.44.

Capobianco, M., Basana, R. and Pesaresi, R., 1995. Beach and nearshore profile evolution at different temporal scales: The case of Duck, North Carolina, U. S. A. *Proceedings of Coastal Dynamics' 95*, pp. 629-638.

Capobianco, M., Larson, M., Nicholls, R. J. and Kraus, N. C., 1997. Depth of closure: a contribution to the reconciliation of theory, practise and evidence. *Proceedings of Coastal Dynamics' 97*. ASCE, pp. 506-515.

Capobianco, M., Hanson, H., Larson, M., Steetzel, H., Stive, M. J. F., Chatelus, Y., Aarninkhof, S. and Karambas, T., 2002. Nourishment design and evaluation: applicability of model concepts. *Coastal Engineering*, 47: 113-135.

Coco, G. Huntley, D.A.and O'Hare, T.J., 2000. Investigation of a self-organisation model for beach cusp formation and development. *Journal of Geophysical Research*, 105: 21991-22002.

Cohen, A., Daubechies, I. and Vial, P., 1993. Wavelets on the interval and fast wavelet transforms, *Applied and Computational Harmonic Analysis*, 1: 54-81.

Coifman, R. R. and Wickerhauser, M. V., 1992. Entropy-based Algorithms for best basis selection, *IEEE Trans. on Inf. Theory*, 38 (2): 713-718.

Davison, A. T., Nicholls, R. J. and Leatherman, S. P., 1992. Beach nourishment as a coastal management tool: An annotated bibliography on development associated with artificial nourishment of beaches. *Journal of Coastal Research*, 8: 984-1022.

Daubechies, I., 1988. Orthonormal bases of compactly supported wavelets. *Communications in Pure and Applied Mathematics*, 41: 909-996.

Daubechies, I., 1992. *Ten Lectures on Wavelets.* Society for industrial and applied mathematics (SIAM). Philadephia.

De Vriend, H. J., 1991. Mathematical modelling and large-scale coastal behaviour: Part 1. Physical process. *Journal of Hydraulic Research*, 29 (6): 727-740.

Dean, R. G., 1977. Equilibrium beach profiles: U. S. Atlantic and Gulf Coastal. *Department of Civil Engineering, Ocean Engineering Report No. 12*, University of Delaware, Newark, Delaware, USA.

Dean, R. G., 1991. Equilibrium beach profiles: characteristics and applications. *Journal of Coastal Research*, 7 (1): 53-84.

Everson, R. M. and Sirovich, L. 1989. A survey of wavelet analysis applied to turbulence data. Centre for Fluid Mechanics Report, No. 89-182.

Farge, M., 1992a. Wavelet transforms and their applications to turbulence. In Annual Rev. Fluid Mech. J. Lumley Eds, Annual Reviews Inc., Vol. 24, pp. 395-457.

Farge, M., 1992b. The continuous wavelet transform of two-dimensional turbulence flows. *In Wavelets and their Applications*. Ruskai, M. B. et al. Eds, Jones and Bartlett, pp. 275-302.

Glahn, H. R., 1968. Canonical correlation analysis and its relationship to discriminate analysis and multiple regression. *Journal of Atmospheric Sciences*, 25: 23-31.

González, M., Medina, R. and Losada, M. A., 1999. Equilibrium beach profile model for perched beaches. *Coastal Engineering*, 36: 343-357.

Goovaerts, P., 1997. Geostatistics for natural resources evaluation. Oxford University Press, New York.

Hallermeier, R. J., 1978. Uses for a calculated limit depth to beach erosion. *Proceedings of the 16th Coastal Engineering Conference*, American Society of Civil Engineers, pp. 1493-1512.

Hallermeier, R. J., 1981. A profile zonation for seasonal sand beaches from wave climate. *Coastal Engineering*, 4: 253-277.

Hashimoto, H. and Uda T., 1982. Field investigation of beach profile changes and the analysis using empirical eigenvectors. *Proceedings of the 18th International Conference on Coastal Engineering*, pp. 1369-1384.

Hasselmann, K., 1988. PIP-s and POP-s: The reduction of complex dynamical systems using principal interaction and oscillation patterns. *Journal of Geophysical Research*, 93 (D9): 11015-11021.

Howd, P. A. and Birkemeier, W. A., 1987. Beach and nearshore survey data: 1981-1984. CERC, Field Research Facility. Tec. Rep. CERC-87-9, U. S. Army Eng. Waterways Expt. Stn., Coastal Eng. Res. Ctr., Vicksburg, MS.

Hotelling, H., 1936. Relations between two sets of variates. *Biometrika* 28: 321-377.

Hsu, T. W., Ou, S. H., and Wang, S. K., 1994. On the prediction of beach changes by a new 2-D empirical eigenvector model. *Coastal Engineering*, 23: 255-2270.

Hudgrins, L. H., 1992. Wavelet analysis of atmospheric turbulence. Ph. D. dissertation, U. Calif. Irvine, 288pp.

IMSL, 1994. *IMSL MATH/LIBRARY User's Manual.* Version 3.0, Visual Numerics, Houston, TX.

Iyama, J. and Kuwamura, H. 1999. Application of wavelets to analysis and simulation of earthquake motions. *Earthquake Engineering and Structural Dynamics*, 28: 255–272.

Jansen, H., 1997. POP analysis of the JARKUS dataset; the IJmuiden Katwijk section. *Fase 2 Rep., Project RKZ-319*, Delft University of Technology, Faculty of Systems and Information Science, the Netherlands.

Komar, P. D. and McDougal, W. G., 1994. The analysis of exponential beach profiles. *Journal of Coastal Research*, 10 (1): 59-69.

Kraus, N. C. and Harikai, S., 1983. Numerical model of the shoreline change at Oasai beach. *Coastal Engineering*, 7(1): 1-28.

Kumar, P. and Foufoula-Georgiou, E., 1994. Wavelet analysis in geophysics: an introduction. In: *Wavelets in Geophysics* (eds E. Foufoula-Georgiou and P. Kumar), pp. 1–43. Academic Press, New York.

Kumar, P., 1997. Wavelet analysis for geophysical applications. *Review of Geophysics*, 35(4): 385-412.

Krystian, W. P., 1990. Introduction to Coastal Protection. *Coastal protection*, pp. 1-14.

Lark, R. M. and Webster, R.., 1999. Analysis and elucidation of soil variation using wavelets. *European Journal of Soil Science*, 50: 185-206.

Lark, R. M. and Webster, R.., 2001. Changes in variance and correlation of soil properties with scale and location: analysis using an adapted maximum overlap discrete wavelet transform. *European Journal of Soil Science*, 52: 547-562.

Lark, R. M., 2004. Decomposing digital soil information by spatial scale. In: Eds. Lagacherie, Ph., Voltz, M. & McBratnery, A. B. *Proceedings of the Global Workshop on Digital Soil Mapping*, Montpellier, France. International Union of Soil Science Pedometrics Commissions.

Larson, M., 1991. Equilibrium profile of a beach with varying grain size. *Coastal Sediments '91*, pp. 905-919.

Larson, M., 1996. Model of beach profile change under random waves. *Journal of Waterway, Port, Coastal, and Ocean Engineering*, 122(4): 172-180.

Larson, M. and Kraus, N. C., 1992. Dynamics of longshore bars. *Proceedings of the 23rd Coastal engineering*, pp. 2219-2232.

Larson, M. and Kraus, N. C., 1994. Temporal and spatial scales of beach profile changes, Duck, North Carolina. *Marine Geology*, 117: 75-94.

Larson, M. and Kraus, N. C., 1995. Prediction of cross-shore sediment transport at different spatial and temporal scales. *Marin Geology*, 126: 111-127.

Larson, M. and Kraus, N. C. and Wise, R. A., 1999a. Equilibrium beach profiles under breaking and non-breaking waves. *Coastal Engineering*, 36: 59-85.

Larson, M., Hanson, H., Kraus, N.C. and Newe, J., 1999b. Short-and long-term response of beach fills determined by EOF analysis. *Journal of Waterway, Port, Coastal and Ocean Engineering*, 125: 285-293.

Larson, M., Capobianco, M., and Jansen, H., 2000. Relationship between beach profiles and waves at Duck, North Carolina determined by canonical correlation analysis. *Marine Geology*, 163: 275-288.

Larson, M., Capobianco, M., Jansen, H., Różyński, G., Southgate, H. N., Stive, M., Wijnberg, K. M. and Hulscher, S., 2003. Analysis and Modelling of Field Data on Coastal Morphological Evolution over Yearly and Decadal Time Scales. Part 1: Background and Linear Techniques. *Journal of Coastal Research*, 19 (4): 760–775.

Lee, G. H. and Birkemeier, W. A., 1993. *Beach and nearshore survey data: 1985-1991 CERC Field Research Facility. Technical Report CERC-93-3*, US Army Engineering Waterways Experimental Station, Vicksburg, Mississippi.

Lee, G. H., Nicholls, R. J., and Birkemeier, W. A., 1995. A conceptual fair-weather-storm model of beach nearshore profile evolution at Duck, North Carolina, U. S. A. *Journal of Coastal Research*, 11: 1157-1166.

Lee, G. H., Nicholls, R. J., and Birkemeier, W. A., 1998. Storm-driven variability of the beach-nearshore profiles at DUCK, North Carolina, USA, 1981-1991. *Marine Geology*, 148: 163-177.

Lippmann, T. C. and Holman, R. A., 1990. The spatial and temporal variability of sand bar morphology. *Journal of Geophysical Research*, 95: 11575-11590.

Lippmann, T. C., Holman, R. A., and Hathaway, K. K., 1993. Episodic, non-stationary behaviour of a double bar system at Duck, North Carolina, U. S. A., 1986-91. *Journal of Coastal Research*, 15: 49-75.

Liu, P. C., 1994. Wavelet spectrum analysis and ocean wind waves. *Wavelets in Geophysics*. Academic Press, New York, pp. 151-166.

Lindsay, R. W., Percival, D. P. and Rothrock, D. A., 1996. The discrete wavelet transform and the scale analysis of the surface properties of sea ice. *IEEE Transactions on Geoscience and Remote Sensing*, 34: 771–787.

Mallat, S. G., 1989. A theory for multiresolution signal decomposition: the wavelet representation. *IEEE Transactions on Pattern Analysis and Machine Intelligence*, 11: 674-693.

Massel, S. R., 2001. Wavelet analysis for processing of ocean surface wave records. *Ocean Engineering*, 28 (8): 957-987.

Matheron, G., 1962. *Traité de Géostatistique Appliqué*, Tome 1. Memoires du Bureau de Recherches Géologiques et Minières, Paris.

Medina, R., Losada, M. A., Dalrymple, R. A., and Roldan, A., 1991. Cross-shore sediment transport determined by EOF method. *Proceedings of Coastal Sediments' 91*. pp. 187-210.

Meneveau, C., 1991. Analysis of turbulence in the orthonormal wavelet representation. *Journal of Fluid Mechanics*, 232: 469-520.

Miller, H. C., 1999. Field measurements of longshore sediment transport during storms. *Coastal Engineering*, 36: 301-321.

Miller, H. C., Birkemeier, W. A., and Dewall, A. E., 1983. Effects of CERC research pier on nearshore processes. Coastal Structure'83, *Proceedings of American Society of Civil Engineers*, pp. 769-784.

Moore, L.J., Sullivan, C. and Aubrey, D.G., 2003. Interannual evolution of multiple longshore sand bars in mesotidal environment, Truro, Massachusetts, USA. Marine Geology, 196: 127-143.

Nairn, R. B. and Southgate, H. N., 1993. Deterministic profile modelling of nearshore process. Part 2. Sediment transport and beach profile development. *Coastal Engineering*, 19: 58-96.

Nicholls, R. J., Birkemeier, W. A., and Lee, G. H., 1998. Evaluation of depth of closure using data from Duck, NC, USA. *Marine Geology*, 148: 179-201.

O'Connor, B. A., Pan, S., Nicholson, J., MacDonald, N. and Huntley, D. A., 1998. A 2D model of waves and undertow in the surf zone. *Proceedings of the 26th Coastal Engineering*, ASCE, pp. 286– 296.

O'Connor, B. A. and Nicholson, J., 1999. Modelling short-term beach profile changes. *Fifth Int. Conf. on Coastal and Port Engineering in Developing Countries*, Cape Town, pp. 277– 287.

O'Hare, T.J. and Huntley, D. A., 1994. Bar formation due to wave groups and associated long waves. *Marine Geology*, 116: 313-325.

Oliver, M. A., Bosch, E. and Slocum, K., 2000. Wavelets and kriging for filtering and data reconstruction. *Proceedings of the 6th International Geostatistics Congress*, Cape Town. CD Rom.

Ostrowski, R., Pruszak, Z., and Zeidler, R. B., 1991. Multi-scale nearshore and beach changes. In B.L.Edge (Editor), Proceedings of the 22nd Conference of Coastal Engineering, ASCE, pp. 2101-2116.

Ostrowski, R., Pruszak, Z., and Zeidler, R. B., 1992. Shoreline evolution from field observations and stochastic analysis, *Hydrotechnical Transactions*, 55: 45-64.

Panizzo, A., Bellotti, G. and Girolamo, P. D., 2002. Application of wavelet transform analysis to landslide generated waves. *Coastal Engineering*, 44: 321-338.

Percival, D. B., 1995. On estimation of the wavelet variance. *Biometrika*. 82: 619-631.

Percival, D. B. and Guttorp, P., 1994. Long-memory processes, the Allan variance and wavelets. In: *Wavelets in Geophysics* (eds E. Foufoula-Georgiou and P. Kumar), pp. 325-344. Academic press, New York.

Percival, D. B. and Mofjeld, H. O., 1997. Analysis of subtidal coastal sea level fluctuations using wavelets. *Journal of the American Statistical Association*, 92: 868-880.

Percival, D. B. and Walden, A. T., 2000. *Wavelet methods for time series analysis.* A volume in the Cambridge Series in Statistical and Probabilistic Mathematics, Cambridge University Press, Cambridge, UK.

Plant, N. G., Holman, R. A. and Freilich, M. H., 1999. A simple model for interannual sandbar behaviour. *Journal of Geophysical Research*, 104(C7): 15755-15776.

Plant, N. G., Holland, K. T., and Puleo, J. A., 2002. Analysis of the scales of errors in nearshore bathymetric data. *Marine Geology*, 191: 71-86.

Plant, N.G., Holland, K.T., Puleo, J.A., 2004. Prediction skill of nearshore profile evolution models. *Journal of Geophysical Research*, 109: C01006.

Press, W. H., Teulolsky, S.A., Vetterling, W.T. and Flannery, B. P., 1992. *Numerical Recipes in Fortran.* 2nd edn. Cambridge University Press. Cambridge.

Pruszak, Z., 1993. The analysis of beach profile change using Dean's method and empirical orthogonal functions, *Coastal Engineering*, 19: 245-261.

Pruszak, Z. and Różyński, G., 1998. Variability of multibar profiles in terms of random sine functions. *Journal of Waterway, Port, Coastal and Ocean Engineering*, 124: 48-56.

Pruszak, Z., and Różyński, G., 2001. Data-driven analysis and modelling of shoreline evolution trends. *Proceedings of Coastal Dynamics' 01*, ASCE, pp. 741-750.

Pruszak, Z., Różyński, G. and Zeidler, R. B., 1997. Statistical properties of multiple bars. *Coastal Engineering*, 31: 263-280.

Pruszak., Z., Różyński, G., Szmytkiewicz, M., and Skaja, M., 1999. Quasi-seasonal morphological shore evolution response to variable wave climate, *Proc. Coastal Sediments'99 Conference, ASCE*, pp. 1081-1093.

Reeve, D, Li, B. and Thurston, N., 2001. Eigenvector analysis of decadal fluctuations in sandbank morphology at Gt Yarmouth. *Journal of Coastal Research*, 17 (2): 371-382.

Reniers, A. J. H.M., Roelvink, J. A. and Walstra, D. J. R., 1995. Validation study of UNIBEST-TC model. Report H2130, Delft Hydraulics, Delft, The Netherlands.

Rivero, F. J. and Sánchez-Arcilla, A., 1994. Propagation of linear gravity waves over slowly varying depth and currents, in Waves '93. In: Magoon, O.T., Hemsley, J.M. (Eds.), *Proceedings of the 2nd International Symposium Ocean Wave Measurement and Analysis*, New Orleans, 1993. ASCE, New York, pp. 518–532.

Roelvink, J. A. and Broker, I., 1993. Cross-shore profile models. *Coastal Engineering*, 21: 163-191.

Romańiczyk, W., Boczar-Karakiewicz, B. and Bona, J. L., 2005. Extended equilibrium beach profiles. *Coastal Engineering*, article in press.

Różyński, G., 2003a. Data-driven modelling of multiple longshore bars and their interactions. *Coastal Engineering*, 48: 151-170.

Różyński, G., 2003b. Coastal nearshore morphology in terms of large data sets. *Institute of the Hydroengineering of the Polish Academy of Sciences (IBW PAN).*

Różyński, G., 2005. Long-term shoreline response of a nontidal, barred coast. *Coastal Engineering*, 52: 79-91.

Różyński, G. and Jansen, H., 2002. Modelling nearshore bed topography with principal oscillation patterns. *Journal of Waterway, Port, Coastal and Ocean Engineering,* 128: 202-215.

Różyński, G. and Reeve, D., 2005. Multi-resolution analysis of nearshore hydrodynamics using discrete wavelet transform. *Coastal Engineering,* 52(9):771-792.

Różyński, G., Larson, M. and Pruszak, Z., 2001. Forced and self-organised shoreline response for a beach in the southern Baltic Sea determined through singular spectrum analysis, *Coastal Engineering,* 43: 41-58.

Różyński, G., Pruszak, Z., Okrój, T. and Zeidler, R. B., 1999. Depth of closure and seabed variability patterns. *Proceedings of ICCE' 98, ASCE,* pp. 2926-2939.

Ruessink, B. G., Wijnberg, K. M., Holman, R. A., Kuriyama, Y. and Van Enckevort, I. M. J., 2003. Intersite comparison of interannual nearshore bar behaviour. *Journal of Geophysical Research,* 108 (C8): 1-12.

Sallenger, A. S., Holman, R. A. and Birkemeier, W. A., 1985. Storm-induced response of a nearshore bar system. *Marine Geology,* 64: 237-257.

Schwartz, R. K. and Birkemeier, W. A., 2004. Sedimentology and morphodynamics of a barrier island shoreface related to engineering concerns, Outer Banks, NC, USA. *Marine Geology,* 211: 215-255.

Short, A. D. and Trembanis, A. C., 2004. Decadal scale patterns in beach oscillation and rotation Narrabeen beaches, Australia-time series, PCA and wavelet analysis. *Journal of Coastal Research,* 20(2):523-532.

Si, B., 2003. Scale and location dependent soil hydraulic properties in a hummocky landscape: a wavelet approach. In: *Scaling methods in Soil Physics* (eds Y. Pachepsky, D. Radcliffe and H. M. Selim), pp. 169-187. CRC Press LLC, Boca Raton, Florida.

Sierra, J. P. and Sánchez-Arcilla, A., 1999. CIIRC-LIM runs for Egmond Pilot Experiment, Report RR-CIIRC/AHC-99-1, University of Catalunya, Spain.

Smallwood, D. O., 1999. Characterization and simulation of gunfire with wavelets. *Shock and Vibration,* 6: 59-72.

Southgate, H. N., 1997. Non-linear methods of analysis for long-term beach and nearshore morphology. *Proceedings of the 27th IAHR Congress,* Theme A.

Southgate, H. N., and Möller, I., 2000, Fractal properties of coastal profile evolution at Duck, North Carolina, *Journal of Geophysical Research,* 105: 11489-11507.

Southgate, H. N. and Nairn, R. B., 1993. Deterministic profile modelling of nearshore process. Part 1. Waves and currents. *Coastal Engineering,* 19: 27-56.

Southgate, H. N., Wijnberg, K. M., Larson, M., Capobianco, M., and Jansen, H., 2003. Analysis of field data of coastal morphological evolution over yearly and decadal time series, Part 2. Non-linear techniques. *Journal of Coastal Research,* 19 (4): 776-789.

Stauble, D. K. and Cialone, M. A., 1996. Sediment dynamics and profile interactions: DUCK94. *Proceedings of 25th International Conference on Coastal Engineering,* Vol. 4, pp. 3921-3934.

Stive, M. J. F., Aarninkhof, S. G. J., Hamm, L., Hanson, H., Larson, M., Wijnberg, K. M., Nicholls, R. J., and Capobianco, M., 2002. Variability of shore and shoreline evolution. *Coastal Engineering,* 47: 211-235.

Thorton, E. B. and Humiston, R. T., 1996. Bar/trough generation on a natural beach. *Journal of Geophysical Research*, 101(C5): 12097-12110.

Traykovski, P., Hay, A. E., Irish, J. D. and Lynch, J. F., 1999. Geometry, migration, and evolution of wave orbit ripples at LEO-15. *Journal of Geophysical Research*, 104: 1505-1524.

Van Rijn, L. C., 1997. Cross-shore sand transport and bed composition. *Proceedings of the Coastal Dynamics '97 Conference*, pp. 88–98.

Van Rijn, L. C., 1998. The effect of sediment composition on cross-shore bed profiles. *Proceedings of the 26th International Conference on Coastal Engineering*. Copenhagen, Denmark. pp. 2495-2508.

Van Rijn, L. C., 2000. General view on sand transport by currents and waves; TRANSPOR2000 and CROSMOR2000 models. Report Z2899.20/2099.30/2824.30, Delft Hydraulics, Delft, The Netherlands.

Van Rijn, L. C. and Wijnberg, K. M., 1994. One-dimensional modelling of individual waves and wave-induced longshore currents in the surf zone. Report R 94-09, Dept. of Physical Geography, Univ. of Utrecht.

Van Rijn, L. C. and Wijnberg, K. M., 1996. One-dimensional modelling of individual waves and wave-induced longshore currents in the surf zone. *Coastal Engineering*, 28: 121–145.

Van Rijn, L.C., Walstra, D.J.R., Grasmeijer, B., Sutherland, J., Pan, S., Sierra, J.P., 2003. The predictability of cross-shore bed evolution of sandy beaches at the time scale of storms and seasons using process-based profile models. *Coastal Engineering*, 47: 295– 327.

Vautard, R., Yiou, P., and Ghil, M., 1992. Singular spectrum analysis: a toolkit for short, noisy, chaotic signals. *Physica D*, 158: 95-126.

Vellinga, P., 1983. Predictive computational model for beach and dune erosion during storm surges. *Proceedings of the Speciality Conference on Coastal Structures '83*, American Society of Civil Engineers, pp. 806-819.

Von Storch, H., Bruns, T., Fischer-Bruns, I., and Hasselmann, K., 1988. Principle oscillation pattern analysis of the 30- to 60-day oscillation in general circulation model equation troposphere. *Journal of Geophysical Research*, 93: 11022-11036.

Webster, R., 2000. Is soil variation random? Geoderma, 97: 149-163.

Webster, R. and Oliver, M. A., 2001. *Geostatistics for Environmental Scientists*. John Wiley & Sons, Chichester.

Wickerhauser, M. V., 1994. *Adapted Wavelet Analysis from Theory to Software*. Wellesley, Massachusetts: A K Peters.

Winant, C. D., Inman, D. L., and Nordstrom, C. E., 1975. Description of seasonal beach changes using empirical eigenvectors. *Journal of Geophysical Research*, 80 (15): 1979-1986.

Wijnberg, K. M. and Terwindt, J. H. J., 1995. Extracting decadal morphological behaviour from high-resolution, long-term bathymetric surveys along the Holland coast using eigenvector analysis. *Marine Geology*, 126: 301-330.

Whitcher, B., Guttorp, P., and Percival, D. B., 2000a. Multiscale detection and location of multiple variance changes in the presence of long memory. *Journal of Statistical Computation and Simulation*, 68: 65-88.

Whitcher, B. J., Guttorp, P. and Percival, D. B., 2000b. Wavelet analysis of covariance with application to atmospheric time series. *Journal of Geophysical Research- Atmospheres*, 105: 14941-14962.

Wright, L. D., Boon, J. D., Kim, S. C. and List, J. H., 1991. Modes of cross-shore sediment transport on the shoreface of the Middle Atlantic Bight. *Marine Geology*, 96: 19-51.

APPENDIX A:

FRF photos

The long pier at Duck (http://www.frf.usace.army.mil/buildings.stm).

Sensor Insertion System at Duck (http://www.frf.usace.army.mil/vehicles2.stm).

Coastal research amphibious buggy (http://www.frf.usace.army.mil/vehicles2.stm).

Table A1: the surveys at Duck corresponding to the calendar month.

No	Survey	No	Survey	No	Survey	No	Survey	No	Survey	No	Survey
1	Jul.81	46	Apr.85	91	Jan.89	136	Oct.92	181	Jul.96	226	Apr.00
2	Aug.81	47	May85	92	Feb.89	137	Nov.92	182	Aug.96	227	May00
3	Sep.81	48	Jun.85	93	Mar.89	138	Dec.92	183	Sep.96	228	Jun.00
4	Oct.81	49	Jul.85	94	Apr.89	139	Jan.93	184	Oct.96	229	Jul.00
5	Nov.81	50	Aug.85	95	May89	140	Feb.93	185	Nov.96	230	Aug.00
6	Dec.81	51	Sep.85	96	Jun89	141	Mar.93	186	Dec.96	231	Sep.00
7	Jan.81	52	Oct.85	97	Jul.89	142	Apr.93	187	Jan.97	232	Oct.00
8	Feb.82	53	Nov.85	98	Aug.89	143	May93	188	Feb.97	233	Nov.00
9	Mar.82	54	Dec.85	99	Sep.89	144	Jun.93	189	Mar.97	234	Dec.00
10	Apr.82	55	Jan.86	100	Oct.89	145	Jul.93	190	Apr.97	235	Jan.01
11	May82	56	Feb.86	101	Nov.89	146	Aug.93	191	May97	236	Feb.01
12	Jun.82	57	Mar.86	102	Dec.89	147	Sep.93	192	Jun.97	237	Mar.01
13	Jul.82	58	Apr.86	103	Jan.90	148	Oct.93	193	Jul.97	238	Apr.01
14	Aug.82	59	May86	104	Feb.90	149	Nov.93	194	Aug.97	239	May01
15	Sep.82	60	Jun.86	105	Mar.90	150	Dec.93	195	Sep.97	240	Jun.01
16	Oct.82	61	Jul.86	106	Apr.90	151	Jan.94	196	Oct.97	241	Jul.01
17	Nov.82	62	Aug.86	107	May90	152	Feb.94	197	Nov.97	242	Aug.01
18	Dec.82	63	Sep.86	108	Jun.90	153	Mar.94	198	Dec.97	243	Sep.01
19	Jan.83	64	Oct.86	109	Jul.90	154	Apr.94	199	Jan.98	244	Oct.01
20	Feb.83	65	Nov.86	110	Aug.90	155	May94	200	Feb.98	245	Nov.01
21	Mar.83	66	Dec.86	111	Sep.90	156	Jun.94	201	Mar.98	246	Dec.01
22	Apr.83	67	Jan.87	112	Oct.90	157	Jul.94	202	Apr.98	247	Jan.02
23	May83	68	Feb.87	113	Nov.90	158	Aug.94	203	May98	248	Feb.02
24	Jun.83	69	Mar.87	114	Dec.90	159	Sep.94	204	Jun98	249	Mar.02
25	Jul.83	70	Apr.87	115	Jan.91	160	Oct.94	205	Jul.98	250	Apr.02
26	Aug.83	71	May87	116	Feb.91	161	Nov.94	206	Aug.98	251	May02
27	Sep.83	72	Jun.87	117	Mar.91	162	Dec.94	207	Sep.98	252	Jun.02
28	Oct.83	73	Jul.87	118	Apr.91	163	Jan.95	208	Oct.98	253	Jul.02
29	Nov.83	74	Aug.87	119	May91	164	Feb.95	209	Nov.98	254	Aug.02
30	Dec.83	75	Sep.87	120	Jun.91	165	Mar.95	210	Dec.98	255	Sep.02
31	Jan.84	76	Oct.87	121	Jul.91	166	Apr.95	211	Jan.99	256	Oct.02
32	Feb.84	77	Nov.87	122	Aug.91	167	May95	212	Feb.99	257	Nov.02
33	Mar.84	78	Dec.87	123	Sep.91	168	Jun.95	213	Mar.99	258	Dec.02
34	Apr.84	79	Jan.88	124	Oct.91	169	Jul.95	214	Apr.99	259	Jan.03
35	May84	80	Feb.88	125	Nov.91	170	Aug.95	215	May99	260	Feb.03
36	Jun.84	81	Mar.88	126	Dec.91	171	Sep.95	216	Jun.99	261	Mar.03
37	Jul.84	82	Apr.88	127	Jan.92	172	Oct.95	217	Jul.99	262	Apr.03
38	Aug.84	83	May88	128	Feb.92	173	Nov.95	218	Aug.99	263	May03
39	Sep.94	84	Jun.88	129	Mar.92	174	Dec.95	219	Sep.99	264	Jun.03
40	Oct.84	85	Jul.88	130	Apr.92	175	Jan.96	220	Oct.99	265	Jul.03
41	Nov.84	86	Aug.88	131	May92	176	Feb.96	221	Nov.99	266	Aug.03
42	Dec.84	87	Sep.88	132	Jun.92	177	Mar.96	222	Dec.99	267	Sep.03
43	Jan.85	88	Oct.88	133	Jul.92	178	Apr.96	223	Jan.00		
44	Feb.85	89	Nov.88	134	Aug.92	179	May96	224	Feb.00		
45	Mar.85	90	Dec.88	135	Sep.92	180	Jun.96	225	Mar.00		

APPENDIX B:

A picture from Lubiatowo

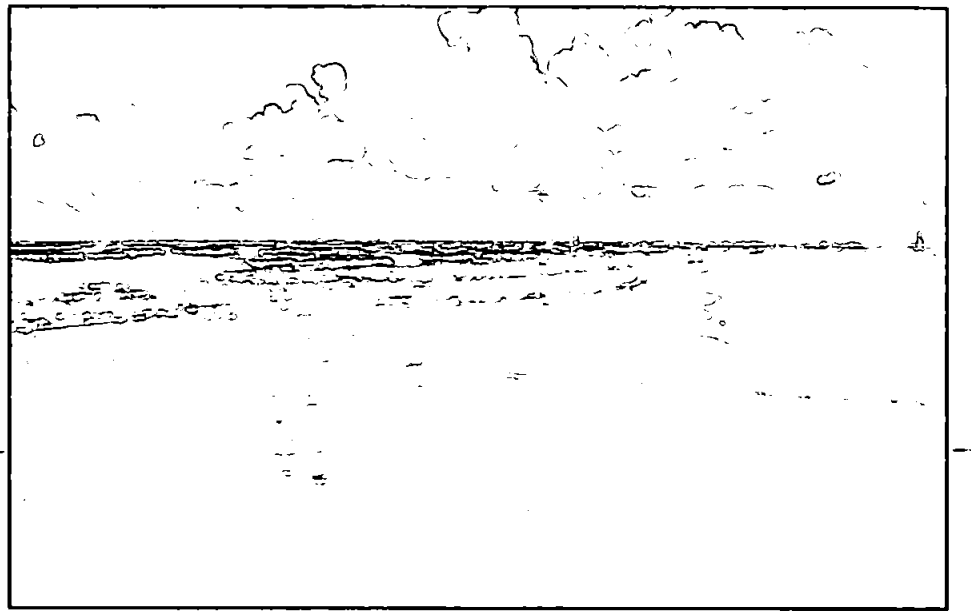

Components of Wavelet Variance of Profile 4 at Lubiatowo

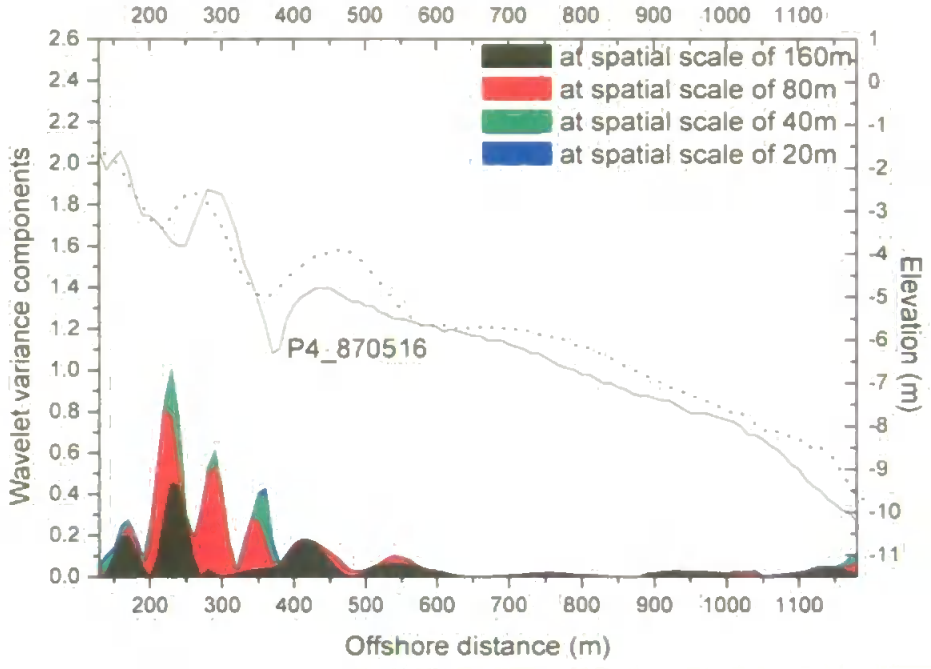

Figure A1 Components of wavelet variance in May 1987 of Profile 4 at Lubiatowo.

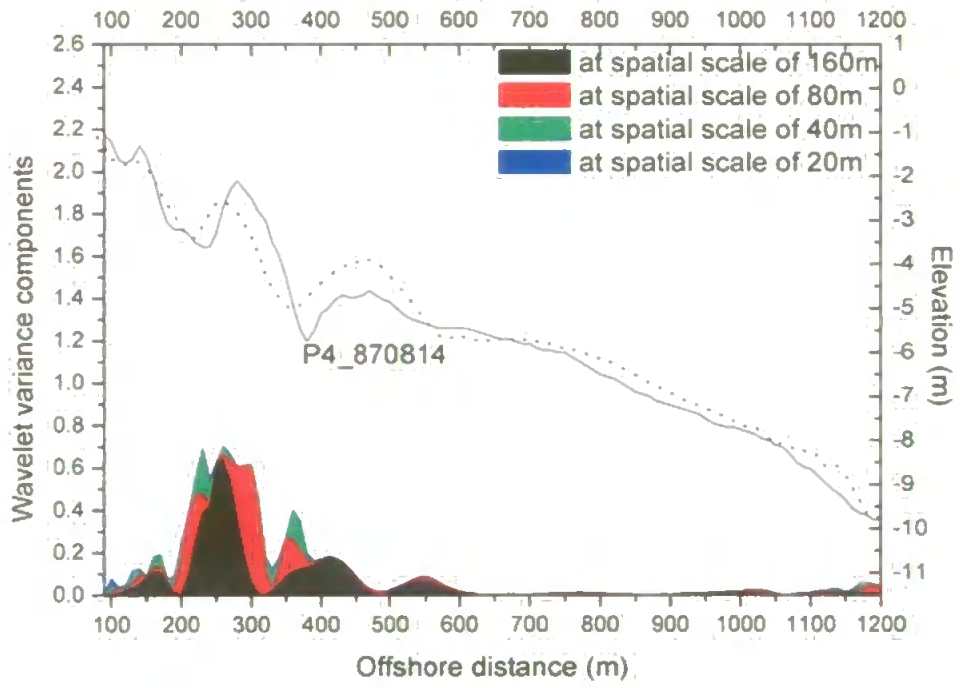

Figure A2 Components of wavelet variance in August 1987 of Profile 4 at Lubiatowo.

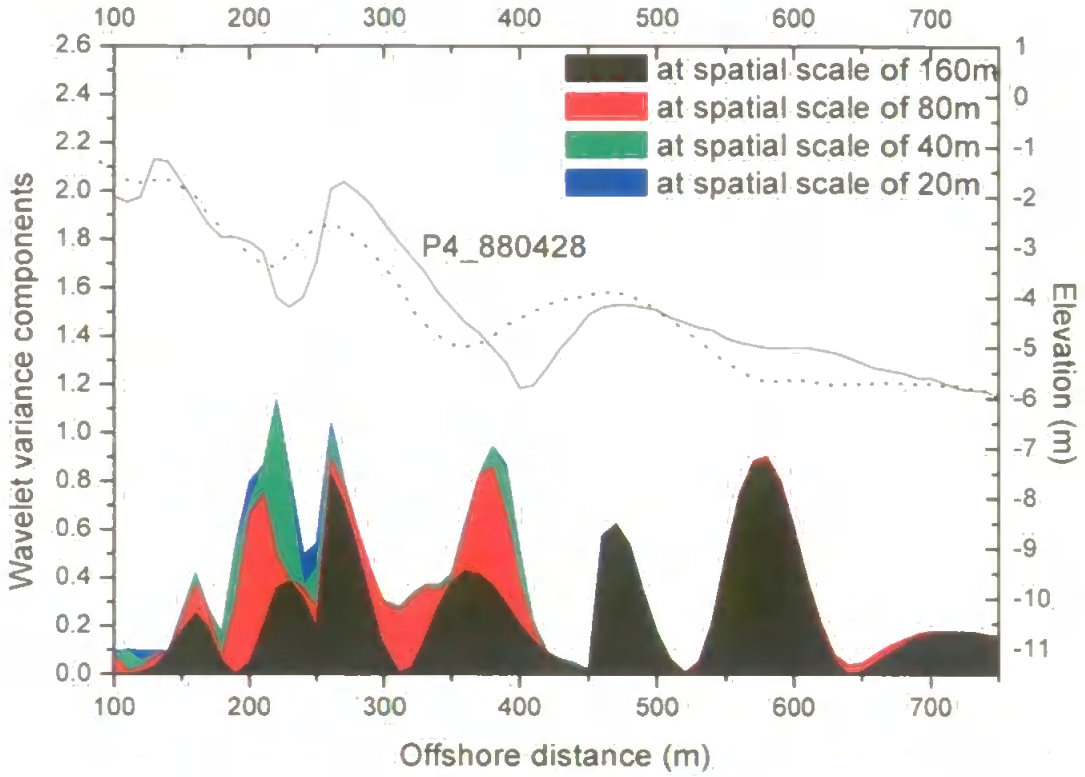

Figure A3 Components of wavelet variance in April 1988 of Profile 4 at Lubiatowo.

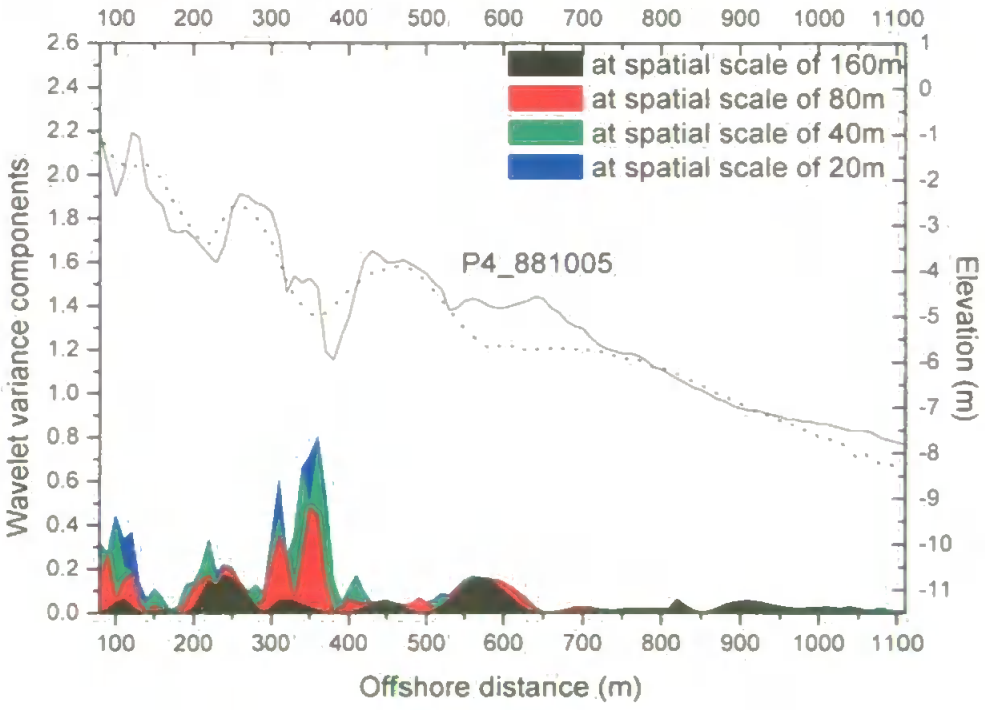

Figure A4 Components of wavelet variance in October 1988 of Profile 4 at Lubiatowo.

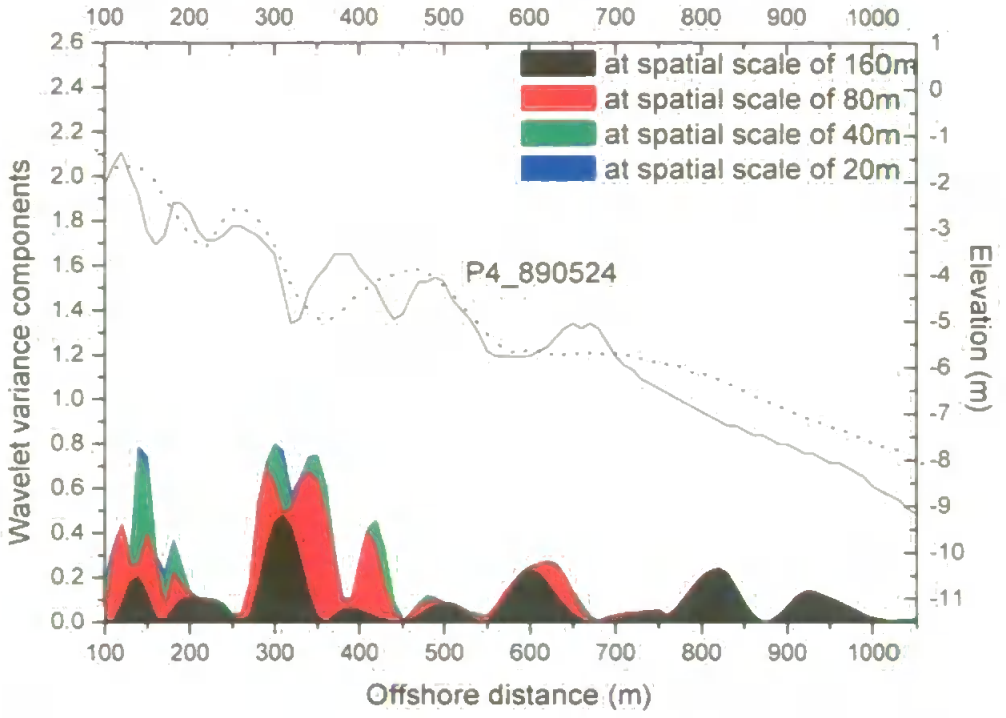

Figure A5 Components of wavelet variance in May 1989 of Profile 4 at Lubiatowo.

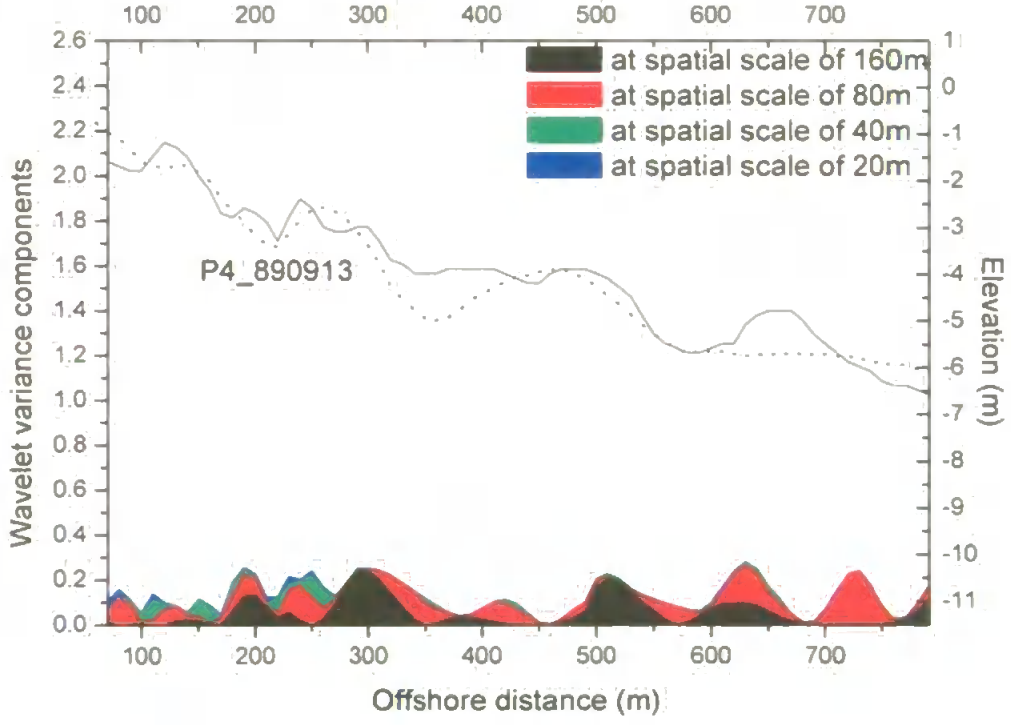

Figure A6 Components of wavelet variance in September 1989 of Profile 4 at Lubiatowo.

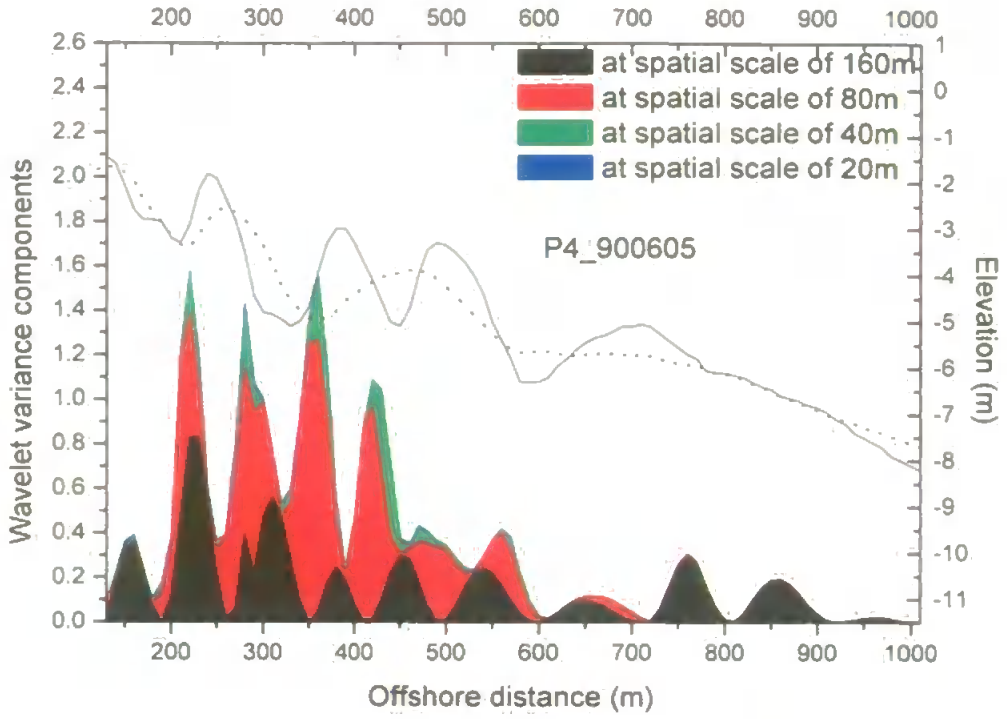

Figure A7 Components of wavelet variance in June 1990 of Profile 4 at Lubiatowo.

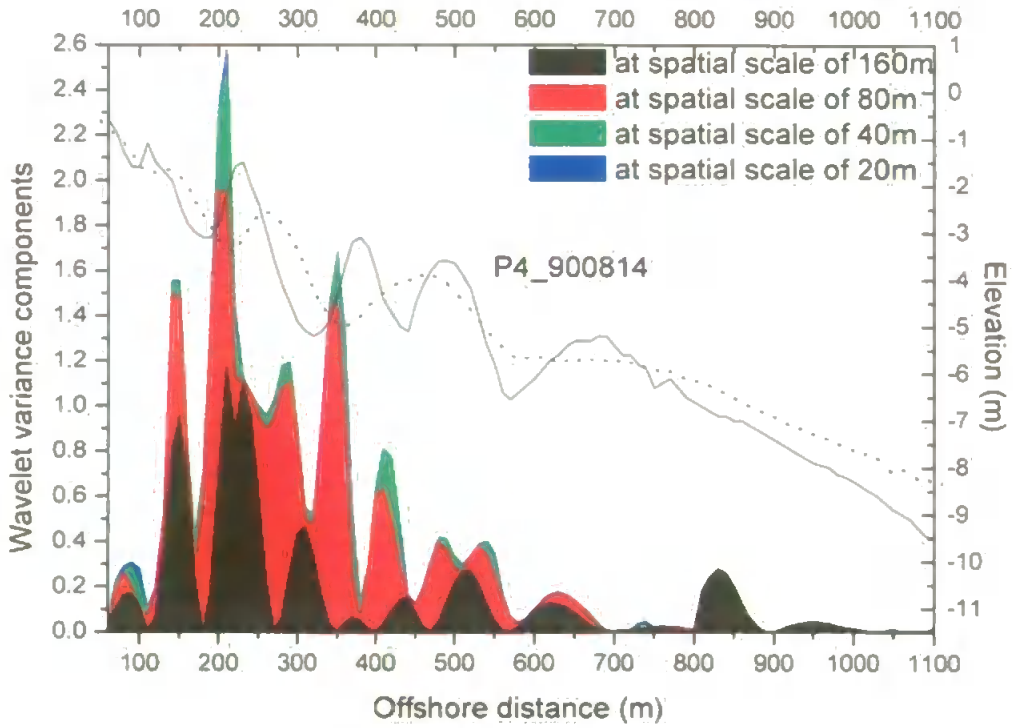

Figure A8 Components of wavelet variance in August 1990 of Profile 4 at Lubiatowo.

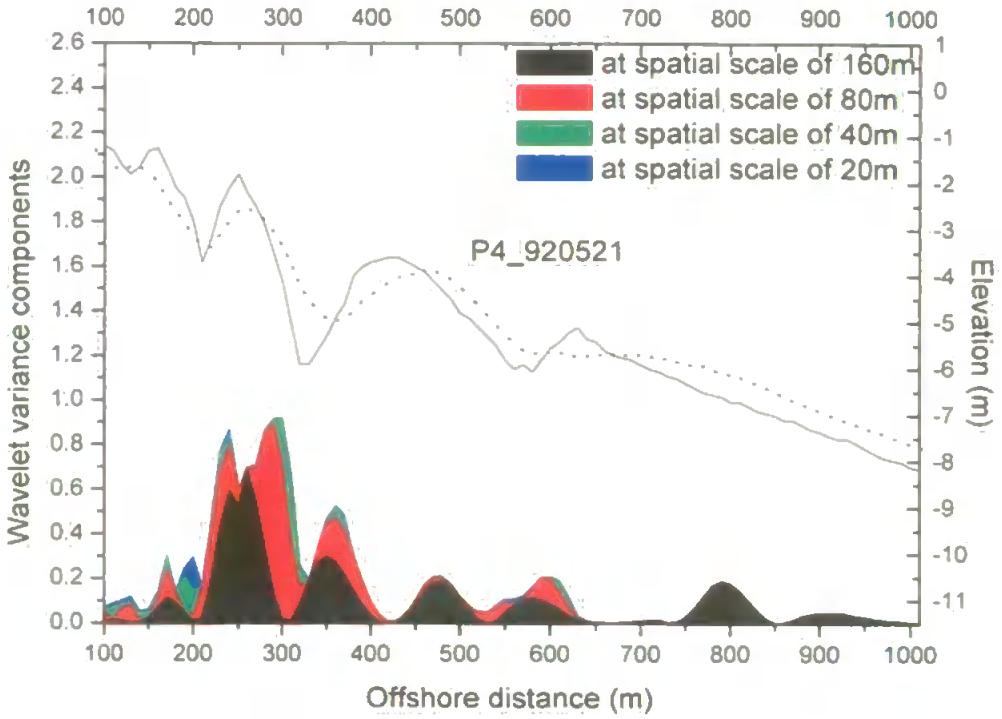

Figure A9 Components of wavelet variance in May 1992 of Profile 4 at Lubiatowo.

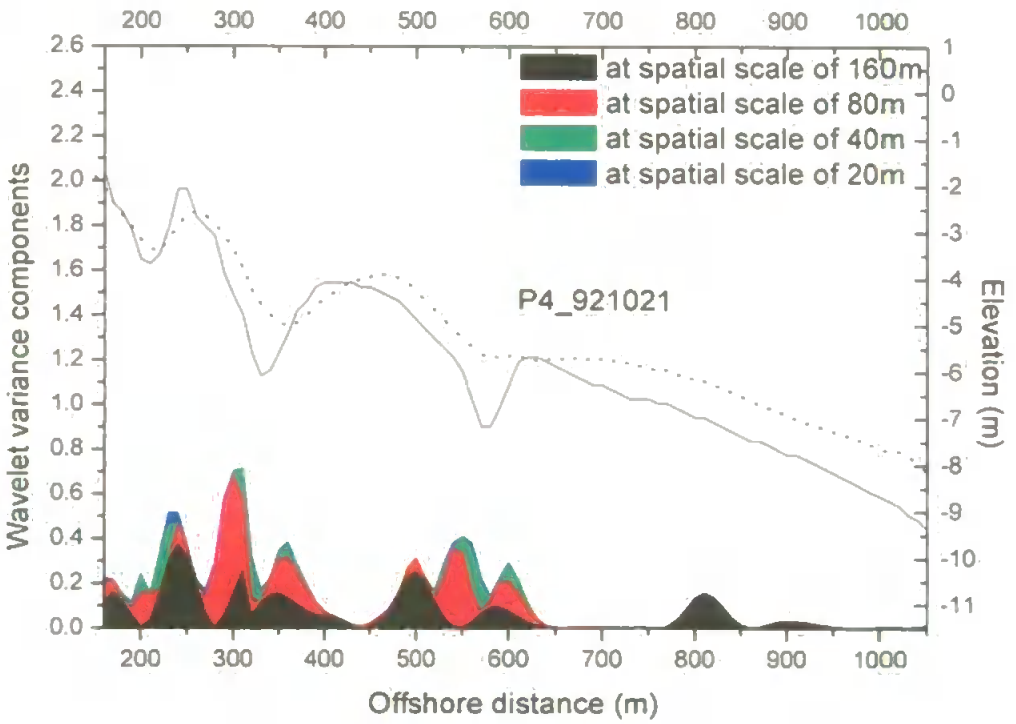

Figure A10 Components of wavelet variance in October 1992 of Profile 4 at Lubiatowo.

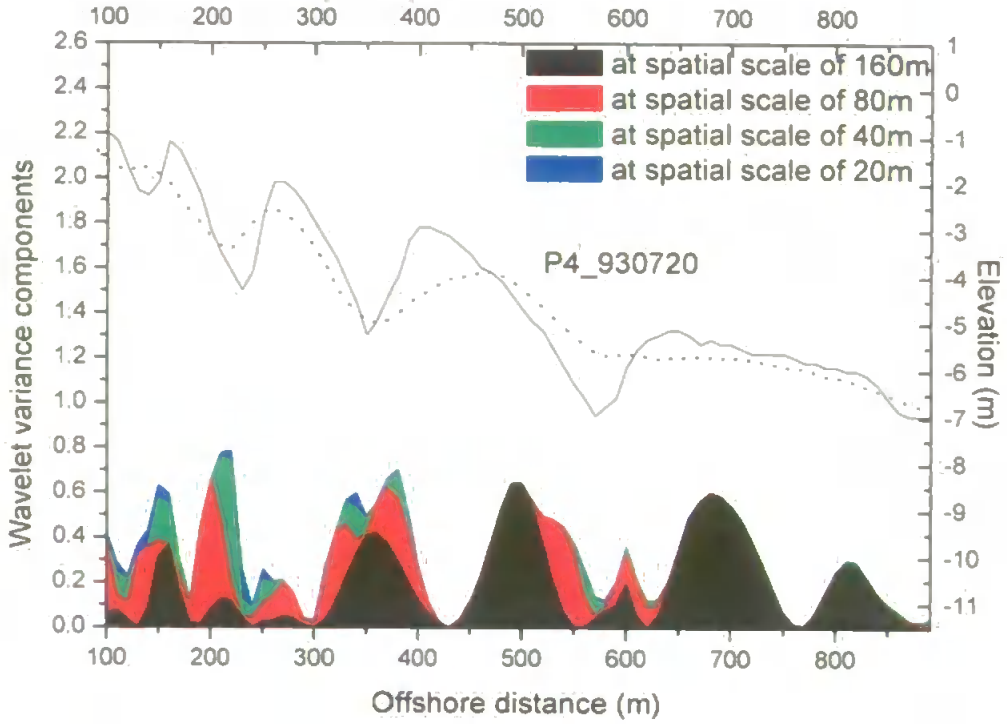

Figure A11 Components of wavelet variance in July 1993 of Profile 4 at Lubiatowo.

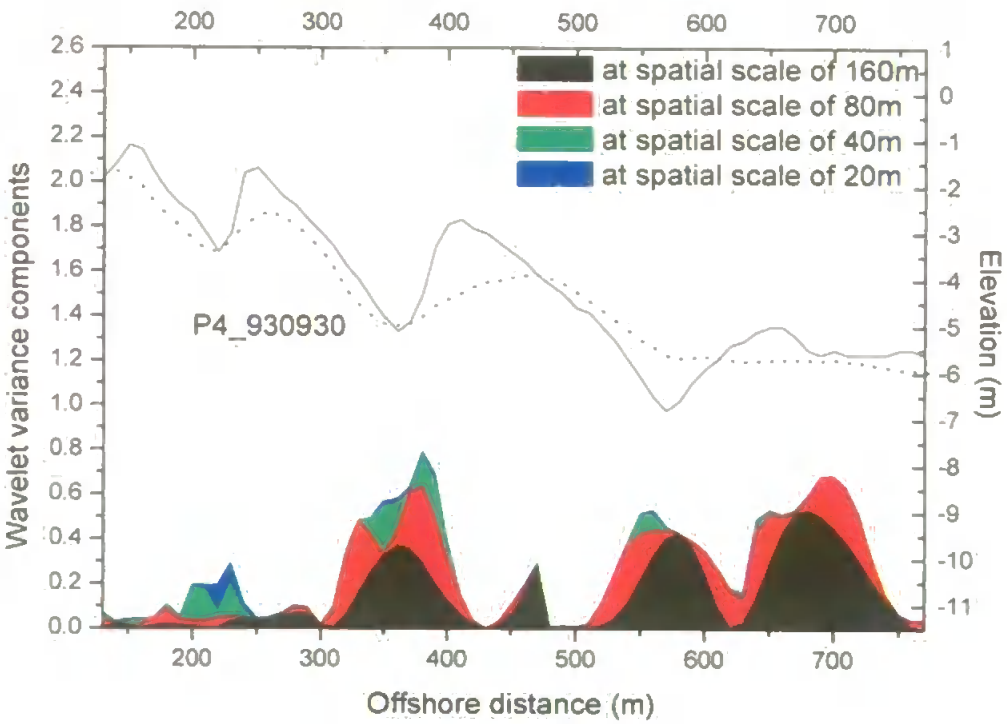

Figure A12 Components of wavelet variance in September 1993 of Profile 4 at Lubiatowo.

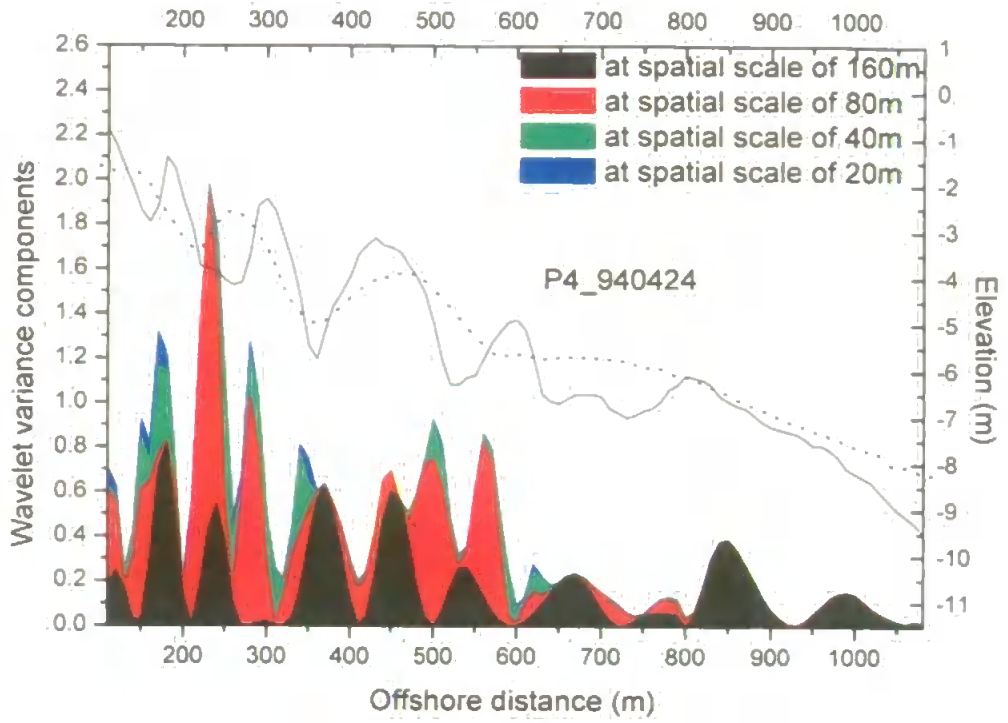

Figure A13 Components of wavelet variance in April 1994 of Profile 4 at Lubiatowo.

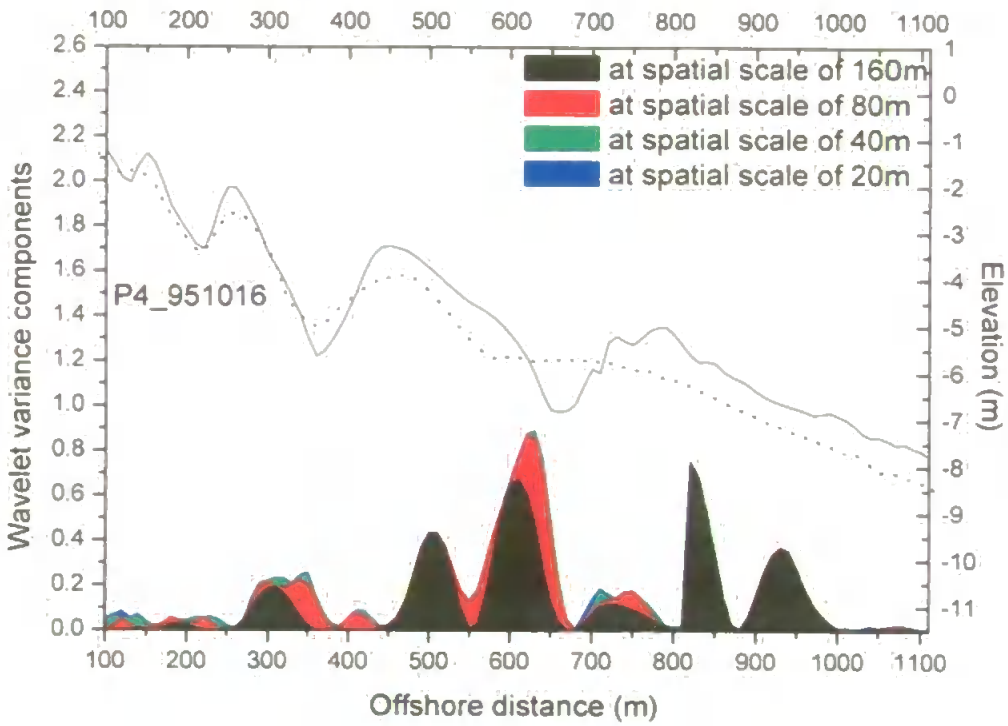

Figure A14 Components of wavelet variance in October 1995 of Profile 4 at Lubiatowo.

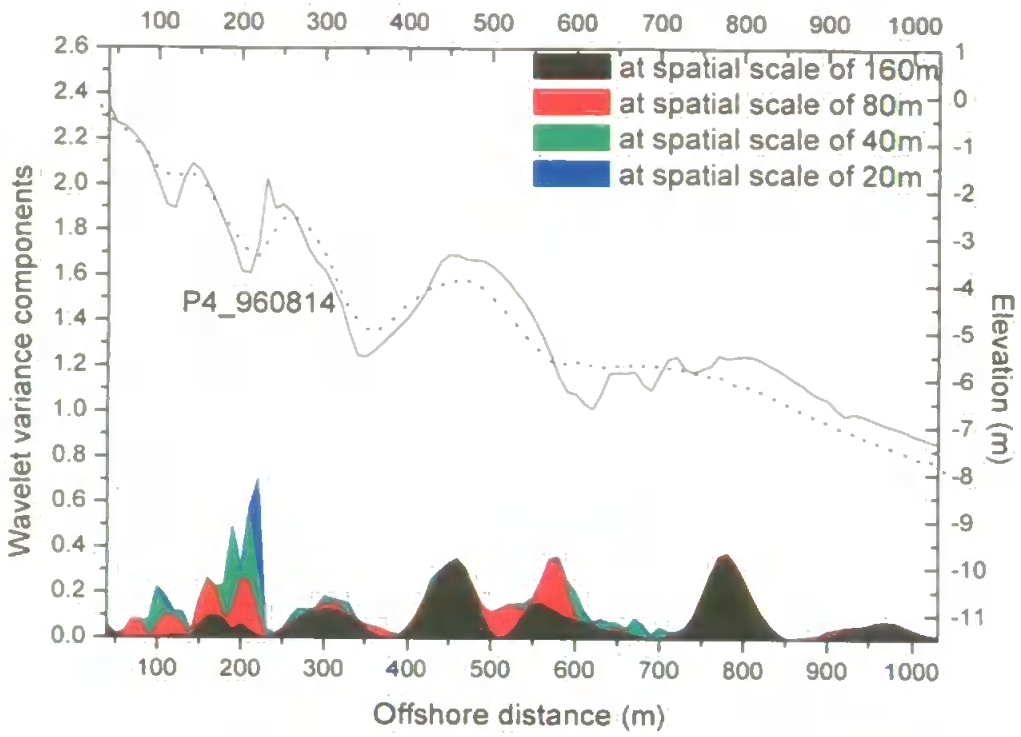

Figure A15 Components of wavelet variance in August 1996 of Profile 4 at Lubiatowo.

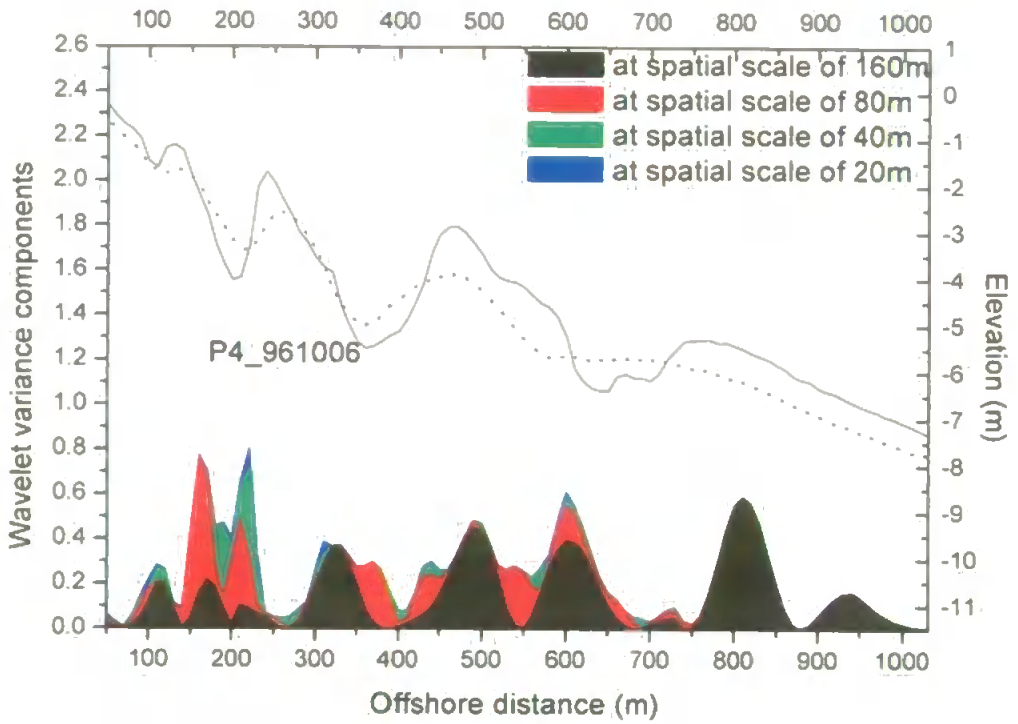

Figure A16 Components of wavelet variance in October 1996 of Profile 4 at Lubiatowo.

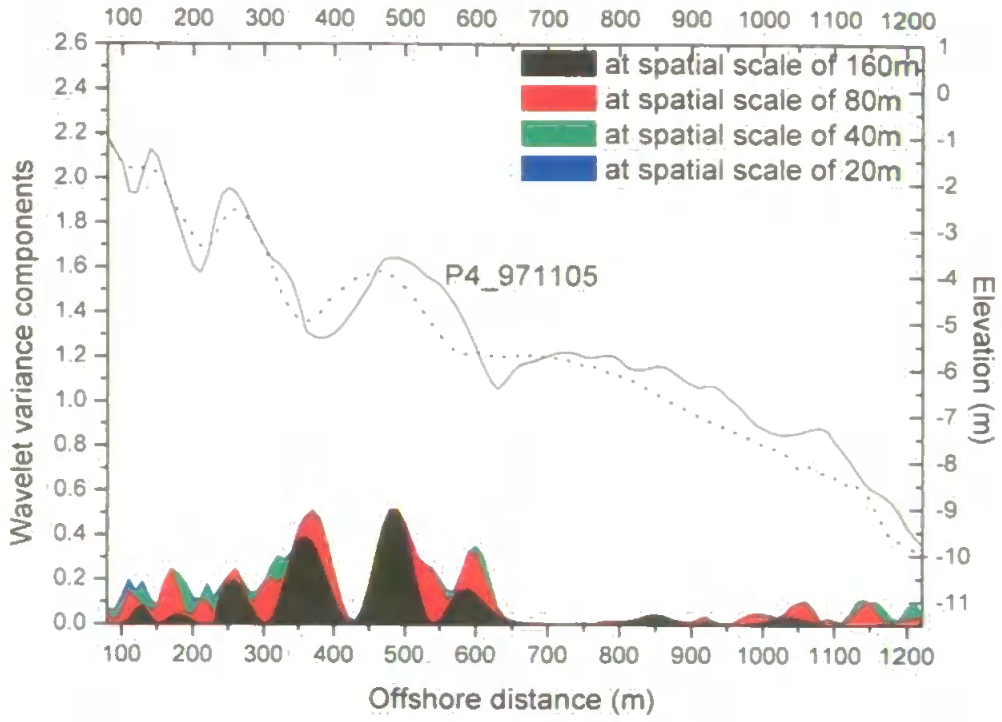

Figure A17 Components of wavelet variance in November 1997 of Profile 4 at Lubiatowo.

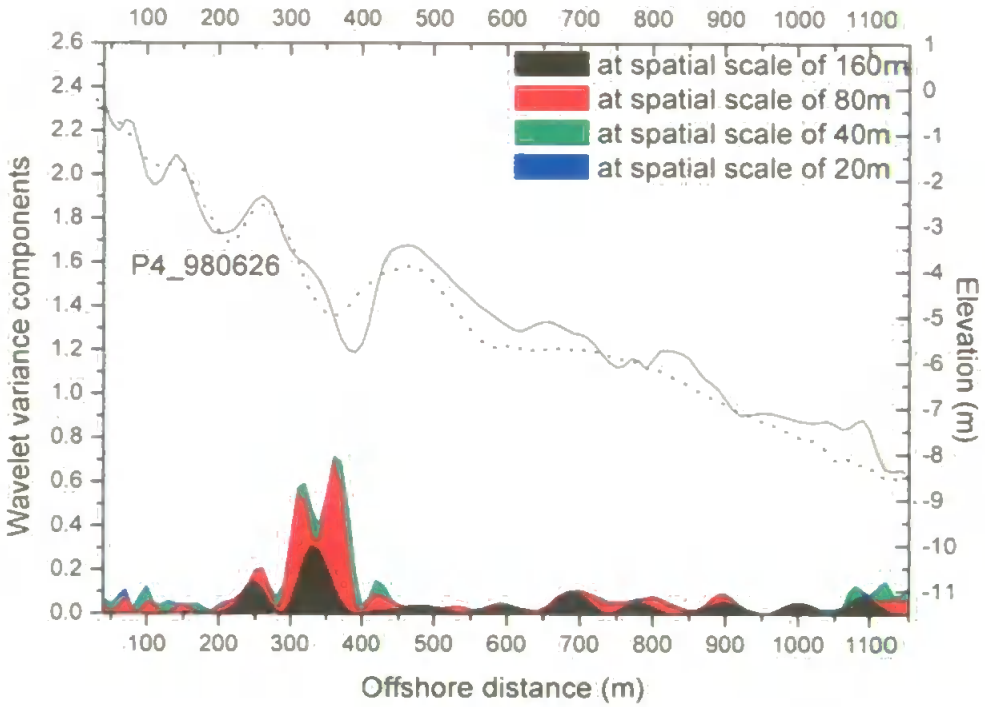

Figure A18 Components of wavelet variance in June 1998 of Profile 4 at Lubiatowo.

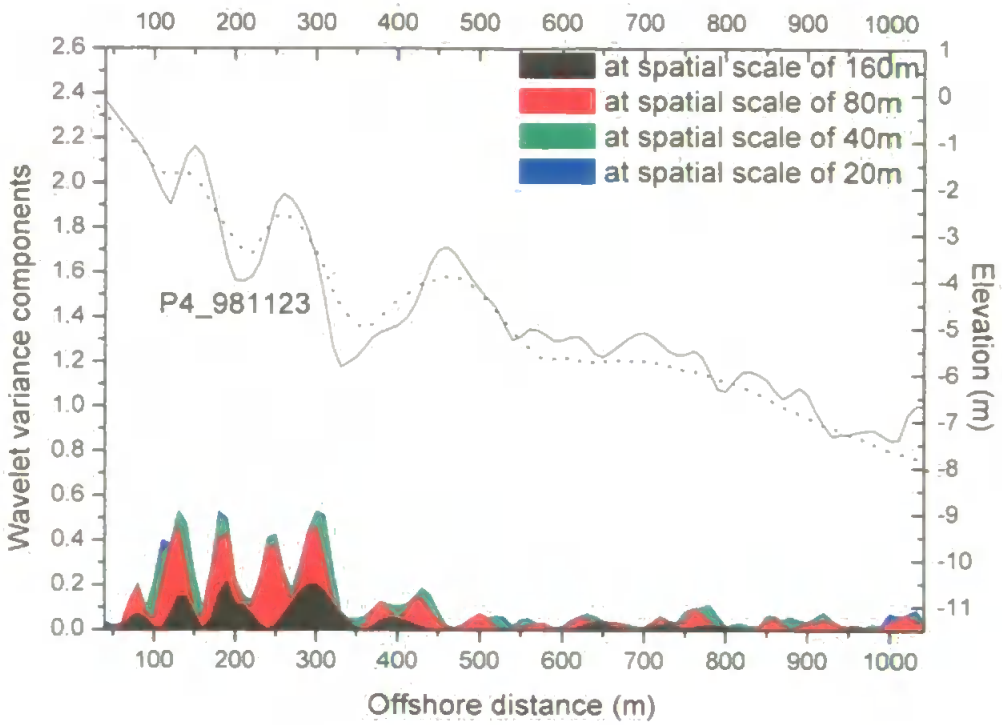

Figure A19 Components of wavelet variance in November 1998 of Profile 4 at Lubiatowo.

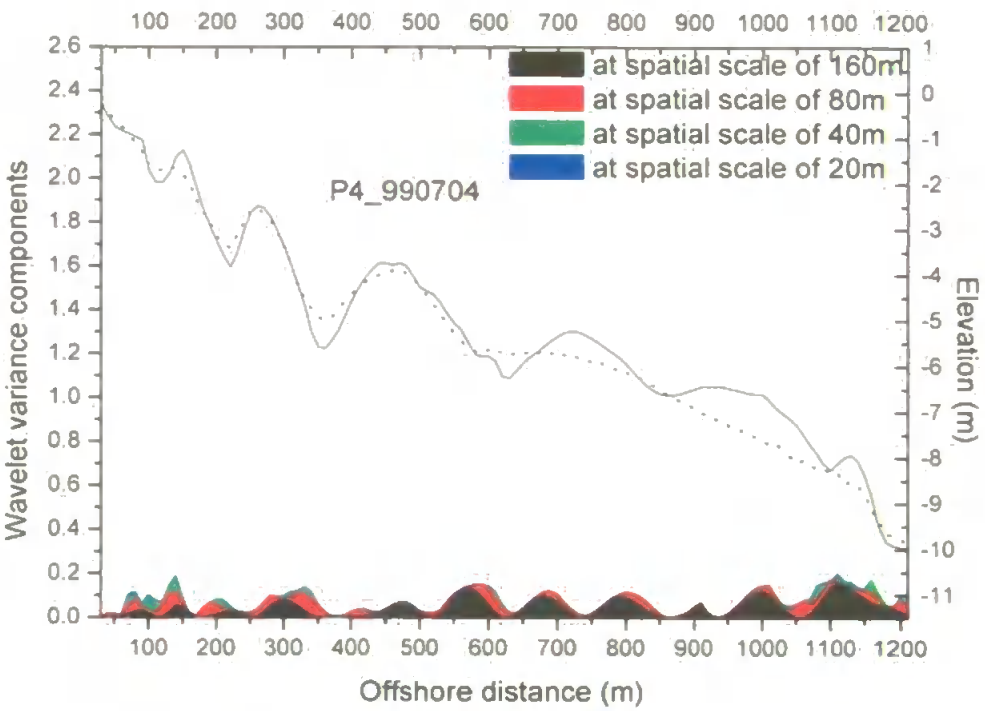

Figure A20 Components of wavelet variance in July 1999 of Profile 4 at Lubiatowo.

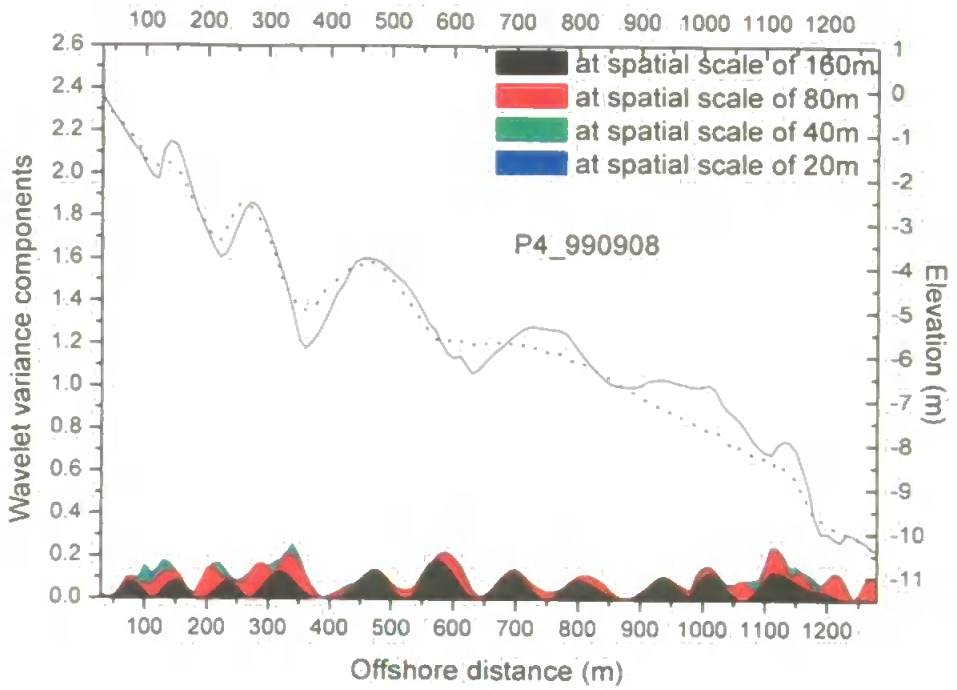

Figure A21 Components of wavelet variance in September 1999 of Profile 4 at Lubiatowo.

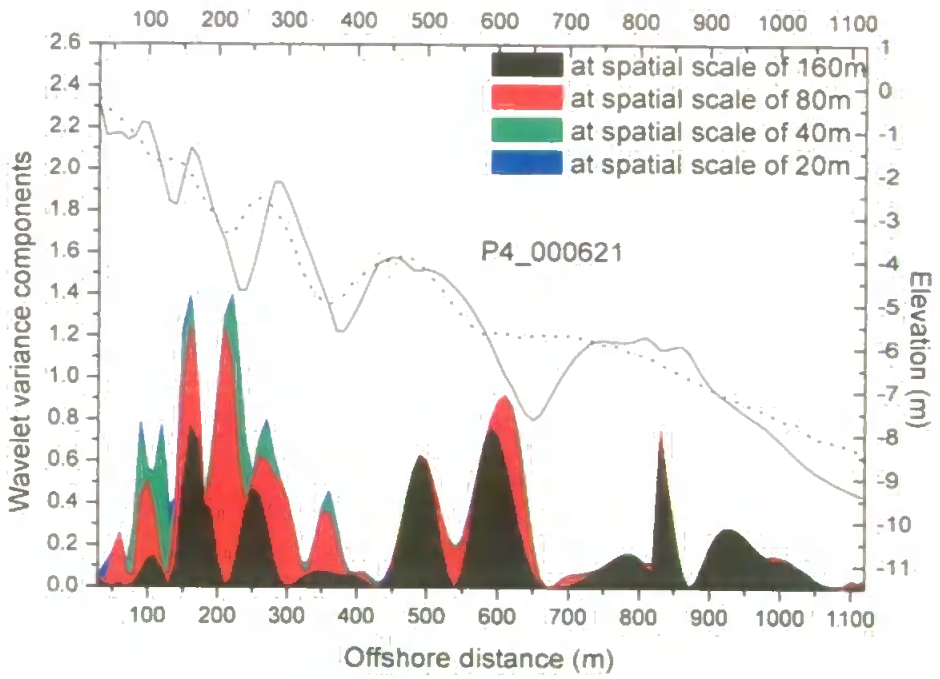

Figure A22 Components of wavelet variance in June 2000 of Profile 4 at Lubiatowo.